Salinas Valley Sediment Sources

Fred Watson, Ph.D,
Mark Angelo, P.E.
Thor Anderson,
Joel Casagrande,
Don Kozlowski,
Wendi Newman,
Julie Hager,
Doug Smith, Ph.D,
Bob Curry, Ph.D

The Watershed Institute

Earth Systems Science and Policy
California State University
Monterey Bay
http://watershed.csumb.edu

100 Campus Center, Seaside, CA,
93955-8001
831 582 4452 / 4431.

All authors reside at:
Watershed Institute,
California State University Monterey Bay

Except:
Mark Angelo,
Central Coast Regional Water Quality Control Board

Lead author contact details:
fred_watson@csumb.edu

ii

Preface

Acknowledgements

Table of Contents

Executive summary, synthesis, and conclusion

E.1   Introduction

Basis

The Salinas River is listed by the Environmental Protection Agency (EPA) under the Clean Water Act's '303d list' as being impaired due to 'sedimentation/siltation'. A plan for management of the total maximum daily load (TMDL) of sediment is thus mandated. This plan must include an assessment of sediment sources in the Salinas Watershed. The present study provides the technical basis for this source analysis, to be used by the Central Coast Regional Water Quality Control Board (CCRWQB) in the development of the Salinas Sediment TMDL.

The precise manner in which 'sedimentation/siltation' is understood to 'impair' the beneficial uses of the Salinas River or its tributaries is yet to be fully described. Sediment is both a natural hindrance and a natural requirement of many of the system's beneficial uses.

Sedimentation is the process whereby sediment drops out of the water column and accumulates on the bottom of a waterbody, or is left behind after the water has gone. This is a natural process that dominates the morphology of the Salinas River. It is a necessary component of the dynamic geomorphic equilibrium that is the ultimate goal of all environmentally sensitive river management. Given this background, excessive sedimentation is possible. In the lower Salinas River (i.e. the section that is listed), it is possible that excessive sedimentation has lead to infilling of deeper parts of the river and the Salinas Lagoon at a higher rate than that which is normally offset by periodic scouring. However, at the outset, it is thought that this possibility is relatively unlikely and almost undetectable when compared with other, much more obvious stressors such as reduction of streamflow, and inputs of anthropogenic chemicals.

We thus take a broader view of all that is implied by the EPA's usage of the terms 'sedimentation/siltation'. Our study is of sediment in general, allowing for the possibility that its impacts may be manifested through suspended sediment *concentration* and sediment *loads* delivered to receiving waters as well as sedimentation *per se*. We also acknowledge that perhaps the only way to

characterize the adverse impacts of sediment in a naturally sediment-dominated system like the Salinas, is to measure that proportion of sediment concentration or load that is due to anthropogenic sources.

Anthropogenic sediment loads in excess of natural loads are assumed to be a hindrance, in the absence of any specific knowledge to the contrary. An aim of the present study is to attempt to delineate anthropogenic versus natural sediment sources, and in doing so, characterize the extent to which there may be a sediment problem in the watershed. This is intended to provoke further study to determine the specific manifestations of such a problem.

Examples where anthropogenic sediment may adversely impact beneficial uses include:

- High concentrations of suspended sediment in the water column may impact the life cycles of fish and other aquatic organisms, through mechanisms such as gill abrasion and reduced visibility for migration and other behaviors (Newcombe & Jensen, 1996). Of particular interest are the potential impacts to migrating South Central-Coast steelhead (*Onchorhynchus mykiss irideus*), which are Federally list as a threatened Evolutionary Significant Unit (ESU).
- High loads of sediment may lead to benthic accumulation both in streams and the ocean. Fine sediment accumulation in otherwise coarse-bedded streams can impact fish spawning and hatching. Sediment accumulation in lagoons and other coastal waters may smother habitat and decrease the habitat volume for organisms that use these waters.

Different types of sediment problem may occur in different parts of the watershed, ranging from the riffle-pool sequences of headwater streams, through to the larger, sandy migration paths of the main stem, to the rearing habitat of the Salinas Lagoon, and to nearby marine habitats.

Sediment problems in general are typical associated with fine material (i.e. clay, silt, and sand) rather than coarse material (e.g. gravel, cobbles, and boulders).

Purpose

The specific aims of the study were to:

- quantify the mean annual sediment load of the River
- quantify the spatial and temporal variability in sediment load
- quantify the major geographic sources of sediment
- quantify the major sources of sediment with respect to specific land uses

Methodology

The study methods focused on characterizing the mean annual sediment load for the whole watershed, for specific geographic areas, and for specific land uses. This load is measured in metric tonnes/km²/yr.

The work was completed in three phases:

1. Data collection
   a. Collection of all existing sediment concentration and load data
   b. Supplementation of existing data with new field data collection, based on gaps in the existing data record – including storm-based monitoring in streams and on farm fields
2. Regional analysis of mean annual load
   a. Statistical characterization of regional hydrology
   b. Statistical characterization of regional sediment load
3. Analyses specific to Valley floor agricultural areas
   a. Timing of sediment load at the Watershed outlet
   b. Longitudinal sequence of land uses and associated sediment loads
   c. Direct monitoring of farm fields
   d. Brief comparison with Revised Universal Soil Loss Equation (RUSLE)

In the regional analysis, the significant episodicity of the system was dealt with by standardizing the data from all sites to *exclude* the uppermost 0.5% of flow magnitudes, which occur too infrequently to form a consistent part of the monitoring record. As the upper 0.5% of flow magnitudes corresponds *roughly* to flood flows, the analysis was termed a 'non-flood' analysis.

E.2 Study area

The study area is the entire watershed of the Salinas River (*c.* 11,000 km²) and Gabilan Creek (315 km²), which drains into the Old Salinas River Channel. In its

lower reaches, the Salinas River flows northward as a large channelized, sand-bed stream within a wide, flat alluvial plain. Steep mountain ranges and tributaries abut the River to the west and east. The climate is Mediterranean, with very little rain for about 8 months of the year. Intense storms are not uncommon in winter. Most streams are non-perennial, including the Salinas River itself, where flows persist in summer only by way of irrigation releases from storage reservoirs upstream.

The dominant land uses of the Watershed are wilderness, grazing, vineyards, row-crops, military reservations, agricultural industries, and urban and residential land. Wilderness and woody vegetation persists mainly in the steep mountains to the west and east, occupying some 41% of the study area. The foothills of these mountains are characterized by grasslands that are primarily used for cattle grazing (51%). Vineyards are rapidly developing as a major land use, occupying approximately 2% of the study area. Row-crop agriculture is a \$3 billion industry in the region, occupying most of the flat Valley floor (7% of the study area). Dense urban and industrial land use is limited to a few small cities and surrounding areas (0.3%).

E.3   Study sites and monitoring protocols

Study sites

Ninety-eight sites on numerous streams in the region were selected for the study (Fig. E.0.1, Tab. 3.1). Sixty-four of these have a past or present daily USGS flow record, and 11 also have existing USGS sediment data. These data were supplemented by field monitoring conducted during the present study at 45 sites (including 3 sites in common with USGS).
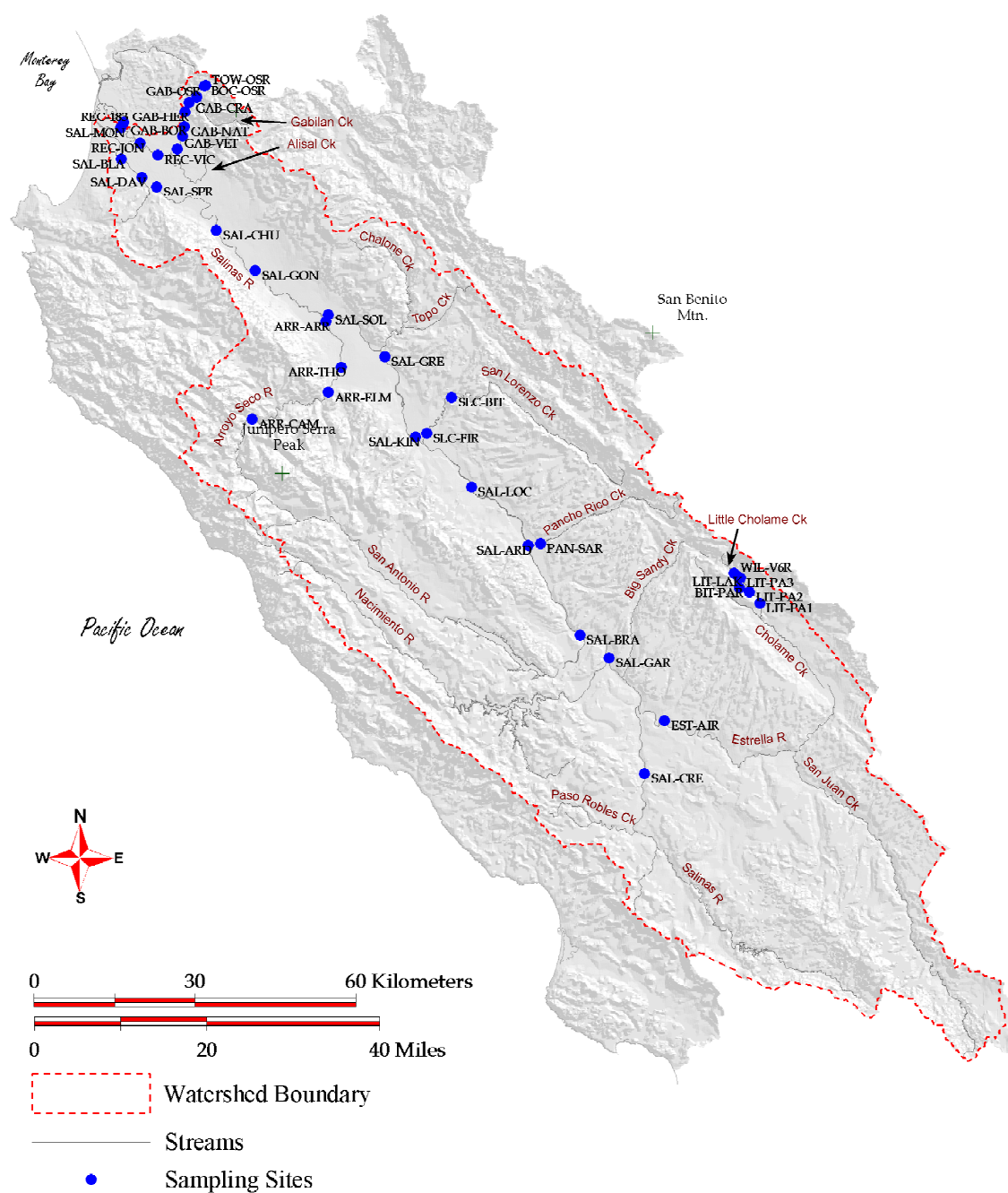
Figure E.0.1. Location of sampling sites (see Table 3.1 for details). See also Figure 7.7 for a closer view of the Gabilan Watershed area.

In addition to the stream sites, monitoring was also conducted at a number of agricultural fields on six anonymous farms.

Monitoring protocols

Monitoring protocols are described in detail in a companion report: 'Protocols for Water Quality and Stream Ecology Research' by Watson et al. (2002). In summary, monitoring teams assembled during the 2000-1 winter and were activated during each of the five major storms that season. Supplemental monitoring also occurred in the following season. A selection of the 45 stream sites and additional farm sites was targeted during each storm. The aim during each storm was to measure water discharge and sediment concentration about 5-10 times at each site, such that a total sediment load could be estimated for the event. In some cases the event-total loads formed the basis of source analyses. In other cases the data were used to construct sediment-rating curves for each site, with mean loads estimated by combining the data with regionalized flow duration statistics.

A variety of techniques were used for sampling. The most typical of which involved using current meters and suspended sediment samplers. Impellor-based current meters were used to measure flow velocity in cross-sections across a stream, with the integrated measurements forming a measurement of discharge in m^3/s. Staff plates were installed at each site, so that discharge measurements could be combined with stage measurements to form discharge-rating curves for each site. DH-48 suspended sediment samplers were used to obtain depth-integrated samples. These were analyzed using vacuum filtration to obtain suspended sediment concentration measurements in mg/L.

E.4 Hydrology

Overview

Over time, the streams of the Salinas Watershed exhibit a wide range of flow conditions. The driest times are in late fall following a dry winter. At this point, the Salinas River is generally dry, with reservoir releases being stopped in mid-Fall to allow channel maintenance access for flood control. The major tributaries are also dry except for brief stretches of perennial flow, generally in the mid-sections of these tributaries, and associated with geologic controls on

groundwater movement. The receded waters expose vast stretches of dry, sandy riverbeds in the lower elevations, ranging to cobbled step-pool sequences in the headwaters.

At the other extreme, the largest storm of a typical year generally causes all streams to flow and connect with one another. Flows from the major tributaries are violent, deep, and capable of transporting large amounts of sediment of all sizes. Upon reaching the lower gradients of the valley floor, they spread out across a wider channel – occasionally exceeding the channel and flooding adjacent agricultural land. Approximately once per decade, the Salinas River floods with flows ranging from several hundred meters to a few kilometers wide in extreme circumstances.

Groundwater in the lower Valley was formerly as shallow as a few feet, but since intense groundwater-based irrigation began in the 1920s, the water table has fallen approximately 50 feet. In the mid-Valley (i.e. near San Lucas and San Ardo), the water table is more stable, with irrigation withdrawals offset by recharge from the Salinas River during summer releases from upstream reservoirs. Future plans are to build a removable dam near the mouth, in order to allow more of the reservoir releases to reach the lower Valley and offset the groundwater overdraft in this area. In the upper Valley near Paso Robles, recent groundwater extraction has lead to more-localized overdrafts.

Flow duration

Flow duration curves were constructed for all 64 past and present USGS sites in the region. These summarize the proportion of time that streamflow exceeds a given magnitude. Seven curves were extracted as being representative of the differing flow regimes through the region (Fig. E.0.2). The dry eastern streams are represented by Cholame Creek (CHO-46), which is dry for over 90% of the time (see Figure). The wetter western streams are represented by the Arroyo Seco River (ARR-ELM), which flows 90% of the time, and has the highest upper-percentile flows in the study area for a given watershed area. The Big Sur River (BSU-BSU) is further west, out of the study area, and has perennial flow exceeding all other streams at all parts of the curve. Regulated streams are exemplified by the Nacimiento River below artificial Lake Nacimiento (NAC-BLD) which has distinct periods of relatively constant flow (benches in the flow duration curve), corresponding to irrigation releases, spillway releases, and

conservation releases. Urban streams are characterized by the Reclamation Ditch (REC-JON), which has anomalously perennial flow and some inflections in its flow duration curve that are indicative of anthropogenically regulated flow.

The progression of flow duration along a single river (e.g. the Arroyo Seco River) is one of declining flow during drier periods, and only slightly increasing flow during wetter periods. This is indicative of pronounced Valley Floor percolation of all flows for over half the time, and continuing percolation diminishing the progression of storm events during wetter periods.

Regional patterns of mean annual non-flood flow

The area under a long-term flow duration curve is the mean annual flow. Further, under the terminology used here, the area under the driest 99.5% of a flow duration curve is the mean annual *non-flood* flow. This is a useful measure for comparing mean flow across multiple sites, after normalization by watershed area. Regional patterns of mean non-flood flow are mapped in Figure E.0.3. Clear patterns are evident, indicating that the mean non-flood flow of an ungauged or partly gauged site can be reliably estimated from nearby sites on the map.

Regionalization of flow duration

The flow duration curve of most streams in the region can be classified into one of four major types: unregulated streams, regulated streams, partly regulated streams, and urban streams. After normalization by watershed area, the flow regime of a given site can be estimated as being identical to the flow regime of a geographically similar site (from Fig E.0.3) of the same class and similar watershed area. This provides a method of regionalizing (i.e. extrapolating) long-term USGS flow records to many short-term or ungauged sites in the region. The method underpins the regional sediment analysis presented below.
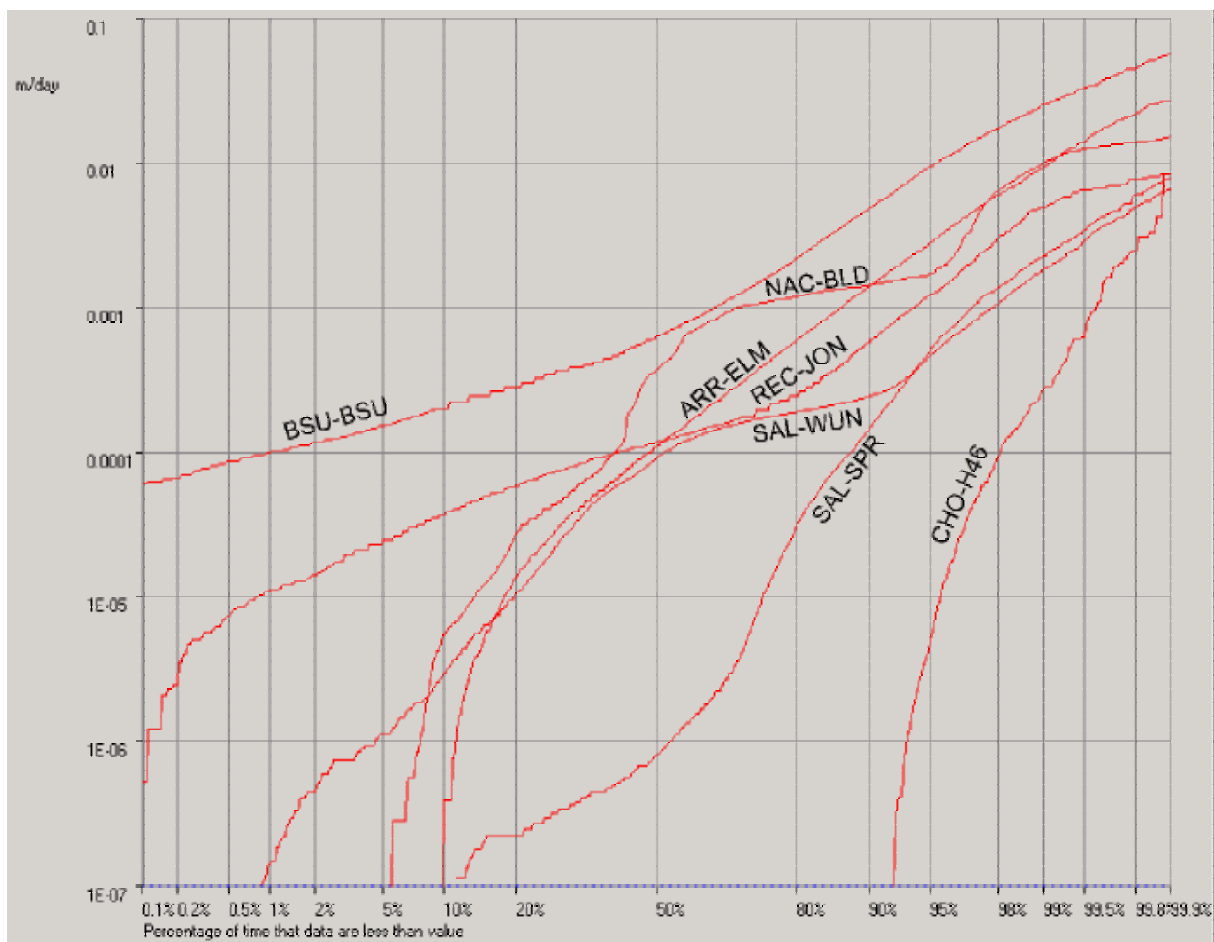
Figure E.0.2. Representative flow duration curves for the Salinas region, normalized by watershed area.
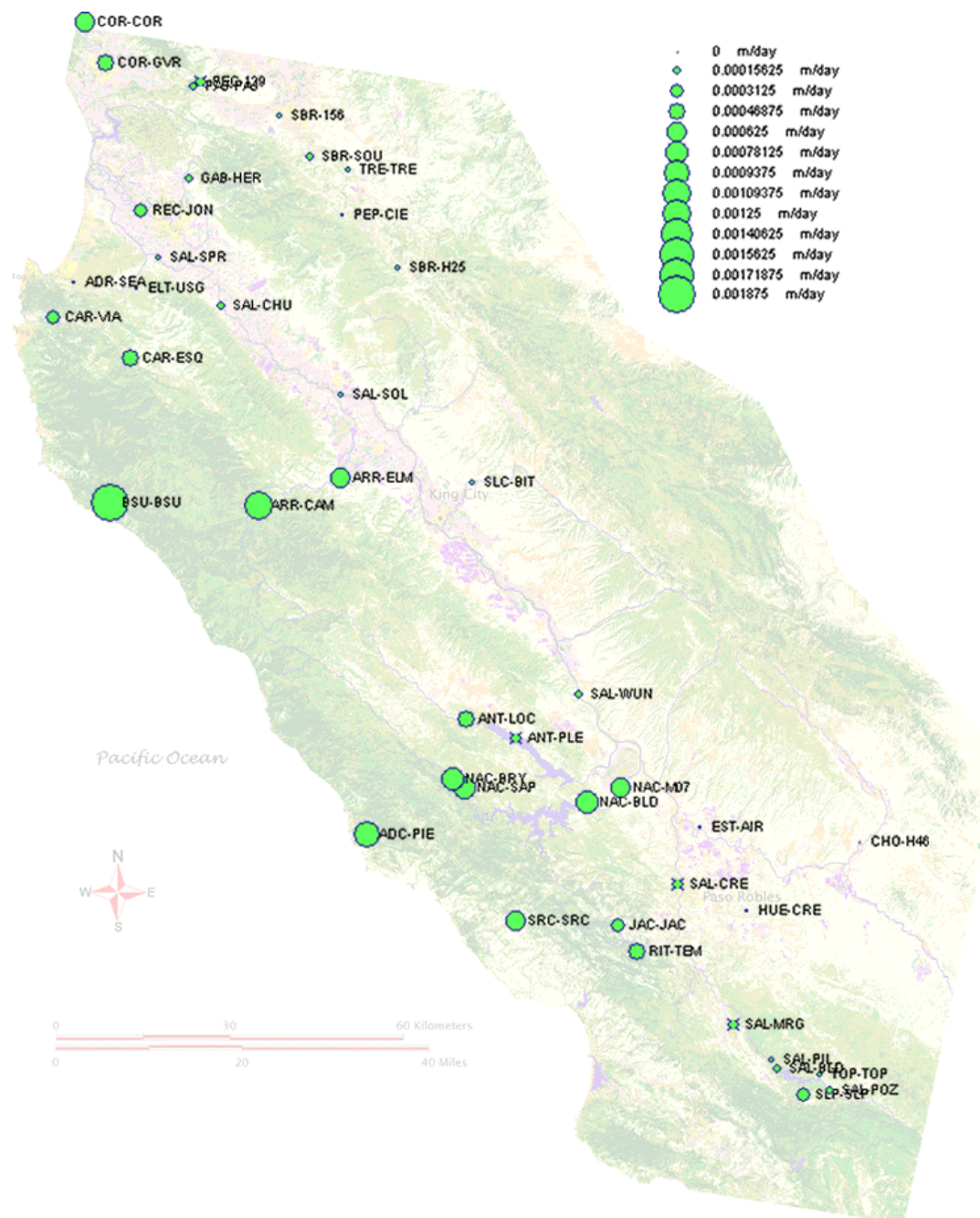
Figure E.0.3. Mean annual non-flood flow for all past and present USGS sites in the Salinas region with at least 10 years of data.

E.5   Sediment load

Mean annual load

Based on a simple analysis of USGS data at Spreckels near the mouth of the Salinas River, the mean annual suspended sediment load of the River is 1.67 million tonnes, or 1.54 million tonnes after correcting for bias in the sampling record. The mean total sediment load (including bedload) is unlikely to greatly exceed 2.0 million tonnes per year. In areal terms, the suspended yield equates to 156 tonnes/km²/yr (1.67 millions tonnes divided by 10,730 km²), which is in the middle of the range worldwide (i.e. the watershed is *not* an outlier or an anomaly world standards).

Degradation and aggradation

Novel methods were developed for estimating degradation and aggradation of streambeds at long-term USGS sites within the study area. These methods utilized the actual field measurements of discharge and flow depth made by the USGS at each site (as opposed to the automatic gauging based on water level).

Apparently due to natural processes, some mountain streams have exhibited long-term channel degradation of 6-12 inches per decade, punctuated by pronounced aggradation after major fires. Others have remained relatively stable. The sediment-starved Nacimiento River below its Dam is degrading steadily at about 6 inches per decade.

The opposite trend is evident for east Valley streams, which are aggrading at a rate of 1-2 feet per decade. Natural processes may also be active here, given the proximity to the San Andreas Fault. But active streambed gravel mining may also play a significant role in some streams.

The main stem of the Salinas River is degrading at a rate of about 1 foot per decade just below the inflow from the Dam releases, and slower some distance downstream. A more-detailed analysis at the lowest USGS site (at Spreckels) revealed a complex pattern of changes. In the long-term, there is no trend, due to the sea-level control not too far downstream. In the medium term, the lowest part of the channel aggrades during prolonged dry periods, and in the short

term, the whole channel is mobilized during intense flows. The streambed effectively liquefies during high flow, forming a sandy, mobile slurry down to 5–7 feet *below* the dry-weather streambed. There are also changes in the upper parts of the channel, where the width at which a given near-channel-full flow is transported varies according to recent flow history, and apparently also due to the emergency grading activities of adjacent landowners following the 1995 floods. The aim of this grading of course is to minimize the flow width of a given flood discharge, in order to minimize the inundation of agricultural land.

Channel sediment storage

Based on the above estimates of channel aggradation and degradation, a simple calculation indicates that the amount of mobile bed material in the main stem of the Salinas River is at least twice the mean annual load. Thus, in-channel sediment storage is a major component of the sediment budget. A slug of sediment emerging from the mountains after a large fire may take many years to be dissipated down through the channel system.

Episodicity

Most sediment transport in the region occurs on only a few days per decade. Half of the 8-year measured load at Spreckels was transported in just 6 days.

Natural causes

Natural phenomena such as fire and tectonic activity may account for a large proportion of the sediment budget of the study area. In the year following the Marble Cone Fire, an Arroyo Seco gauging site representing 2.8% of the Salinas Watershed is estimated to have delivered an additional sediment load equivalent to the mean annual load of the entire Salinas watershed. Further, streambed aggradation estimates suggest that much of this material was still being transported out of Arroyo Seco for at least 5 years afterwards. There is also evidence to suggest that high sediment loads in the eastern Salinas Watershed (at Pancho Rico Creek) may be associated with proximity to a particularly active part of the San Andreas Fault.

Spatial variability

The spatial distribution of sediment sources is highly variable. Sediment sources can vary greatly from place to place in a way that changes from year to year. The USGS station on Arroyo Seco at the campground (ARR-CAM) drains an area only 2.8% of the size of the full Salinas watershed measured at Spreckels (SAL-SPR). Yet ARR-CAM contributed 60% of the annual load measured at SAL-SPR 1972, and just 1.4% of the Spreckels load in 1974.

E.6   Regional analysis of non-flood loads

The RLDCL method

A new method of analyzing sediment data to discern regional patterns of sediment load was developed. The method, termed the Regional Load Duration Curve LOWESS (RLDCL) method, combines regionalized flow duration curves (see above) with sediment rating curves to produce load duration curves – i.e. curves indicating the duration of time for which specific sediment loads are exceeded at a site.   The area under these curves is an estimate of the mean annual suspended sediment load for the site. The area under the 99.5 percentile is here termed the mean annual 'non-flood' suspended sediment load. The term 'LOWESS' refers to an objective smoothing method used to develop sediment-rating curves for sites with very large data sets of non-uniformly distributed suspended sediment data.

The method is incremental – estimates can easily be improved by the addition of new monitoring data. It is well suited to situations where long-term flow data are available from many sites, but sediment concentration data are generally only available for short, sporadic monitoring records.

Results

The resulting estimates of mean annual non-flood suspended sediment load for selected sites in the study area are shown in Table 0.1 and Figure 0.4. The regional average non-flood load, taken at Spreckels is 64 t/km^2/yr. Adding in the estimated 'flood' load increases this value to 246 t/km^2/yr, which is in the same order of magnitude as the 8 year average of daily loads calculated earlier (156 t/km^2/yr). Assuming 100% trapping efficiency in large dams, the regional average non-flood load per unit of contributing land area is 78 t/km^2/yr. The

effect of changing conditions over time (e.g. pre- and post-dam) is not considered.

Site code	Watershed area (km2)	Regional flow duration curve used	USGS-LOWESS or CCoWS-manual sediment rating curve used	Dates of suspended sediment measure-ments	Number of suspended sediment measurements	Estimated 99.5 percentile flow (Q99.5%) (ML/day)	Estimated mean annual non-flood flow (Qave99.5%) (mm/yr)	Estimated 99.5 percentile suspended sediment load (L99.5%) (t/km2/day)	Estimated mean annual non-flood suspended sediment load (Lave99.5%) (t/km2/yr)	Annual estimate for fraction of watershed area below large dams (t/km2/yr)
ANT-LOC	562.0	ANT-LOC	USGS-LOWESS	1965-1974	3011	7006.1	143.9	27.6	76.30	
ANT-PLE	717.4	ANT-PLE	USGS-LOWESS	1961-1965	213	4924.0	76.5	12.6	31.60	
ANT-SAM	528.4	ANT-LOC	USGS-LOWESS	1961-1965	731	6586.4	143.9	34.1	81.21	
ARR-ARR	780.6	ARR-ELM	CCoWS	2000-2002	18	11034.5	201.3	25.6	76.60	
ARR-CAM	285.8	ARR-CAM	USGS-LOWESS	1962-1984+	6877	8849.9	472.1	12.5	27.42	
ARR-ELM	622.7	ARR-ELM	CCoWS	2000-2001	19	8802.7	201.3	1.6	7.29	
BIT-PAR	5.4	CHT-RWY	CCoWS	2001-2001	3	1.4	1.4	0.1	0.10	
LIT-LAK	18.1	CHT-RWY	CCoWS	2001-2001	5	4.9	1.4	0.2	0.27	
LIT-PA2	44.8	CHT-RWY	CCoWS	2001-2001	4	12.1	1.4	0.1	0.14	
LIT-PA3	27.8	CHT-RWY	CCoWS	2001-2001	4	7.5	1.4	0.1	0.08	
NAC-BRY	380.7	NAC-BRY	USGS-LOWESS	1960-1971	3100	11156.4	287.0	14.5	30.55	
NAC-SAP	419.6	NAC-SAP	USGS-LOWESS	1971-1974	1096	14576.2	305.9	25.3	39.74	
PAN-SAR	159.1	SLC-BIT	CCoWS	2000-2001	7	295.6	15.4	78.2	280.16	
REC-183	315.9	REC-JON	CCoWS	2001-2002	26	1016.8	52.0	25.6	88.93	
REC-JON	275.9	REC-JON	CCoWS	2000-2002	75	888.0	52.0	22.2	77.93	
RIT-TEM	47.1	RIT-TEM	USGS-LOWESS	1967-1972	1827	1024.6	183.7	23.8	51.04	
RTT-H46	7.6	RIT-TEM	USGS-LOWESS	1967-1972	1827	166.1	183.7	5.2	11.19	
SAL-BRA	6365.7	SAL-WUN	CCoWS	2000-2001	11	21752.0	55.7	0.8	3.76	4.60
SAL-CHU	10451.0	SAL-CHU	USGS-LOWESS	1966-1969+	1029	32461.2	35.6	11.9	48.79	59.73
SAL-CRE	1007.8	SAL-CRE	CCoWS	2001-2001	13	8464.9	65.0	1.4	5.85	8.21
SAL-GRE	8699.4	SAL-CHU	CCoWS	2000-2001	22	27020.6	35.6	23.2	78.77	96.43
SAL-LOC	7291.5	SAL-WUN	CCoWS	2000-2002	15	24915.6	55.7	17.9	50.16	61.41
SAL-SOL	9200.3	SAL-SOL	CCoWS	2000-2001	4	22715.2	31.4	10.9	29.50	36.11
SAL-SPR	10729.7	SAL-SPR	USGS-LOWESS	1969-1979+	3652	31387.1	25.4	21.8	63.94	78.27
SLC-BIT	606.7	SLC-BIT	CCoWS	2000-2001	7	1127.3	15.4	6.0	13.65	
WIL-V6R	16.4	CHT-RWY	CCoWS	2001-2001	3	4.4	1.4	7.4	9.59	

Table 0.1. Estimated 99.5 percentile flow, mean annual non-flood flow, 99.5 percentile suspended sediment load, and mean annual non-flood suspended sediment load for selected sites in the Salinas Watershed. These data are mapped in Figure 0.4.

[1] '+' denotes earlier USGS data that are now supplemented by CCoWS measurements.
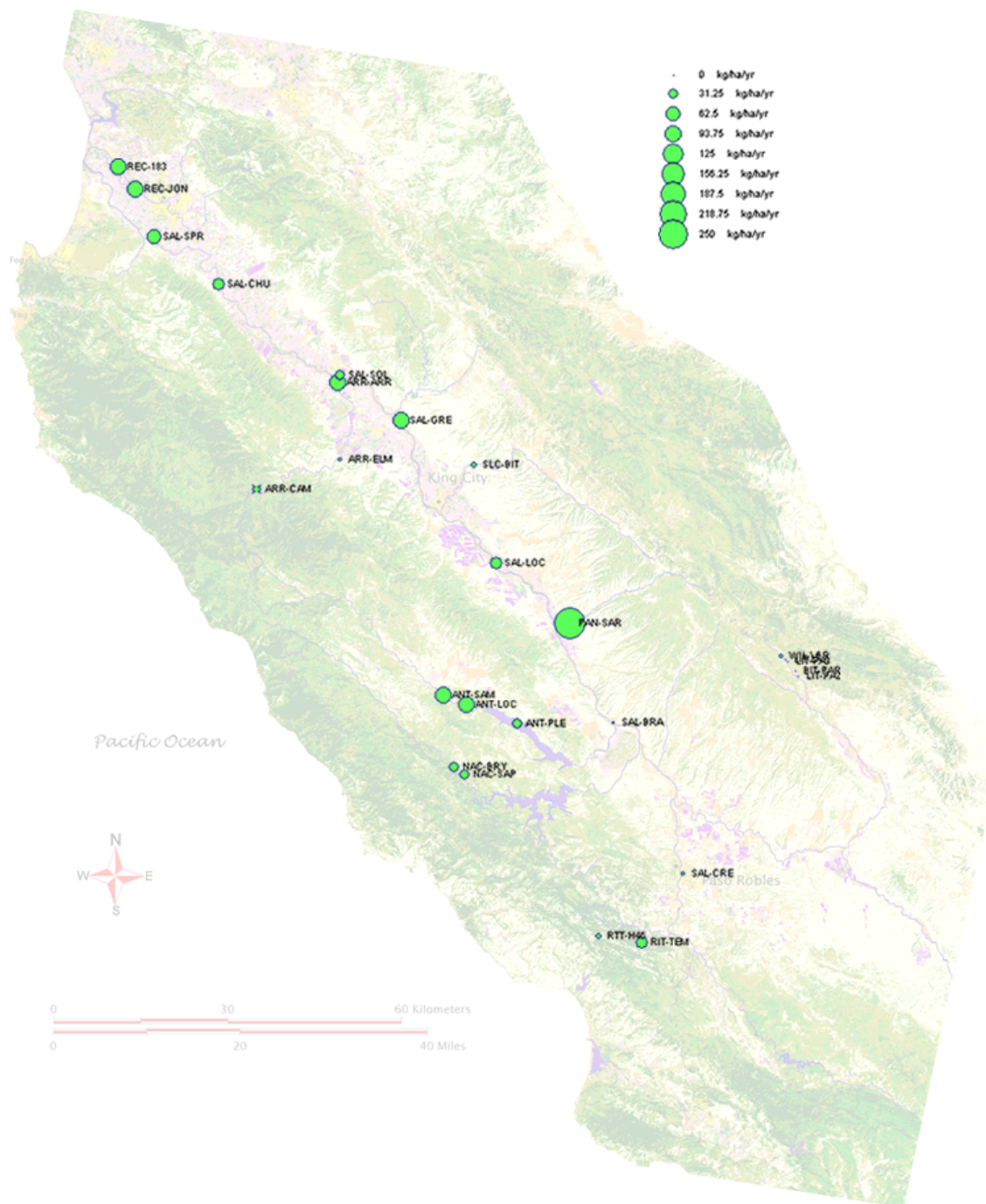
Figure 0.4. Estimated average annual non–flood suspended sediment load passing selected sites in the Salinas Watershed.

Turning to specific geographical areas within the study area, the lowest non-flood loads occur in the National Forest and the dry, eastern grazing lands. The National Forest loads exhibit low sediment yield (7.3 – 40 t/km²/yr) because, despite being the dominant source of runoff due to its mountainous climate, suspended sediment concentrations from these forested areas are very low (e.g. Nacimiento River, upper Arroyo Seco River). Loads from the dry grazing lands are also low (0.08 – 14 t/km²/yr) because they yield almost no runoff at all, except during floods (e.g. San Lorenzo Creek, Little Cholame Creek, upper Salinas River).

Higher than average non-flood loads (76 – 89 t/km²/yr) are observed in foothill areas, where rain falls each year, and there is some form of significant land use apart from National Forest or other reserves (e.g. lower Arroyo Seco River, San Antonio River, Reclamation Ditch). These areas include vineyards, military training, row-crop agriculture, and dense urban land use.

The highest loads (280 t/km²/yr) were estimated for Pancho Rico creek, a remote watershed with mainly grazing and dry-agricultural uses. Near its headwaters, this creek intersects the San Andreas Fault zone, displaying spectacular cliffed banks hundreds of feet high. The present study measured very high suspended-sediment concentrations (SSC) at this site during early 2001. The resulting uniquely high loads may be due to sampling coincidence, the natural influence of tectonic activity, a general property of the land use in the watershed, or a distinct event such as fire or earthquake. Further investigation is warranted.

On the main stem of the Salinas River itself, the uppermost reaches exhibit low estimated non-flood sediment yield (5.9 t/km²/yr, scaling to 8.2 t/km²/yr if area upstream of Salinas Dam is excluded). This is to be expected from the relatively low-intensity land-uses of this dry part of the study area. Downstream at Bradley, below the reservoir inflows, the estimated yield is also low, at 3.8 t/km²/yr (scaling to 4.6 t/km²/yr excluding land upstream of reservoirs). Any hypothesized influence of high sediment yields associated with recent intense residential and viticultural development in the Paso Robles area is not reflected in these data.

Below Bradley, the estimated mean annual non-flood loads increase significantly. At San Lucas, the load is 50-61 t/km²/yr, which may be due to the Pancho Rico Creek anomaly, nearby vineyard development, channel degradation and bank erosion, or sampling bias. Further downstream at Greenfield the estimated mean annual non-flood load increases to 79-96 t/km²/yr, again due either to nearby vineyards and row-crop agriculture, channel changes, or sampling bias. Channel degradation may be a significant factor, accounting for about 20-40 t/km²/yr for each of these two reaches (assuming 36 km & 34 km reach lengths, 100 m active channel width, 0.03 m/yr degradation, 2 t/m³ bulk density, and 6000 km² watershed area).

The estimated mean annual non-flood load at Soledad, downstream of Greenfield, is 30-36 t/km²/yr, a low figure that may be due to the addition of low-yielding watershed area including the wooded country in and around the Pinnacles National Monument. At Chualar, downstream of Soledad, the non-flood load increases again to 49-60 t/km²/yr. The channel both aggrades and degrades at this near-sea-level site depending on winter storm severity, but a slight net long-term decline of about half a foot per decade appears to be evident in the record. This amounts to 9 t/km²/yr at Chualar, and could explain much of the increase in load between Soledad and Chualar (assuming 30 km reach length, 100 m width, 0.015 m/yr degradation, 2 t/m³ bulk density, 10,000 km² watershed area).

Note that an alternative explanation for any of the changes estimated as one moves down the Salinas Watershed is uncertainty due to sparse data. For example, the mean annual non-flood load estimate at Soledad is based on just four suspended sediment samples (see Section 6.3.2 for a justification of the approach). Most other main stem sites have more data, but are still sparsely sampled at high flow, where the most information on sediment budgets is obtained. Further, the sediment-rating curves for most main stem sites are imprecisely determined. There is a great degree of scatter about any central concentration-flow relationships.

Notwithstanding the above caution, the estimated load increases again downstream at Spreckels to 64-78 t/km²/yr. Long-term channel degradation would be minimal here, due to the proximity of the ocean. Degradation of only 2 t/km²/yr is estimated for the 18 km reach, assuming degradation of 7 cm per decade. Sampling bias is unlikely, given the relatively long record at Spreckels,

and the fact that the Chualar sampling was conducted during a fairly typical flow year. Additional land use inputs are thus the most likely source of the increased loads. Loads of about 500 t/km²/yr are suggested, most likely from the intense agricultural land use in this part of the study area.

Comparison with global FAO data shows that the Salinas data do not contradict global trends in sediment load versus watershed area. Indeed, both data sets contradict (for watersheds smaller than 10,000 km²) the simplistic common statement that sediment per unit area should decrease with increasing watershed area.

Long-term spatial patterns of flood load

Figure 0.4 is representative of suspended sediment loads carried in streams 99.5% of the time, which approximately corresponds to non-flood loads (i.e. those less than channel-full, see Section 6.5). In the 19-year record on the Arroyo Seco River at Greenfield, 61% of the suspended sediment load was passed by the lowest 99.5% of flows. The corresponding figures from the 10-year record on the Salinas River at Spreckels and the 6-year record on the Nacimiento River at Bryson are 26% and 34% respectively.

'Flood' loads therefore account for about 39–74% of the total load to receiving waters in the long term. These are not explicitly accounted for by the present study, although extrapolation suggests that the overall spatial pattern of flood loads is not significantly different to the spatial pattern of non-flood loads (Fig. 6.16).

Bedload

The regional analysis focused on suspended load, and excluded bedload. Bedload is often thought to comprise only about 1–5% of total sediment load (Emmett, 1984; Renau & Dietrich, 1991). In the Salinas River, the bedload fraction has been estimated as 1% (McGrath, 1987). Local exceptions to this low rate may occur in northern parts of the study area with granitic geology, such as the northern Gabilan Range, the northwestern Santa Lucia Range (including small parts of the Arroyo Seco watershed), and the Sierra de Salinas. The bedload fraction may reach 50% in the northern Santa Lucias (Hecht 2000, citing Kondolf, 1982). Kondolf (1997) suggests that the bedload fraction is a 'few

percent' in lowland rivers to 15% in mountain streams, and ranging to 60% in some parts of the world (e.g. Israel). Tooth (2000) notes a number of studies showing bedload far greater than suspended load in ephemeral streams. A reasonable amount of bedload data exists for the Carmel Watershed (Hampson, 1997; MEI, 2002). Hampson (1997) presents data implying a 27% bedload fraction for 5 years of data on the lower Carmel. Inman & Jenkins (1999) cite studies in Southern California streams that estimate bedload as comprising between about 10% and 73% of total load, summarized as 10% for watersheds greater than 500 km^2 and 15% and higher for smaller watersheds,

E.7 Analyses specific to Valley Floor sites

The source of higher sediment loads in the lower main stem of the Salinas River was investigated through four supporting analyses:

Timing of sediment transport

A quantitative analysis of a regional rainfall event was conducted, describing the progression of a flood wave down the Salinas River, and comparing the timing of peaks in flow with the timing of peaks in sediment concentration. The highest concentrations of suspended sediment were transported past monitoring sites during and shortly after rainfall, while the highest flows occurred some days later. This is indicative of a sediment source that is closer to the monitoring sites than the principal source of flow. It is most readily explained as two independent phenomena: initially, a significant amount of sediment is discharged into the main stem from either the City of Salinas and/or agricultural areas adjacent to the River, then one to two days later, a relatively sediment-free flood wave arrives from high rainfall areas in the distant mountains. It is the timing of sediment transport that implicates local sources such as urban or agricultural areas, at concentrations that may impair beneficial uses. In-channel sources would be more likely to correlate with flow magnitude, and thus would occur later in the event.

Detailed study of Gabilan Creek

Gabilan Creek, a tributary to the Old Salinas River, flows through a range of land uses and geomorphic settings in sequence. It is thus a good place to study the event-based details of flow routing and sediment transport in a intensely

modified, non-perennial, Mediterranean watershed. Intense monitoring was conducted during the five major storms of the 2000-1 season. The total flow and load passing each of 13 bridges was quantified during each of 3-5 storm events and plotted as a longitudinal sequence down the stream (Figs 0.5 & 0.6).

Results from the longitudinal sequence are dominated by the total percolation of all flow above the Boronda Road site. In this slightly drier-than-average year, the Creek largely behaved as two separate, disconnected surface flow systems: the headwater and early agricultural floodplain section above Boronda Road, and the urban and coastal agricultural section below Boronda Road.

Gabilan Creek is perennial in its uppermost tributaries, which deliver water with low sediment concentration from generally wooded slopes to alluvial valleys at the start of the main Salinas floodplain. There is some evidence for higher sediment loads being delivered from grazed slopes with limited riparian vegetation. Percolation rates are very high above the alluvium, with associated deposition of sediment offset by increased loading from localized sources. Strawberry agriculture in this area may be a significant sediment source, given very high concentrations of sediment in the Creek, which is bordered by strawberry fields with plastic-lined channels draining directly into the stream.

Figure 0.5. The Gabilan Creek Watershed, showing the location of sites monitored during the present study.
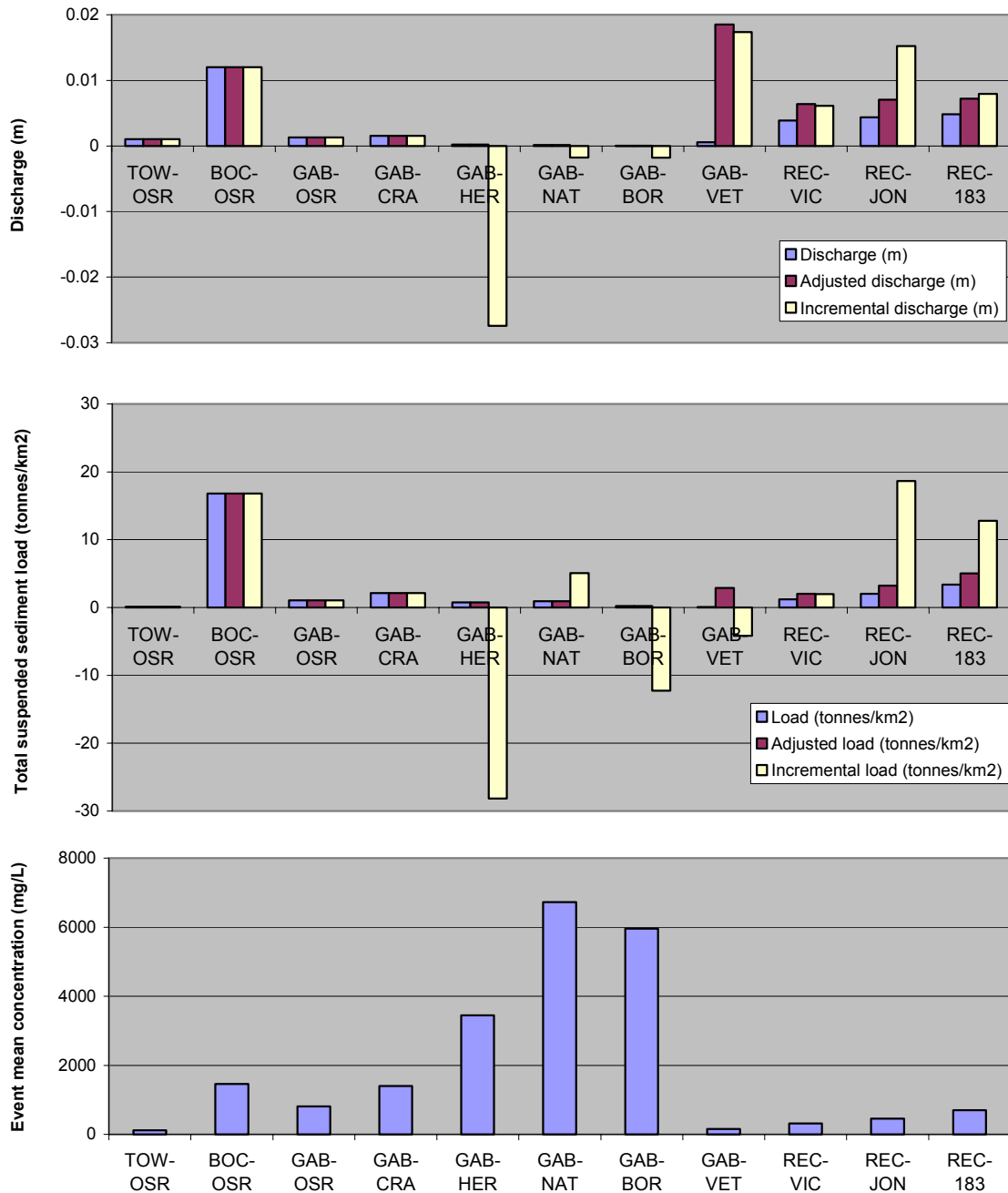
Figure 0.6. Total discharge, suspended sediment load, and event mean concentration along Gabilan Creek for three of the five storm events of the 2000–1 season. Note: 'adjusted load' is load that is specific to the watershed below the flow discontinuity at Boronda Road; 'incremental load' is specific to just the reach between the indicated site, and the next upstream site (if present).

In the lower system, perennial flow originates from urban areas at relatively low sediment concentrations. During storms, the flow per unit watershed area from urban land greatly exceeds that from any other land and so, despite the low sediment concentration, the total sediment load from urban land may be significant. Below the agricultural areas downstream of the City of Salinas however, the load per unit area increases greatly. In-channel sources are highly unlikely, due to the hardened, channelized nature of the stream at this point (known as the Reclamation Ditch) with little space for sediment storage. Calculations based on the incremental load at San Jon Road and Highway 183 suggest a local sediment yield of 337 to 722 t/km^2/yr. Both the reach above San Jon Road and the reach above Highway 183 have a mix of undulating agricultural land uses and urban storm water discharges.

The following conclusions were drawn from the Gabilan Creek study:

- Determination of watershed sediment budgets in non-perennial systems is confounded by the dominant influence of episodicity, percolation, and in-channel sediment storage, even when detailed storm-based monitoring is conducted at multiple sites simultaneously for a whole storm season. Conclusions based on monitoring data are thus limited. Decisions based on these data should be cognizant of the inherent uncertainty in the results.
- There is evidence that row-crop agricultural lands contributed the highest suspended sediment loads per unit area under the conditions experienced in 2000-1, although significant urban sources cannot be ruled out.
- There is good evidence that urban lands contributed the greatest volume of runoff per unit area.
- There is some evidence for significant input of coarse material (transported as bedload) from strawberry lands.
- There is some evidence that sediment load from grazing lands can be high if not mitigated by stream-bank vegetation.
- More conclusive results based on in-stream monitoring could be gained through long term (5-10 years) storm-based monitoring programs capable of sampling from large flood flows. The high cost of such programs could be partly offset by carefully thought out improvements in site selection.

On-farm monitoring

Given the frequent, but inconclusive, suggestion of high agricultural sediment loads in the previous analyses, direct on-farm monitoring was conducted in collaboration with selected farmers. This aimed to quantify a range of sediment loads that could be expected to be delivered from row-crop agricultural land under various scenarios. Monitoring was conducted both during irrigation events, and during rain events. In each case, the total event load was characterized by measuring discharge and sediment concentration every 10-30 minutes during the event – typically lasting one day. The results are shown in Table 0.2, along with the wide range of parameters describing each site and each event.

Event loads varied widely, between 0 and 55 t/km², with little obvious correlation to site or event parameters (Note that these figures are *not* yet annual figures). Sloping, fallow agricultural land might be expected to yield high loads, but these appear to be able to be offset by management measures such as composting and reduction of soil-saturation using buried perforated pipe (tile-drains). On the other hand, extremely flat land can yield median event loads if sufficient water is applied. In the absence of mitigating measures, there is a general correlation between the instantaneous rate of application of water to the land, and the sediment load. This is most apparent under linear irrigation systems, which move slowly over a field, applying water at a high rate to only a portion of the field at any one time.

A very approximate scaling of the above event-based measurements to mean annual totals was attempted. This involved assumptions of a 'typical' event yielding 5 t/km², with between 5 and 20 'typical' irrigation events per year, between 5 and 15 'typical' rainfall events per year, on farm detention varying between 0% and 100%, and in-channel sediment delivery ratios of between 50% and 100%. The resulting estimate range of mean annual total sediment loads from row-crop areas was between 0 and 175 t/km²/yr.

This figure is similar to the estimated regional mean annual total sediment load (156 t/km²/yr), but somewhat lower than other estimates for agricultural areas based on the differential load between sequential sites on both the Reclamation Ditch and the main stem of the Salinas River. The discrepancy could be due to sampling bias – only a few farms could be sampled, on only a few occasions – or

it could be due to the use of conservative figures in the scaling of event totals to mean annual totals. Clarification on potential agricultural sediment sources would be obtained through exercises such as a 5-year program of monitoring all storms passing sites draining purely agricultural sub-watersheds. A 5-year program would be required to "guarantee" at least one above-average flow year. A sub-watershed-scale effort (e.g. 10 km^2) would facilitate anonymity and allow for simultaneous assessment of the effectiveness of existing sediment detention measures.

Agricultural land has the potential to deliver significant sediment loads to streams at very high mean concentrations. However, a wide range of management practices are in place that can reduce this load to zero under all but the most extreme weather conditions. The level of adoption of these practices determines where agricultural land use as a whole falls in the range of sediment producing areas. This level is unknown and should be determined in order to clarify the true state of agricultural water quality management.

Field	Date	Soil texture	Slope	Slope x surface erodibility	Crop	Crop stage	Soil state	Detention before sampling point?	Irrigation or rainfall	Area water applied to (m2)	App. rate (mm/hr)	Peak app. rate (mm/hr)	App. Duration (min)	Applied (mm)	Runoff (mm)	Runoff Coeff.	Sed. loss (tonnes /km2 /event)	EMC (mg/L)	Loss per net app. (tonnes /km2/mm)
D1	19-Feb-01	L, SL	0% - 2%	0.28%	None	Fallow	Cultivated	None	Rainfall	51230	3.8	13.3	220.00	14.0	1.49	10.7%	54.15	36,310	4.33
B3	28-Jun-00	L	~0-2%	0.28%	Red & green	Mature (last water)	Sealed	None	Linear	14731	34.35 / 5.67	34.35 / 5.67	45.37 / 275	26.0	1.36	5.2%	17.85	13,122	0.73
B2B	28-Jun-00	L	~0-2%	0.28%	Lettuce	Early (2nd water)	Sealed?	None	Linear	21535	46.6 / 4.03	46.6 / 4.03	24.19 / 280	18.8	1.62	9.4%	13.98	8,647	0.81
A2	30-Jun-00	FSL	~0-2%	0.20%	Red & green	Mature - last	Partly sealed	None	Sprinkler	13315	8.7	8.7	188.00	27.2	2.56	9.4%	7.77	3,033	0.32
C1	22-Jul-00	SiCL	0.01%-0.03%	0.01%	Cauliflower	Mid (17 days since	Cultivated		Sprinkler	28387	10.1	10.1	301.00	50.4	0.79	1.6%	7.03	8,868	0.14
B2A	22-Jun-00	L	~0-2%	0.28%	Broccoli	Early (2nd water)	Cultivated	None	Linear	15834	31.42 / 3.75	31.42 / 3.75	24.93 / 209	13.1	0.94	7.2%	5.86	6,235	0.48
D1	12-Feb-01	L, SL	0% - 2%	0.28%	None	Fallow	Cultivated	None	Rainfall - tail	51230	5.0	7.5	24.00	2.0	0.46	23.0%	5.53	12,010	3.59
D2	19-Feb-01	L, SL	0% - 5%	0.70%	None	Fallow	Cultivated	None	Rainfall	38490	3.8	13.3	220.00	14.0	0.83	5.9%	5.42	6,561	0.41
C1	02-Aug-00	SiCL	0.01%-0.03%	0.01%	Cauliflower	Mid (28 days since	Cultivated	None	Sprinkler	28387	8.4	8.4	345.00	48.4	1.51	3.1%	4.72	3,127	0.10
D1	11-Feb-01	L, SL	0% - 2%	0.28%	None	Fallow	Cultivated	None	Rainfall - tail	51230	1.6	3.0	137.00	3.8	0.35	9.2%	2.02	5,840	0.59
D2	12-Feb-01	L, SL	0% - 5%	0.70%	None	Fallow	Cultivated	None	Rainfall - tail	38490	5.0	7.5	24.00	2.0	0.20	10.2%	1.16	5,721	0.65
E3	24-Nov-01	LS	1% - 3.5%	0.23%	Brus. Spr.	Mature	Not cultivated	None	Rainfall	18723	4.7	7.2	240.00	16.0	0.10	0.6%	0.97	9,731	0.06
A1	30-Jun-00	FSL	~0-2%	0.20%	Red & green	Mature - last	Partly sealed	None	Sprinkler (artificial)	14698	8.7	8.7	188.00	27.2	2.30	8.5%	0.88	384	0.04
A2	23-May-00	FSL	~0-2%	0.20%	Leaf lettuce	2 weeks	Mostly sealed	None	Sprinkler (artificial)	31736.5	6.0	6.0	84.00	8.4	0.30	3.6%	0.77	2,541	0.09
A1	23-May-00	FSL	~0-2%	0.20%	Leaf lettuce	2 weeks	Mostly sealed	Some water and	Sprinkler (artificial)	31736.5	6.0	6.0	84.00	8.4	0.11	1.3%	0.39	3,575	0.05
F1	28-29-Nov-01	C	6.8%	0.82%	None	Fallow	Composted, Sealed	None	Rainfall	42673	1.2	2.5	251.00	5.1	0.07	1.4%	0.35	4,986	0.07
E2	24-Nov-01	LS	1% - 6%	0.35%	Brus. Spr.	Mature	Not cultivated	Wetland	Rainfall	50392	2.0	7.2	240.00	16.0	0.14	0.9%	0.30	2,091	0.02
D2	11-Feb-01	L, SL	0% - 5%	0.70%	None	Fallow	Cultivated	None	Rainfall - tail	38490	1.6	3.0	137.00	3.8	0.14	3.6%	0.28	2,084	0.08
E1	24-Nov-01	LS	1% - 6%	0.35%	Brus. Spr.	Mature	Not cultivated	None	Rainfall	50392	3.7	7.2	240.00	16.0	0.36	2.3%	0.20	544	0.01
E4	24-Nov-01	LS	1% - 6%	0.35%	Brus. Spr.	Mature	Not cultivated	None	Rainfall	75127	7.7	7.2	240.00	16.0	0.03	0.2%	0.01	390	0.00
B1	28-29-Nov-01	L	~0-2%	0.28%	None	Fallow	Cultivated	None	Linear		35.66 / 3.57	35.66 / 3.57		31.2	0.00	0.0%	0.00	0	0.00
C1	Pre-5-Jul-00	SiCL	0.01%-0.03%	0.01%	Cauliflower	Pre-transplant			Sprinkler	28387	9.0	9.0	540.00	81.0	0.00	0.0%	0.00	0	0.00
F2	28-29-Nov-01	C	8.8%	1.06%	None	Fallow	Composted, Not-sealed	None	Rainfall	4736	1.2	2.5	251.00	5.1	0.00	0.0%	0.00	0	0.00
G1	28-Dec-01	L, GSL	~2-5%	0.98%	Vines	Dormant	Light grass cover	None	Rainfall		0.2	0.8	1920.00	5.7	0.00	0.0%	0.00	0	0.00
G1	02-Jan-02	L, GSL	~2-5%	0.98%	Vines	Dormant	Light grass cover	None	Rainfall		1.3	1.5	540.00	11.3	0.00	0.0%	0.00	0	0.00

Table 0.2. Summary of runoff and sediment data for a variety of agricultural fields under discrete irrigation or rainfall events. Note that linear irrigation systems only apply water to a fraction of the irrigated area at any given instant. The paired values for application rate and duration reflect both instantaneous irrigated areas and total irrigated areas.

Comparison with RUSLE

The Revised Universal Soil Loss Equation (RUSLE) is widely used in the United States by agronomists from the Natural Resources Conservation Service for the estimation of plot scale soil loss from agricultural areas. It is a model mainly based on data from the eastern states. In order to provide an avenue for comparison of the present study's results with RUSLE methodology, some simple RUSLE estimates of mean annual soil loss were made for the field monitoring during the study.

The resulting estimates range from 124 t/km²/yr to 1243 t/km²/yr, depending mainly on farm slope. This range overlaps other estimates made during the study, confirming a general agreement between different methods of sediment yield estimation.

Summary of agricultural sediment yield estimates

Table 0.3 summarizes the different estimates of agricultural sediment yield made during the study. The discrepancies between the various methods highlight the uncertainty in the general field of long-term sediment yield estimation for specific land-uses. However, the estimates tend to indicate sediment yields for agricultural areas that are higher than the regional average, and much higher than would be expected of the same, flat land under pre-European conditions. Similar patterns are observed elsewhere, such as the Chesapeake Bay watershed, where a progression of sediment yield was estimated by Pasternack et al. (2001) from early-European (33–134 t/km²/yr), through peak agricultural and forest activity between 1820 and 1920 (401 – 1216 t/km²/yr), to post-dam and post-urban times (75 – 87 t/km²/yr).

Estimation Method	Land use	Section in this report	Event total yield (t/km²)	Mean annual non-flood suspended yield (t/km²/yr)	Mean annual suspended yield (t/km²/yr)	Mean annual total yield (t/km²/yr)	Ag. tailwater ditch conc. (mg/L)	Event mean stream conc. (mg/L)	Peak main–stem conc. (mg/L)
Monitoring record	Regional	5.1			156	~ < 250			
De–biased monitoring record	Regional	5.1			144				
RLDCL	Regional	6.6		64 – 78	246 – 300				
RLDCL	Ag. dominated	6.6.2, E.8		200 – 500	667 – 1667	883 – 2083			
Main–stem hydrograph timing	Ag. **OR** urban	7.2						? ~1,000	? ~3,500
Gabilan longitudinal sequence	Ag. dominated	7.3.5	4 – 6	337–722	~ > 500			~6,000	
On–farm measurement	Agriculture (sheet & rill)	7.4.6	0 – 55			~ ≤175	~35,000		
RUSLE	Agriculture (sheet & rill) (flat to moderate)	7.5				124 – 1243			
USLE (SCS, 1984a, b)	Row–crop (sheet & rill) (mod. to steep)	7.5				1120 – 2236			

Table 0.3. Summary of sediment–yield and SSC estimates involving row–crop agriculture in the Salinas Valley.

E.8 Synthesis

Dominant characteristics of the system

The Salinas Watershed is the largest coastal watershed in California. Its creeks and rivers are non-perennial throughout most of their length. The land is dry for most of the year, excepting the Valley Floor, which is one of the most productive areas of intensive irrigated agriculture in the nation. Occasionally, the rivers flood, inundating large tracts of productive and residential land, and delivering a significant mass of sediment and pollutants to the Monterey Bay National Marine Sanctuary.

Streambed percolation is the dominant control on the hydrology of the Salinas River and its major tributaries. The entire volume of water borne in the region's headwaters is subsumed into the bed of the large rivers during the first few storms of each season. This water becomes groundwater recharge, especially in the lower Valley, which experiences a net groundwater overdraft due to pumping for irrigation.

The mean annual in-channel suspended sediment load of the Salinas River is approximately two million tonnes per year. Adding in bedload and out-of-channel loads carried during floods, the mean annual total sediment load is unlikely to greatly exceed 2.0 millions tonnes per year. These are median figures by world standards.

The load varies greatly from year to year, and from day to day. The record includes annual loads varying from 60 tonnes to 15 million tonnes. Half of the total suspended load measured in 8 years was transported in just 6 days.

The location of significant sediment sources also varies greatly. The contribution of one of the major tributaries varied from 60% of the total suspended load to just 1.4% of the total suspended load in a 3-year span.

Some of the highest annual loads can be explained by natural causes. A single forest fire initiated the delivery of over 2 million tonnes of sediment in the first subsequent year, with continuing effects on geomorphology and sediment load lasting at least 5 years. Some of the highest loads per unit area currently

emerge from a canyon 3 km from the San Andreas Fault, and 20 km from the epicenter of a Magnitude 6.0 earthquake in 1966.

The river channels of the system store large amounts of sediment, capable of accounting for the mean annual load many times over. Downstream of releases from two large reservoirs, the main stem of the Salinas River is degrading 30 cm (1 foot) each decade over 100 m of channel width (at a location 154 km from the ocean). Closer to the ocean, the degradation rate is lower, about 15 cm per decade. The streambed material removed by the river during degradation processes accounts for a significant proportion of the mean annual suspended sediment load of the entire watershed, perhaps as much as half.

During high flow, the bed of the Salinas River effectively liquefies down to depths 5–7 feet below the normal bed elevation. After the flow recedes, most of the original bed elevation is restored within weeks, but some of the degradation persists for about a year. Conversely, prolonged drought in the main-stem can lead to the accumulation of sediment over several years as headwater storms deposit their sediment load into the dry Valley floor streambed.

Comparative analysis of sediment yield per unit area

A regional analysis of sediment sources was performed. This analysis considered all sediment load that is transported during the lowest 99.5% of flow conditions. Such periods were termed *'non-flood'* periods for the purposes of the present study, based on the fact that the 99.5 percentile flow is generally of a similar magnitude to the channel-full flow.

The regional average mean annual non-flood suspended sediment yield is about 64 t/km^2/yr – increasing to 78 t/km^2/yr if one excludes the area upstream of large dams. Wooded, natural land occupies 41% of the greater Salinas watershed (including the Salinas and Gabilan watersheds) and has a non-flood suspended sediment yield of about 7 to 81 t/km^2/yr. Grassland used primarily by cattle occupies a further 51% of the watershed, and yields lower non-flood sediment loads (0.1 – 14 t/km^2/yr) from a generally very dry climate. Vineyards occupy about 2%, with an as yet uncertain mean sediment load. Similar uncertainty surrounds the load from urban areas (0.3% of the study area). Row-crop agriculture is the most intense land use from the perspective of *potential* sediment yield, occupying about 7% of the greater watershed with much of it

remaining fallow during the winter storm season. The mean annual non-flood suspended sediment yield of row-crop agriculture is somewhat higher than the regional average yield, and may be as high as 200–500 t/km²/yr. Considerable uncertainty surrounds this estimate, which was examined using five different methods. Channel degradation below large reservoirs is a significant source of sediment, but one that is best compared with other sources in absolute terms (tonnes/yr) rather than after dividing by watershed area. This comparison is made below.

Preliminary sediment budget

The regional analysis of non-flood suspended sediment yield is considered by the authors as the best way to compare sediment sources around the region, because it makes the comparison using a methodology common to all sites and a long-term averaging period. It is, however, limited by the fact that 'non-flood' suspended sediment only comprises a portion of the total sediment yield. Therefore, an attempt is made here to compile a complete, total sediment budget for the Salinas Watershed above Spreckels, based on all the information generated during the study. This budget relies on numerous weak assumptions about the episodicity of suspended load, and the fraction of total yield that is transported as bedload. The budget it summarized in Table 0.4 and explained as follows.

Down the left hand side of the Table, the watershed area is divided into representative geographic areas, each comprising various land uses, but generally dominated by a particular land use. The western slopes of the Watershed are divided into three bands of the Santa Lucia Ranges: northern, middle, and southern. Special account is taken of sediment trapping by large reservoirs. The eastern side of the watershed is considered as a whole – the 'Eastern Ranges' comprising the Gabilan Range, portions of the Diablo Range, and the associated foothills including the far southeastern San Juan Creek area. The intense agriculture of the northern Valley Floor is treated as a separate area. Areas dominated by vineyards and urban land are not included because of lack of data. Vineyards generally fall on the geographic and geomorphic boundary between foothill grazing land and intense agricultural land. Urban loads are probably fairly high on a per area basis, but negligible compared to the remainder of the Watershed above Spreckels.

Representative geographic area	Dominant land cover	Estimated fraction of Spreckels Watershed represented (%)	Estimated land area represented (km2)	<= Q99.5% ~= 'non-flood' (t/km2/yr) Lo	Mid	Hi	Q99.5 frac.	> Q99.5% ~= 'flood' (t/km2/yr) Lo	Mid	Hi	Total suspended (t/km2/yr) Lo	Mid	Hi	Record	Unbiased	Bedload fraction	Bedload (t/km2/yr) Lo	Mid	Hi	Total sediment yield (t/km2/yr) Lo	Mid	Hi	Total sediment yield (Mt/yr) Lo	Mid	Hi	Reservoir Total sediment yield (t/km2/yr) Lo	Mid	Hi
Salinas Watershed at Spreckels	All	100.0%	10729.7		**64**		**30%**		**149**			**213**		156	**144**	**5%**		**11**			**224**			**2.407**				
(as above - excluding land above dams)	All	81.7%	8765.0		**78**		**30%**		**183**			**261**				**5%**		**14**			**275**			**2.407**				
Northern Santa Lucia	Wooded	12.5%	1341	7	17	**27**	30%	16	40	**63**	**23**	57	**90**	718	**163 / 84**	30%	10	24	39	33	81	129	0.045	0.109	0.172	411 / 263		433 / 278
Middle Santa Lucias	Wooded, military	17.0%	1824	**31**	56	**81**	30%	72	131	189	103	187	270			20%	26	47	**68**	129	233	338	0.236	0.426	0.616			
San Antonio & Nacimiento dam trapping (98%)	"	**15.6%**	1675																	0.212	0.383	0.554						
Middle Santa Lucias - excl. dam trappings	"	17.0%	1824	3.3	5.9	8.5	30%	8	14	20	11	20	28			20%	2	4	6	13	23	34	0.024	0.043	0.062			
Southern Santa Lucia	Wooded, grazing (coastal)	17.0%	1824	**11**	31	**51**	30%	26	72	119	37	103	170			30%	16	44	**73**	52	148	243	0.096	0.269	0.443	**314**	**467**	**619**
Santa Margarita Dam trapping (85%)	"	**2.7%**	**290**																				0.013	0.036	0.060			
Southern Santa Lucia - excl. dam trappings	"	17.0%	1824	10	27	45	30%	22	63	104	32	90	149			30%	13	37	**61**	45	128	210	0.083	0.233	0.383			
Eastern ranges	Wooded, grazing (inland)	46.0%	4936	**0.1**	7	**14**	30%	0.2	16	33	0	24	47			20%	0.1	6	**12**	0.4	29	58	0.002	0.145	0.288			
Pancho Rico Ck	Wooded, grazing (anomaly)	**1.5%**	**159**		**280**		30%		653			933				20%		233			1167		0.000	0.186	0.000			
Valley floor	Agriculture	**6.0%**	**644**	**200**	350	**500**	30%	467	817	1167	667	1167	1667			20%	167	292	417	833	1458	2083	0.536	0.939	1.341			
Channel degradation (per unit Spreckels Watershed area)	All	**100.0%**	**10730**	9.9	12	17	30%	23	29	39.1	33	41	55.9			20%	8	10	14	**41**	**52**	**70**	**0.444**	**0.555**	**0.750**			
Sum of contributions to Spreckels																							1.133 / 47%	2.209 / 92%	2.996 / 124%			

Table 0.4. Preliminary total sediment budget for the Salinas Watershed above Spreckels.

Across the top of Table 0.4, the sediment budget is built up from several components: the suspended load passing during the lower 99.5% of flows (here referred to as the 'non-flood' load); the suspended load passing during the highest 0.5% of flows; the bedload, and the total yield. Each of these components are represented on a per-area basis, and then the total yield is also represented in absolute terms (tonnes/yr). These data are all ultimately based on the RLDCL analysis that formed the primary geographically comparative tool of the study. For methodological comparison, columns are given for the mean suspended yield based just on the period of sampling record for selected sites, and on a reconstructed record with climatic variation removed using the method of Inman & Jenkins (1999). Further methodological comparison is given in the columns at the far right, which show total yields computed using reservoir sedimentation analysis. Throughout the whole table, values in **bold** indicate primary, objective estimates. Other values involve some level of subjective judgment on the part of the authors.

Two scaling factors warrant special mention. The factor used to scale from 'non-flood' suspended load to total suspended load was fixed at 30% for all areas. In the 10-year record at Spreckels, 26% of the load was transported at flows lower than the 99.5th percentile. In the upper Arroyo Seco River, the corresponding figure is 61%, from a 19-year record. However, the Arroyo Seco figure reduces to 27% if the four fire-affected years from 1978 – 1981 are excluded. This not to say that the fire-years should be ignored, but rather to emphasize the way in which estimation of the long-term properties of the system are very difficult to estimate even from almost 19 years of daily suspended sediment measurements. For the sediment budget, a uniform figure of 30% was chosen as an estimate of the long-term regional average proportion of suspended load passed during flows lower than the 95th percentile.

The second scaling factor is the bedload fraction. This is often discussed in the literature as an uncertain value due to the difficulty of making bedload measurements in all rivers at all flows. Most authors cite a few studies and then estimate a range of bedload fractions based on these studies and their own qualitative expertise (see Section 1E.6 above). Estimates less than 5% or 10% are common, but these appear to be biased by temperate studies. The value for arid mountainous areas can be as high as 60%, declining with watershed areas above 500 km². Much of the Salinas Watershed is semi-arid, falling between temperate and arid. The local data appear to suggest a relatively high bedload fraction,

based on studies in the Carmel Watershed, and the high ratio of reservoir sedimentation rates to long-term average suspended sediment transport rates. The values used in the sediment budget thus range from 30% (for partly granitic mountainous areas) to 20% for most other tributary areas to 5% for the Salinas Watershed measured at Spreckels.

These factors lead to mean annual total sediment yield estimates made using consistent methodology (the RLDCL method) ranging between about 28 t/km^2/yr for the eastern ranges and 1400 t/km^2/yr for intensive agricultural areas. Multiplying by the estimated proportion of the Watershed represented by each representative geographic area, this leads to a range of absolute mean annual total sediment yields of 145,000 tonnes/yr for the eastern ranges to 939,000 tonnes/yr for intensive agricultural areas[1]. At this point, estimated inputs from channel degradation can be added in at about 555,000 tonnes/yr (assuming 185 km of river, 100 m wide, 0.015 m/yr mean degradation rate, 2 t/m^3 bulk density). The total of all RLDCL-based estimates of contributions to the yield at Spreckels is 2.2 million tonnes/yr, while the independent RLDCL-based estimate made using the Spreckels data themselves is 2.4 million tonnes/yr. The shortfall of the estimated inputs is 8% of the Watershed total, well within the range of errors expected for all aspects of the present methodology.

The budget is summarized graphically in Figure 0.7 showing the geographic distribution of yield-per-area, and Figure 0.8 showing the geographic distribution of yield in tonnes/yr. These figures also show the estimated breakdown of yield into bedload, 'non-flood' suspended load, and 'flood' period suspended load. The comparison between the non-flood suspended loads is that most objective and thus most reliable. Addition of the other terms increases the uncertainty considerably.

---

[1] This is equivalent to about 0.7 mm/yr or 1 inch of soil every 35 years, assuming a bulk density of 2 tonnes/m^3.
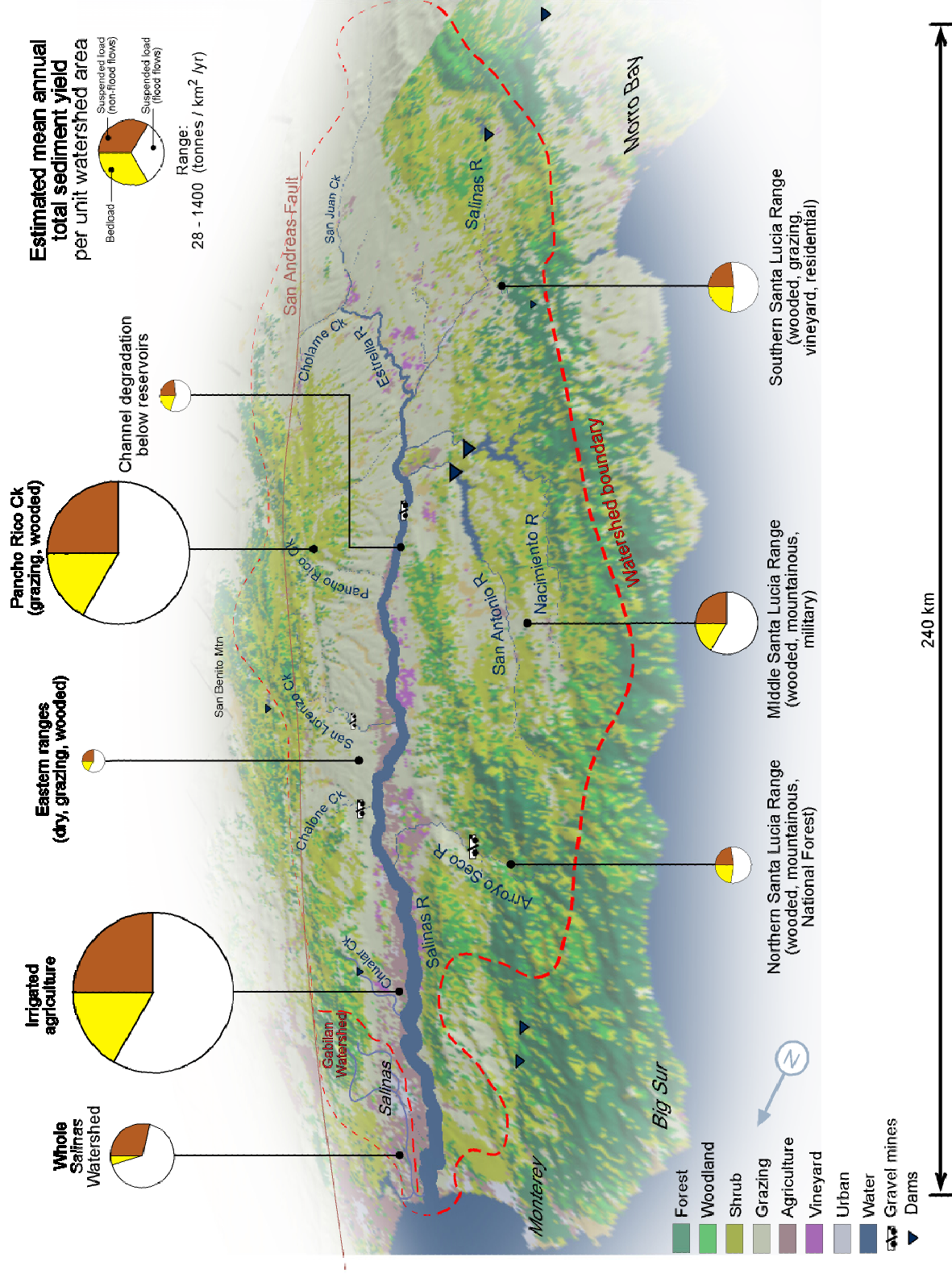
Figure 0.7. Estimated mean annual sediment yield per unit area (tonnes/km²/yr) from sections of the Salinas Watershed. Based on suspended sediment sampling in streams. The size of each pie-chart corresponds to the yield.
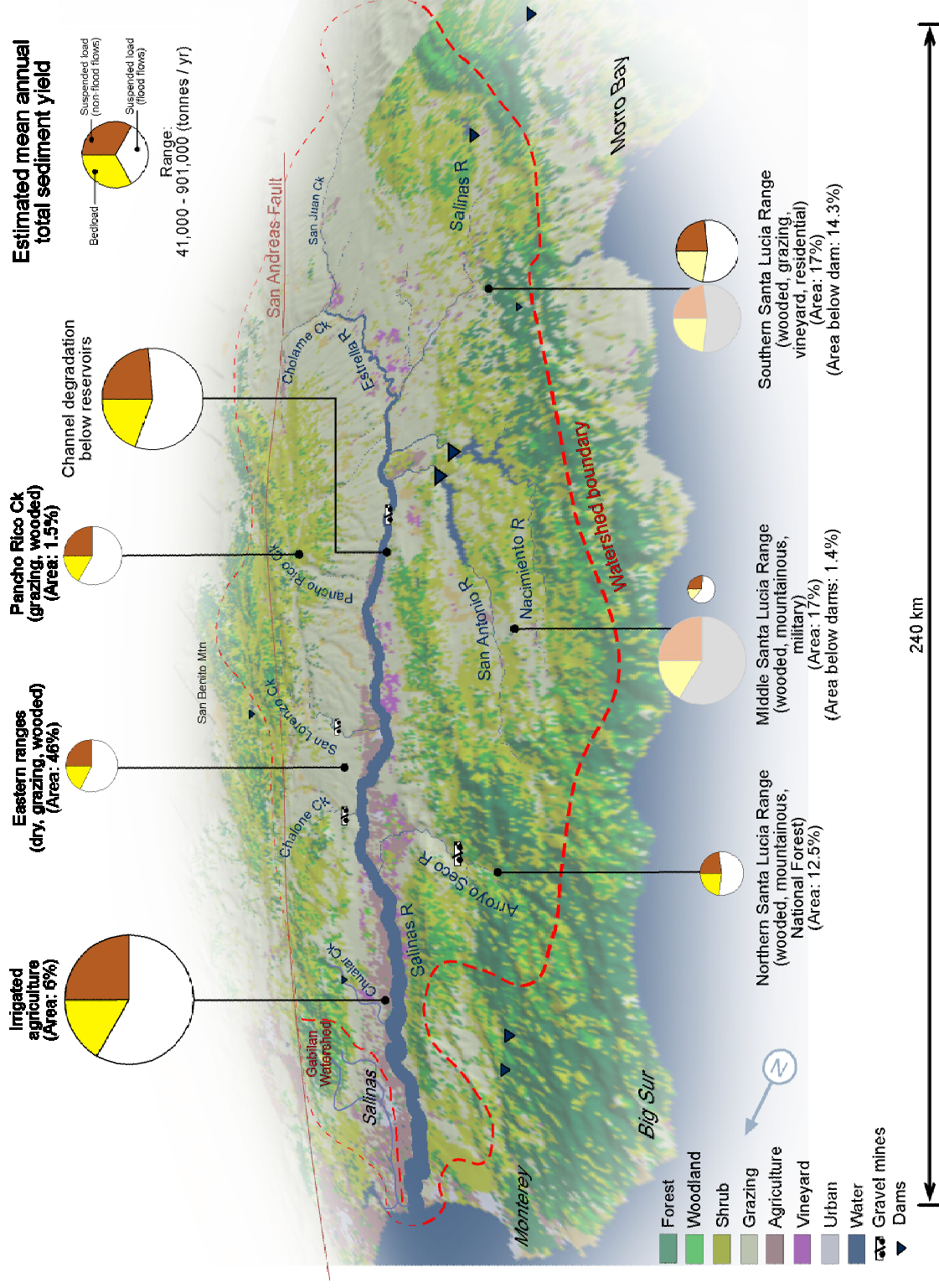
Figure 0.8. Estimated mean annual sediment yield (tonnes/yr) from sections of the Salinas Watershed. Percentage areas add to 100% of the area upstream of Spreckels. Based on suspended sediment sampling in streams. Adjustments are shown for sediment trapped behind dams. The size of each pie–chart corresponds to the yield.

Under the present preliminary sediment budget, intensive agriculture representing approximately 6% of the watershed area is estimated to be the largest contributor of suspended and total sediment load to the Salinas River at Spreckels in the long term. This is an uncertain estimate. Refinement of methods and data sets could change the ranking of the agricultural contribution. Primary estimates of the agricultural load were based on measured increases in suspended sediment load as streams pass through agricultural areas. Secondary support for the general magnitude of these estimates was given by a number of other field and model-based techniques. For example, the most direct measurements of the agricultural load, made directly on farms, suggested a much lower contribution from agriculture. The present estimates should be confirmed in future by detailed sampling from moderate-sized, purely agricultural watersheds. This has not been possible to date.

Channel degradation is estimated to be the second ranked contributor to the sediment load. Again, uncertainty prevails. The existence of long-term channel degradation was strongly suggested by an analysis of long-term channel scour at USGS gauging sites, but the estimate of its contribution to total load was based on approximations of the mean degrading channel width, the length of degrading channel, and the bulk density of channel sediment. While the large dams are almost certainly the cause of channel degradation, they are also the cause of a similar magnitude of sediment trapping in the upstream reservoirs.

The contribution of the remainder of the Salinas Watershed (approximately 94% of the area) is of approximately the same magnitude as both the agricultural and channel degradation sources. The western (Santa Lucia) ranges of the watershed are estimated to contribute a slightly larger load than the eastern ranges. However, there is evidence for very high loads from isolated eastern range localities.

There are two major caveats to be placed on these interpretations:

1. The above patterns were completely altered in the years immediately following a large fire in the Santa Lucia Ranges. Natural events like this can completely disrupt and over-ride any systematic judgment of sediment source areas.

2. The methods used in the study, while state of the art, are imperfect. There are significant differences between estimates made using various methods, which may never be fully resolved.

Decisions based on these interpretations should be cognizant of the uncertainty in the analysis, and the extreme variability of nature.

Conclusion

It is likely that the aquatic ecosystems in and downstream of the Salinas Watershed have developed in such a way as to be tolerant of massive episodic sediment loads and sedimentation, and reasonably high chronic sediment loads and sedimentation. Against this natural background, the anthropogenic sediment load *per se* probably has little adverse effect. Consideration of the quantity and effects of the load of agricultural material transported with sediment (e.g. DDT) is beyond the present scope.

A more significant role may be played by anthropogenic sources in respect of sediment concentration – as opposed to sediment load. Row-crop agriculture may be the most important cause of high suspended-sediment concentrations in the lower Salinas River. Mean concentrations of 35,000 mg/L are measured directly from fields, and are thereafter diluted to about 6,000 mg/L in small streams, and are one of two possible causes of spikes of between 1,000 and 3,500 mg/L in the main-stem of the Salinas River during the periods immediately following rain (the other possible cause being urban runoff from the City of Salinas). These concentrations exceed those that would be present in the stream in the absence of intensive land uses such as row-crop agriculture and cities.

These conclusions are based on analyses that attempted to account for sediment yield at a range of time scales. However, it is possible that anthropogenic sources would be play a relatively minor role in suitably large events (such as the 100-year flood).

Numerous measures for reducing sediment concentration and sediment load from agricultural fields are in effect in the study area. Further adoption of these measures is possible. A number of diverse groups comprised of landowners and

other stakeholders are at present developing approaches to further voluntary improvement of nonpoint source water quality in general.

E.9 Future work

The present study provides the first attempt to quantify sediment sources in the greater Salinas Watershed on a regional scale. Although a regional breakdown of sediment yields for major land uses was achieved, very considerable uncertainties remain. Some of these are unavoidable consequences of the complex, episodic processes governing erosion and sediment transport. Others may be improved through further work:

Further sampling

- Continued sediment sampling at selected existing sites during storms will improve the regional RLDCL estimates of geographically stratified sediment load
- Establishment of new sites draining moderately sized areas of a single land use will clarify the contribution of specific land uses. In particular, a number of agricultural drainage watersheds remain ungauged
- Establishment of new sites below recently established, sloping vineyards may elucidate the potential role of viticulture in the overall sediment budget
- Establishment of a program of high-temporal-resolution (e.g. hourly) sediment sampling of a site on the lower Salinas River during major storms (e.g. Davis Road) – in order to better quantify the total load to the Sanctuary, and the timing of this load
- Sampling of many more rainfall (and irrigation) events from specific row-crop fields, vineyards, and urban construction sites
- Measurement of the spatial variability of the bedload fraction of total sediment load. Lack of sufficient bedload measurements is a long-recognized weakness in understanding the Salinas sediment budget (see McGrath, 1987).

Further analyses and new techniques

- Better quantification of the amount of sediment unaccounted for by flows above standard quantiles, such as the 99.5[th] percentile.

- Sensitivity analysis of the dependence of estimates of long-term sediment yield on:
  - Sampling bias in the sparse CCoWS data
  - Sampling bias in the daily USGS data
  - Negative bias in the fitting of power functions to sediment-discharge data
  - Standardization of the regional analysis at the 99.5th percentile
  - Uncertainty in the bedload fraction
- A spatial simulation model of erosion and sediment transport. Although the appropriate expertise exists (Watson & Rahman, 2002; Watson & Vertessy, 2002; Watson et al., 2001a, b), it was decided at the outset of the present study that insufficient data and process understanding existed that could warrant an honest modeling study. At the conclusion of the study, it is felt that much of the complexity in the data that now exist could be simplified by using the data to constrain an appropriate erosion and transport model.

Refinement of scope

In the broader context of water quality management, some of the most important avenues of further work are:

- Field study and socio-economic valuation of the specific beneficial uses of the water bodies of the region
- Targeted study of specific instances where these beneficial uses may be being adversely impacted by sediment and pollutants – e.g. study of the effects of high sediment concentration on fish life cycles in the greater Salinas Watershed
- Alignment of studies by beneficial use rather than by pollutant – i.e. "Sources and effects of water quality on Species X" rather than "Sources of Pollutant X".

1   Introduction

1.1   Background – TMDLs

The principal instrument of non point–source pollution reform in the United States is the Clean Water Act (1972, amended 1977). This Act mandates that all impaired water bodies in the United States be listed, and that a plan should be set in place to deal with the impairment. The list is known as the 303d list, and the plans are known as Total Maximum Daily Load (TMDL) plans. Each TMDL should address the respective impairment by managing the load of the pollutant causing the impairment.

In California, TMDLs take the form of documents issued by the EPA, resulting from studies and investigations lead by Regional Water Quality Control Boards and their subcontractors. Each TMDL document must contain statements defining the following elements (EPA, 1999):

- problem identification (with reference to defined beneficial uses of the water body)
- identification of water quality and target values
- source assessment
- linkage between water quality targets and sources
- allocations (of overall pollutant loading capacity to sources)
- follow–up monitoring and evaluation plan

The Salinas River in the Central Coast of California is listed as being impaired due to[2]:

- Sedimentation/siltation
- Salinity/TDS/Chlorides
- Pesticides
- Nutrients

As shown in Figure E.1.1, 'sedimentation/siltation' is by far the most common 'pollutant/stressor' listed on the 1998 Californian 303d list.

---

[2] http://www.swrcb.ca.gov/tmdl/docs/303dtmdl_98reg3.pdf
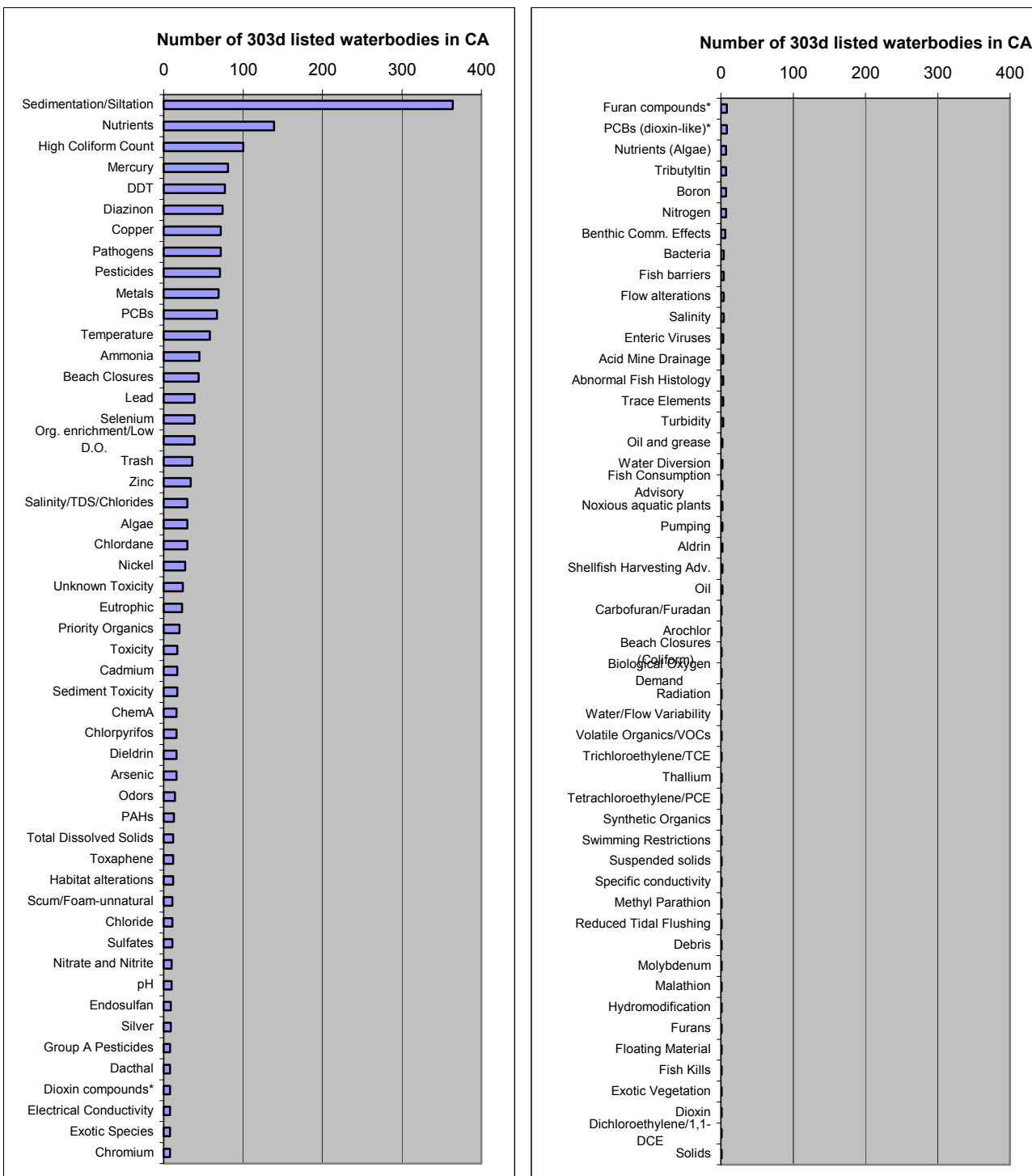
Figure E.1.1. Pollutants listed on the 1998 Californian 303d list, ranked by number of waterbodies listed as being impaired due to each pollutant. Source data: http://www.swrcb.ca.gov/news/nrichard/elec303d.dbf.

1.2 Importance of sediment

The precise manner in which sediment is understood to 'impair' the beneficial uses of the Salinas River or its tributaries is yet to be fully described. Indeed the problem of poor definition of the importance of sediment is widespread in the growing field of TMDL development (Moore et al., 2001; see also NRC, 2001). Sediment is both a natural hindrance and a natural requirement of many of the Salinas system's beneficial uses.

Sedimentation is the process whereby sediment drops out of the water column and accumulates on the bottom of a waterbody. This is a natural process that dominates the morphology of the Salinas River. It is a necessary component of the dynamic geomorphic equilibrium that is the ultimate goal of all environmentally sensitive river management. Given this background, excessive sedimentation is possible. In the lower Salinas River (i.e. the section that is listed), it is possible that excessive sedimentation has lead to infilling of deeper parts of the river and the Salinas Lagoon at a higher rate than that which is normally offset by periodic scouring. However, at the outset, it is thought that this possibility is relatively unlikely and almost undetectable when compared with other, much more obvious stressors such as reduction of streamflow, and inputs of anthropogenic chemicals.

We thus take a broader view of all that is implied by the EPA's usage of the terms 'sedimentation/siltation'. Our study is of sediment in general, allowing for the possibility that its impacts may be manifested through suspended sediment *concentration* and sediment *loads* delivered to receiving waters as well as sedimentation *per se*. We also acknowledge that perhaps the only way to characterize the adverse impacts of sediment in a naturally sediment-dominated system like the Salinas, is to measure that proportion of sediment concentration or load that is due to anthropogenic sources.

Anthropogenic sediment loads in excess of natural loads are assumed to be a hindrance, in the absence of any specific knowledge to the contrary. An aim of the present study is to attempt to delineate anthropogenic versus natural sediment sources, and in doing so, characterize the extent to which there may

be a sediment problem in the watershed. This is intended to provoke further study to determine the specific manifestations of such a problem.

1.2.1   Potential sediment problems

Examples where anthropogenic sediment may adversely impact beneficial uses include:

- High *concentrations* of suspended sediment in the water column may impact the life cycles of fish and other aquatic organisms, through mechanisms such as gill abrasion and reduced visibility for migration and other behaviors (Newcombe & Jensen, 1996). Of particular interest are the potential impacts to migrating South Central–Coast steelhead (*Onchorhynchus mykiss irideus*), which are Federally list as a threatened Evolutionary Significant Unit (ESU).

- High *loads* of sediment may lead to benthic accumulation both in streams and the ocean. Fine sediment accumulation in otherwise coarse-bedded streams can impact fish spawning and hatching. Sediment accumulation in lagoons and other coastal waters may smother habitat and decrease the habitat volume for organisms that use these waters. Oceanographic measurements at 1 km depth have suggested that under certain conditions the Salinas River and its entrained material flow beyond the coastline down to the depths of 3 km or more in the Monterey Canyon (Farnsworth, 2000; Johnson et al., 2001). This is achieved by way of hyperpycnal flows, whose density due to entrained sediment is greater than cold, ocean-floor seawater.

Different types of sediment problems may occur in different parts of the watershed, ranging from the riffle-pool sequences of headwater streams, through to the larger, sandy migration paths of the main stem, to the rearing habitat of the Salinas Lagoon, and to nearby marine habitats.

Sediment problems in general are typically associated with fine material (i.e. clay, silt, and sand) rather than coarse material (e.g. gravel, cobbles, and boulders).

The role of sediment as a vehicle for the transport of adsorbed anthropogenic substances such as DDT is the subject of future TMDL studies in the region targeted specifically at those substances.

1.2.2 Potential sediment benefits

Sediment is also a benefit or requirement for the proper functioning of environmental systems. The focus of one of the few previous works on Salinas River sediment (McGrath, 1987) sought sediment for beach replenishment in Monterey Bay. This study concluded that the River's sediment contributed a small amount to beach supply in the Bay, relative to larger sources from relic dunes along the coast.

Fine sediments in the slow moving waters of the region's lagoons and sloughs may provide essential substrate for organisms that process anthropogenic chemicals. At the outset however, it is unlikely that these systems are limited by sediment supply.

1.3 Purpose

The purpose of the present study was to study the sources of sediment in the Salinas Watershed, in order to provide supporting technical information for the Salinas River sediment TMDL. The work was primarily designed to be the basis of the TMDL source analysis, and was secondarily intended to assist in evaluating the extent of any sediment problems in the watershed. To these ends, the following specific aims were identified:

- quantify the mean annual sediment load of the River
- quantify the spatial and temporal variability in sediment load
- quantify the major geographic sources of sediment
- quantify the major sources of sediment with respect to specific land uses

1.4 Methodology

1.4.1 Monitoring

Prior to the study, existing sediment load data were available from early USGS monitoring programs, but recent data were sparse. Available data were generally unsuited to the purposes of the study due to the lack of focus on the major geographic provinces, and on land use relationships.

Therefore, a detailed monitoring program was undertaken. This served not only as a means of obtaining new, targeted data, but also as a means of observing the Salinas Valley system in its dynamic state, and formulating hypotheses as to its processes and functions.

Monitoring was conducted at three spatial scales, from large to small:

- Storm-based monitoring of river sediment loads at many points within the Salinas River watershed (up to 11,000 km^2)
- Storm-based monitoring of stream sediment loads at many points within the Gabilan Creek sub-watershed (up to 315 km^2)
- On-field monitoring of erosion and sediment delivery from row-crop lands and vineyards (*c.* 0.05 km^2)

In each case, the paradigm was to wait for storms and then measure sediment concentration and water discharge as frequently as possible during those storms. Chapter 3 describes the monitoring program in detail.

1.4.2 Hydrologic and geomorphic setting

The dominant hydrological and geomorphic characteristics of the system are described in Chapters 4 and 5. The hydrologic system is characterized as being largely non-perennial, and highly episodic. Many sites are dry or nearly so for most of the time, and when flowing, do so rather intensely. Thus, an analysis based on flow duration curves was adopted as the most appropriate means of describing the overall flow regime and comparing the differences between sites. The geomorphic behavior of the system is similarly episodic. Analyses are presented that quantify dramatic changes in the sandy channels typical of the region, as well as the considerable impact of natural forces such as fire, and seismic activity.

1.4.3 Regional source analysis

The primary analysis of sediment sources was at the regional scale of the whole watershed (11,000 km^2) in Chapter 6. This involved the development of a new method for inter-comparison of sediment monitoring data designed to cope with sparse data on sediment concentrations at many sites supplemented by a relatively dense arrangement of long-term USGS flow gauging sites. The method

resulted in a map of the geographic sediment sources for the watershed, and an involved interpretation of this map with respect to land use.

1.4.4 Valley floor analyses

The regional analysis highlighted row-crop agriculture and vineyards as a potentially large anthropogenic source of sediment, but was weakened by unavoidable uncertainties in the results. In Chapter 0, subsequent effort thus concentrated on these areas, in order to provide confirmation or refutation of the regional results.

Four techniques were used, the first looked more closely at the timing of sediment arriving at the bottom of the watershed, in order to indicate if the associated sources were proximate or distant. The second technique examined a longitudinal sequence of sampling sites along a single stream adjoining by varying land uses. The third technique measured sediment directly from row-crops and vineyards in cooperation with growers. The fourth technique applied more traditional modeling using the Revised Universal Soil Loss Equation (RUSLE) in order to place the work in general within the well-known context provided by RUSLE within the United States.

2   Study area

2.1   Introduction

The study area is the entire watershed of the Salinas River (*c.* 11,000 km^2) and Gabilan Creek (315 km^2), which drains into the Old Salinas River Channel via Tembladero Slough (Figs 2.1 and 2.2) (Armstrong et al., 1997). The present–day Salinas River primarily drains to the ocean at two points. The larger outlet is at the seasonal mouth of the Salinas Lagoon. The smaller outlet is through a floodgate to the side of the Lagoon, from which the River's waters flow down the Old Salinas River Channel to Moss Landing Harbor, Elkhorn Slough, and the Pacific Ocean. During summer, when the lagoon is closed to the Ocean, the Old Salinas River Channel is the only outlet.

2.2   Physiography

The Salinas Valley is oriented sub–parallel to the coast along a NNW to SSE axis. It is about 30 km wide and 250 km long. To the west, it is bounded by the Santa Lucia Range, rising to 1787 m at Junipero Serra Peak. To the east, it is bounded by the Gabilan and Diablo Ranges, rising to 1597 m at San Benito Mountain (just outside the watershed). The northern valley floor is a coastal plain about 10 km wide. In the south, the lands immediately around the River become more undulating.

Legend:
- Salinas Valley Watershed
- County boundaries

Monterey County

San Luis Obispo County

0   300   600 Kilometers

0   200   400 Miles
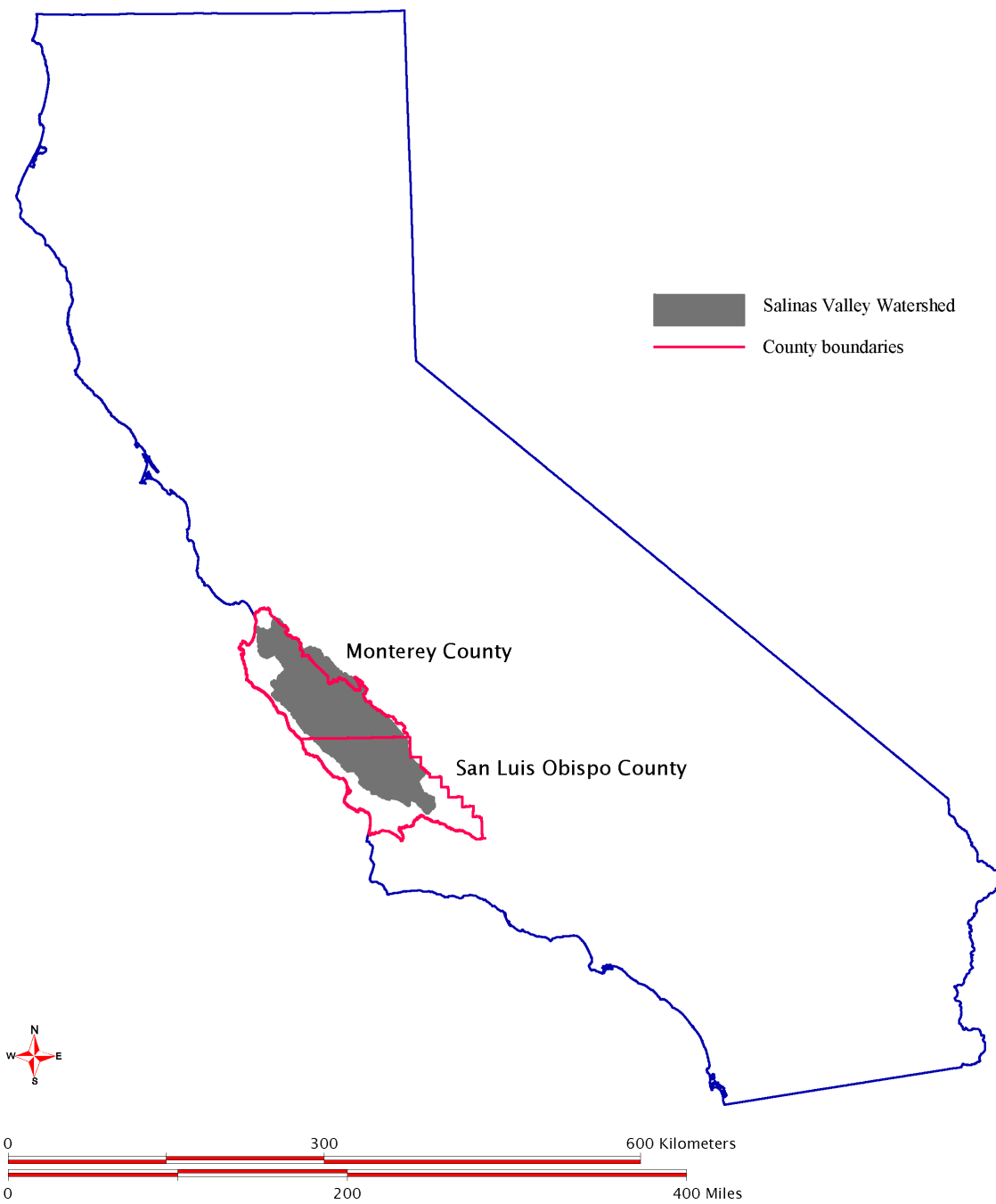
Figure 2.1. Location of the study area in California.
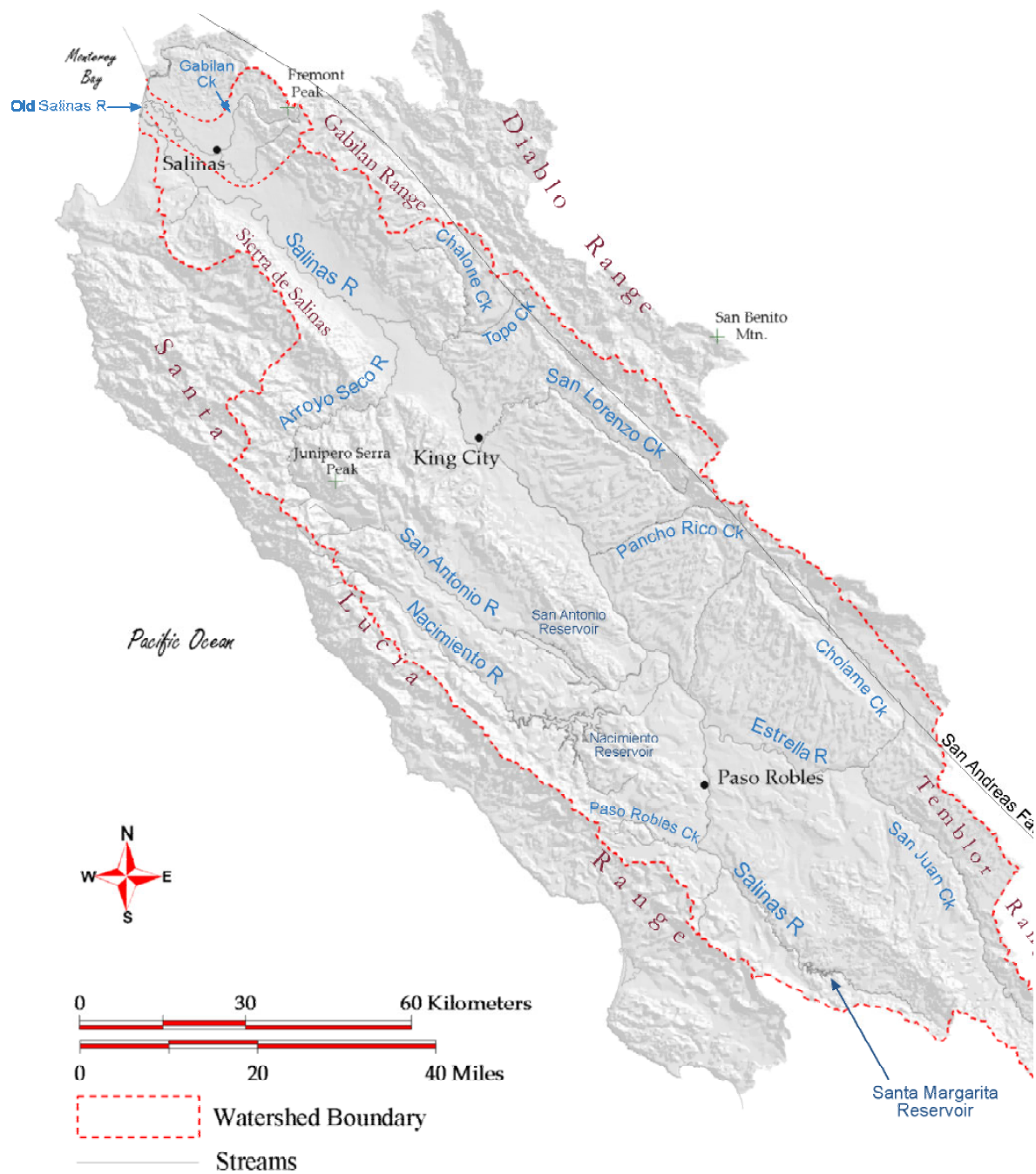
Figure 2.2 Location and physiography of the Salinas and Gabilan Watersheds on California's Central Coast.

2.3   Geology

A discussion of the geologic history of the Salinas watershed can shed light on the expected natural background sediment budget of the Salinas Valley. In general, the Salinas watershed is pinched between two great faults of the Pacific-North American plate boundary, leaving a landscape of crushed and fractured bedrock, high uplift rates and high erosion rates. The series of elevated river terraces flanking the modern Arroyo Seco River is clear evidence that tectonic uplift and rapid erosion still dominate the region. High sediment yield is a hallmark of such 'youthful' landscapes. The geologic history of the Salinas Valley watershed can be broken into two episodes that are relevant to this study: 1) pre-Quaternary geology and 2) Quaternary geology.

The Salinas Valley watershed contains a great diversity of pre-Quaternary rocks and geologic structures, testament to a complex evolution. Between 1500 m and 3000 m of sedimentary rock and unconsolidated alluvium lie perched upon granite bedrock beneath the Salinas Valley floor. The deeper strata are oil-bearing near San Ardo, and the younger strata compose the vast shallow aquifers that span the length of the Salinas Valley. The oldest bedrock in the Santa Lucia and Gabilan ranges from 10 million to over 100 million years ago. These rocks, including granitic, metamorphic and deep-marine sedimentary rocks, originated in the northwestern part of the Mojave Desert as the southern continuation of the Sierra Nevada (Mattinson and James, 1985; Kistler and Champion, 2001). The older granitic and metamorphic rocks were uplifted between 5 and 10 km, then dropped down to deep-marine conditions where they were draped by mudstone of the 10 million year old Monterey Shale. These rocks, including the Monterey Shale, were transported westward on the Garlock Fault, then northward on the San Andreas Fault. The San Andreas Fault parallels the eastern watershed boundary, and the entire Salinas watershed located west of the San Andreas Fault is continuing a northward migration at between 3 and 6 cm/yr. This ancient and modern fault activity continues to produce a broad zone of folded, fractured, and crumbled crust. As this masticated crust is uplifted to the surface, it is among the most easily eroded sediment sources in the Salinas basin; likewise it is very prone to slope failure, adding yet more natural background sediment to the Salinas River system.

The Quaternary (<2 million year) history includes further uplift of the Santa Lucia and Gabilan Ranges, down-dropping of the Salinas Valley floor, and deposition of sediments in a wide range of depositional environments. Approximately 2 million years ago the Santa Lucia Range stood higher than today (Ducea et al., 2003). A broad apron of steep alluvial fans transported sediment eroded from the range out to subsiding Salinas Valley floor. The remnants of those large fans are present between Arroyo Seco and Spreckels. The sediment derived from the uplift and denudation of the local mountains accounts for the great thickness of Quaternary sediment (>600 m; Hansen et al., 2002) underlying the Salinas Valley floor. Those sand and gravel deposits, interstratified with lenses and layers of mudstone left by sporadic rapid marine transgression events compose the Salinas Valley aquifer system. At the mouth of the valley, the sea level fluctuations of the past 2 million years produced a complex interstratification of dune, estuarine, river, and beach deposits, with the greatest transgression reaching the location of Gonzalez.

The Santa Lucia Mountains have been rapidly rising (>1 mm/ year) for the past 2 million years (Ducea et al., 2003). The combination of rugged topography, high relief, and fractured bedrock has made landslides a very important part of sediment budget of the Santa Lucia Range for at least the past 2 million years (Ducea et al., 2003; Willis et al., 2001).

2.4 Soils

Soils for the study area are mapped as part of the statewide STATSGO database, part of nationwide state-scale mapping program. The STATSGO soil parameter that is most relevant to a sediment source analysis is the K-factor for slope erodibility, designed for use within Universal Soil Loss Equation (USLE) family of models (Renard, 1997):

$$A = 2.24\,R\,K\,L\,S\,C\,P$$

where A is soil erosion from an area, R is a storm or daily erosivity index, K is a soil erodibility factor, L is a slope length factor, S is a slope steepness factor, C is factor due to land cover and management, and P is a factor due to cropping practices. This equation demonstrates that the K-factor measures just soil properties associated with the fundamental cohesiveness of the soil, with

factors due to climate, gradient, cover, and practice being incorporated into other terms.

Figure 2.3 maps the K-factor of Salinas Watershed soils. Because STATSGO records a *distribution* of soil properties for each discrete spatial map unit, some aggregation of the data were performed in order to obtain this map, as follows (M. Angelo, CCRWQCB, pers. comm.). For each map unit (polygon) there can be as many as 21 'components' or, put simply, soil types occupying a specified percentage area of the map unit. Each soil type can have up to 6 vertical layers, giving as many as 126 combinations of soil types with different layer structures for a single spatial map unit. A single K-factor (incorporating rock inclusions) for each map unit was computed as the area-weighted and thickness-weighted average of the K-factor for each soil layer (or partial layer) within 12 inches of the surface. This is the value mapped in Figure 2.3.

The most potentially erodible (i.e. high K-factor) soils are in the moderately sloped, dry, grazing-dominated county east of the Salinas River in the middle and southern parts of the watershed; and in the flat row-crop agricultural northern Valley floor alluvial plain.
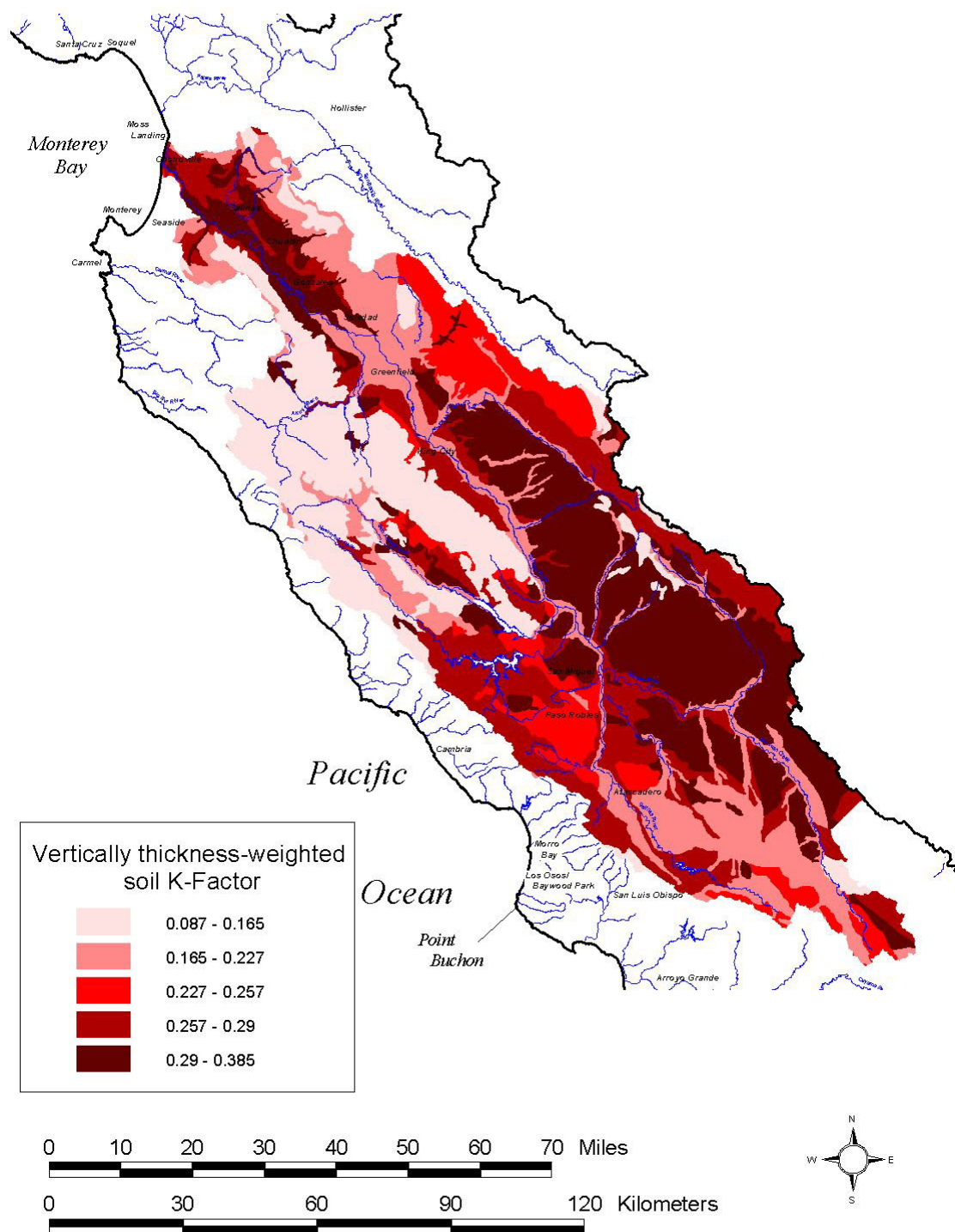
Figure 2.3. Potential soil erodibility in the Salinas Watershed, derived from the STATSGO database (GIS analysis by Mark Angelo, CCRWQCB).

It is useful to also consider a map showing the combined influence of the slope gradient (*S*) and erodibility (*K*) influences. This is shown in Figure 2.4, which was obtained by taking the depth-weighted K-factor for each soil type, multiplying by specified minimum and maximum slope values, and then weighting by soil-type area to give two erodibility-gradient (*KS*) values (minimum and maximum) for each map unit. For simplicity, the final mapped value was taken as the mean of minimum and maximum values (M. Angelo, pers. comm.).

In this map, the erosivity indicated for the row-crop lands of the northern Valley floor is much reduced, once the very flat slopes of these lands is taken into account. The southeast grazing lands remain important, with their moderate slopes. Increasing in prominence, once slope is considered, are the steep wooded mountains of the Los Padres National Forest in the Santa Lucia Mountains to the west, and of the generally BLM-owned lands of the Diablo and Gabilan ranges in middle and northern east.
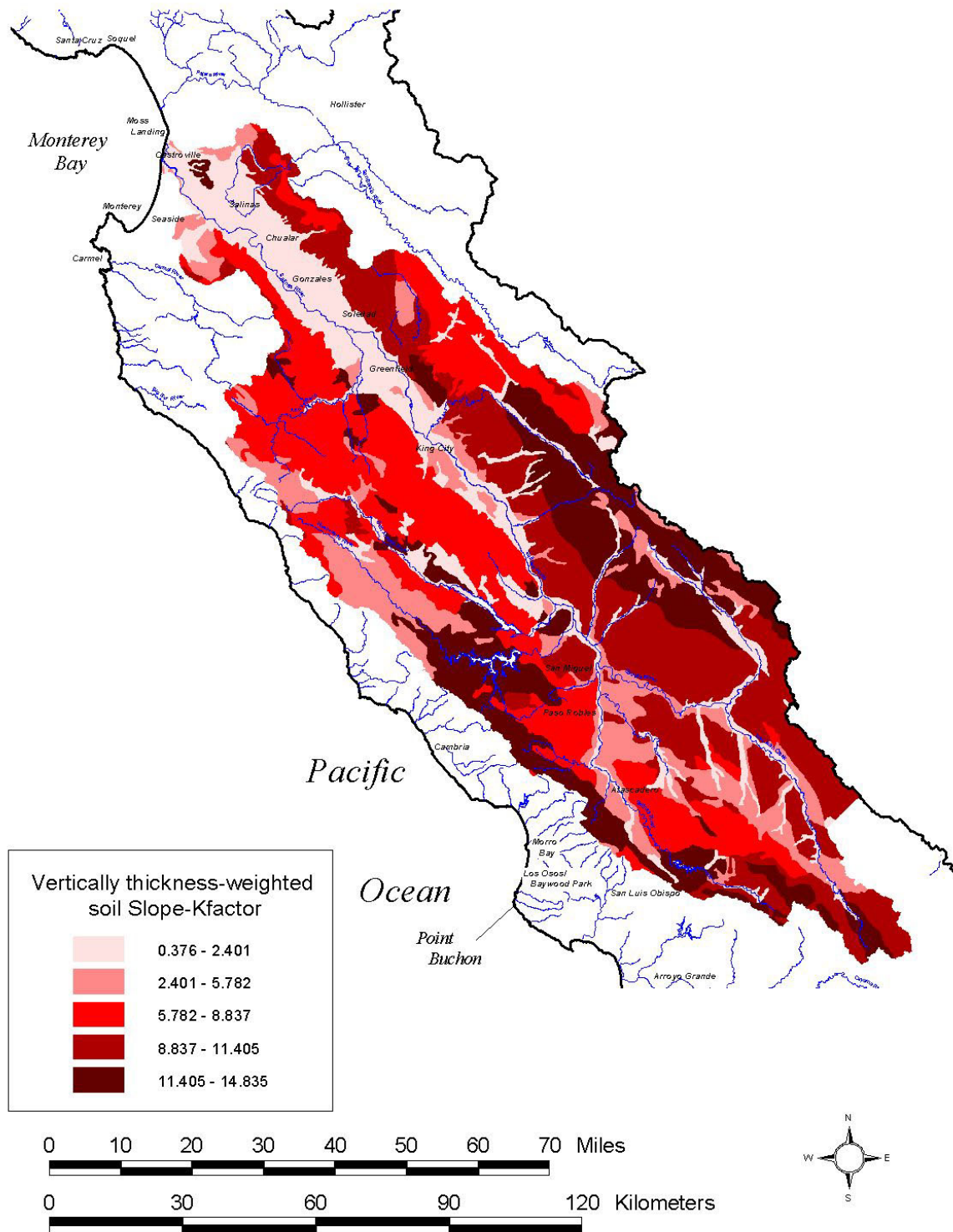
Figure 2.4. Potential soil erodibility (*K*) multiplied by slope gradient (*S*) for the Salinas Watershed (GIS analysis by Mark Angelo, CCRWQCB).

2.5 Land use and land cover

In areal terms, human use of the study area is dominated by tilled agriculture and grazing (Fig. 2.5). The flat northern valley around the City of Salinas is one of the world's most productive vegetable growing areas. In the middle and south valley around King City and Paso Robles, some of the world's largest contiguous vineyards are rapidly becoming established. Grazing and feed croplands dominate the foothills adjacent to the valley-floor. These are backed by steep scrub and forested slopes managed mainly as National Forest or Bureau of Land Management lands.

2.6 Climate

The climate of the study area is predominantly Mediterranean with long, dry summers and short, wet winters. A strong coastal influence occurs within about ten kilometers of the ocean, where fog is experienced at many times during the warmer months.

The highest rainfall occurs in the Santa Lucia Mountains to the west, with maximum mean annual precipitation reaching 1140 mm at Mining Ridge (Source: CCoWS analysis of 21.5 years of MCWRA ALERT data). In Monterey the mean annual precipitation is 475 mm. The central and southeastern portions of the study are arid, with mean annual precipitation of 292 mm at King City and 317.5 mm at Paso Robles.

The more coastal northerly sites experience a low seasonal temperature range. Mean monthly temperature at Salinas in the north ranges from 11°C to 17°C. Atascadero is a southerly, more inland site with a seasonal range of 7°C to 22°C.

The hydrology of the watershed is described in Section 4.
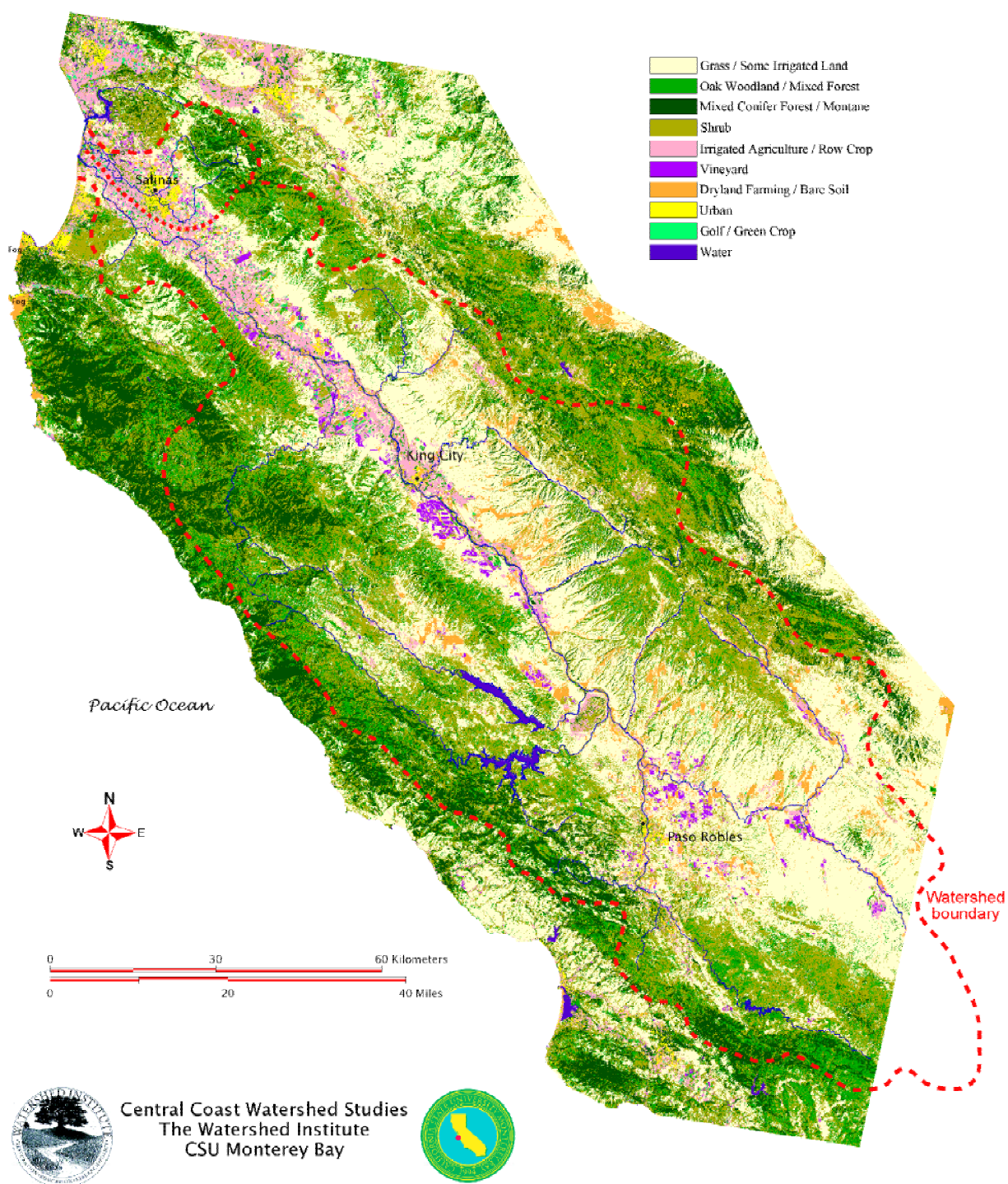
Figure 2.5. Land use and land cover within the study area: the Salinas and Gabilan Watersheds.

Figure 2.7. Overview of the lower Salinas Valley, from the Sierra de Salinas (foreground) looking north to Fremont Peak and the Gabilan Range. Photo: Fred Watson, Nov 1999.

Figure 2.7. Santa Lucia firs on the slopes of Cone Peak in the Ventana Wilderness. Photo: Fred Watson, Nov 2000.

Figure 2.9. The lower Salinas River and surrounding fallow agricultural land after heavy rains in early 2001. Photo: Wendi Newman, 11 Mar 2001.

Figure 2.9. Stream runoff flowing over row–crop agricultural field. Photo: Fred Watson, 11 Feb 2000.

Figure 2.11. New vineyards in the San Ardo region. Photo: Fred Watson.

Figure 2.11. Grape harvesting operations. Photo: Fred Watson, Oct 2001.

Figure 2.13. Dryland agriculture in the Hames Valley, on the western side of the Salinas Watershed. Photo: Fred Watson.

Figure 2.13. Dryland agriculture in the Bitterwater Valley, on the eastern side of the Salinas Watershed. Photo: Fred Watson, Summer 2000.

Figure 2.15. Gray pines among grazing slopes in the Gabilan Range above the Salinas Valley. Photo: Fred Watson, Summer 2000.

Figure 2.15. Dryland cattle ranch in the eastern Salinas Watershed. Photo: Fred Watson.

Figure 2.17. Urban construction site in the City of Salinas during winter. Photo: Fred Watson, 11 Feb 2000.

Figure 2.17. Runoff from urban construction site entering Natividad Creek in the City of Salinas. Photo: Fred Watson, 11 Feb 2000.

Figure 2.19. Streambed gravel mining (wide areas at bottom left and top right). Photo: Fred Watson, 3 Oct 2002.

Figure 2.19. Streambed gravel mining. Photo: Fred Watson, Fall 2000.

2.7 Riparian vegetation

The natural flora surrounding larger streams in the study area is dominated by a number of tree species, including willows (*Salix* spp.), cottonwood (*Populus* spp.), and oaks (*Quercus* spp.). A common native shrub is coyote brush (*Bacharis pilularis*), and willow re-growth is found in many of the dry river beds.

The invasive flora is profuse in some areas, and relatively absent in others. Formerly used for bank stabilization, the noxious giant grass *Arundo donax* has overtaken the native flora along most of the lower Salinas River (Oakins, 2001). Other non-native species include the shrub tamarisk (*Tamarisk* spp.) and numerous annual grasses such as wild oats (*Avena fatua*) and rattlesnake grass (*Briza* spp.).

2.8 Threatened and endangered and extinct species

The most prominent federally listed threatened species of the Central Coast is the steelhead trout (*Onchorhynchus mykiss irideus*). This is an anadromous fish that spawns in some tributaries of the Salinas River, migrating there from the ocean. It once existed in much greater numbers than today.

The red-legged frog (*Rana aurora draytonii*) is federally listed as a threatened species. It lives in perennial pools in sandy areas. The arroyo toad (*Bufo microscaphus californicus*) is an endangered species, often found in non-perennial streams with low gradients and sandy or gravelly beds. The Salinas Valley is the northern limit of its historic range. The species' occurrence in the Salinas watershed is now limited to the San Antonio River above Lake San Antonio[3].

Bell's vireo (*Vireo bellii pusillus*) is listed as an endangered bird species and utilizes willow-dominated riparian habitat.

Prominent species that are locally extinct in the study area include the grizzly bear (*Ursa arctos*), and Merriam's chipmunk (*Tamis merriami*).

---

[3] http://www.r5.fs.fed.us/sccs/species/arroyo-toad.htm

3 Study sites and monitoring protocols

3.1 Study sites

All sites referred to in the text are listed in Table 3.1. Of the 98 sites listed from the study area and surrounding region, 64 have a daily USGS flow record (many are no longer current), and 11 have a USGS suspended-sediment concentration (SSC) monitoring record. In addition, 45 sites were sampled for SSC during the present study by the CCoWS team, with 3 sites in common with the USGS sediment record. At 8 of the CCoWS sites, USGS flow gauging data could be used to supplement sediment measurements but at the remaining sites flow gauging was conducted by CCoWS. The CCoWS sampling sites are mapped in Figure 3.1.

Flow and sediment data from all past and present USGS sites were used. In addition to the USGS sites, the CCoWS sites were selected in order to sample the major geographic provinces of the study area, and the major land use types. The major constraint for site selection was the location of County bridges allowing safe public access for monitoring during high flows. Other selection criteria are listed in Watson et al. (2002, Sec. 3.1.1). Each site was given a two-part name, with the first part of the name describing the waterbody, and the second part describing the name of the road used to access the site, or some other identifying feature. For example, the Salinas River at Spreckels is named SAL-SPR during the present study.

Table 3.1. Selected USGS and CCoWS monitoring sites used in this study (see Figure 3.1 for map).

CCoWS site code	Waterway	Bridge/Road	NearbyLocality	USGS ID	USGS name	Watershed area	Unit	Earliest USGS daily flow	Latest USGS daily flow	Earliest USGS SSC	Latest USGS SSC	N USGS SSC	Earliest CCoWS SSC	Latest CCoWS SSC	N CCoWS SSC	Used in FDC analysis (1)	Used in LDC analysis (2)
ADC-PIE	Arroyo De La Cruz	No bridge?, Nr Piedras Blancas	Piedras Blancas	11142500	ARROYO DE LA CRUZ NR SAN SIMEON CA	106.71	km2	01-Oct-50	30-Sep-79							Yes	No
ADR-SEA	Arroyo Del Rey	Unknown bridge, At Seaside	Seaside	11143300	ARROYO DEL REY A DEL REY OAKS CA	35.74	km2	01-Oct-66	30-Sep-78							Yes	No
ALI-OSR	Alisal Ck	Old Stage Rd	Salinas	11152570	ALISAL C NR SALINAS CA	36.78	km2	01-Oct-70	30-Sep-74							Yes	Yes
ANT-LOC	San Antonio R	Interlake Rd	Lockwood	11149900	SAN ANTONIO R NR LOCKWOOD CA	562.03	km2	01-Oct-65	30-Sep-00	01-Nov-65	30-Sep-74	3011				Yes	Yes
ANT-PLE	San Antonio R	Unknown old br. nr Pleyto (submerged)	Lockwood	11150000	SAN ANTONIO R A PLEYTO CA	717.43	km2	01-Oct-29	30-Sep-65	03-Dec-61	28-Feb-65	213				Yes	Yes
ANT-SAM	San Antonio R	Sam Jones Rd	Lockwood	11149700	SAN ANTONIO R A SAM JNS BR NR LOCKWOOD CA	528.36	km2	01-Jul-58	30-Sep-65	14-Nov-61	31-Jul-65	731				Yes	Yes
ARR-ARR	Arroyo Seco R	Arroyo Seco Rd	Soledad	11152050	ARROYO SECO BL RELIZ C NR SOLEDAD CA	780.60	km2	01-Oct-94	30-Sep-00				15-Mar-00	03-Jan-02	18	Yes	Yes
ARR-CAM	Arroyo Seco R	Los Padres NF Campground	Soledad	11151870	ARROYO SECO NR GREENFIELD CA	285.75	km2	01-Oct-61	04-Feb-98	01-Oct-62	30-Sep-84	6877	27-Oct-00	26-Jan-01	7	Yes	Yes
ARR-ELM	Arroyo Seco R	Elm Rd (USGS stn) (Green br.)	Soledad	11152000	ARROYO SECO NR SOLEDAD CA	622.71	km2	01-Oct-01	30-Sep-00				24-Mar-00	05-Mar-01	19	Yes	Yes
ARR-THO	Arroyo Seco R	Thorne Rd	Soledad			718.21	km2						28-Oct-00	26-Jan-01	9	No	No
BIT-PAR	Bitterwater Cyn	Parkfield Rd	Parkfield			5.36	km2						05-Mar-01	06-Mar-01	3	No	Yes
BSU-BSU	Big Sur R	Pfeiffer Big Sur SP, Weyland Camp br.	Big Sur	11143000	BIG SUR R NR BIG SUR CA	120.43	km2	01-Apr-50	30-Sep-00							Yes	No
CAR-ESQ	Carmel R	Esquiline Rd	Carmel Valley	11143200	CARMEL R A ROBLES DEL RIO CA	499.87	km2	01-Aug-57	30-Sep-00							Yes	No
CAR-VIA	Carmel R	Via Mallorca	Carmel	11143250	CARMEL R NR CARMEL CA	640.37	km2	18-Jan-62	30-Sep-00	27-Jan-81	31-Mar-81	64				No	No
CH1-RWY	Chualar Ck Trib (S)	Railway Culvert	Chualar			4.10	~km2						14-Mar-01	31-Jan-02	11	No	Yes
CHO-H46	Cholame Ck	Hwy 46	Cholame	11147800	CHOLAME C NR SHANDON CA	587.93	km2	01-Oct-58	30-Sep-72							Yes	No
CHT-RWY	Cholame Ck Trib	Railway Bridge	Cholame	11147700	CHOLAME C TRIB NR CHOLAME CA	23.98	km2	01-Oct-58	30-Sep-65							Yes	No
CHU-CCR	Chualar Ck	Chualar Canyon Rd	Chualar			59.39	km2						14-Mar-01	14-Mar-01	1	No	No
CHU-CRR	Chualar Ck	Chualar River Rd	Chualar			81.00	~km2						14-Mar-01	17-Mar-02	11	No	No
CLR-CLR	Clear Ck	Clear Creek Rd	Idria	11154700	CLEAR C NR IDRIA CA	36.57	km2	01-Oct-93	30-Sep-00							Yes	No
COR-COR	Corralitos Ck	Unknown bridge, Nr Corralitos	Corralitos	11159150	CORRALITOS C NR CORRALITOS CA	27.45	km2	01-Oct-57	11-Oct-72							Yes	No
COR-GVR	Corralitos Ck	Green Valley Rd	Corralitos	11159200	CORRALITOS CA FREEDOM CA	72.00	km2	01-Oct-56	30-Sep-00							Yes	No
COW-198	Cow Ck	Hwy 198 ?	Priest Valley	11150800	COW C NR SAN ARDO CA	12.43	km2	01-Oct-60	30-Sep-64							Yes	No
ELT-USG	El Toro Ck	USGS stn	Spreckels	11152540	EL TORO C NR SPRECKELS CA	82.71	km2	01-Oct-61	30-Sep-00							Yes	No
EP1-ROG	Espinosa Lake inflow	Rodgers Rd	Castroville			2.02	km2						12-Nov-01	12-Nov-01	1	No	No
EST-AIR	Estrella R	Airport Rd	Paso Robles	11148500	ESTRELLA R NR ESTRELLA CA	2,387.9	km2	01-Oct-54	26-Sep-98				05-Mar-01	09-Mar-01	5	Yes	No
EST-H46	Estrella R	Hwy 46	Paso Robles	11148000	ESTRELLA R NR PASO ROBLES CA	2,038.3	km2	01-Oct-39	30-Sep-41							Yes	No
GAB-BOR	Gabilan Ck	Boronda Rd	Salinas			104.30	km2						08-Mar-00	19-Feb-01	9	No	No
GAB-CRA	Gabilan Ck	Crazy Horse Rd	Salinas			90.40	km2						17-Apr-00	19-Feb-01	48	No	No
GAB-HER	Gabilan Ck	Herbert Rd	Salinas	11152600	GABILAN C NR SALINAS CA	94.70	km2	01-Oct-70	30-Sep-00				13-Apr-00	19-Feb-01	28	Yes	No
GAB-NAT	Gabilan Ck	Natividad Rd	Natividad			98.70	km2						14-Apr-00	19-Feb-01	16	No	No
GAB-OSR	Gabilan Ck	Old Stage Rd	Salinas			41.50	km2						08-Mar-00	19-Feb-01	54	No	No
GAB-VET	Gabilan Ck	Veterans Park Bridge	Salinas			107.70	km2						17-Apr-00	19-Feb-01	23	No	No
GVC-GVR	Green Valley Ck	Green Valley Rd	Corralitos	11159400	GREEN VALLEY C NR CORRALITOS CA	18.26	km2	01-Oct-63	30-Sep-67							Yes	No
HUE-CRE	Huerhuero Ck	Creston Rd	Paso Robles	11147600	HUERHUERO C NR CRESTON CA	261.59	km2	01-Oct-58	30-Sep-72							Yes	No
JAC-JAC	Jack Ck	No Bridge?, Nr Templeton	Templeton	11147000	JACK C NR TEMPLETON CA	65.53	km2	01-Oct-49	30-Sep-78							Yes	No
LIT-LAK	Little Cholame Ck	Lake Driveway	Parkfield			18.14	km2						05-Mar-01	06-Mar-01	5	No	Yes
LIT-PA1	Little Cholame Ck	Parkfield Rd (1st above Parkfield)	Parkfield			94.64	km2						05-Mar-01	09-Mar-01	4	No	Yes
LIT-PA2	Little Cholame Ck	Parkfield Rd (2nd above Parkfield)	Parkfield			44.76	km2						05-Mar-01	09-Mar-01	4	No	Yes
LIT-PA3	Little Cholame Ck	Parkfield Rd (~3rd above Parkfield)	Parkfield			27.82	km2						05-Mar-01	09-Mar-01	4	No	Yes
MOR-HWY	Morro Ck	Hwy 1	Morro Bay	11142080	MORRO C A MORRO BAY CA	62.16	km2	01-Oct-70	30-Sep-78							Yes	No

Code	River	Crossing / Location	Place	Station No.	Station Name	Area	Unit	Start	End	Start 2	End 2	Rec	Survey Start	Survey End	n	Q1	Q2
NAC-BLD	Nacimiento R	X-ing at Perim. & River Rds (blw dam)	Camp Roberts	11149400	NACIMIENTO R BL NACIMIENTO DAM NR BRADLEY CA	852.11	km2	01-Oct-57	30-Sep-00							Yes	No
NAC-BRY	Nacimiento R	Bryson Hespiera Rd	Bryson	11148800	NACIMIENTO R NR BRYSON CA	380.73	km2	01-Oct-55	30-Sep-71	01-Nov-60	30-Sep-71	3100				Yes	Yes
NAC-HIG	Nacimiento R	Highwater Bridge	Camp Roberts	11149500		959.33	km2	01-Oct-39	30-Sep-57				07-Jun-00	08-Sep-00	1	No	No
NAC-M07	Nacimiento R	Mlle 7	Camp Roberts	11149500	NACIMIENTO R NR SAN MIGUEL CA	917.86	km2	01-Oct-39	30-Sep-57							Yes	No
NAC-SAP	Nacimiento R	No bridge, Below Sapaque Ck	Bryson	11148900	NACIMIENTO R BL SAPAQUE C NR BRYSON CA	419.58	km2	16-Sep-71	30-Sep-00	01-Oct-71	30-Sep-74	1096				Yes	Yes
NAT-LAU	Natividad Ck	Laurel Drive	Salinas			28.97	km2						17-Apr-00	17-Apr-00	1	No	No
PAJ-MAI	Pajaro R	Main St (Watsonville)	Watsonville	11159500	PAJARO R A WATSONVILLE CA	3,294.4	km2	01-Oct-11	30-Sep-73							Yes	No
PAJ-PAJ	Pajaro R	Pajaro Rd ?	Aromas	11159000	PAJARO R A CHITTENDEN CA	3,071.7	km2	01-Oct-39	30-Sep-00							Yes	No
PAJ-SAR	Pajaro R	Unknown bridge, Nr Sargent	Gilroy	11154500	PAJARO R A SARGENT CA	1,307.9	km2	01-Oct-40	30-Sep-41							Yes	No
PAN-SAR	Pancho Rico Ck	Sargents Rd	San Ardo			159.09	km2						24-Mar-00	16-Feb-01	7	No	Yes
PEC-129	Pescadero Ck	Near Hwy 129	Aromas	11158900	PESCADERO C NR CHITTENDEN CA	26.42	km2	11-Sep-70	30-Sep-81							Yes	No
PEP-CIE	Pescadero Ck	Cienaga Rd	Paincines	11156700	PESCADERO C NR PAICINES CA	99.20	km2	01-Jul-59	07-Oct-70							Yes	No
PER-PER	Perry Ck	No bridge ?, Perry Ck	Cambria	11142240	PERRY C A CAMBRIA CA	59.31	km2	21-Nov-87	11-Jul-89							Yes	No
RAT-HWY	Rat Ck	Hwy 1	Lucia	11142800	RAT C NR LUCIA CA	2.12	km2	01-Oct-60	30-Sep-63							Yes	No
REC-183	Reclamation Ditch	Hwy 183	Castroville			315.90	km2						08-Jan-01	19-Feb-01	25	No	Yes
REC-JON	Reclamation Ditch	San Jon Rd	Salinas	11152650	RECLAMATION DITCH NR SALINAS CA	275.90	km2	01-Oct-70	03-Feb-86				13-Apr-00	12-Nov-01	73	Yes	Yes
REC-VIC	Reclamation Ditch	Victor Way	Salinas			263.30	km2						26-Oct-00	19-Feb-01	31	No	No
RIT-TEM	Santa Rita Ck	Templeton Rd	Templeton	11147070	SANTA RITA C NR TEMPLETON CA	47.14	km2	01-Oct-61	30-Sep-94	01-Oct-67	30-Sep-72	1827				Yes	Yes
RTT-H46	Santa Rita Ck Trib	Unnamed old bridge?, Nr Hwy 46	Templeton	11147040	SANTA RITA C TRIB NR TEMPLETON CA	7.64	km2	01-Aug-67	30-Sep-72	01-Oct-67	30-Sep-72	1827				Yes	Yes
SAL-ARD	Salinas R	San Ardo	San Ardo			6965.8	km2						19-Apr-00	11-Nov-01	10	No	No
SAL-BLA	Salinas R	Blanco Rd	Marina			10970.6	km2						13-Mar-00	05-Mar-01	28	No	No
SAL-BLD	Salinas R	No bridge, Below Dam	Santa Margarita	11144600	SALINAS R BL SALINAS DAM NR POZO CA	290.08	km2	01-Oct-73	09-Apr-86							Yes	Yes
SAL-BRA	Salinas R	Bradley Rd	Bradley			6365.72	km2						24-Mar-00	09-Mar-01	11	No	No
SAL-CHU	Salinas R	Chualar River Rd	Chualar	11152300	SALINAS R NR CHUALAR CA	10451	km2	01-Oct-76	30-Sep-00	07-Dec-66	30-Sep-69	1029	15-Mar-00	03-Jan-02	31	Yes	Yes
SAL-CRE	Salinas R	Creston Rd	Paso Robles	11147500	SALINAS R A PASO ROBLES CA	1007.77	km2	01-Oct-42	30-Sep-00				11-Feb-01	09-Mar-01	13	Yes	Yes
SAL-DAV	Salinas R	Davis Rd	Marina			10867.4	km2						15-Mar-00	03-Jan-02	21	No	No
SAL-GAR	Salinas R	River Rd (Nr East Garrison)	Camp Roberts			4436.35	km2						10-Jan-01	16-Feb-01	6	No	No
SAL-GON	Salinas R	River Rd Gonzales Bridge	Gonzales			10276.3	km2						15-Mar-00	09-Mar-01	24	No	No
SAL-GRE	Salinas R	Greenfield	Greenfield			8699.39	km2						15-Mar-00	09-Mar-01	22	No	No
SAL-KIN	Salinas R	King City	King City			8422.62	km2						15-Mar-00	06-Mar-01	12	No	No
SAL-LOC	Salinas R	Lockwood Rd	San Lucas			7291.53	km2						24-Mar-00	03-Jan-02	15	No	No
SAL-MON	Salinas R	Del Monte Rd	Marina				km2						15-Mar-00	09-Mar-01	18	No	No
SAL-MRG	Salinas R	Unknown bridge, Nr Santa Margarita	Santa Margarita	11145500	SALINAS R NR SANTA MARGARITA CA	385.91	km2	01-Apr-22	30-Sep-49							Yes	No
SAL-PIL	Salinas R	Las Pilitas Rd	Santa Margarita	11145000	SALINAS R AB PILITAS C NR SANTA MARGARITA CA	295.26	km2	28-Jul-42	03-Oct-75							Yes	No
SAL-POZ	Salinas R	Pozo Rd	Pozo	11143500	SALINAS R NR POZO CA	182.08	km2	01-Nov-39	30-Sep-83							Yes	No
SAL-SOL	Salinas R	Hwy 101 at Soledad	Soledad	11151700	SALINAS R A SOLEDAD CA	9200.28	km2	01-Oct-68	30-Sep-00				15-Mar-00	14-Feb-01	4	Yes	Yes
SAL-SPR	Salinas R	Hwy 68	Spreckels	11152500	SALINAS R NR SPRECKELS CA	10729.7	km2	01-Oct-29	30-Sep-00	01-Oct-69	30-Sep-79	3652	15-Mar-00	07-Mar-01	10	Yes	Yes
SAL-WUN	Salinas R	Wunpost Rd	Bradley	11150500	SALINAS R NR BRADLEY CA	6544.74	km2	01-Oct-48	30-Sep-00							Yes	No
SBR-156	San Benito R	Hwy 156	Hollister	11158600	SAN BENITO R A HWY 156 NR HOLLISTER CA	1,572.1	km2	01-Oct-70	30-Sep-00							Yes	No
SBR-H25	San Benito R	Hwy 25	Hollister	11156500	SAN BENITO R NR WILLOW CREEK SCHOOL CA	644.91	km2	01-Oct-39	30-Sep-00							Yes	No
SBR-HER	San Benito R	Unnamed ? Jeep Trail, Nr Hernandez	Hernandez	11156000	SAN BENITO R BL M C NR HERNANDEZ CA	279.72	km2	01-Oct-49	30-Sep-63							Yes	No
SBR-SOU	San Benito R	Near Southside Rd	Hollister	11158500	SAN BENITO R NR HOLLISTER CA	1,517.7	km2	01-Oct-49	30-Sep-83							Yes	No
SCC-SCC	San Carpoforo Ck	Old Bridge, San Carpoforo Ck	Piedras Blancas	11142550	SAN CARPOFORO C NR SAN SIMEON CA	89.61	km2	01-Oct-77	30-Sep-78							Yes	Yes
SLC-BIT	San Lorenzo Ck	No bridge, Bitterwater Rd (USGS stn)	King City	11151300	SAN LORENZO C BL BITTERWATER NR KING CITY CA	606.70	km2	01-Oct-58	30-Sep-00				24-Mar-00	13-Feb-01	7	Yes	Yes
SLC-FIR	San Lorenzo Ck	First Street (G15, King City)	King City	11151500	SAN LORENZO C A KING CITY CA	673.98	km2	01-Oct-42	30-Sep-45				15-Mar-00	06-Mar-01	10	Yes	No
SLC-LON	San Lorenzo Ck	No bridge ?, Nr Lonoak	Lonoak	11151000	SAN LORENZO C NR KING CITY CA	543.90	km2	01-Apr-40	30-Sep-42							Yes	No
SLP-SLP	Salsipuedes Ck	Bridge unknown, Salsipuedes Ck	Pozo	11144200	SALSIPUEDES C NR POZO CA	15.31	km2	01-Oct-69	30-Sep-83							Yes	No
SRC-SRC	Santa Rosa Ck	No bridge ?, Santa Rosa Ck	Cambria	11142200	SANTA ROSA C NR CAMBRIA CA	32.37	km2	01-Aug-57	30-Sep-72							Yes	No
SSC-SSR	San Simeon Ck	San Simeon Rd	Cambria	11142300	SAN SIMEON C NR CAMBRIA CA	68.12	km2	01-Oct-87	11-Jul-89							Yes	No

SUL-SUL	Sulphur Springs Cyn	Sulphur Spring Rd	Fort Hunter	11149650	SULPHUR SPRINGS CYN NR JOLON CA	13.36	km2	01-Oct-67	30-Sep-69				Yes	No
TEM-MOL	Tembladero Slough	Molera Rd	Castroville			380.00	~km2			08-Mar-00	12-Nov-01	1	No	No
TOM-TOM	Toro Ck (Nr Morro)	Toro Creek Rd	Morro Bay	11142100	TORO C NR MORRO BAY CA	36.26	km2	01-Oct-70	30-Sep-78				Yes	No
TOP-TOP	Toro Ck (Nr Pozo)	No bridge ?, Toro Ck Nr Pozo	Pozo	11144000	TORO C NR POZO CA	24.76	km2	01-Oct-60	30-Sep-83				Yes	No
TOW-OSR	Towne Ck	Small br nr Old Stage Rd	Salinas			9.70	km2			08-Mar-00	18-Feb-01	26	No	No
TRE-TRE	Tres Pinos Ck	No bridge, Near Hwy 25	Tres Pinos	11157500	TRES PINOS C NR TRES PINOS CA	537.73	km2	01-Oct-40	30-Sep-00				Yes	No
WCT-H25	Willow Ck Trib	Hwy 25	Paicines	11156450	WILLOW C TRIB NR SAN BENITO CA	3.21	km2	01-Jul-64	30-Sep-69				Yes	No
WIL-V6R	Wild Ck (CCoWS)	V6 Ranch dirt Rd	Parkfield			16.42	km2			05-Mar-01	09-Mar-01	3	No	Yes

(1) Only sites with USGS flow data were used in the FDC analysis (see Section 4.4).

(2) Sites included in the LDC analysis had either USGS flow data or could be regionalized to have USGS flow estimates (see Section 4.7), and had either USGS sediment data or a suitable sample distribution of CCoWS data (see Section 6.3).

Figure 3.1. Location of sampling sites (see Table 3.1 for details). See also Figure 7.7 for a closer view of the Gabilan Watershed area.

3.2 Monitoring protocols

The companion report 'Protocols for Water Quality and Stream Ecology Research' by Watson et al. (2002) describes the details of all sediment sampling and analysis protocols associated with the study. The strategy was to build up a database of paired discharge estimates and suspended sediment concentrations for each site – leading to a sediment–rating curve for each site. In turn, discharge estimation was based around a database of paired stage and discharge measurements – leading to a discharge–rating curve for each site. Stage (water level) was measured using staff plates installed at each site. Discharge was measured using a variety of techniques, depending on flow rate and site conditions, as detailed in Watson et al. (2002, Sec. 4.1). The most common technique involved transects across the flow measuring flow velocity using hand–held impellors. Suspended sediment was typically sampled using a DH–48 sampler, and then analyzed in the CCoWS laboratory using vacuum filtration (Watson et al., 2002, Sections 4.2 & 5.1).

Sediment sampling was initiated in early 2000, with most sampling done during the 2000–1 storm season, and some supplemental sampling during the 2001–2 season. During the 2000–1 season, crews were maintained on standby consisting of up to 14 staff and students. Once storms were forecast, weather radar was monitored until intense rain was imminent. Crews of 2–3 people were then mobilized in 4–6 hour shifts around the clock for 1–3 days, and then in daylight hours until flows had receded. The primary task of the crews was to obtain 3–6 suspended sediment samples per site, per event. Ideally, the samples would be taken before, during, and after the peak in the hydrograph, so that it was clear that all parts of the hydrograph were sampled. Discharge measurements were also taken whenever a site was flowing at a stage that differed significantly from stages at which previous discharge measurements had been made. Further details are given in Watson et al. (2002, Sec. 3.2).

3.3 SSC versus TSS

The terms suspended–sediment concentration (SSC) and total suspended solids (TSS) are confusing. Their intuitive meaning does not adequately describe the standard analytical methods that bear their name, and the results of methods can differ considerably (Gray et al., 2000; Glysson & Gray, 2002). In the United

States, SSC analyses (archived by USGS with parameter code 80154) conform to a protocol described by ASTM (2000), which typically involves filtering entire samples in the lab. Conversely, TSS analyses (USGS parameter code 00530) conform to an APHA standard method (APHA et al., 1995), which typically involves taking aliquots to get a small enough sample that will not clog filters. SSC analyses are much more accurate indicators of the amount of sediment transported by streams, while TSS analyses can significantly underestimate the suspended load (Gray et al., 2000).

None of the data in the present study were produced using the (less appropriate) TSS method. USGS samples are analyzed using a method equivalent to the ASTM SSC method. For the present study, the data were obtained from USGS as daily mean concentrations. Usually, these are based on one sample per day, but on days wit highly varying flow, a daily average is computed based on flow weighted averaging of multiple samples (USGS, accessed 2003). Similarly, all CCoWS samples were analyzed using a method that is equivalent to or better than the ASTM SSC method. This method *always* filters entire samples, with no sub-sampling – achieving this using vacuum suction and multiple large-diameter filters. The method was designed for the present study by CCoWS lab staff after consulting with the USGS sediment analysis lab (formerly) in Salinas.

4 Hydrology

4.1 Overview

The Salinas River and most of its tributaries are only locally perennial. Perennial reaches are typically located where an impermeable layer is the substrate or is found in the shallow subsurface. Where the tributaries reach the Salinas Valley, they typically dry up, losing flow to the permeable alluvium of the unconfined Salinas aquifer. Only storm flows make it across wide sandy washes to the main stem of the Salinas River. These are typical traits of dryland rivers globally (Tooth, 2000).

The course of the major rivers and tributaries (e.g. Salinas, Arroyo Seco, Estrella) is confined within well-defined channels. The banks are often leveed and stablized by adjacent landowners using concrete 'rip-rap'. The 100-year annual flood peak in the lower Salinas River at Spreckels is estimated as 3739 m^3/s (see Table 4.1). In 1995, a record peak of 2690 m^3/s (95,000 cfs) escaped the banks in many places, causing unwanted flooding and sedimentation over agricultural lands. Statistically, this is the 34-year annual flood.

Unlike most of central and southern California, all water needs are met from within the watershed itself. Irrigation is the dominant consumptive use of water. Irrigators use on-site pumps to withdraw ground water from between 10 and 50 m (30–150 ft) below the surface (MCWRA web data, 2002). Surface flows are impounded at a number of large reservoirs for both flood control and groundwater recharge. A major use of the two largest reservoirs, Nacimiento (413,216 ML) and San Antonio (466,133 ML), is to release water in summer to recharge the unconfined aquifer of the Salinas Valley.

Despite the winter-retention of some of the surface flow that would otherwise have reached the ocean, there has been a local overdraft in the lower valley since irrigated agriculture boomed in the late 1920s (Montgomery Watson et al., 1998a). Prior to this, groundwater was sufficiently shallow that the lower valley supported swamps and lakes that are now farmed, as shown in a 1901 map produced by the USDA (Fig. 4.1). Early explorers and their horses encountered quicksand in the River (Fisher, 1945), an indication of *upward* groundwater pressure in the surface aquifer (Harr, 1962; Hillel, 1998).

Groundwater level data for the region are archived by the USGS through the early 1980s, with peak monitoring activity in the late 1970s. USGS data from 1976 to 1978 were averaged for each monitoring well and plotted as overlay to the 1901 data in Figure 4.2. Groundwater decline of approximately 20 feet is evident in the areas closest to the coast, increasing as one moves away from the coast. The temporal progression of groundwater development in the Valley is illustrated in Figure 4.3, which shows data from the relatively long record of the USGS-archived well southwest of Salinas (Site 363856121413701). A data point from the 1901 USDA map is included, estimated as 15 ft ±5 ft, as are the major water resources milestones of the region: the dates of commencement of gravity irrigation, groundwater irrigation, and groundwater replenishment from the two large dams. For comparison, the total acreage under irrigation, and specifically under lettuce (currently the dominant irrigated crop) is shown. The respective data align well and indicated that around 1928, when groundwater pumping technology achieved widespread use, farming rapidly switched from wheat and barley (see Newman et al., 2003) to irrigated crops such as lettuce. Concurrently, ground water levels began steadily declining at an average rate of 5.6 inches per year, through the early 1980s when the USGS record ends. Analyses of other well records in the region (not shown) concur with the pattern shown for the well to the southwest of Salinas.

Modern records for the Valley as far inland as San Ardo are kept by MCWRA, and indicate a continuing overdraft as evidenced by long-term declines in groundwater levels in the Northern Salinas Valley. The long-term (1958–1994) mean annual overdraft from the Salinas Valley Ground Water Basin (extending inland to San Ardo) is 19,000 acre feet, or 3.6% of the groundwater pumped for urban and agricultural uses (Montgomery Watson et al., 1998a, b). Most of the overdraft is experienced in the 'East Side' groundwater area on the eastern side of the valley between Salinas and Gonzales, and in the 'Pressure' groundwater area on the west side of the valley between Gonzales and the coast. The 'Forebay' and 'Upper Valley' groundwater areas between Gonzales and San Ardo have relatively steady long-term groundwater levels, although the net outcome of the early 1990s drought and recent increases in rural development in these areas may yet to be fully realized in the groundwater level data.
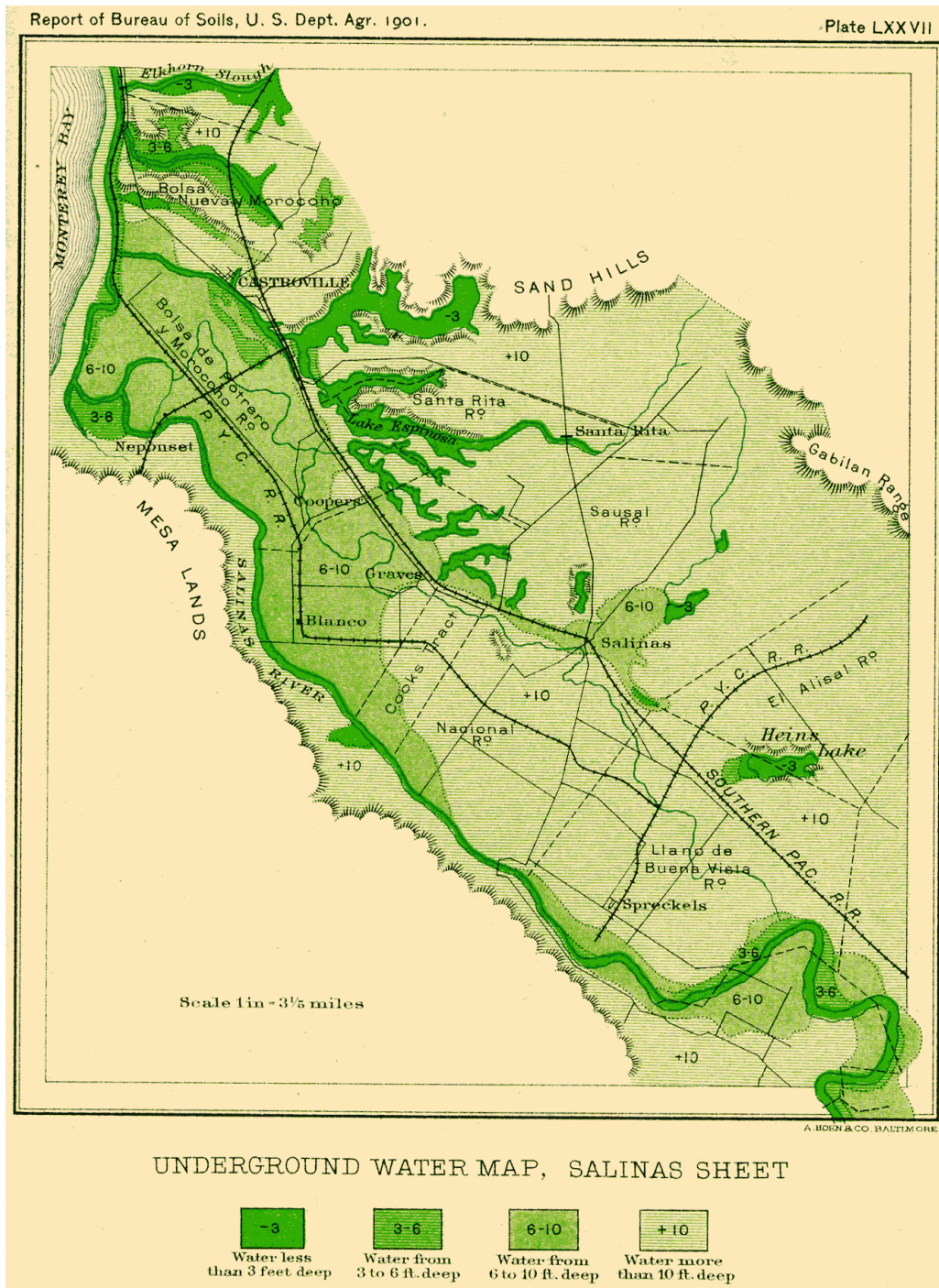
Figure 4.1. Groundwater levels at the turn of the 20th century.

78
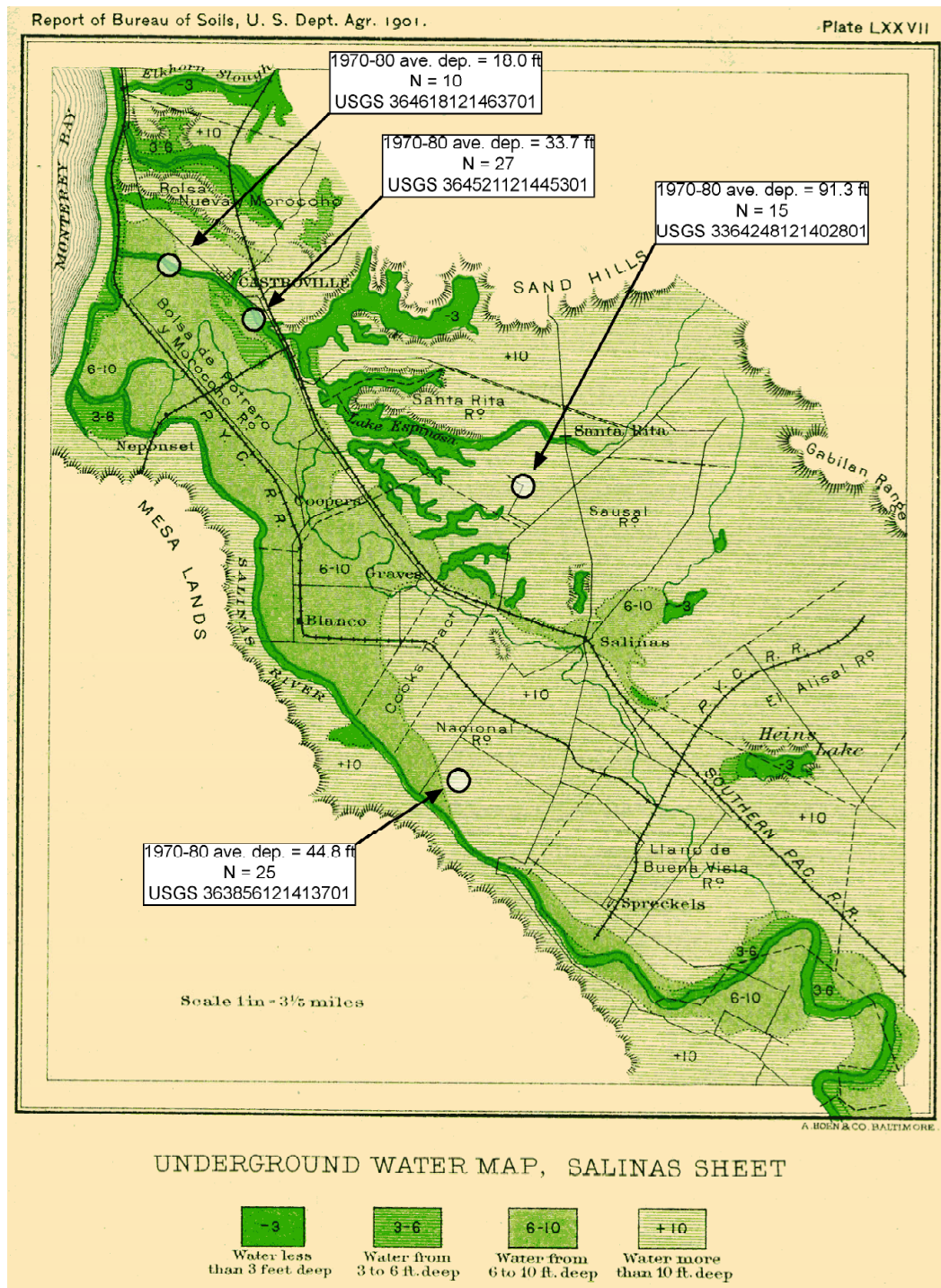
Figure 4.2. Declining groundwater in the northern Salinas Valley: comparison between groundwater levels (depth below surface) mapped in 1901 and levels averaged from 1970–1980 USGS well data (limited to wells with at least 10 data points between 1970–1980).
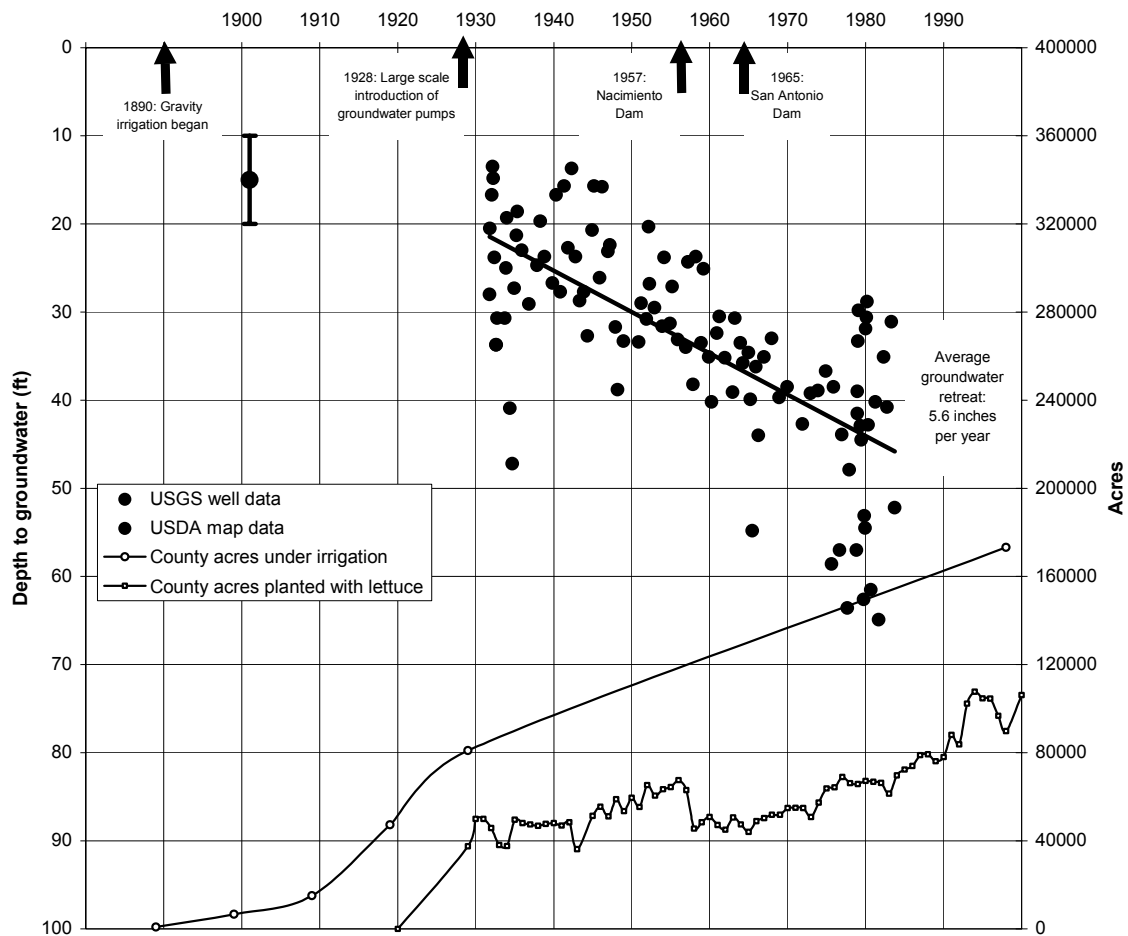
Figure 4.3. Timeline of groundwater development in the northern Salinas Valley.

Further south, in San Luis Obispo County, there is both long-term decline and long-term increase in groundwater level. Along Highway 46 east of Paso Robles, residential, golf course, and viticultural developments (Fig. 4.4) overlie a hydro-geologic basin where groundwater levels have declined up to 100 feet since 1959 (Fugro West, 2002, Figs 34 & 43). On the other hand, groundwater levels have risen over 40 feet since the 1970s in the Creston area 15 km south of Highway 46 (Fugro West, 2002, Figs 34 & 39). The net situation for the Paso Robles basin is a relatively steady groundwater reserve.

The modern-day Salinas River has two seasons. The regular winter season is modified by reservoir detention but still carries the peak flows of the large unregulated tributaries such as Arroyo Seco. The lower river may then dry up completely before the first summer releases are made. These are designed to flow almost to the ocean before percolation is complete, and typically run at between 10 and 15 m^3/s at the reservoir outlet. In fall, the releases stop, and there is a period where farmers have limited heavy-equipment access to the river bed in order to make local preparations for the risk of coming winter floods (see below).

Current plans (MCWRA & USACE, 2001) include the possibility of an inflatable dam near the Salinas River Mouth that would allow more rapid reservoir releases without loss of irrigation water to the ocean. This would temper the groundwater decline of the Northern Valley.

Figure 4.4. Rural-residential and viticultural development along Highway 46 east of Paso Robles. Photos: Fred Watson, 3 Oct 2002.

4.2 Hydro-statistics

Stream flow and sediment transport in the region is highly episodic. It is thus important to compute some fundamental hydrologic statistics that quantify this. Table 4.1 shows the results of a flood frequency analysis of annual peak flows for selected USGS sites in the Salinas Watershed. The analysis assumed a log Pearson Type III (LP3) distribution for peak flows, calculated according to Kite (1977, Eq. 9-52), Interagency Advisory Committee on Water Data (1982), and Pilgrim & Doran (1987). The theoretical mean annual flood (MAF) can be estimated as the 2.33 year event from a series of annual peak flows (Dunne & Leopold, 1978). At Spreckels, this estimate of the MAF is 264 m^3/s (9,333 cfs). The actual sample mean of the 66 year record of annual peak flows at Spreckels is slightly higher, 462 m^3/s (16,300 cfs), the 3.19 year event.

The ratio of rare floods to the mean annual flood is an indication of the episodicity of runoff in the watershed. At Spreckels, the ratio of the 100 year flood to the theoretical mean annual flood is 14.2, indicating significant episodicity when compared with, say, East Coast temperate streams, where values between 3 and 8 are more typical (Dunne & Leopold, 1978; Sutton et al., 1996).

Site	USGS ID	USGS name	Length of record used (years)	Watershed area (km2) (USGS)	Peak discharge (m3/s), by recurrence interval							
					1.01 yr	2 yr	2.33 yr ~= MAF	5 yr	10 yr	20 yr	50yr	100 yr
SAL-CRE	11147500	Salinas R. nr Paso Robles	55	1010	2.86	133.37	163.28	314.08	447.94	575.09	729.72	(835.46)
SAL-WUN	11150500	Salinas R. nr Bradley	51	6566	1.83	168.23	223.80	602.52	1095.61	1735.14	2809.72	(3796.97)
SAL-SOL	11151700	Salinas R. nr Soledad	26	9228	1.35	98.09	138.14	501.69	1198.40	2482.58	(5691.94)	
SAL-CHU	11152300	Salinas R. nr Chualar	23	10469	1.28	215.77	287.77	747.60	1281.56	1897.32	(2797.20)	
SAL-SPR	11152500	Salinas R. nr Spreckles	66	10764	0.14	185.36	264.29	808.00	1445.41	2144.40	3074.51	(3738.74)
ARR-CAM	11151870	Arroyo Seco R. nr Greenfield	39	293	18.18	202.63	230.24	348.30	436.39	511.70	(595.87)	
ARR-ELM	11152000	Arroyo Seco R. nr Soledad	95	632	15.72	209.10	244.43	416.25	569.48	721.23	919.19	(1066.36)
ARR-ARR	11152050	Arroyo Seco R. blw Reliz Cr nr Soledad	6	787	29.46	275.29	324.48	592.63	(877.19)			
NAC-SAP	11148900	Nacimiento R. blw Sapaque Cr. nr Bryson	29	420	12.23	392.10	473.62	879.46	1239.37	1584.90	(2013.20)	
NAC-BLD	11149400	Nacimiento R. blw Dam	43	852	0.96	45.58	56.55	115.44	172.53	231.01	(308.14)	
ELT-USG	11152540	El Toro Cr nr Spreckles	39	83	0.03	2.25	3.00	8.36	15.92	26.55	(46.17)	
EST-AIR	11148500	Estrella R nr Estrella	43	2388	0.04	14.13	21.89	109.39	313.09	739.20	(1924.36)	
SLC-BIT	11151300	San Lorenzo Cr blw Bitterwater Cr nr King City	42	603	0.82	30.73	39.73	100.54	182.06	293.42	(495.13)	
GAB-HER	11152600	Gabilan Cr nr Salinas	26	95	0.34	6.80	8.20	15.61	22.97	30.85	(41.96)	

Table 4.1. Flood frequency analysis for selected sites in the Salinas Watershed. Estimated peak discharges are listed for a variety of recurrence intervals. Estimated peak flows are most accurate for recurrence intervals shorter than the period of record, and less accurate for longer recurrence intervals (parenthesized figures).

4.3 Regional peak flow patterns

It is useful to compare peak flows of a given recurrence interval amongst gauged sites in the region. The use of frequency data and relatively short recurrence intervals eliminates sampling bias associated with particular records. A comparison using the 2-year recurrence interval highlights processes occurring during the large storms that can be expected to occur about every one to four years. Figure 4.5 plots 2-year peak flow against watershed area. The flow data have been normalized[4] by watershed area, and so are plotted in depth units (mm/day) instead of volume units (e.g. m^3/day). This removes the trivial correlation between flow and area in the data. The sites have been grouped and colored according to their location along the east–west gradient of declining precipitation as one moves inland.

The 2-year peak flow in small watersheds equates to about 100 mm/day, but these peaks decline rapidly to about 1 mm/day as the flood waves move down the watershed. There are a number of factors that are likely to contribute to this condition. Firstly, most storms in the region do not occur over the entire watershed simultaneously, so as watershed area increases, the peak number of storm cells per unit area should decrease. Secondly, stream channels do not convey flood waves perfectly. Flow is retarded, and flood peaks are spread out over time as water moves downstream. Figure 4.5 shows only the peak flow, not the duration of these peaks, which increases with area (data not shown). Finally, the Salinas Region's streams in particular exhibit very high percolation rates, presumably enhanced by the well-pumping of near surface groundwater. Entire headwater storms are frequently subsumed into the streambed, leaving an entirely dry channel downstream. This is especially so early in the rainy season.

---

[4] The word 'normalize' is here used in the sense common in the natural sciences whereby one variable is simply divided by another, to which it is considered relative.
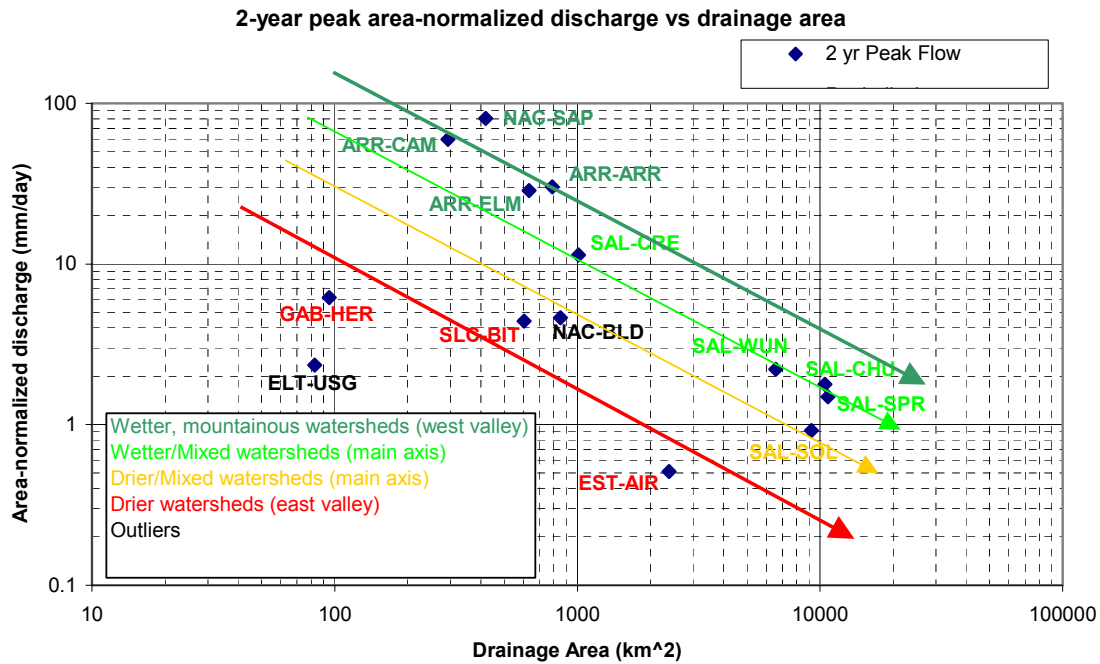
Figure 4.5. 2–year peak discharge per unit area versus drainage area for selected USGS sites in the Salinas Watershed (see Table 3.1 for site codes).

4.4 Regional flow duration patterns

A flow duration curve from a long-term daily flow gauging site is a statistically unbiased measure of the magnitudes of daily flows passing the site, and the historical duration of flow at each magnitude. Flow duration curves (FDCs) provide a useful adjunct to flood frequency analysis. They are simply a plot of the magnitude of flow versus the percentage of time that the flow is less than that magnitude. Typically, flow is plotted on a log axis, and time is plotted on a probability scale (an axis that inverts the log-normal distribution that flow data typically exhibit). This has the effect of producing an approximately straight line for most sites, which helps with comparison between sites. Unlike the comparison of peak flows from a frequency analysis (above), flow duration curves provide information about the duration of flow, and the total volume of water being transported past various sites in a watershed.

A selection of FDCs from diverse parts of the Salinas Watershed (and nearby) are compared in Figure 4.7a. The only perennial stream in the comparison is the Big Sur River at Big Sur (BSU-BSU). This is a steep, rocky stream draining directly to the ocean from some of the highest and wettest peaks of the coastal Santa Lucia ranges. The Big Sur Valley is deeply incised through most of its length, with only a narrow floodplain forming in the last one or two kilometers above a short estuary. The FDC is a straight line with no zeroes, indicating a perennial stream with a lognormal distribution of flow in time, as would be expected for a stream whose flow distribution is controlled mainly by rainfall (also approximately lognormally distributed) without significant human or subsurface influence.

Before making a comparison with other streams, it is easiest to normalize flow by watershed area to yield a set of FDCs expressed in depth units (m/day), as shown in Figure 4.7b. Here, we can see that on a per-area basis, the Big Sur River is statistically the wettest in the data set, at all times. The Arroyo Seco River at Elm Rd (ARR-ELM) is the most similar to the Big Sur River, but has access to a larger flood plain, and a greater volume of unfilled sub-surface alluvial storage (even though the gage itself is partly on bedrock). Therefore, the FDC reveals that ARR-ELM dries up completely for 10% of days, during which

time the river upstream either percolates or flows hyporheically[5]. During wetter times, ARR-ELM displays an un-interrupted straight line FDC like BSU-BSU, albeit uniformly drier than BSU-BSU given its more inland location in the rain shadow of the Santa Lucia Range.

Another stream with a largely natural flow regime Cholame Creek at Highway 46 (CHO-H46). This stream is located in the far southeastern arid zone of the Salinas Watershed, largely devoid of trees. The stream is dry for over 90% of days, but experiences fairly strong flow when significant rains fall. Again, the site has a smooth FDC indicative of unmodified flow.

Figure 4.6. USGS field crew measuring an annual peak flow on the Salinas River at Spreckels. Photo: Thor Anderson, 7 March 2001.

---

[5] Approximately 33% to 49% of the mean annual flow from the Arroyo Seco River becomes groundwater recharge before reaching the Salinas River (EDAW 2001)
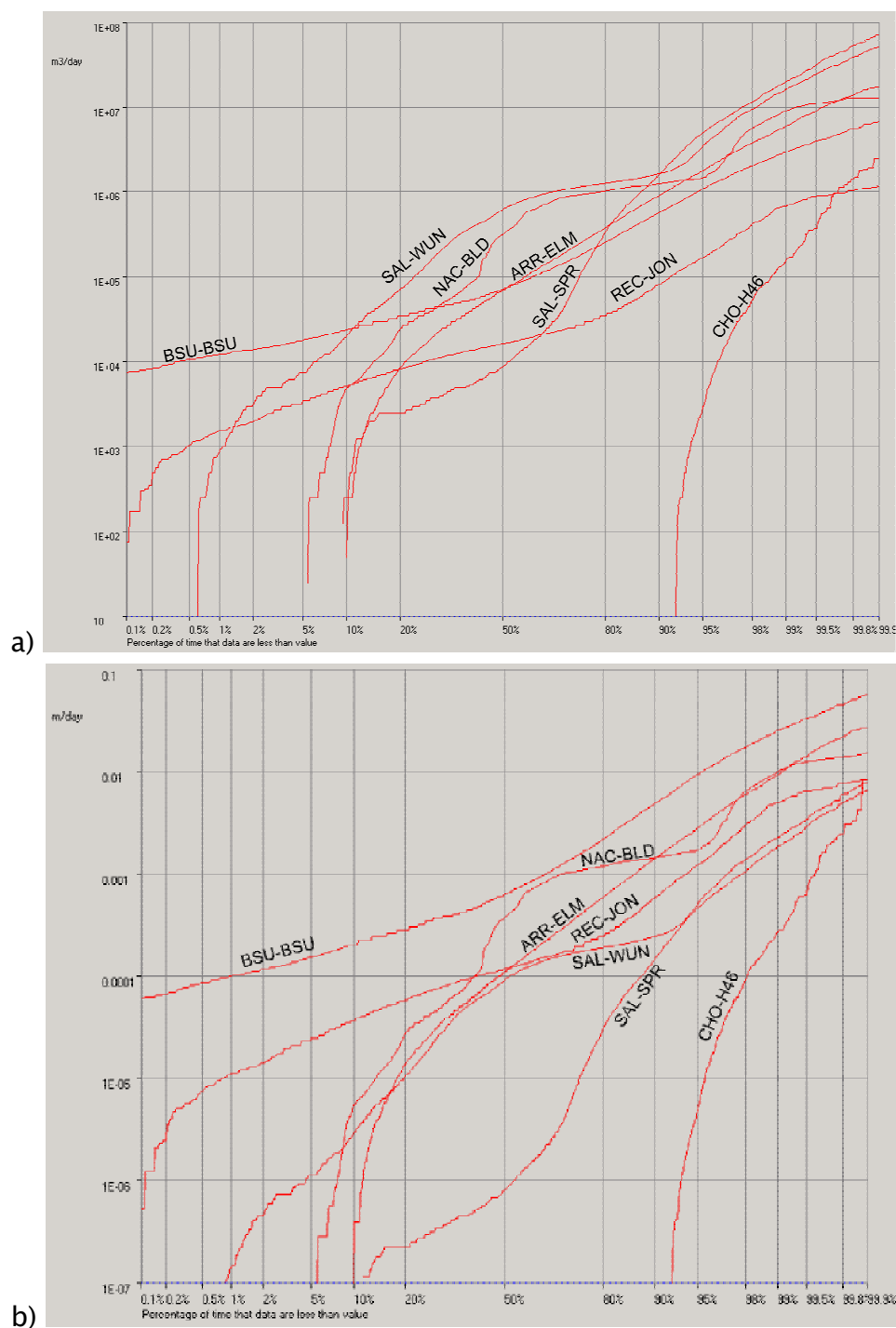
Figure 4.7. Flow duration curves for selected USGS sites in the Salinas Watershed: a) flow expressed in m³/day; b) flow normalized by watershed area, m/day (see Table 3.1 for site codes).

A good example of a stream with a highly modified flow regime in the region is the Nacimiento River below the Nacimiento DAM (NAC–BLD). The perennial, or near–perennial Nacimiento River emerges from high mountains into foothills at Fort Hunter Liggett before flowing into Lake Nacimiento. The Dam is operated so as to retain winter flows, flood control storage permitting, and then to release water down the river in summer for deliberate percolation into alluvial aquifers used for irrigation. Under an agreement with CDFG, a non–drought minimum release of 25 cfs (0.7 m^3/s) maintains a fish population dominated by Sacramento Suckers in the cobbled reach below the dam, and above the confluence with the Salinas River (MCWRA & USACE, 2001)[6].

The FDC for NAC–BLD reflects this modified flow regime, as indicated by the two plateaus in the curve at just over 0.001 m/day and just over 0.01 m/day, and an inflection in the curve at about 0.0001 m/day. The plateau at 0.001 m/day represents the extended periods during which a relatively constant irrigation release of just over 400 cfs (10^6 m^3/day) passes the site. The leveling off of the curve at 0.01 m/day corresponds to the success of the Dam in limiting floods to just over 4000 cfs (10^7 m^3/day). The inflection at 0.0001 m/day may be an indication that the typical conservation release is about 40 cfs (10^5 m^3/day), although the curve also indicates that at times there is no flow.

A typical urban stream is exemplified by the former (and future) gage at the Reclamation Ditch at San Jon Rd (REC–JON, Fig. 4.7), just below the City of Salinas. Upstream of the City of Salinas, Gabilan, Natividad, and Alisal Creeks are non–perennial. Gabilan Creek in particular is completely dry for most of the year at and below Herbert Road, despite a perennial boulder stream that persists in its wooded headwaters. However, once these streams combine in Carr Lake, and the urban drainage of the City and the tailwater of additional agricultural areas are incorporated, the FDC indicates that the stream is very–nearly perennial at San Jon Road, being dry for less than 0.1% of days. Ironically, this may be the more natural flow regime for streams of the formerly swampy northern Valley.

---

[6] Note that the minimum release from Lake San Antonio is lower – 3 cfs.

Two sites on the main stem of the Salinas River are included in Figure 4.7. The Salinas River at Wunpost[7] is the first main stem site below the influence from Lakes San Antonio and Nacimiento. Above these influences, the Salinas River is a wide, completely dry, sandy wash for most of the year. Below these influences, the FDC at SAL-WUN clearly indicates a plateau at $>10^6$ m^3/day (>400 cfs) corresponding exactly to the summer irrigation releases (Fig. 4.7a). The curves are thus a useful quantification of the altered two-season flow regime of the lower and middle Salinas River. Much further downstream at Spreckels (SAL-SPR), most of the summer releases have percolated into the stream bed, leaving a steady plateau in the FDC of about 2000 m3/day (0.8 cfs) trickling under Highway 68. Otherwise, SAL-SPR appears to have a relatively natural, straight-line FDC – mostly determined by the unregulated (although still heavily percolated) floods from its major hydrological tributary, the Arroyo Seco River.

4.5 Flow duration along a single River

The hydrologic importance of streambed percolation in the understanding of flow regimes of the Salinas Watershed is most clearly demonstrated by comparing FDCs from three sites in a sequence down the Arroyo Seco River, as shown in Figure 4.8. The uppermost site is ARR-CAM, at the National Forest campground. This site has almost perennial flow, through a narrow canyon with numerous bedrock controls interspersed between narrow, cobbled floodplains. The next gauged site, ARR-ELM, is about 20 km downstream. The FDC illustrates that approximately ten percent of the time, none of the water flowing past ARR-CAM makes it to ARR-ELM as surface flow. However, during the wetter half of the time, the flow at the two sites is almost identical, despite intervening inflows from Vaqueros and Piney Creeks. These more inland tributaries appear to contribute negligibly to overall flow. ARR-ELM is still within the bedrock-controlled portion of the watershed. The next site downstream, ARR-ARR is surrounded by the huge expanse of the Salinas Valley alluvium, just upstream of the Salinas River. As shown by its FDC, this site flows less than half the time. The channel is wide and sandy with almost no pools, and therefore no residual water at all during no-flow periods. A large amount of water from upstream is completely absorbed by the aquifer before reaching this site, including the flow from the first one or two winter storms. When it does flow however, the

---

[7] The USGS "Salinas at Bradley" site is actually at Wunpost (SAL-WUN). This is some distance from Bradley, where there is a CCoWS site called SAL-BRA.

discharge is approximately equal along the length of the River[8]. The system is illustrated in Figure 4.9.

The steepness of the FDC is another measure of the episodicity of a stream. So, despite the fact that the size of storm peaks diminishes as one moves downstream (on a per-area basis), the stream on the whole becomes more episodic due to percolation losses to the alluvial aquifer. This is most likely typical of the watershed as a whole. Given that in this system, percolation joins climate as a dominant source of episodicity, the hypothesis can be made that groundwater depletion in the past 75 years has reduced the regularity and duration of flow in the Rivers and Creeks that lie above the unconfined aquifer of the Salinas Valley. An analysis of this possibility and its potential biological effects is left for future work.

---

[8] Note that Figure 4.8 shows ARR-ARR has having slightly higher flows than its upstream counterparts in the upper 10th percentile because of sampling bias associated with the short (1994-2000) data set for ARR-ARR.
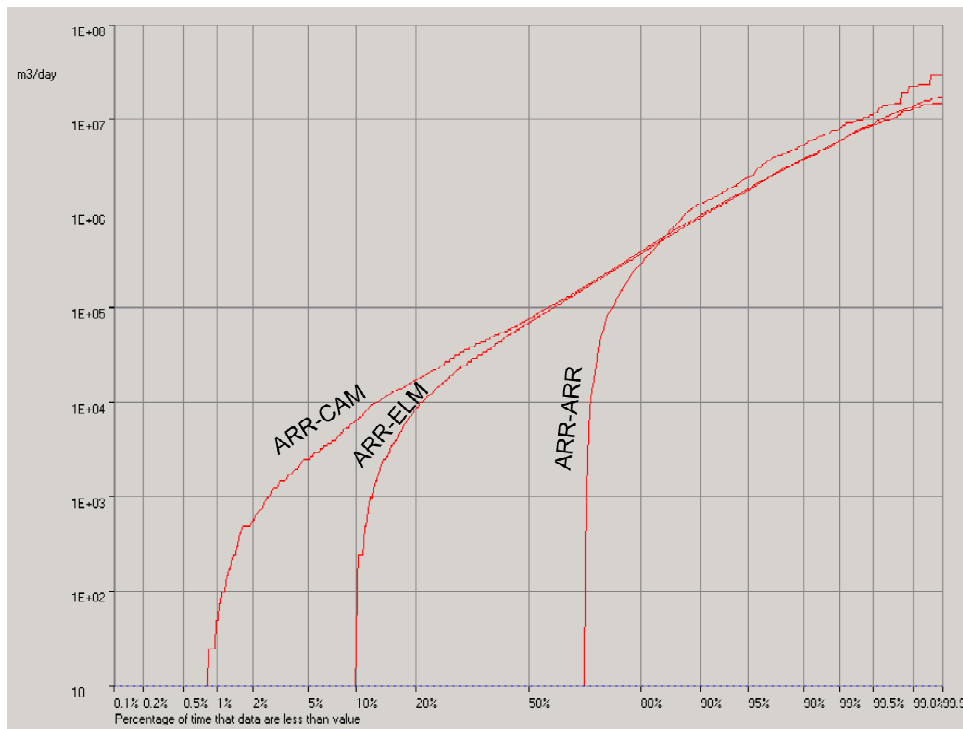
Figure 4.8. Flow duration curves for three USGS sites on the Arroyo Seco River, illustrating the effects of percolation between upstream (ARR–CAM) and downstream (ARR–ARR) sites.
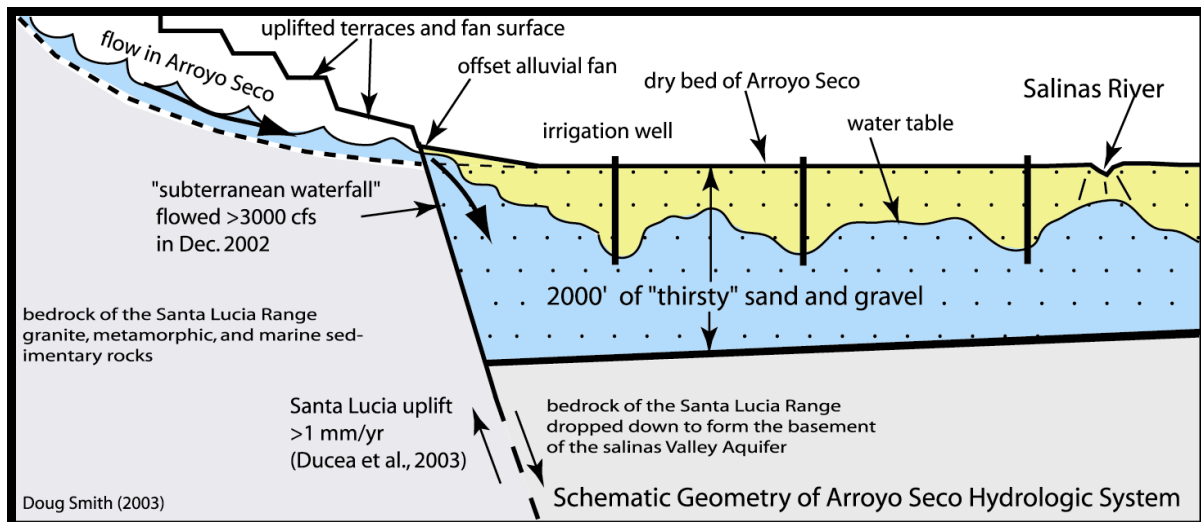
Figure 4.9. Schematic diagram of percolation of the Arroyo Seco River into the aquifer system of the Salinas Valley.

4.6 Classification and modification of flow regimes

Flow duration curves for all USGS gauged sites in the region of the Salinas Watershed are overlaid in Figure 4.10a (expressed in m³/day). Most of the variation between the curves shown is due to differences in watershed area, so it is better to work with area-normalized data expressed in m/day, as in Figure 4.10b. The normalized data align well. Once the initial jump from no-flow to flow is made (left end of each curve), the curves generally exhibit the same slope. The alignment improves when sites with less than 10 years of record are eliminated, and the remaining sites are grouped into four further categories (Fig. 4.11):

- unregulated streams with largely natural flow regimes,
- regulated streams immediately downstream of large reservoirs,
- partly regulated streams with a large reservoir somewhere in their watershed,
- and urban streams.

Anthropogenic changes in flow regime are due to factors such as reservoir regulation and urbanization (Fig. 4.11) as well as groundwater decline (not analyzed here). In addition to obvious climatic influence, natural changes in flow regime may be brought about by factors such as fire. Hecht (1993) documented increased summer flows in the Arroyo Seco River following the Marble-Cone fire of 1977, due to increased infiltration and decreased removal of moisture from the soil following vegetation removal by fire.

4.7 Regionalization of flow duration data

In hydrology, regionalization is the process of estimating the properties of a site by inference, using information on the properties of sites in the nearby region. At its most complicated, regionalization may involve multivariate geo-statistical interpolation of parameters based on information from thousands of nearby sites. At its simplest, regionalization is simply the assumption that the properties of two sites are identical if they are sufficiently proximate – the "nearest neighbor" approach.
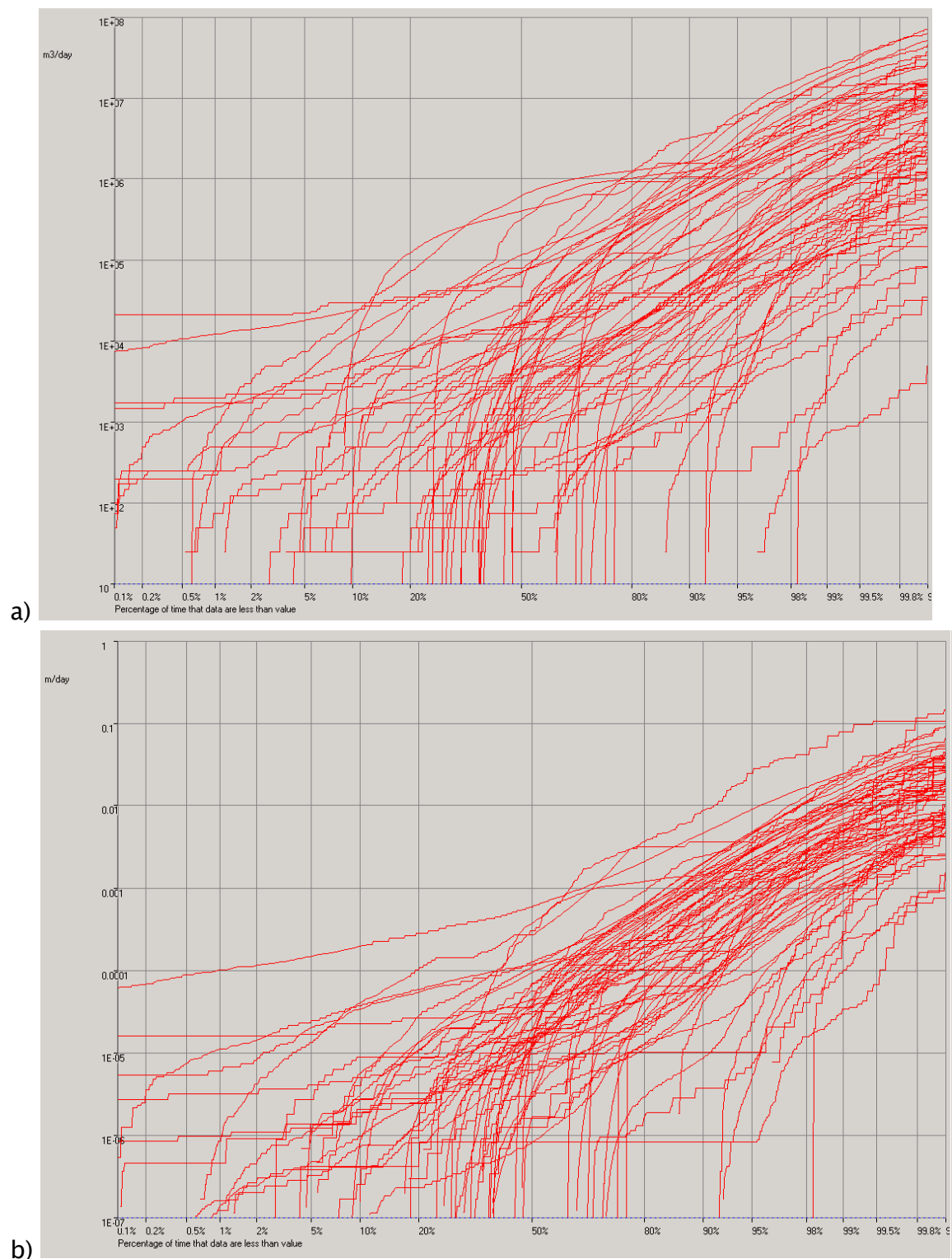
Figure 4.10. Flow duration curves for all present and historic USGS sites in the Salinas Watershed and nearby: (a) in m3/day, and (b) in normalized by watershed area, in m/day.

a – Unregulated streams

b – Regulated streams

c – Partly regulated streams

d – Urban streams
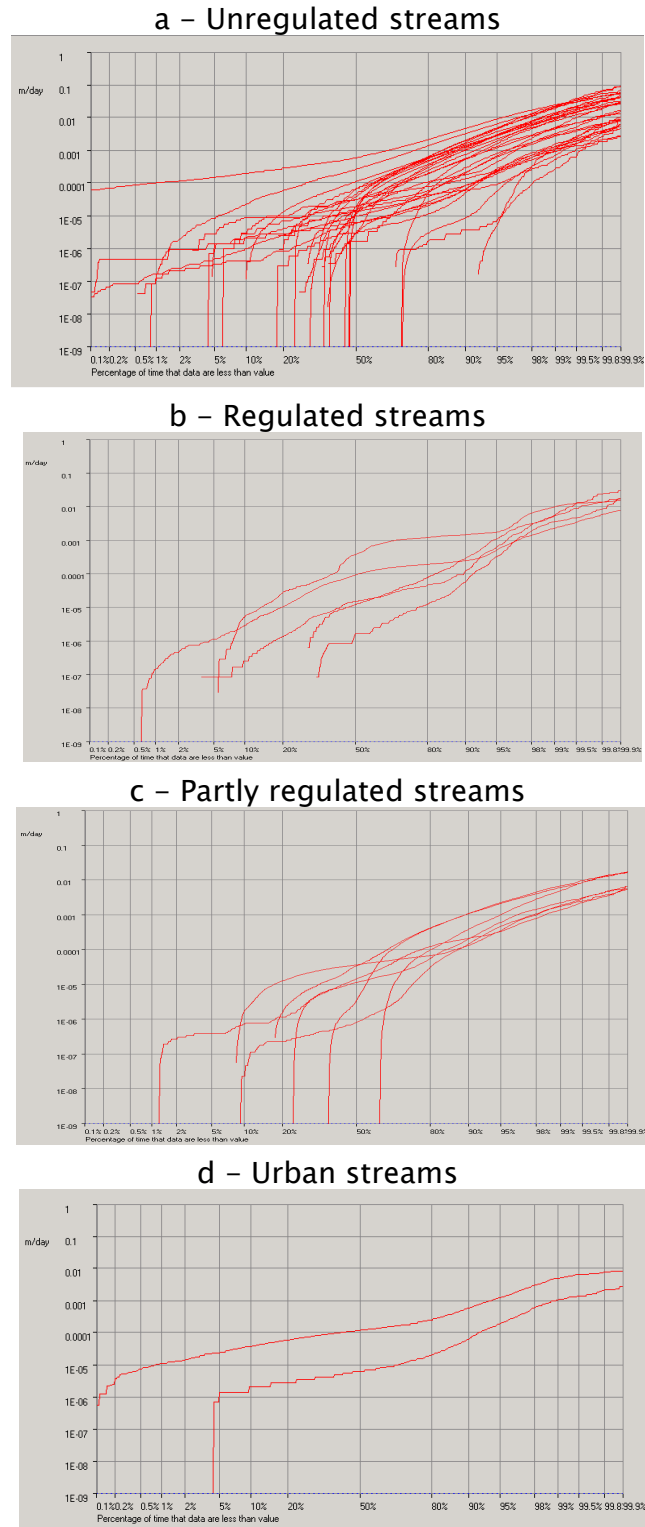
Figure 4.11. Area-normalized flow duration curves for sites with more than 10 years of data – grouped into four categories of flow regime.

The factors discussed above explain much about the *shape* of individual flow duration curves – including effects of geomorphology, percolation, land use, and artificial regulation of flow. The *magnitude* of these curves is determined by climate and watershed processes, and in particular, the mean watershed runoff. Thus, by comparing FDCs across the whole region, a picture of regional climate and runoff patterns is obtained. Further, by performing this analysis using FDCs rather than simply looking at mean annual runoff, specific parts of the flow regime can be examined. For example, our analysis of regional sediment loads (Section 6) is limited to flows less than the 99.5 percentile – a value that is obtained directly from the flow duration curve. As described in Section 6, the 99.5 percentile flow is approximately equal to the channel-full flow.

The overall variation in flow magnitude evident in the area-normalized curves of a given type (regulated, unregulated etc.), revealed as vertical shifts in the curves relative to each other, is due to climate and watershed runoff processes. This can be illustrated by mapping the cumulative flow, or in the case of Figure 4.12, the cumulative flow up to the 99.5 percentile (the non-flood flow, See Section 6.5). The map reveals clear patterns in the mean non-flood flow, with more runoff in the high Santa Lucia Ranges to the west of the Salinas Watershed, declining to much lower runoff in the east. Some of the anomalies to this pattern are due to sampling bias in short gauging records. This can be reduced by only plotting data from stations with at least 10 years of record, as in Figure 4.13.
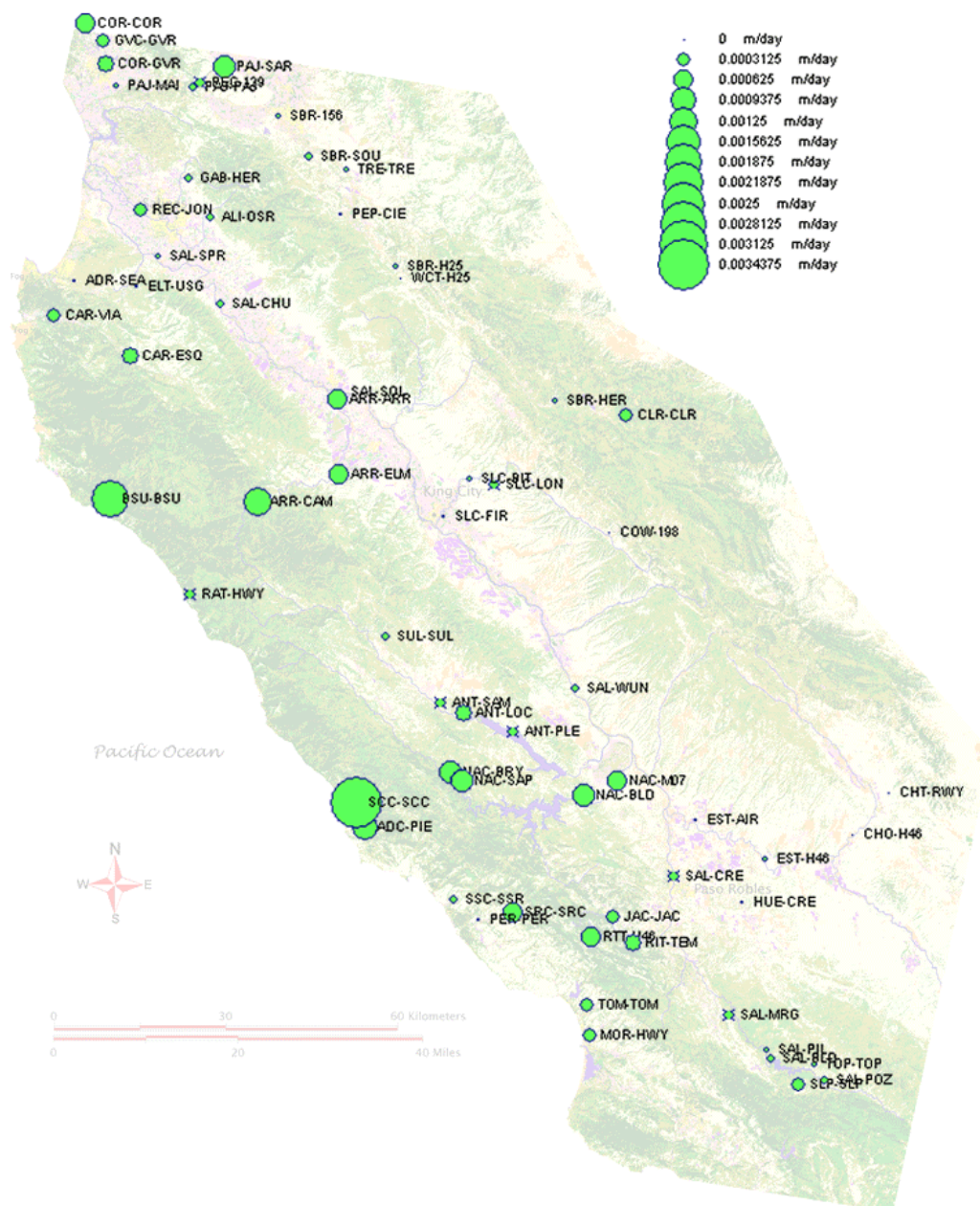
Figure 4.12. Mean non-flood daily flow for USGS sites in the Central Coast region, normalized by area.

The dominant trend is the west–east inland decline in mean flow. The most coastal site, Big Sur River (BSU–BSU) has by far the most flow per unit watershed area. Just to the east, lies the Arroyo Seco Watershed, with the second highest areal flow in its headwaters (ARR–CAM). Similarly eastward, but to the south, are the headwaters of the Nacimiento River (NAC–BRY) with the third highest flow, along with a small watershed at Arroyo De La Cruz near San Simeon (ADC–PIE). Just east of Nacimiento is the San Antonio Watershed (ANT–LOC), with the next highest flows. Moderately high flow originates from a line of smaller tributary watersheds rising in the lower, more southerly portions of the Santa Lucia Range as it passes to the west of Atascadero, turning more eastward to the north of Paso Robles (JAC–JAC, RIT–TEM, SAL–POZ, SLP–SLP). The eastern tributaries of the Salinas have fewer historical flow gages. The low, dry southeast has a few long–term gages revealing very low mean flow (HUE–CRE, CHO–H46, 11148500) in the HuerHuero Creek and Estrella River watersheds, the latter being the largest tributary watershed of the Salinas. Some distance to the north, San Lorenzo Creek has similarly low mean flow, although slightly higher than the Estrella area due to the high mountains of the Diablo Range in the far east.

Summing these tributaries together, the main stem of the Salinas River exhibits flow more indicative of its expansive, dry, eastern tributaries than of its small, wetter, western tributaries. The mean flow is further reduced by net loss to groundwater that is later transpired and evaporated back into the atmosphere after use for irrigation. To a limited extent, one can infer the influence of tributaries as changes in the mean Salinas flow above and below the major confluences. For example, the Salinas at Chualar (SAL–CHU) has more per-watershed-area flow than upstream at Soledad (SAL–SOL), due to the inflow from Arroyo Seco (ARR–ELM).

There are very few anomalies to these broad regional patterns. An example is the Reclamation Ditch below the City of Salinas (REC–JON), which has higher flow than would be expected based on regional patterns, due to urban features such as impervious surfaces and lawn watering.
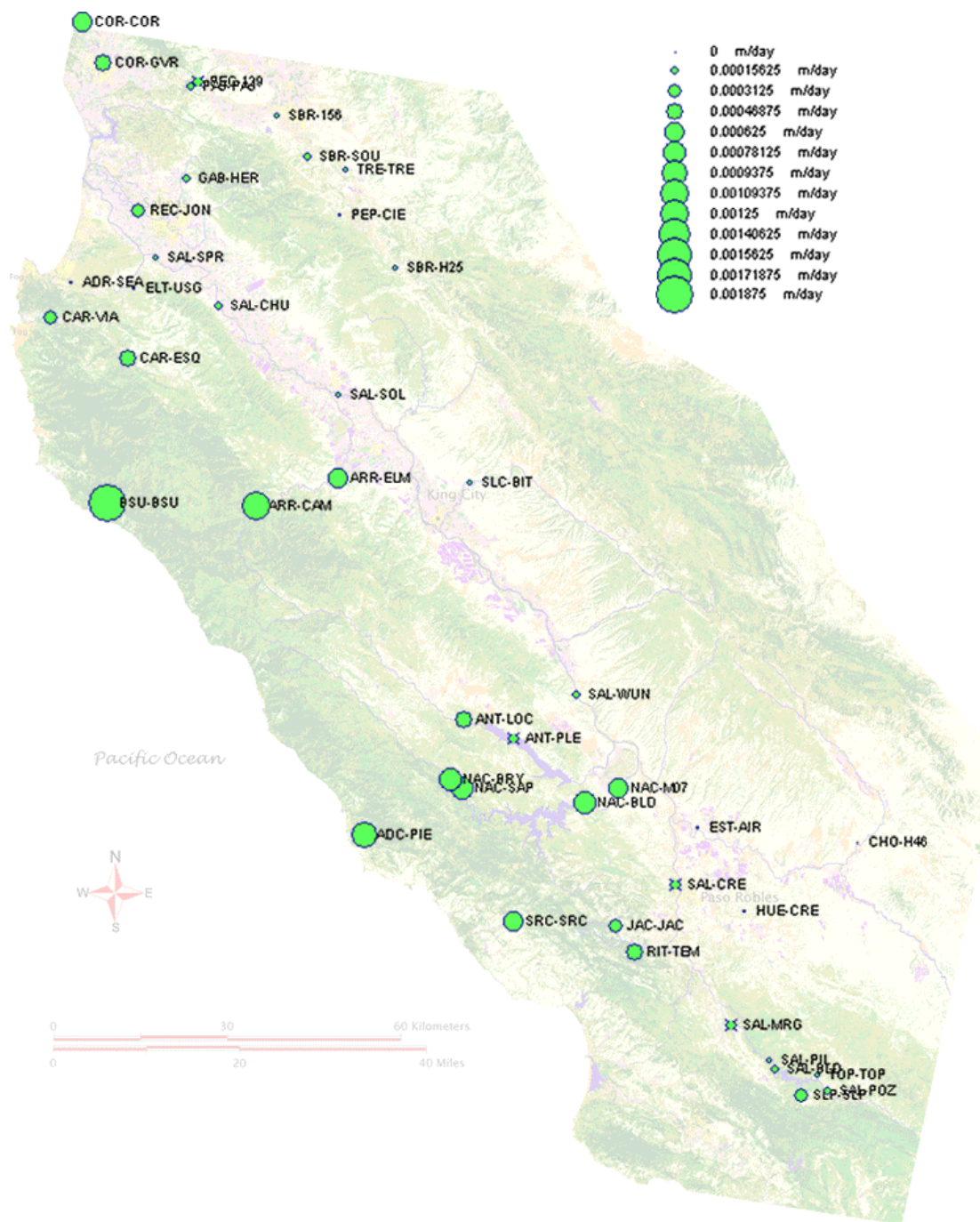
Figure 4.13. Mean non-flood daily flow for USGS sites in the Central Coast region having at least 10 years of record.

Based on these observations, a simple regionalization is possible: the flow duration curve for any ungauged site in the region of the Salinas Watershed can be estimated as being equal to the flow duration curve of a nearby gauged site, possibly from a different stream, provided that:

- watershed area is normalized (i.e. the gauged curve is multiplied by the ratio of the ungauged watershed area to the gauged watershed area),
- watershed area is similar (ideally within 25%),
- the two watersheds are close to each other with respect to coastal–inland and mountain–foothill climate gradients,
- the percolation potential of the two sites is similar, with respect to access to unfilled alluvial aquifer volume, and percolation properties of the stream bed,
- the watersheds are either both urban or both non–urban,
- the streams are either unregulated, or if regulated then in a similar manner and to a similar extent.

A quantitative evaluation of the accuracy of this regionalization strategy is beyond the scope and need of the present work. More comprehensive, objective, accurate schemes may be developed in future. The scheme as presented underlies the analysis of long-term regional sediment loads in the following Section.

5   Sediment load

5.1   Mean annual load

The mean annual sediment yield of a watershed is an indicator of the overall stability of its landscape. It provides closure on the analysis of erosion levels from the component landscapes of the watershed, and it quantifies the total delivery of sediment and associated material to receiving waters. The USGS took ten years of daily, measurements of suspended sediment concentration (mg/L) at the Spreckels site, draining almost all of the Salinas Watershed (1970–1979). More than one sample was taken on high flow days with strongly varying flow, resulting in a more accurate estimate of the daily load (tonnes/day) than would be gained by multiplying the main daily concentration (mg/L) and flow (m^3/day). The mean annual load calculated from these data is 1.67 million tonnes (1.84 million US tons[9]) of suspended sediment per year. The data are biased by their position within the long–term climate record. Inman & Jenkins (1999) removed some of this bias by fitting a sediment–rating curve to the data and using it to estimate annual sediment load for a longer record based on flow measurements (1944–1995). Their estimate of the mean yield was 1.54 million tonnes/yr.

McGrath (1987) concluded that out–of–bank flows tend to be depositional, and the resulting out–of–bank sediment transport is less than 10% of the in–channel load. In a detailed analysis seeking to identify sources of sand to Monterey beaches, the same author concluded that bedload is approximately only 1% of the total load of the river. This is consistent with other west coast studies that consider error due to exclusion of bedload to be insignificant when compared to errors in estimation of suspended load (Renau & Dietrich, 1991). Local exceptions may occur in granitic areas in the northern part of the study area (Hecht, 2000, citing Kondolf, 1982; MEI, 2002). It is suggested that in–channel suspended sediment transport is the dominant, most important component of the present synoptic analysis of Salinas River sediment sources. Allowing for these factors and the measurement error typically associated with suspended sediment sampling, the long–term average total sediment load of the Salinas River is thus unlikely to greatly exceed, say, 2.0 million tonnes per year.

---

[9] The tonne is a metric unit exactly equal to 1000 kg. One tonne is 1.1023 US tons.

In areal terms, the mean suspended yield at Spreckels is 156 tonnes/km²/yr (hereafter abbreviated to t/km²/yr), after dividing 1.67 million tonnes by the watershed area of 10,730 km². De-biasing for climate variation modifies this estimate to 144 t/km2/yr (Inman & Jenkins, 1999). This value is in the mid-range for coastal streams in California of similar geology (Inman & Jenkins, 1999 – Fig. 5.1) and in Oregon (Renau & Dietrich, 1991 – 190 t/km²/yr). It is also in the mid-range for global streams of similar area (Walling, 1994). Globally, yields of over 1000 t/km²/yr are reported from areas such as sub-Himalayan India, the loess agricultural soils of the North China Plain, and the Amazonian slopes of the Andes. Walling's map reports Californian loads typically higher than 500 t/km²/yr, which is significantly higher than the Salinas estimate. This may be due the lower sediment delivery ratio one would expect from a watershed slightly larger than Walling's range (100 – 10,000 km²).
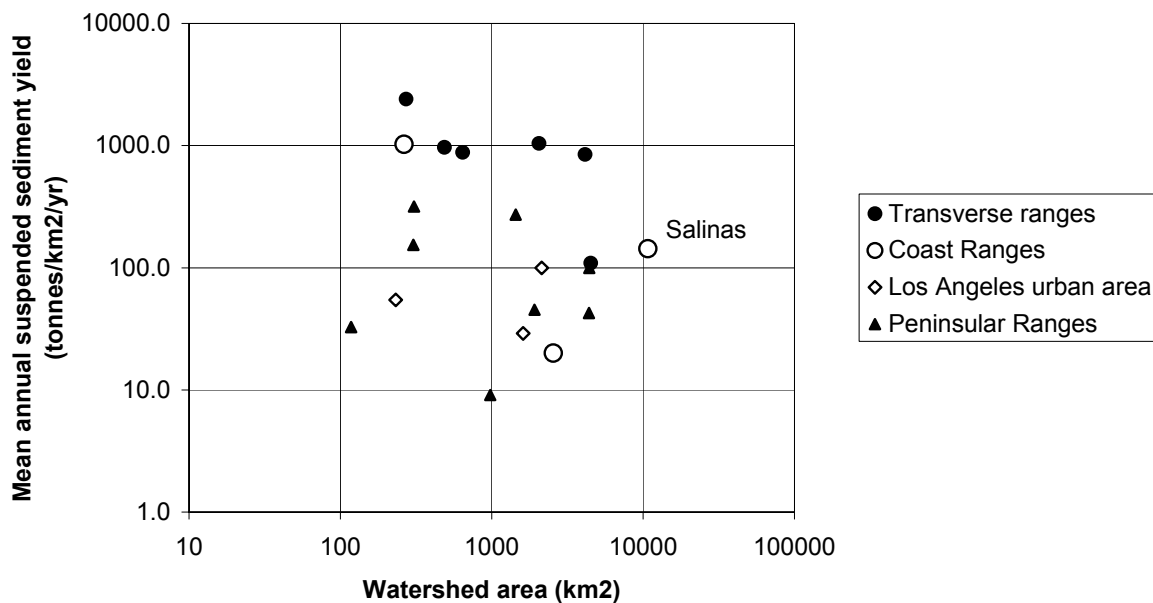
Figure 5.1. Mean annual suspended sediment yield for coastal California streams (data from Inman & Jenkins, 1999).

5.2 Channel degradation and aggradation

5.2.1 Definition and significance

Channel degradation and aggradation refers to long-term net scour or deposition of sediment in the streambed, such that the mean elevation of the streambed changes over time. By measuring degradation and aggradation, one can estimate the magnitude of processes relating to long-term storage of sediment in channels, to the role of the streambed as a source of sediment itself, and to the long-term dispersal of sediment waves.

Degradation of the channel can:
1. increase delivery of sediment downstream from the degrading reach;
2. lower the interface between the groundwater and stream, possibly leading to the lowering of the surrounding water table;
3. and consequently lead to loss of riparian vegetation due to movement of water out of the root zone.
4. Banks can become destabilized due to loss of root mass.
5. The channel can then widen and in the process deliver increased amounts of sediment due to increased bank erosion.

Aggradation of the channel can:
1. Cause increased flood potential due to loss of channel capacity.
2. Cause channel to widen to accommodate flows.
3. Increase bank erosion – thereby exacerbating the problem (positive feedback).

5.2.2 Methods

The USGS maintains stage-discharge curves for each gauging station by periodically making direct measurements of streamflow from time to time. These are recorded on USGS Form 9-207, which lists the width of flowing water (W), the cross-sectional area of flow (A), the water level stage, and the discharge – amongst other things. By dividing the cross-sectional area by the width of flowing water, we obtain a measure of the mean depth of flowing water. Subtracting this from the elevation of the water surface (WSE, the stage relative

to the gage datum) gives a measure of the mean depth of the streambed under flowing water ($\overline{BE}$):

$$WSE = Gage\ datum + Stage \tag{1}$$

$$\overline{BE} = WSE - \frac{A}{W} \tag{2}$$

The mean bed elevation will vary both with the degradation and aggradation of the bed, and with discharge. The effect of degradation and aggradation can be isolated by stratifying the data according to flow width. By examining just the data for narrow flow widths, the changes in thalweg elevation can be examined over time.

In the results presented below, mean bed elevation was computed as above for every USGS flow measurement made at each gage (typically between 200 and 700 measurements over several decades). The data were stratified by flow width and grouped by water year. Water years with less than three measurements within a given flow–width class were discarded. Flow–width classes pertaining to out–of–channel flow were also discarded, with channel–full flow being roughly estimated from plots of stage versus flow width. The remaining data were plotted as time series.

5.2.3 Results: Central Santa Lucia Range streams

Results for the Arroyo Seco River (ARR–ELM) and Big Sur River (BSU–BSU) are shown in Figure 5.3. A long–term streambed degradation of about 3 feet is evident in the Arroyo Seco River, interrupted by two distinct pulses of sediment. The second of these, in 1978, corresponds exactly with the first heavy rains following the Marble Cone fire, which burned almost the entire watershed in 1977. This aggradation event has been previously documented both at Arroyo Seco River (9 ft, Roberts et al., 1984, cited by Hecht, 2000) and the Carmel River (up to 1 ft, Hecht, 2001). The first pulse, in the early 1960s, is not so easily explained, for there were no fires in the Arroyo Seco watershed at time[10], nor were there any particularly unusual streamflow conditions. The site is just

---

[10] Source: GIS data downloaded from the California Dept. of Forestry and Fire Protection, Fire and Resource Assessment Program (CDF–FRAP), http://frap.cdf.ca.gov.

downstream from a large gravel mining operation. Future work should compare these streambed degradation data with mining extraction records.

The Big Sur River shares a watershed boundary with the Arroyo Seco River, and drains directly to the coast. Its was also heavily impacted by the Marble Cone fire, the effects of which are clearly revealed in the history of streambed elevations (Fig. 5.3). Other, smaller fires occurred in the watershed 1972 and 1996. The return to pre-fire trend at both sites appears to occur over about 3–5 years. This duration of sediment dispersal agrees with the duration measured by Sutherland et al. (2002) in the Navarro River of the northern California coast, where the dispersal of a single landslide input was tracked over 5 years in a gravel-bed stream. Note that these authors found no evidence of *translation* of the sediment wave, thus refuting notions that a sediment wave moves as a discrete 'slug' down a river.

Figure 5.2. The Arroyo Seco River just upstream of the gravel mine and Elm Rd gauging site. Photo: Fred Watson, 3 Oct 2002.

106
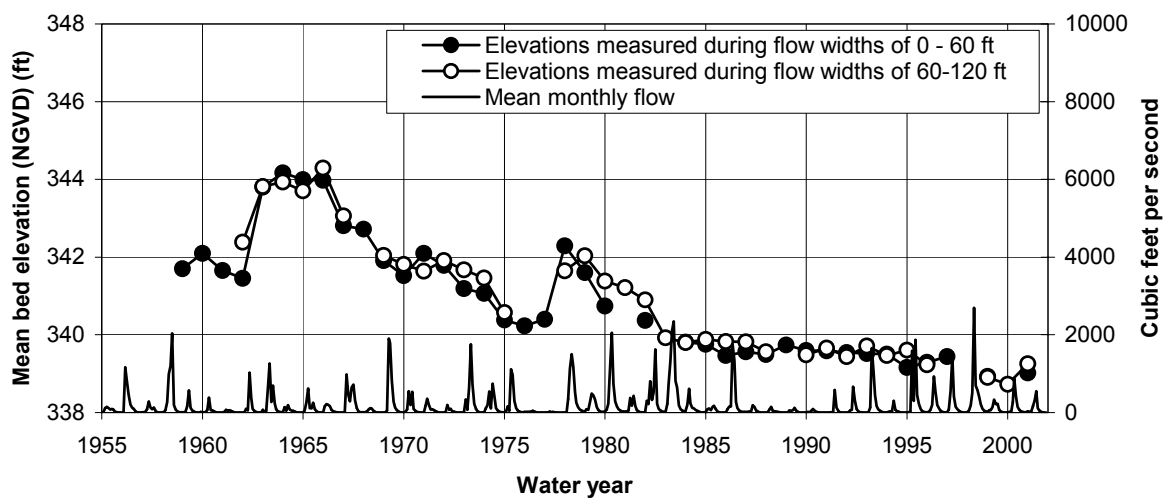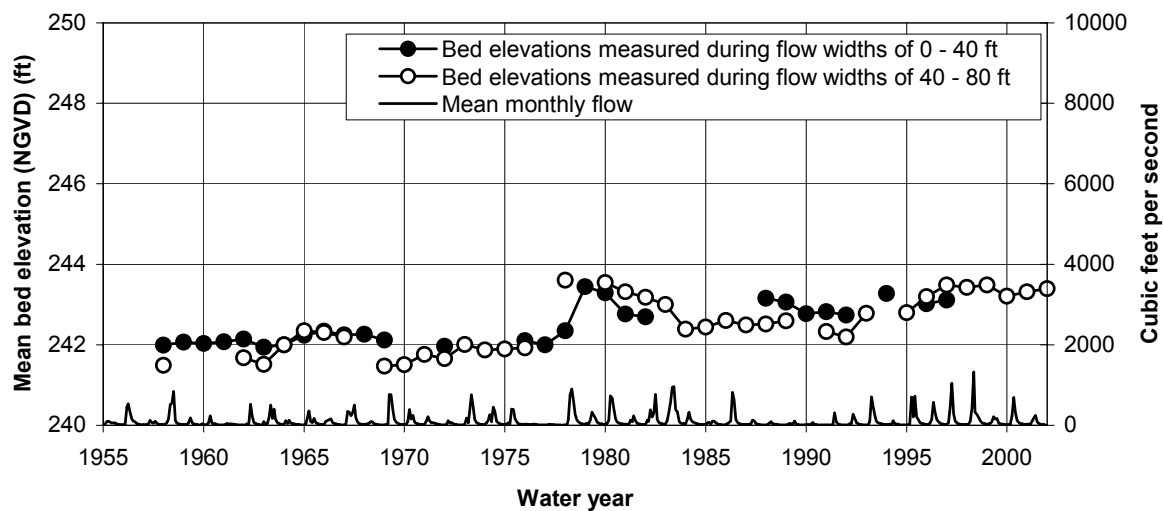
Figure 5.3. Annual streambed history for Central Santa Lucia Range streams, derived from width-stratified mean streambed elevation.

Figure 5.4. Fence (at left) partially buried by sediment after forest fires in the Santa Margarita Valley (southern Salinas Watershed). Photo: Fred Watson, Nov 2000.

5.2.4 Results: Southern Santa Lucia Range streams

In the southern Santa Lucias, online data were available for the Nacimiento River both upstream and downstream of Lake Nacimiento, and for the San Antonio River upstream of Lake San Antonio (Fig. 5.6). Both watersheds were burned over a wide area by the South Kirk fires in 1999, but streamflows have been diminished since that time. The unregulated San Antonio site (ANT–LOC) has been experiencing steady degradation of just over 1 foot per decade, and the unregulated Nacimiento site (NAC–SAP) has been stable. Downstream of the reservoir, the Nacimiento River channel (NAC–BLD) has been steadily degrading for the past 40 years at a rate of about half a foot per decade.

Figure 5.5. The uniform, sediment–starved cobble bed of the Nacimiento River below Lake Nacimiento. Photo: Thor Anderson.

a – ANT–LOC
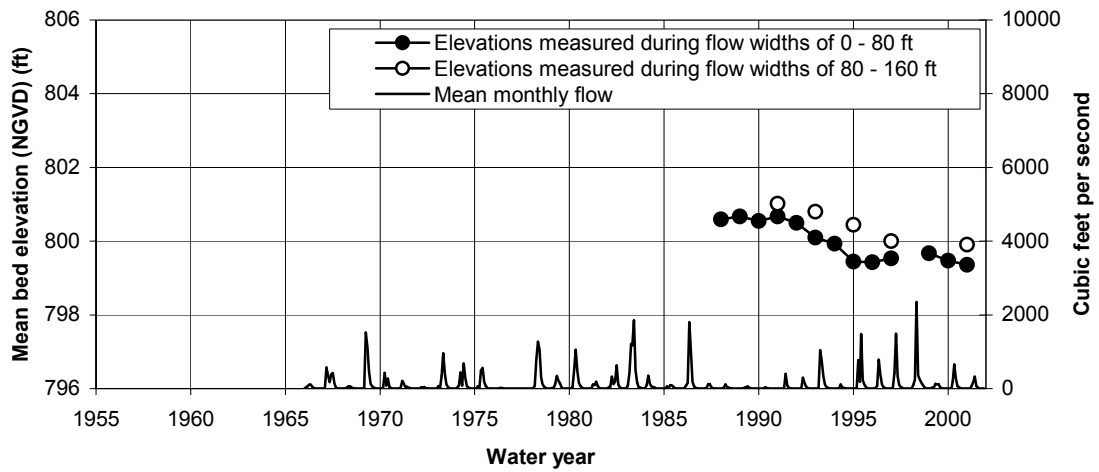
b – NAC–SAP
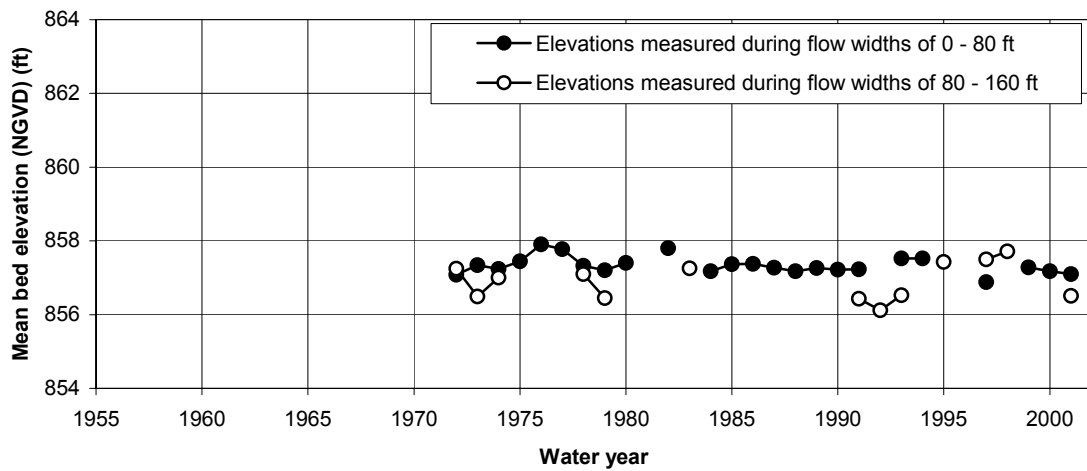
c – NAC–BLD
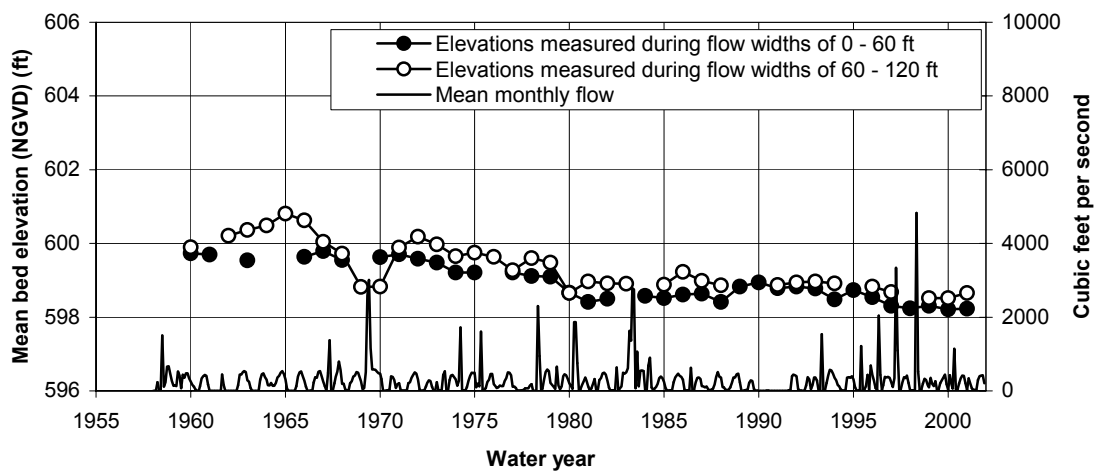
Figure 5.6. Annual streambed history for Southern Santa Lucia Range streams, derived from width–stratified mean streambed elevation.

5.2.5 Results: Gabilan Range streams

On the eastern side of the Salinas Valley, in the Gabilan Range, the situation is quite different to that in the Santa Lucias (Fig. 5.8). The gage on San Lorenzo Creek as it reaches the Salinas Valley (SLC–BIT) has been moved twice during the period of data, each time resulting in a discontinuity in the streambed elevation record (Friebel et al., 2001). However, aggradation of about 2 feet per decade is clearly evident in much of the period where the gage has been stationary. As with the Arroyo Seco River, the gage is immediately downstream of a gravel mining operation, which may explain the degradation and then stabilization of the streambed elevation in recent years. Future work should examine this, and also the cause of the severe degradation in the late 1970s.

A longer record is available for the San Benito River near Willow Creek School (SBR–H25). This site is outside the Salinas Watershed, but drains similar San Andrean terrain with mixed woodlands, grazing, and some dryland agriculture. Like San Lorenzo Creek, a steady aggradation of about 1 foot per decade is evident (interspersed with frequent moving of the gage and datum).

Figure 5.7. Gravel mining on San Lorenzo Creek, just above the USGS gaging site (left of image). Photo: Fred Watson, 3 Oct 2002.

a – SLC–BIT
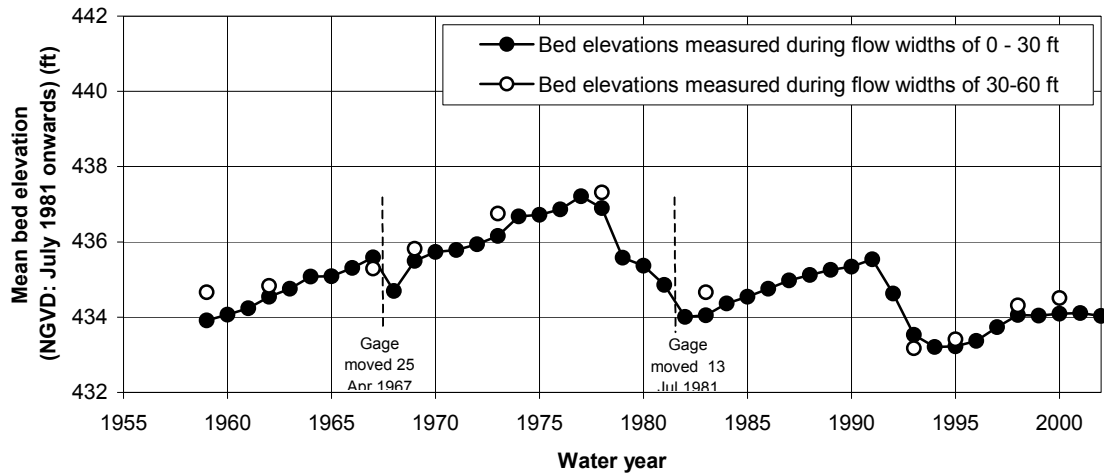
b – SBR–H25 (on same time scale as above)
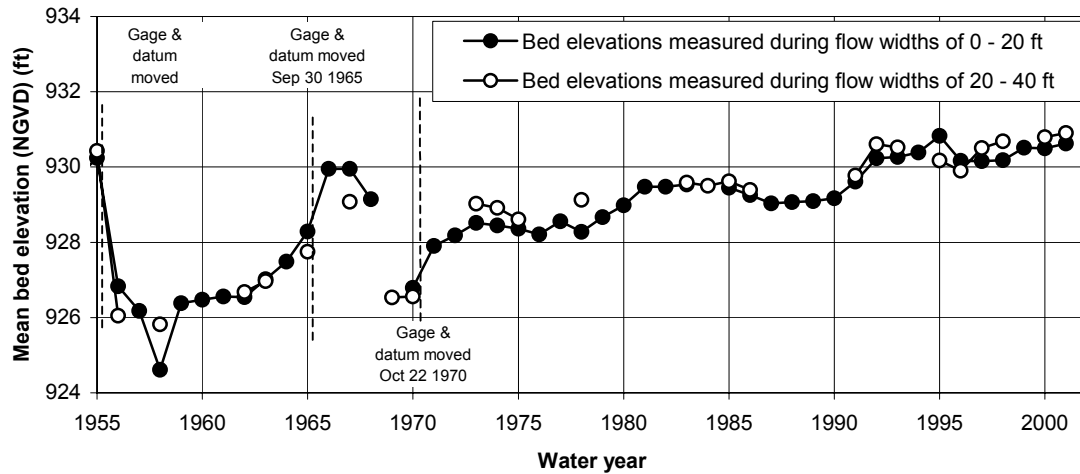
c – SBR–H25 (full time scale)
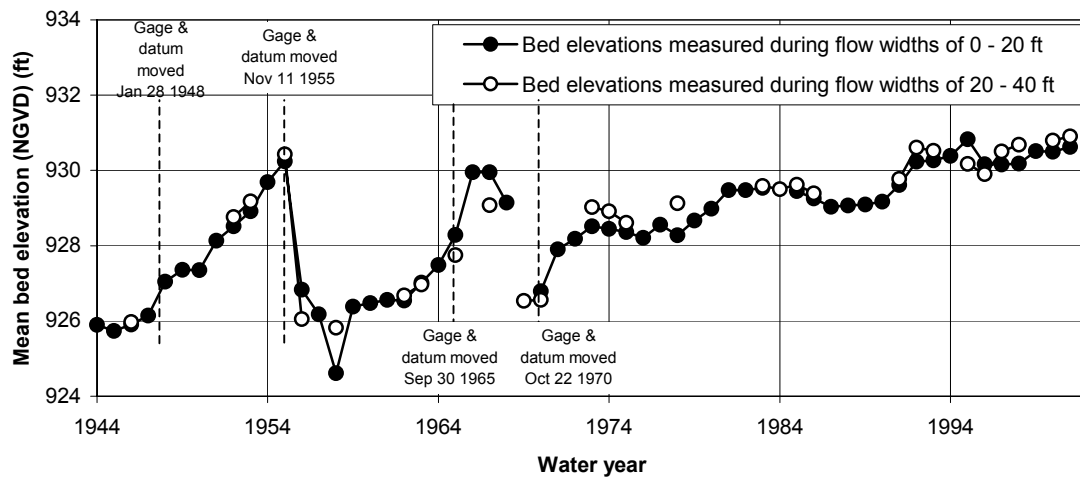
Figure 5.8. Annual streambed history for Gabilan Range streams, derived from width–stratified mean streambed elevation.

5.2.6 Results: Main stem Salinas River

By comparison with the tributary streams, the main stem of the Salinas River exhibits a lesser amount of long-term degradation or aggradation (Fig. 5.9). At Wunpost (SAL-WUN), about 10 km downstream from the sediment-hungry dam releases coming in from the Nacimiento and San Antonio Rivers, the Salinas River degrades about 1 foot per decade (see Fig. 5.10 for photographic evidence). During the 1995 floods, the annual degradation was higher than average, and a few years of aggradation then followed before the longer-term degradation trend was resumed. Degradation of streambeds below dams is well document both globally (Kondolf, 1997) and locally – in the Carmel River (Curry & Kondolf, 1983). Hampson (1997) reviewed data from the lower Carmel River indicating long-term degradation rates of 1 to 3 feet per decade.

Downstream at Soledad (SAL-SOL) and Chualar (SAL-CHU), the River gradient flattens out somewhat, and only the slightest long-term degradation is indicated from the relative short data set.

Finally, near the River mouth, the Spreckels site (SAL-SPR) exhibits no long-term trend. However, the streambed at this site has undergone considerable inter-annual change in elevation. In 1993, the channel degraded 2-3 feet, mainly in the innermost 100 feet of its width. Then, during the 1995, the wider sections (100-200 feet width) degraded while the inner sections (<100 feet) aggraded. Earth-moving operations in the years since 1995 are discussed in Section 5.2.8.
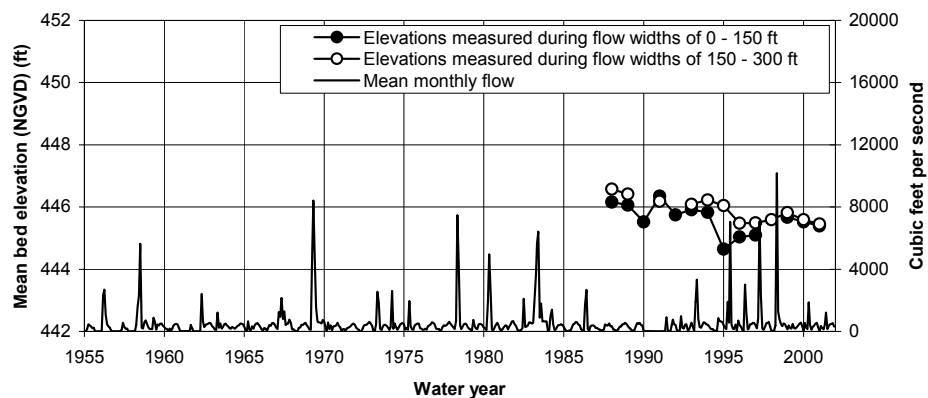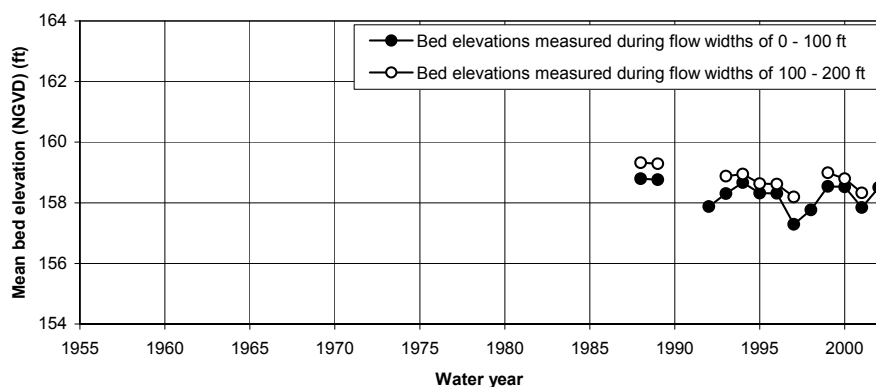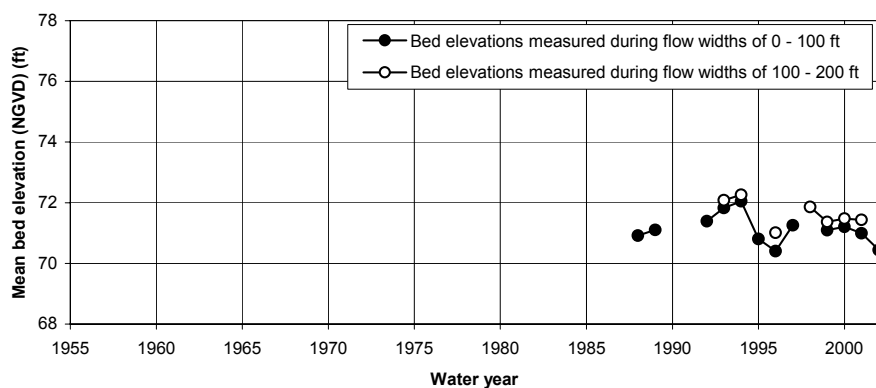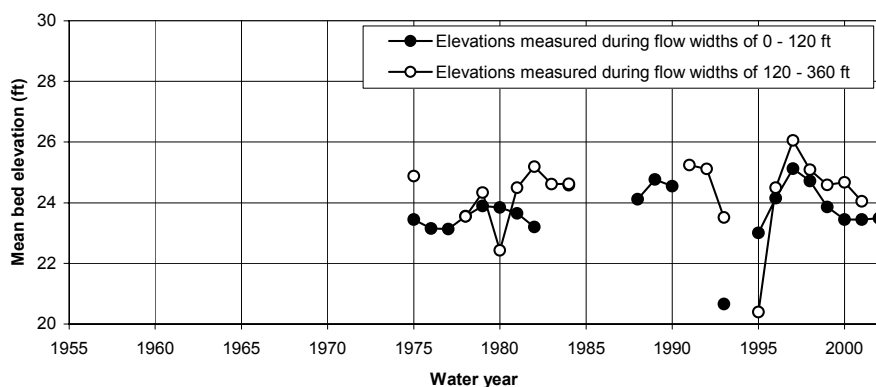
Figure 5.9. Annual streambed history for main stem Salinas River, derived from width–stratified mean streambed elevation.

Figure 5.10. The Salinas River a few miles upstream of San Ardo: in the early 1900s, and in late 2002. The most obvious change is the dramatic increase in riparian vegetation facilitated by summer irrigation releases from large dams just upstream (Lake San Antonio and Lake Nacimiento). The comparison also suggests significant channel incision, in agreement with channel scour analyses based on USGS flow measurements. Incidental changes include the construction of Highway 101 (foreground), and the San Ardo oilfield (background). Old photo: courtesy of U.C. Berkeley. New photo: Fred Watson, 3 Oct 2002.

5.2.7 Results: detailed analysis of Spreckels data

The Spreckels data are examined in more detail in Figure 5.11, which plots the mean streambed elevation associated with every measurement in the USGS data set for Spreckels (as opposed to averaging the measurements within water years). The measurements are color-coded into stream-width classes, so that elevation comparisons can easily be made between sections of similar flow width. Figure 5.11a shows the full record, and Figure 5.11b shows the period surrounding the late 1990s floods. Also shown is the water surface elevation, just above the streambed elevation.

Perhaps the most prominent feature of these more-detailed data is that during the instant of high flows, the streambed elevation drops 5 to 7 feet below the previous dry-weather level, and then rapidly almost regains that elevation once flow reverts back to dry-weather levels. Similar observations have been made elsewhere using scour pins (Pickup & Warner, 1976). During the high flows, the water surface elevation rises well above dry-weather levels. The implication is that the streambed is liquified during high flows, down to perhaps surprising depths, well beyond what can be seen in dry weather. For example, prior to 1995 a 0–50' wide flow in 1993 had a mean streambed elevation of 24 feet, as did a 100–150' wide flow in 1994. Then, in early 1995, 600–800' wide flows rose to flood the channel beyond its levees. In the weeks afterwards, the river returned to lie within its banks, but the 200–400' wide flows now passed over a mean streambed elevation as low as 17 feet. As the waters further subsided, a considerable amount of sediment was re-deposited where the liquified sediment once moved, for later that year, 50–200' wide flows moved over a mean streambed elevation of between 22 and 24 feet. The mild storms of 1996 brought 300–400' wide flows again, but this time at a much higher bed elevation of 24–27 feet. The next time the river flow was measured at less than 50' wide flow, was a year later, in 1997, at a mean streambed elevation of 25 feet.

Complimenting the observation of high flows scouring the channel which is then re-filled in the following year, are observations made during prolonged periods where flushing flows are absent. An example is the late 1980s, where no large flows occurred for many years, and the streambed reached its highest sustained narrow-width elevation.
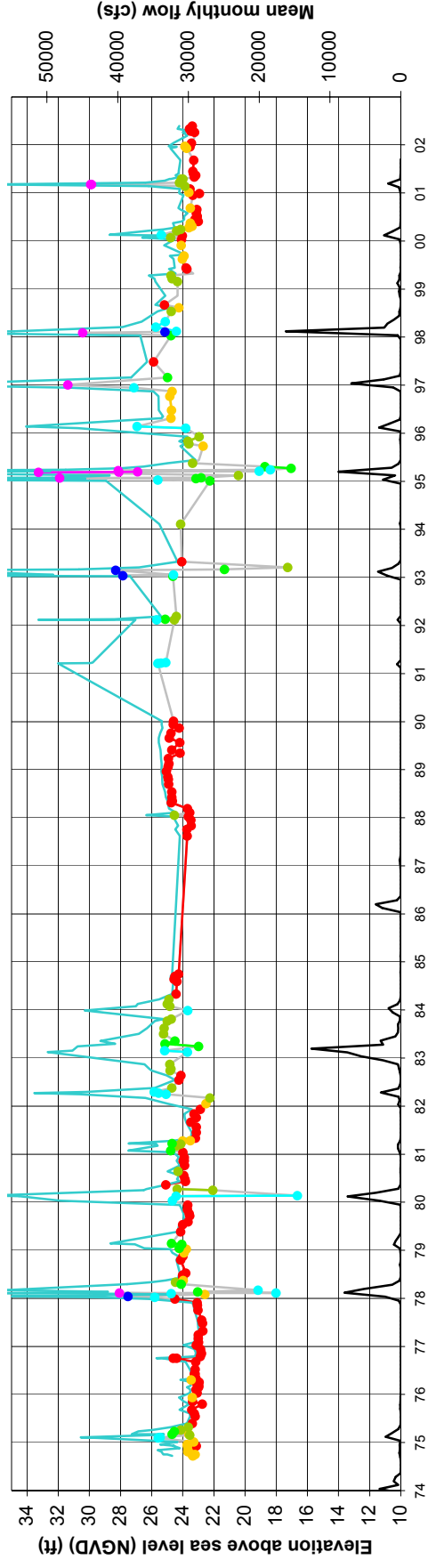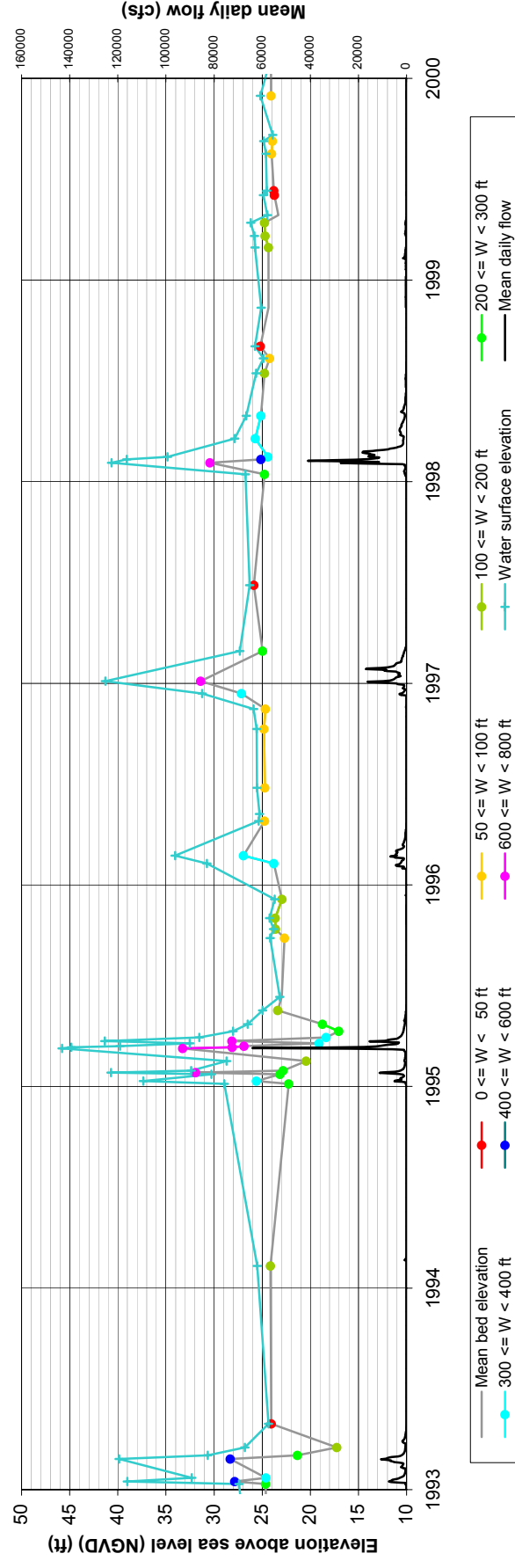
Figure 5.11. Streambed history at SAL-SPR, estimated using discharge-rating-curve anomalies.

5.2.8 Channel maintenance using earth–moving equipment

Previous sea water levels in the Holocene were lower than at present, leading McGrath to conclude that the present flood plain is a primarily depositional landscape that has aggraded to its current level in recent geologic history. Current human activity works against this natural cycle. Since the 1995 floods, landowners along the lower reaches of the Salinas River have operated under the banner of the Salinas River Channel Coalition to minimize the risk of flooding on agricultural lands by using earth–moving equipment in the river channel (Fig. 5.12). Their permits do not allow levees to be increased. Rather, the aim is to improve the efficiency of the existing channel by bulldozing vegetation and accumulated sediment from the bottom of the channel towards its sides. In terms of hydraulic routing, this amounts to an increase in the hydraulic radius and a decrease in the roughness, or resistance to flow. In theory, a given discharge should then be able to be conveyed by the channel at a lower water surface elevation. The procedure is contentious, because of its destructive impacts on flora and fauna of the riverbed, and potentially on the passage of endangered steelhead trout. Grading must now occur away from a seasonally staked–out low–flow channel that meanders within the main channel.

Figure 5.12. Channel grading and vegetation removal for flood control – Salinas River at Spreckels. Photo: Thor Anderson, Fall 2000.

The significance of in-stream habitat in the Salinas River is poorly defined. Its natural historic context is one of periodic deep scour and destruction of benthic habitat, with intervening periods where seasonal aquatic ecology may play an important role in the life cycles of species such as the steelhead trout (Snyder, 1913). The best management of the channel bottom is not readily evaluated without a solid understanding of its stream ecologic values.

Of interest to the present work is the efficacy of the flood-control grading itself. Figure 5.15 plots the width of flowing water surface at which measured streamflow discharges have been carried during the period of the USGS data set at Spreckels. At a given discharge, a narrow width implies an efficient channel, and a wide width implies an inefficient one. Flooding is minimized if discharges larger than about 10,000 cfs can be carried at flow widths less than about 500 feet. A closer examination of higher flows in given in Figure 5.16.

Examining Figures 5.15 and 5.16 in detail, it can be seen that between the 1970s and the 1980s, the river became less efficient (wider flows) in its conveyance of discharges between about 10 and 1000 cfs, and slightly more efficient at carrying higher flows (>10,000 cfs). This is consistent with a channel cross-section changing from more triangular to more rectangular. However, in the early 1990s, all discharges above 1000 cfs spread water over a wider surface than was previously the case. A high flow in 1993 was slightly wider than a flow of similar magnitude in 1980. By the time of the 1995 event, flood flows in the 10,000 to 20,000 cfs range widened to over 750 feet, where before they had been contained within 350 to 550 feet. Agricultural land was inundated. After a few years of channel maintenance through grading activities, similar flood flows in 1997 and 1998 were narrowed to 400 feet again, indicating that the grading had achieved its purpose. Most recently, however, the width of 10,000 to 20,000 cfs flows has again widened to over 600 feet in 2001. More-detailed analysis is required in order to explain this, and to more closely relate channel changes to both fluvial and mechanical causes.

Figure 5.14. The Salinas River at Chualar River Road in summer (looking north). Photo: Fred Watson, Oct 1999.

Figure 5.14. The Salinas River at Chualar River Road during high flow in winter (looking north). Photo: Fred Watson, 11 Feb 2000.
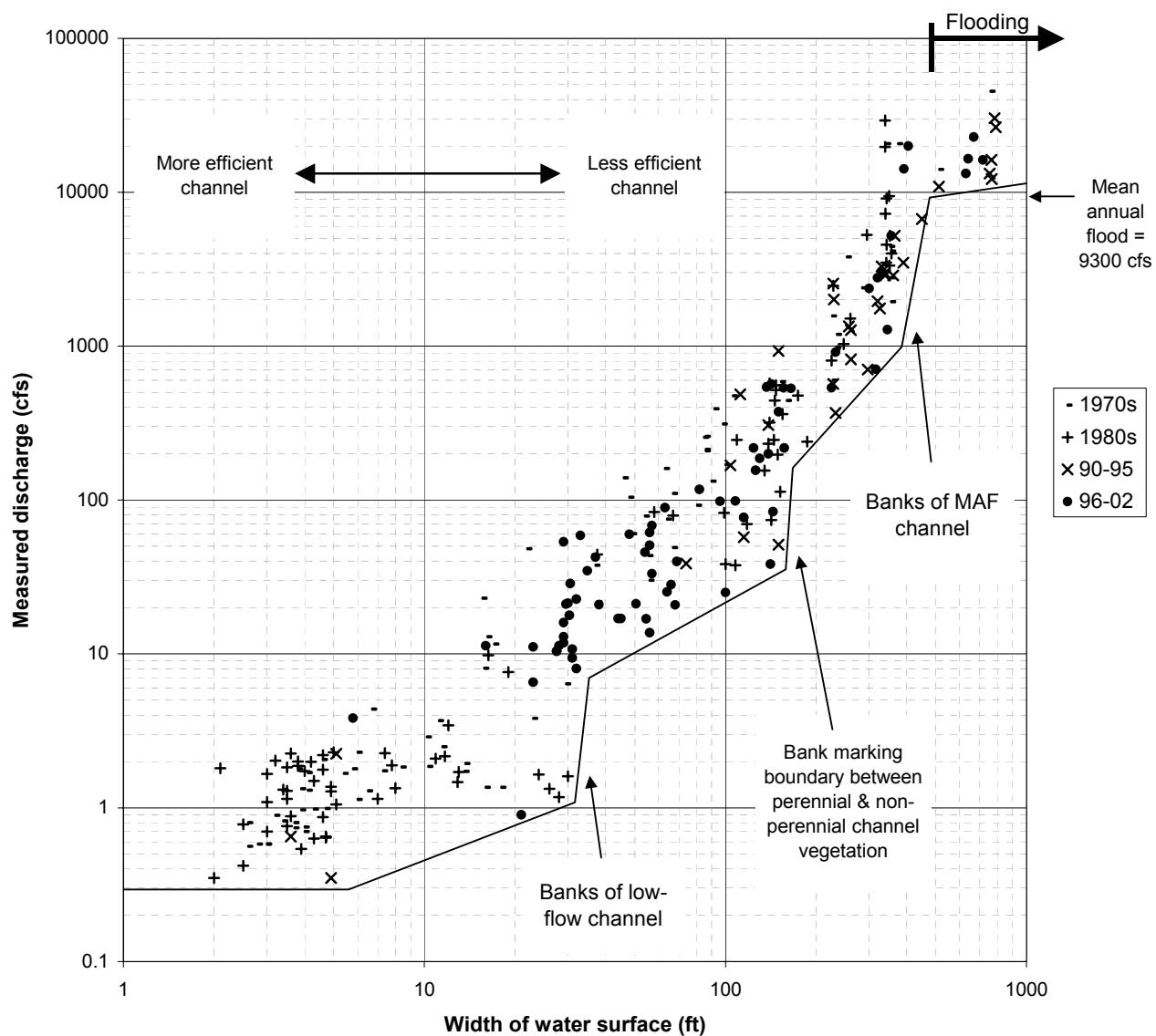
Figure 5.15. Changes over time in the width of flowing water surface required to carry given streamflow discharges – Salinas River at Spreckels (SAL–SPR).
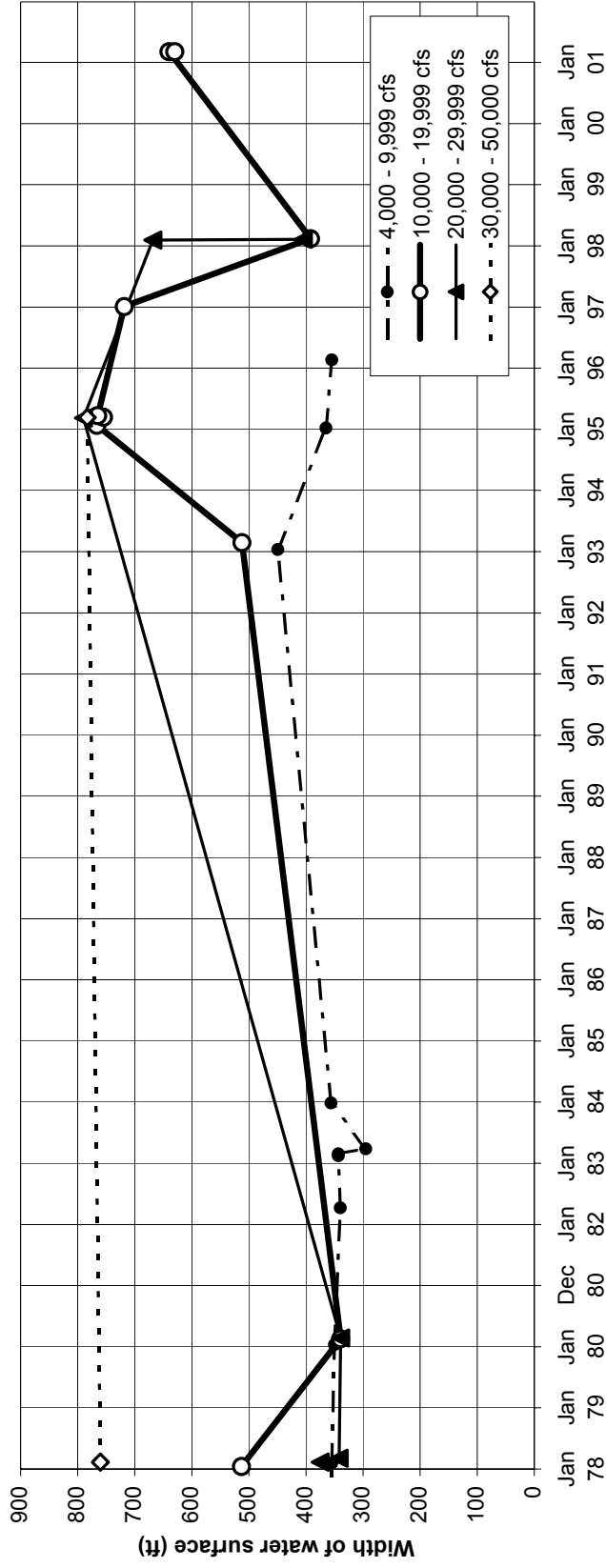
Figure 5.16. Changes over time in the width of flowing water surface required to carry large streamflow discharges – Salinas River at Spreckels (SAL–SPR). NB: flood flows are approximately those above 10,000 cfs.

5.2.9 Channel sediment storage

Long-term degradation and aggradation in the streams of the Salinas Watershed has been observed previously. McGrath (1987), reporting USGS data, noted that channel scour of approximately 4 feet occurs in the main Salinas River channel. This broadly concurs with the present analyses. In the main stem, there is evidence for a cycle of scour during large flow events, balanced by deposition in the intervening periods – this being a previously recognized phenomenon (Leopold et al., 1964).

Changes in channel sediment storage resulting from scour and deposition are a major component of the sediment budget of the watershed. The main stem of the Salinas River below Paso Robles Creek near Templeton is approximately 200 km long. The total mass of mobile sediment in this reach may be roughly, but conservatively estimated as 5 million tonnes – assuming, for the moment, a 50 m width of mobile bed material, a mobile depth of 0.25 m (9.8 inches), and a bulk density of 2 tonnes/m^3. The total mobile bed sediment in the main stem is thus more than twice the mean annual load. An implication of this conclusion is that not all the bed is mobilized and transported to the ocean in an average year. The residence time of a given slug of bed sediment is hypothesized to be many years. The best evidence for this is perhaps the fact that the streambed elevation of rivers such as the Arroyo Seco and the Big Sur is raised immediately after large fires, and gradually declines thereafter over many years.

5.3 Episodicity of suspended sediment load

While the Salinas Watershed contains small areas of moist climate, its dominant characteristics are more akin to dryland rivers – including high temporal and spatial variability of sediment yield (Inman & Jenkins, 1999; Tooth, 2000). Sediment transport in the Salinas Watershed is highly episodic. Table 5.1 lists the 10 largest daily loads on record at two sites in the watershed. During 8 years of USGS record, over half the sediment transport at Spreckels occurred during just 6 days. Similarly, half the 19-year total load of Arroyo Seco at the National Forest campground was passed in just 10 days.

The time series of estimated annual total suspended sediment yields at SAL–SPR and ARR–CAM (Fig. 5.17) shows variation over more than five orders of magnitude (237,000x) between the lowest and highest annual yields.

5.4 Natural causes of extreme loads

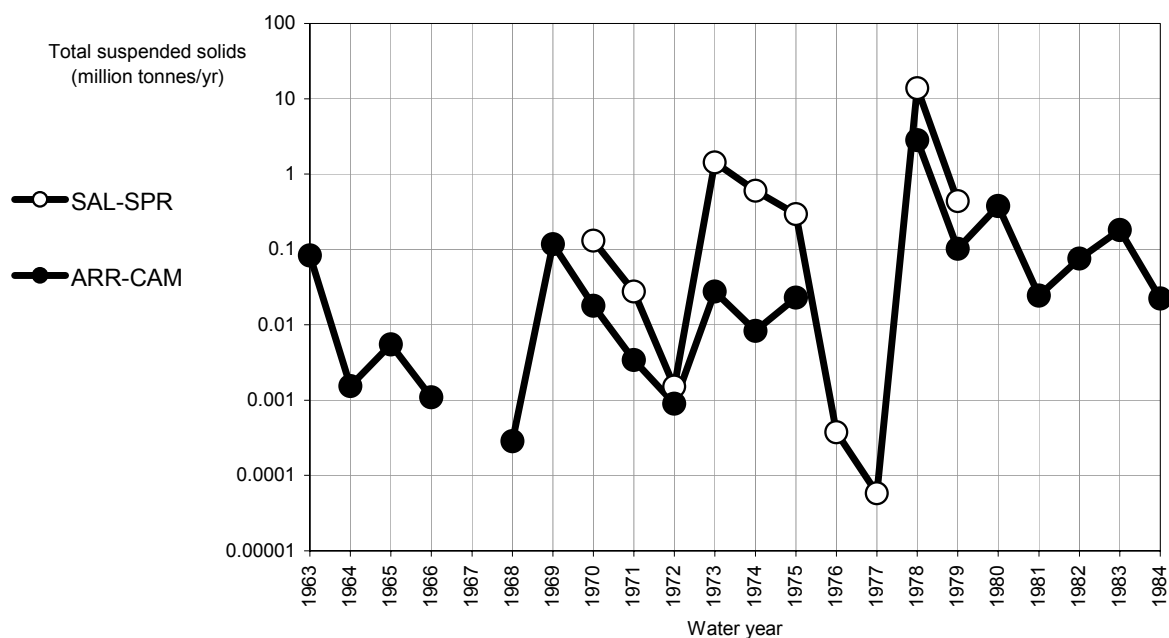The largest ten daily loads at each of the above sites occurred in the winter of

Figure 5.17. High variability in total annual suspended sediment loads in the Salinas Watershed.

1977/8. This was the first winter following the Marble Cone Fire in July 1977.

This fire remains the largest in California since 1932, having burnt 719.8 km^2 (177,866 acres) of wilderness (CDF, 2002), some of it in the upper Arroyo Seco watershed. Figure 5.18, taken after the Kirk Complex fire in 1999, illustrates the massive soil erosion that occurs during the first few rains after intense fire.

The large loads of 1977/8 cannot be explained by heavy rains alone. The effect of fire is strongly implicated. Figure 5.19 plots suspended sediment concentration versus stream discharge at ARR–CAM. Days from the 1978 water year are plotted separately, showing that larger stream discharges occurred in years other than 1978, but did not produce the largest concentrations or the largest sediment loads. A marked increase in sediment concentration occurred during 1978, irrespective of stream discharge. The estimated suspended sediment yield was more than 100,000 tonnes/day for 11 days spread throughout the 1977–78 winter (see also Figures 5.20 and 5.21). The total for the top ten days (Table 5.1) was 2.06 million tonnes. From Figure 5.19, it is estimated that concentrations were approximately ten times higher for a given discharge than in other years, suggesting that the Marble Cone fire caused something on the order of two million tonnes of suspended sediment to be delivered from the Arroyo Seco watershed. This is more than the mean annual suspended sediment yield of the entire Salinas Watershed. The fire was caused by a sequence of natural events, including snow (breaking branches off trees on 3 Jan 1974), drought, and culminating in lightning (Griffin, 1978). Neighboring tributaries of the Salinas River may have been similarly affected, as evidenced by

SAL-SPR	Years of record 8		ARR-CAM	Years of record 19	
Date	10 largest daily suspended solids loads (megatonnes/day)	Cumulative percentage of total record	Date	10 largest daily suspended solids loads (megatonnes/day)	Cumulative percentage of total record
11-Feb-78	2.67	16.0%	7-Feb-78	0.41	10.5%
14-Feb-78	1.92	27.5%	16-Jan-78	0.25	17.0%
5-Mar-78	1.91	38.9%	14-Jan-78	0.23	22.9%
12-Feb-78	0.83	43.9%	6-Feb-78	0.22	28.5%
6-Mar-78	0.83	48.8%	4-Mar-78	0.20	33.6%
13-Feb-78	0.69	52.9%	5-Jan-78	0.14	37.2%
10-Feb-78	0.44	55.6%	22-Dec-77	0.13	40.5%
15-Feb-78	0.40	58.0%	23-Dec-77	0.13	43.8%
17-Jan-78	0.35	60.1%	12-Feb-78	0.13	47.0%
4-Mar-78	0.33	62.1%	9-Feb-78	0.12	50.2%

Table 5.1. The 10 largest daily suspended sediment loads on record in the Salinas River, and the upper Arroyo Seco River.

the record suspended loads observed at Spreckels that year. Similar impacts of the fire have been demonstrated elsewhere in the Santa Lucia range using reservoir sedimentation analysis (Hecht, 1981).

Figure 5.18. Deep erosion of wilderness slopes following the 1999 Kirk Complex fire in the Ventana Wilderness. Photos: Fred Watson, Oct 2000.
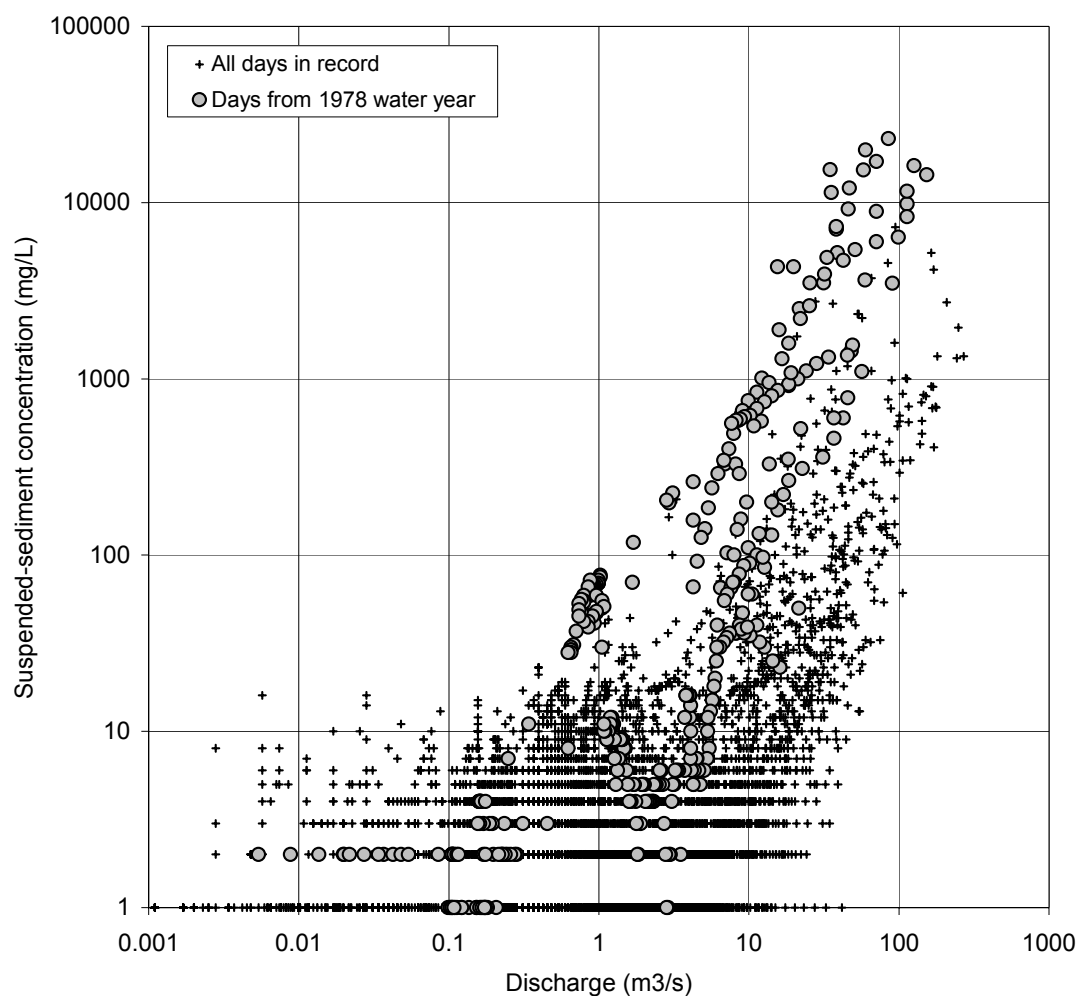
Figure 5.19. Sediment rating curve for Arroyo Seco at the National Forest Campground (ARR-CAM), with the post-fire year 1978 highlighted.
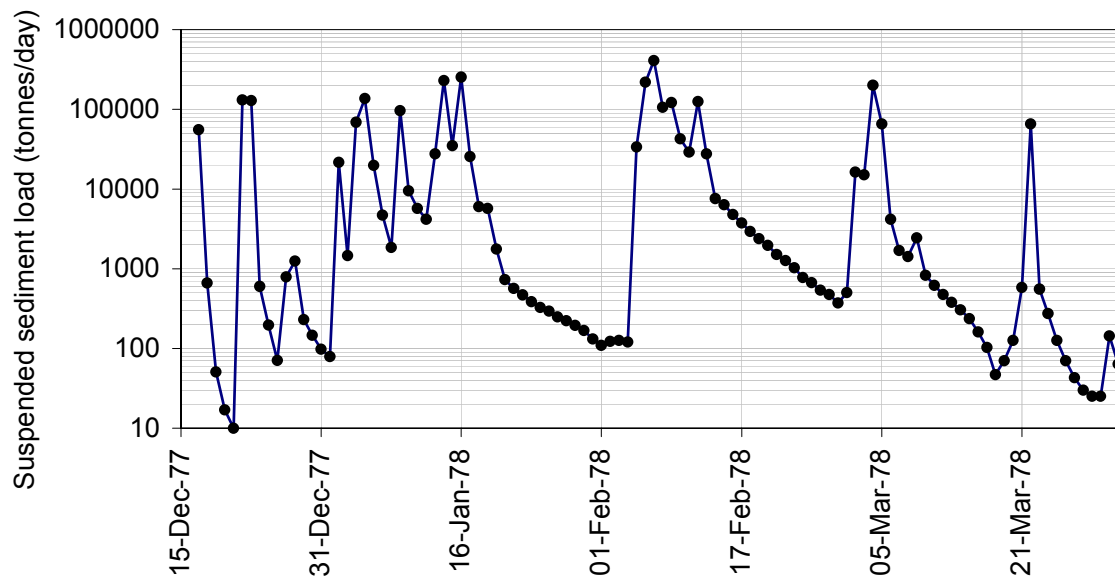
Figure 5.20. Time series of estimated suspended sediment load at ARR–CAM – winter of 1977–78.
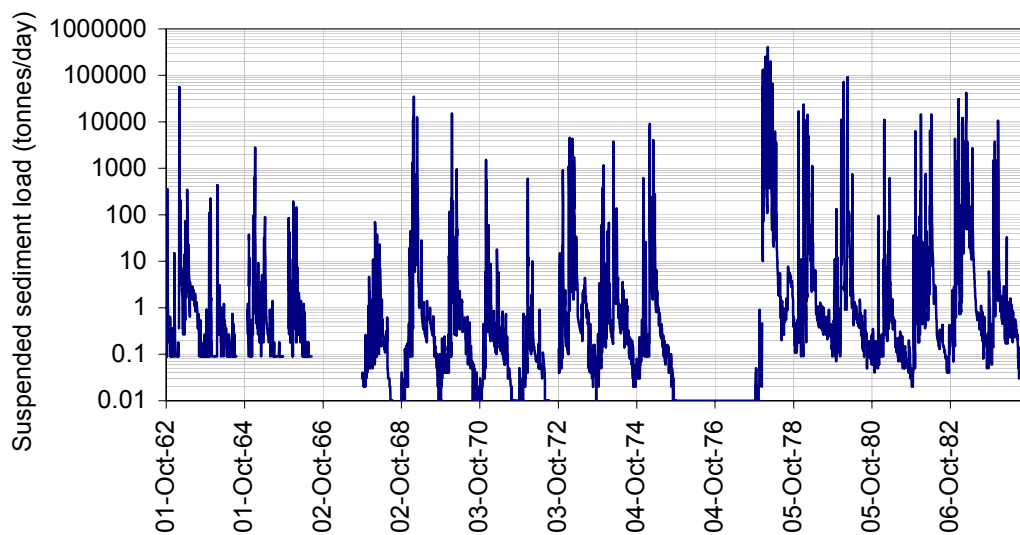

Figure 5.21. Time series of estimated suspended sediment load at ARR–CAM.

5.5 Spatial variability of suspended sediment load

The spatial distribution of sediment sources is highly variable. The USGS station on Arroyo Seco at the campground (ARR–CAM) drains an area only 2.8% of the size of the full Salinas watershed measured at Spreckels (SAL–SPR). Yet ARR–CAM contributed 60% of the annual load measured at SAL–SPR in 1972, and just 1.4% of the Spreckels load in 1974 (Fig. 5.22).
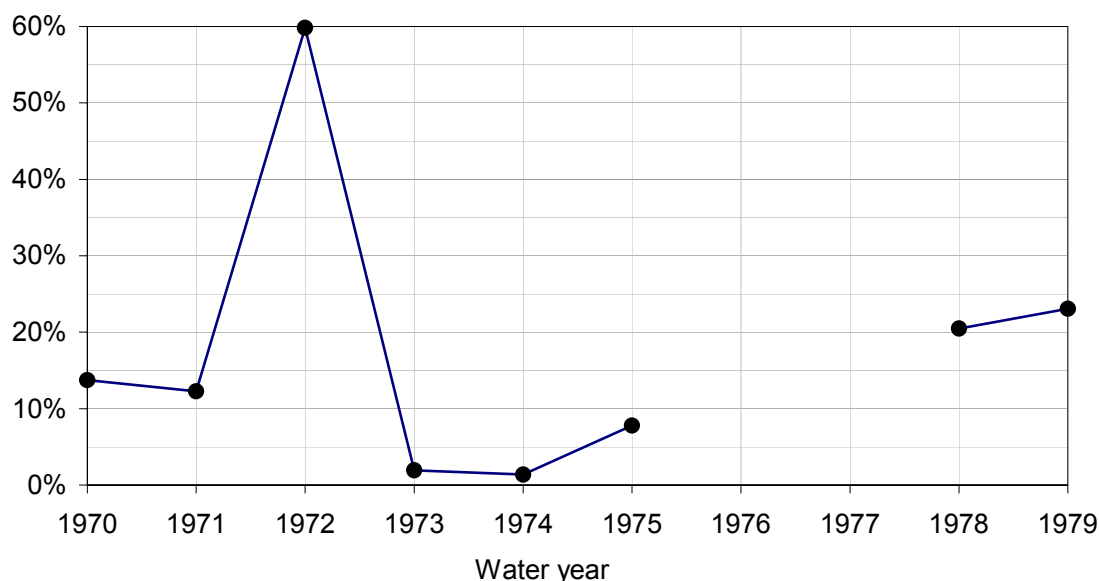

Figure 5.22. Annual suspended sediment load contribution from ARR–CAM, as a fraction of the total load near the mouth of the watershed at SAL–SPR.

This is problematic for sediment management, because localized areas of high sediment yield may just be transient phenomena, and not indicative of symptomatic problems with land use in the corresponding watersheds. There is evidence in the region that in–channel storage of sediment may persist for many years before a given parcel of sediment is finally delivered to the ocean (Curry & Kondolf, 1983).

6 Regional analysis of non-flood loads

The present study was motivated by the requirement to establish a Total Maximum Daily Load (TMDL) for sediment in the Salinas River. Part of the process is an analysis of the sources of sediment in the Salinas River. The present chapter forms the basis of this source analysis.

6.1 Review of techniques for spatial mapping of sediment load

Perhaps the most useful piece of information for sediment management of large landscapes is a map of sediment sources. This is also one of the most difficult pieces of information to obtain. A variety of techniques have been demonstrated.

The Universal Soil Loss Equation (USLE) approach (Renard, 1997) predicts erosion from the land based on maps of the governing parameters, such as rainfall, soil type, land cover, and land use. It is calibrated against numerous plot scale measurements of soil erosion, primarily centered in the eastern United States. It does not, however, take into account gully erosion or in-stream deposition and storage processes, and so cannot be used to estimate sediment sources at large scales (Trimble & Crosson, 2000).

A more recent approach is the use of radionuclide and other tracers (e.g. Olley et al., 1993). This can be applied by using simple numerical mixing models to infer the respective tributary contributions to sediment below a confluence by looking at ratios between specific natural radionuclides such as ^{226}Ra:^{232}Th and ^{40}K:^{232}Th, derived in turn from differences in tributary geology (Wallbrink & Fogarty, 1998). Similarly, the anthropogenic nuclear-testing tracer, ^{137}Cs, can be used to infer a recent soil-derived origin for sediment samples in stream channels. Tracer techniques have advantages relating to utility in measuring the integrated effect of all processes occurring on time-scales longer than typical stream monitoring programs, and consistent with time scales of in-channel sediment storage. The methods rely on the existence of clear radionuclide signatures in the various parts of a watershed. These signatures have a limited resolution, and so tracer studies should be used in conjunction with other approaches.

The most direct approach to quantifying the watershed-scale transport of sediment is to work with actual measurements of sediment load in streams. Ideally, one would have long-term daily records of streamflow and sediment concentration at multiple sites. A map of sediment sources could then be constructed by computing daily load as the product of flow and concentration and summing over many decades of record to provide estimates of the mean annual load at each gauged site. In practice, although many sites are gauged for flow, too few sites have daily sediment data, and the only maps that can be constructed are done so at continental (Church, accessed 2002) or global (Walling, 1994) scales, or as small studies at the scale of a few 10's of km^2 (the Salinas Watershed, by contrast, is 10,730 km^2 at Spreckels).

A compromise to the direct approach is a statistical manipulation of direct in-stream measurements of flow and sediment concentration. Shen and Julien (1993) term this the "flow duration – sediment rating curve (FDSRC) method" (see also, USACE, 1989). This involves estimating long term average load from the area under a load duration curve (LDC) (a plot of sediment load versus the percentage of time that the instantaneous load less than that value). Firstly, a sediment-rating curve (SRC) is constructed by fitting a simple equation (usually a power function) to a plot of measured sediment concentration versus measured streamflow. Suspended sediment data are usually used, as bedload data are rare. A flow duration curve (FDC) is then computed from the observed flow record using standard hydrological techniques (Gordon et al., 1992). The LDC is the product of the FDC and the SRC. The area under the LDC is the long-term average load, provided the record is long enough to contain the largest expected daily loads.

The FDSRC method is attractive because it makes good use of plentiful flow data, and of often scant sediment concentration data that may be biased toward the measurement of sediment during either dry or wet periods. It relies on a long flow record, unbiased toward small or large events. It assumes that a well-determined SRC exists, with not too much scatter about the fitted line relating sediment concentration to flow. It remains, however, subject to sampling bias introduced for example when all sediment data for a site were affected by a specific event like a fire or gravel mining activity.

6.2 The RLDCL method: overview

A similar method is introduced here, which we term the "regionalized load duration curve LOWESS" method (RLDCL). The method is derived from the FDSRC method of computing load statistics from direct measurements of flow and sediment concentration. The method extends the FDSRC method by regionalizing FDCs to estimate flow regimes for infrequently gauged sites, and by using LOWESS smoothing (see below) to remove non-uniformity effects in the fitting of SRCs to sites with larger concentration-flow records. This results in the ability to statistically estimate long-term sediment load regimes for many more sites in a landscape than would otherwise be possible. It only estimates loads for sites that have, at least some, actual field measurements of sediment concentration and flow, but it does not require that a long term flow gaging record exists for each site. The accuracy of the resulting load estimates increases as more sediment-flow measurements are made at each site over time.

The tenets of the method are:

- short-term sediment analyses are misleading
- sediment regimes can only be characterized by taking account of long-term patterns
- long-term flow regimes can be regionalized by simple geographic translation of flow records after accounting for slight changes in watershed area (see Section 4.7)
- sediment concentration data cannot be regionalized in heterogeneous landscapes
- site-specific sediment concentration & flow data can be combined with regionalized flow regime data to estimate site-specific sediment load regime data

6.3 The RLDCL method: development of sediment rating curves

6.3.1 Sediment rating curves for USGS data

A typical record of sediment concentration versus flow data is shown in Figure 6.1a for the USGS station at Santa Rita Creek near Templeton (RIT-TEM) (47 km²). The data, plotted on logarithmic axes show a typical indeterminate scatter

at low flow, rising to a relatively well-defined relationship between concentration and flow for flows greater than about 1 m³/s (35 cfs). It is conventional to fit power functions to such data, as these are the most accepted form for sediment transport capacity relationships (Julien & Simmons, 1985; Prosser et al., 2001). Power functions have previously been fitted to Salinas data (Inman et al., 1998). In this case, a 3-parameter power function has been fitted. The three parameters, scale, offset, and power, control respectively: the overall magnitude of the curve, the asymptotic minimum SSC concentration, and the slope of the increase of SSC with discharge:

$$C = Scale \left(Q + Offset \right)^{Power} \tag{3}$$

An optimal fit was achieved by linearizing the power function, and using a secant optimization scheme to maximize the R-squared of the resulting 2-parameter linear regression through alterations of the third parameter. The resulting equation for RIT-TEM is:

$$C = 32.02 \left(Q + 0.2133 \right)^{1.478} \tag{4}$$

The problem with this regression fit, and with many others one encounters in the literature, is that the data are non-uniformly distributed (many more low flow data than high flow data), and their variance is heteroskedastic (more variant at low flow than high flow). Apart from precluding any statistical conclusions we may wish to draw from our 'line of best fit', this strongly biases the location of the fitted line to match low flow data. It can be see from the Figure that the 'line of best fit' is consistently misaligned with (higher than) the data for the highest, and most important 8 data points.

Point for point, the high flow data are much more important to long-term load estimation than the low flow data. This fact has been illustrated in Section 5.3, and is especially true when considering that the high flow values have already been de-emphasized by the logarithmic scale used to linearize the relationship.

Given this poor result, an objective scheme must be sought that effectively re-samples the original data set to give equal weight to data from all magnitudes of (in this case log) flow, rather than all points in time. A LOWESS smoothing (Cleveland, 1979; Hirsch et al., 1993) accomplishes this, as shown in Figure 6.1b. The smoothing algorithm is a computationally intensive scheme that

iteratively fits linear regression lines to overlapping, windowed subsets of the data and combines these to produce a single, objective line of best fit. The Tarsier environmental modeling framework (Watson et al., 2001) was used to compute both LOWESS and power function fits in the present work. The outcome can be manipulated by choice of a single 'tension' parameter, in this case 0.3, that controls the smoothness of the line. Figure 6.1b shows that the LOWESS fit is more faithful to the data than the 3-parameter power function (Fig. 6.1a). This is not surprising, as the LOWESS fit has considerably more degrees of freedom (one for each original unique data point) than the three parameters of a single regression line. LOWESS is a more sophisticated and objective technique for dealing with non-uniform regression than previous techniques applied to the Salinas River data, such as piecewise loglinear regression as used by Farnsworth (2000).

It is, however, convenient, and informative to be able to derive a simple equation for the sediment-rating curve. Therefore, in Figure 6.2a, a 3-parameter power function has been fitted in turn to the LOWESS fit. The power function is able to reproduce all of the well-determined variance in the LOWESS fit, and achieves a simple, 3-parameter representation of the original data that is objective, and now unbiased with respect to (the logarithm of) flow magnitude. The two power functions are compared in Figure 6.2b, which shows that the better match throughout the full range of data points achieved by the LOWESS-derived power function. The empirically derived equation for this function for the RIT-TEM data is:

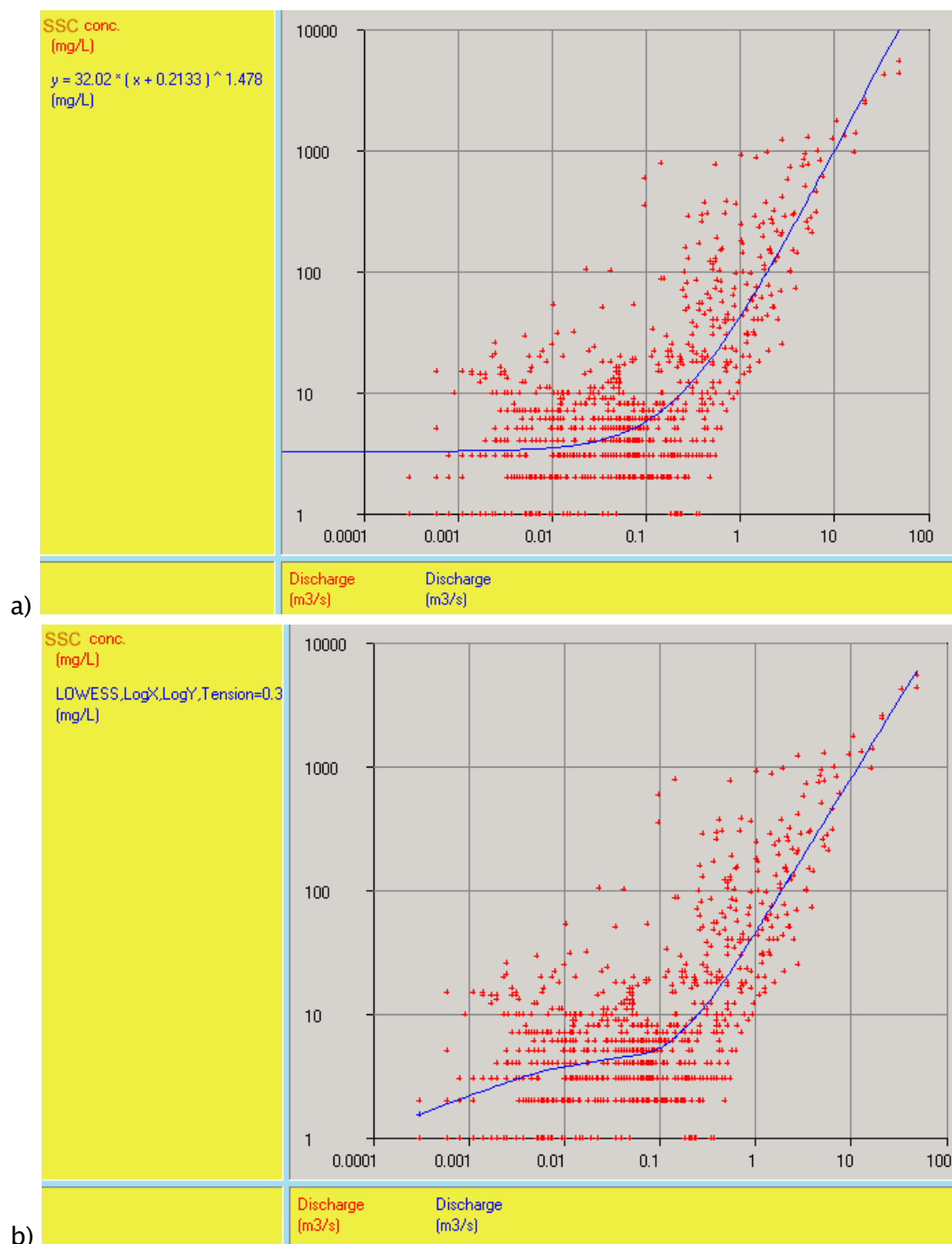$$C = 39.35 \left(Q + 0.123 \right)^{1.297}$$
(5)

Figure 6.1. USGS sediment concentration versus flow (discharge) at Santa Rita Creek near Templeton (RIT–TEM): a) with power function sediment rating curve fitted; b) with LOWESS sediment rating curve fitted.
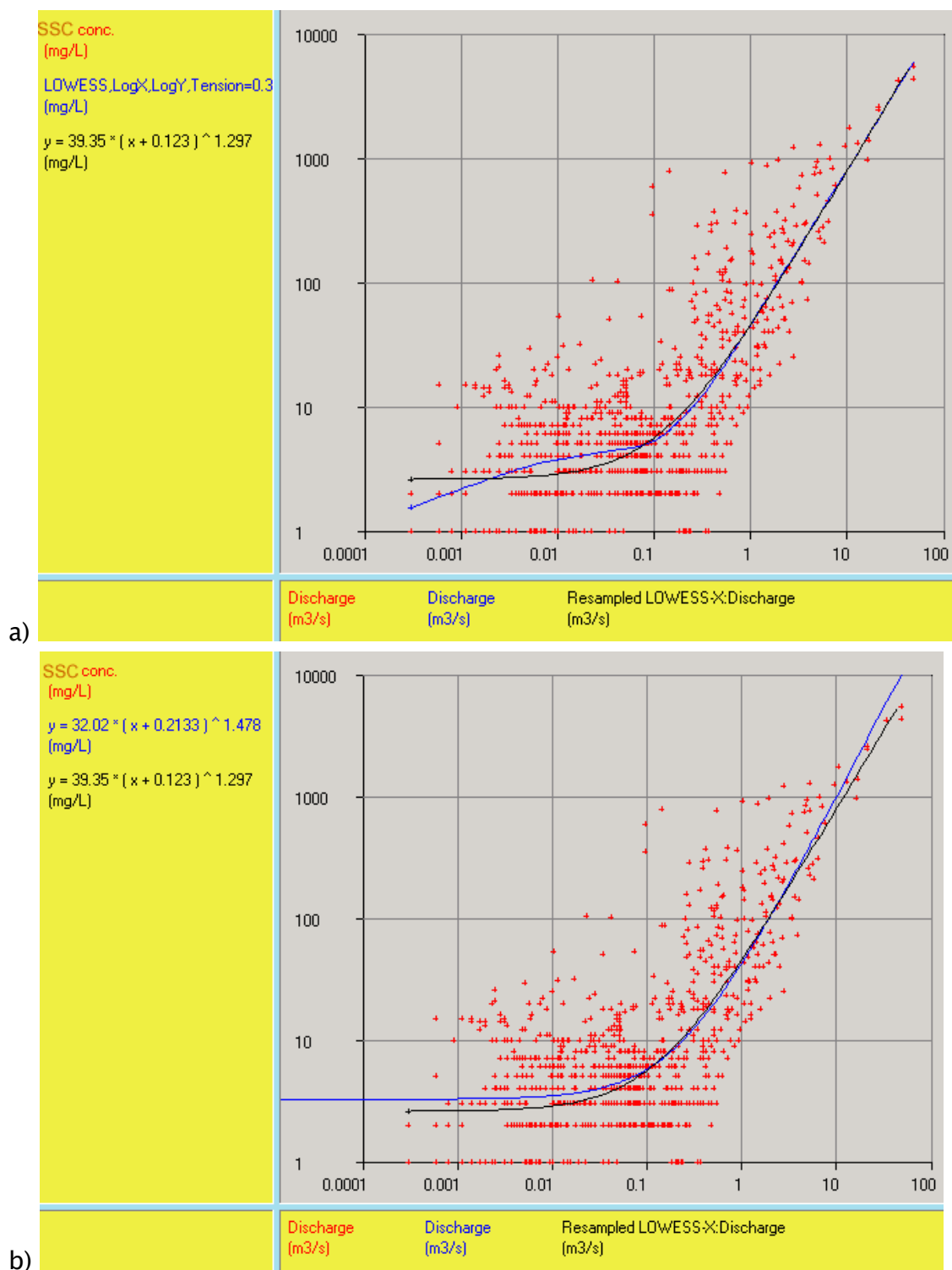
Figure 6.2. Power function fit to LOWESS fit to Santa Rita Creek sediment data: a) comparison of LOWESS fit and subsequent power function fit; b) comparison between original and LOWESS_derived power function fits.

The above procedure for fitting sediment rating curves to large USGS data sets was applied to all sites in the region of the Salinas Watershed. Results for the lower Salinas River (SAL-SPR) and the Arroyo Seco River (ARR-CAM) are shown in Figure 6.3. A good fit is obtained for SAL-SPR, which exhibits a fairly stable rating curve at moderate to high flows. This observation is indicative of a river that is transport-limited, such that sediment load is controlled more by the capacity of the river's flow to transport sediment, rather than the supply of sediment to the river. This is consistent with the geomorphic setting of the river with a very low longitudinal slope situated within a managed, but still active, flood plain. An episodic, supply-limited river would be expected to display a wider range of sediment concentration for a given flow level, representing periods of high supply and low supply of sediment, only limited by transport capacity when supply is at a maximum. This pattern is observed at ARR-CAM (Fig. 6.3b), which is generally a clear mountain stream, but was shown earlier (Section 5.4) to experience large increases in sediment supply after major fires. The fitted curves for ARR-CAM are objective, and unbiased with respect to flow levels, but for a given flow level, they tend to follow the temporally dominant sediment load regime of the non-fire, clean-water periods.
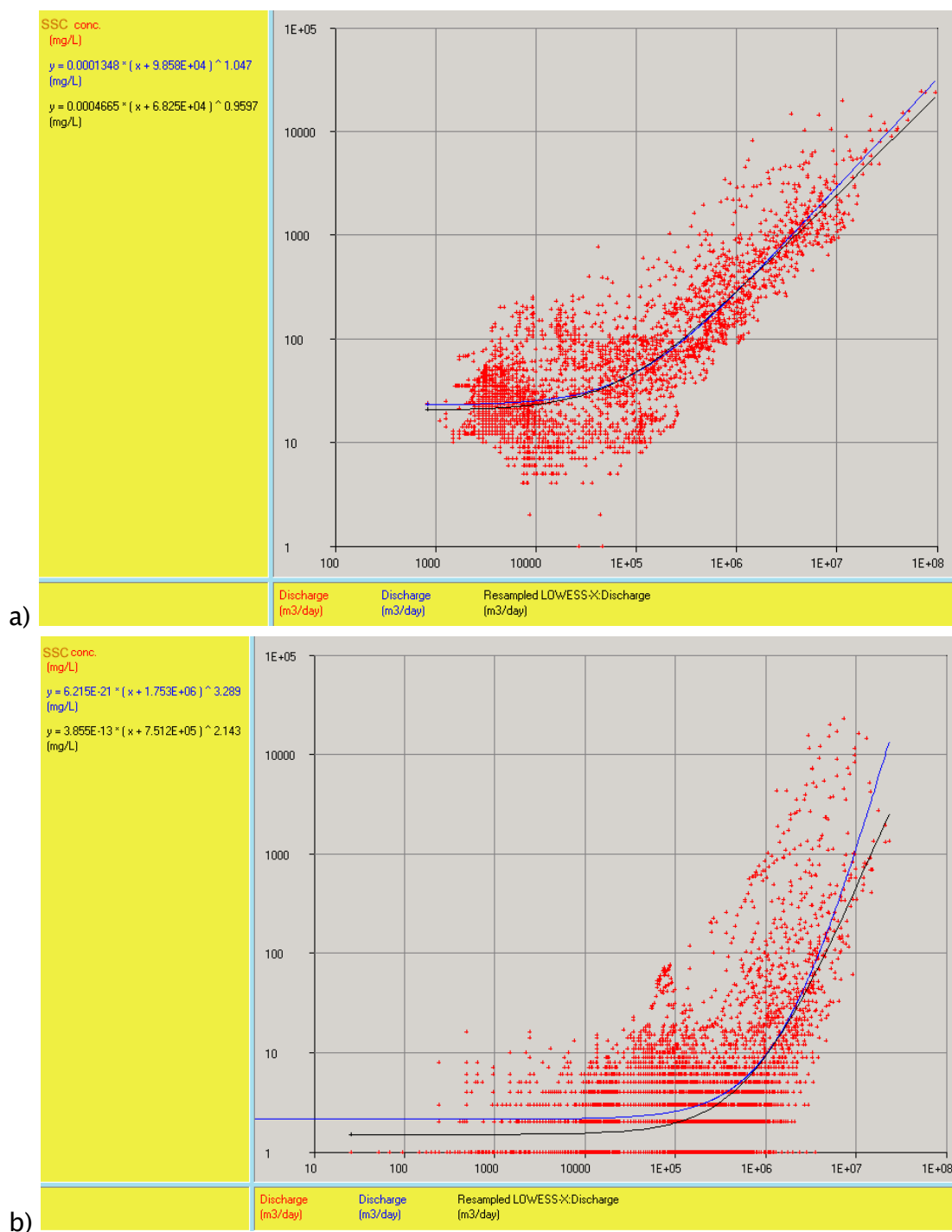
a)

b)

Figure 6.3. Direct (blue) and LOWESS–derived (black) 3–parameter power functions fitted to USGS total suspended solids concentration versus discharge data at: a) Salinas River at Spreckels (SAL–SPR); and b) Arroyo Seco near the National Forest campground (ARR–CAM).

6.3.2 Sediment rating curves for CCoWS data

The sites for which the USGS has archived measurements of sediment concentration in the region of the Salinas Watershed are too few, and often too old to provide a complete picture of the contemporary sediment transport dynamics of the Salinas River and its tributaries. This sparseness of gaging sites is one of the reasons that CCoWS began a comprehensive, storm-based sediment monitoring program. Sediment rating curves for the CCoWS data were created using a different technique than for the USGS data. The data were collected predominantly during storm periods, under a monitoring plan designed to obtain measurements before and after each major storm, and during the peak flow associated with each major storm (Watson et al., 2002). Ambient, non-storm measurements were made occasionally from those streams with perennial flow (the minority).

The CCoWS data are thus biased differently than the USGS data. The shortness of the data set introduces bias because one or two consecutive years of data are unlikely to be completely representative of the long-term regime; the storms that were measured may not be representative of the years in which they occurred. Also, despite a hydrograph-sensitive monitoring protocol (see Watson et al., 2002), the storm hydrograph may not have been observed enough times to characterize the variation in the rating curve during, say, hysteresis associated with the rising and falling limbs of the hydrograph. In some years, significant storms do not even occur. Finally, as with the USGS data, the formulation of sediment rating curves assumes that a relationship exists between sediment concentration and flow.

Notwithstanding the above pitfalls, it may frequently be observed in the field that certain streams tend to be more sediment-laden than others when all other factors appear to be equal. Short-term, targeted data sets such as the CCoWS data collected for the present study, are sufficient to quantify such observations, providing indications of sediment levels suitable for quantitative comparison amongst large numbers of sites, and setting the groundwork for longer-term reduction in the uncertainty of any resulting conclusions.
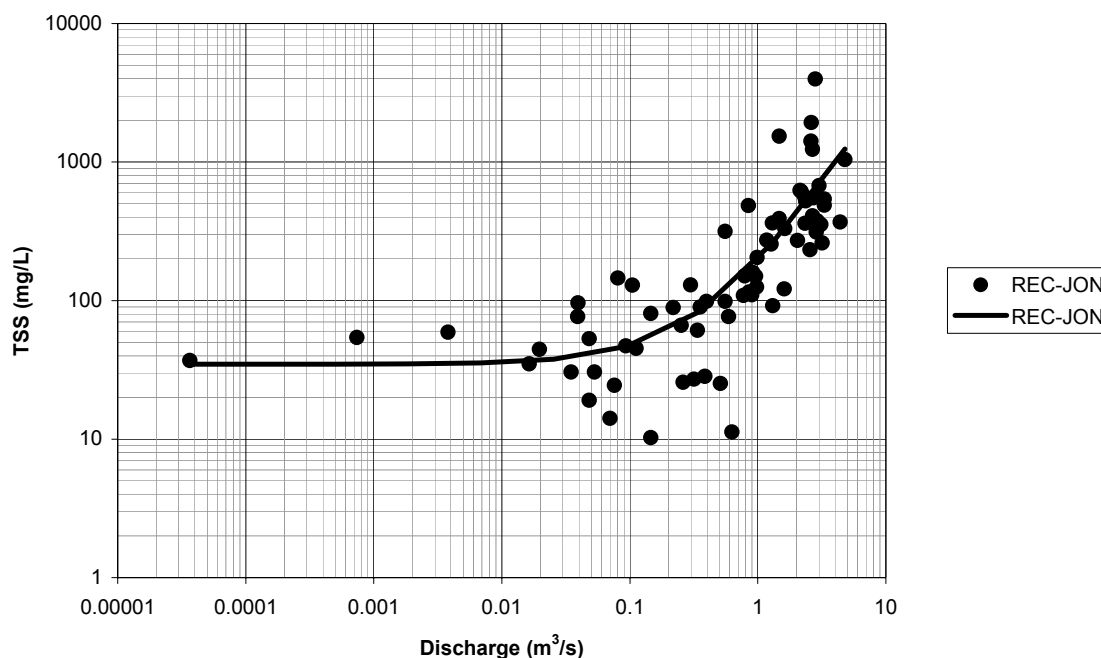
Figure 6.4. Sediment rating curve for CCoWS site REC–JON.

Data from one of the better–sampled CCoWS sites, the Reclamation Ditch at San Jon Road (REC–JON), are shown in Figure 6.4. A clear trend is evident, with non–zero suspended sediment at low–flows, rising rapidly in concentration during higher flows. Although we note that the most concentrated sediment was recorded at less than the highest flow. About five storm events are represented in the data. The curve was fitted by eye using a 3–parameter power function of the same form as used for the USGS–LOWESS fits.

Given that the curve fittings are to become a basis for an assessment of long–term mean sediment load, it is important to minimize curve–fitting error at the highest flows and concentrations because the majority of sediment load is transported at high flows. Therefore, in this, and all other manual curve fits, an effort was made to closely match the SSC recorded during the *highest observed flow*. An automated procedure, such as was used for the USGS data, was not used for the curve fits to CCoWS data, because such a procedure would be more susceptible to errors due to sampling bias in small data sets.

Data from two much less frequently visited sites are shown in Figure 6.5. The sites are located in adjacent sub–watersheds in the eastern part of the Salinas

Valley. Pancho Rico Creek at Sargents Road (PAN–SAR) is a 159 km^2 watershed noted in the field to yield particularly turbid water. San Lorenzo Creek at Bitterwater Road (SLC–BIT) is a larger watershed (608 km^2) just to the north. Both watersheds contain land used predominantly for grazing. For given flow rates, PAN–SAR yielded more than ten times as much suspended sediment during the times of observation. Sampling bias and differences in watershed area are unlikely to explain such large differences, although further sampling from different events in different years would help clarify this. Simple 3–parameter power functions were fitted to these data, and used to represent the data in further quantitative analysis (see below). The gravel mine just upstream of SLC–BIT may have either a positive or negative effect on suspended sediment concentrations, most likely varying with the flow rate. However, concentrations at SLC–BIT are, in general, not distinctly different from other sites in the data set, while the concentrations measured at PAN–SAR are the highest in the data set. Possible explanations for high sediment concentrations at Pancho Rico Creek are included in the discussion in Section 6.6.1.
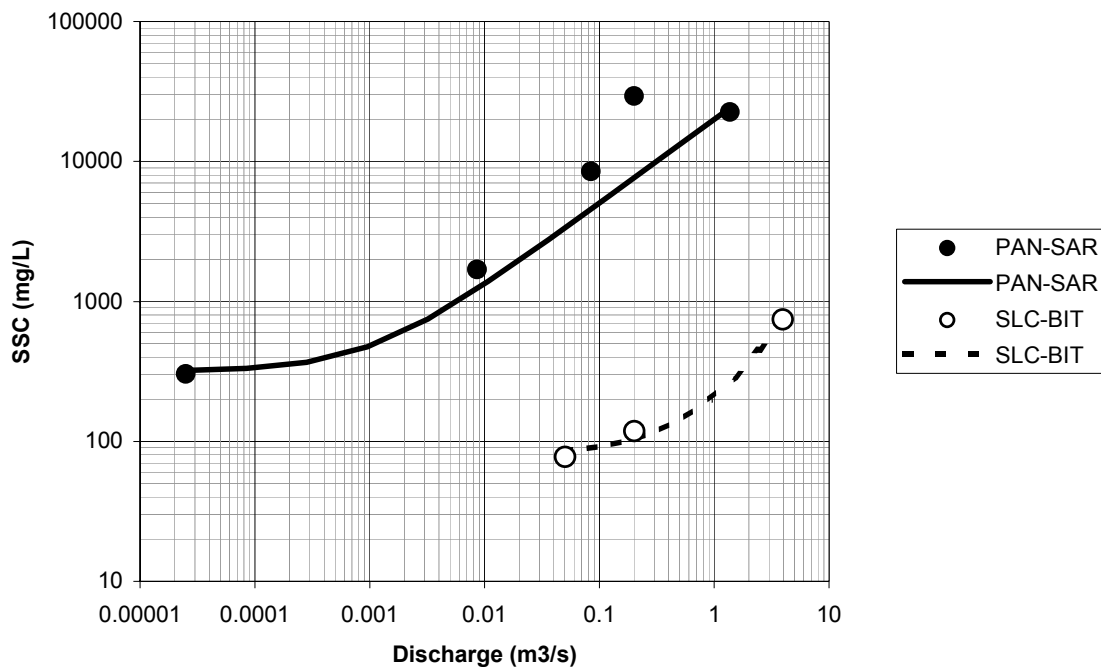

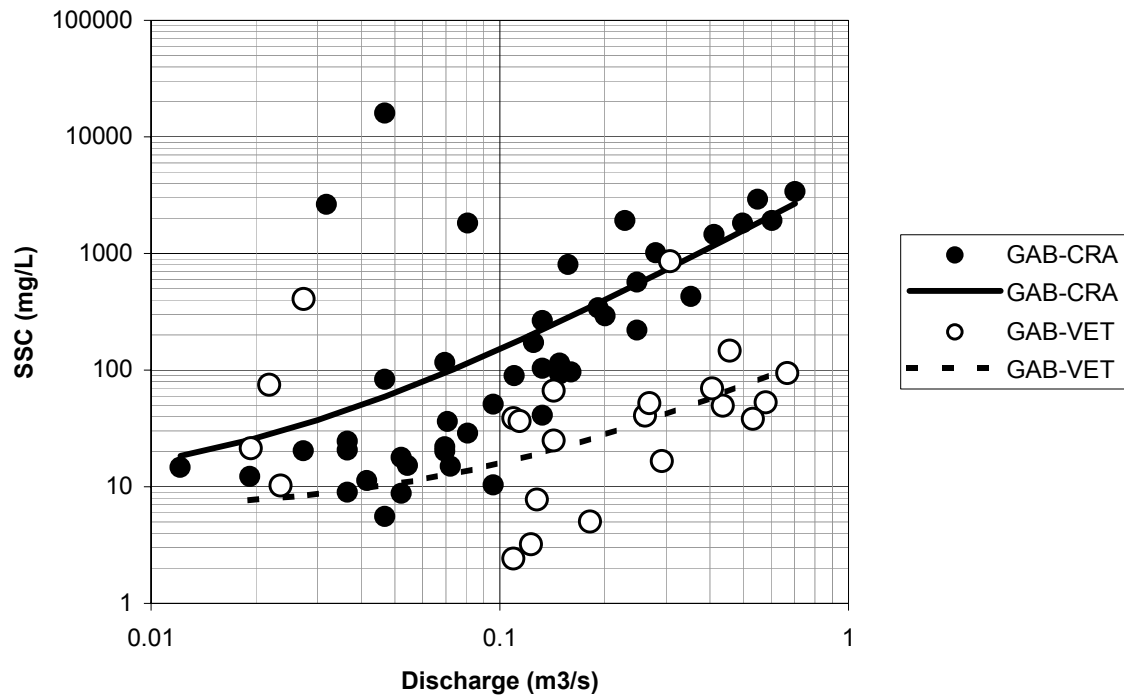Figure 6.5. Sediment rating curves for PAN–SAR and SLC–BIT.

Figure 6.6. Sediment rating curves for GAB–CRA and GAB–VET.

A final pair of CCoWS monitoring sites are examined in Figure 6.6. These sites on Gabilan Creek at Crazy Horse Road (GAB–CRA) and Veteran's Park (GAB–VET) were sampled reasonably frequently, during a number of small storms. During most storms, most of the headwater flow of Gabilan Creek percolates into the ground upon reaching the Salinas Valley floor below Old Stage Road. Crazy Horse Road is at the upper end of the losing reach below Old Stage Road, but far enough down to experience significantly diminished flood peaks relative to Old Stage Road. Veteran's Park is at the bottom of the losing reach, in the City of Salinas, but above most of the urban inputs. Only the largest headwater flood waves reach this site. Because of these groundwater percolation effects, and the associated deposition of all sediment in all but the larger storms, the sediment rating curves for these sites are not well defined. Both sites appear to receive sporadic (and probably highly localized) sediment spikes at low flows, and only the base of an increasing trend is evident. Further, the observed flows do not span enough of the estimated flow duration curve for these sites (see Section 4.7) for the data to be considered representative. Therefore, the fitted curves

shown in the Figure were not used in any further analysis. Other, data-poor sites were similarly screened from further analysis.

The data from these sites remain useful however. Firstly, the data may be supplemented by future monitoring, perhaps providing a longer-term data set containing larger storm peaks in future. Secondly, the data clearly show that GAB-VET is cleaner under low flows and small peak flows than GAB-CRA. This is consistent with field observation and interpretation. GAB-CRA is just downstream of a major row-crop production area with many un-vegetated strawberry fields exposed during winter and plastic-lined strawberry fields with direct hydraulic connections to the stream (Fig. 6.7). GAB-VET is further downstream, but below a much longer section of losing streambed, and apparently fed by groundwater. A high school just upstream pumps groundwater into the storm drain system in order to keep its basement dry (City of Salinas engineers, pers. comm.).

Figure 6.7. Plastic-lined strawberry field with direct connection of runoff to stream. Photo: Fred Watson, Jan 2001.

6.3.3 The RLDCL method: final sediment–rating curve parameters

The final set of sediment–rating curve parameters is summarized in Table 6.1. The parameters correspond to terms in Equation 3 in Section 6.3.1.

Site code	USGS-LOWESS or CCoWS-manual sediment rating curve used	Dates of suspended sediment measurements	Number of suspended sediment measurements	Sediment-rating curve parameters		
				Scale (mg/L)/(m3/s)	Offset (m3/s)	Power
ANT-LOC	USGS-LOWESS	1965-1974	3011	9.211	0.303	1.246
ANT-PLE	USGS-LOWESS	1961-1965	213	7.088	0.160	1.373
ANT-SAM	USGS-LOWESS	1961-1965	731	4.595	0.550	1.472
ARR-ARR	CCoWS	2000-2002	18	2.000	3.000	1.400
ARR-CAM	USGS-LOWESS	1962-1984+	6877	0.005	10.954	2.387
ARR-ELM	CCoWS	2000-2001	19	1.800	2.000	0.900
BIT-PAR	CCoWS	2001-2001	3	8000.000	0.000	0.830
LIT-LAK	CCoWS	2001-2001	5	7000.000	0.000	0.800
LIT-PA2	CCoWS	2001-2001	4	3300.000	0.000	1.020
LIT-PA3	CCoWS	2001-2001	4	2000.000	0.000	0.900
NAC-BRY	USGS-LOWESS	1960-1971	3100	0.118	4.549	1.705
NAC-SAP	USGS-LOWESS	1971-1974	1096	0.048	5.577	1.864
PAN-SAR	CCoWS	2000-2001	7	20000.000	0.001	0.600
REC-183	CCoWS	2001-2002	26	120.000	0.400	1.400
REC-JON	CCoWS	2000-2002	75	125.000	0.400	1.400
RIT-TEM	USGS-LOWESS	1967-1972	1827	34.905	0.149	1.387
RTT-H46	USGS-LOWESS	1967-1972	1827	80.049	0.123	1.540
SAL-BRA	CCoWS	2000-2001	11	0.800	30.000	1.000
SAL-CHU	USGS-LOWESS	1966-1969+	1029	10.000	7.000	1.000
SAL-CRE	CCoWS	2001-2001	13	0.500	60.000	1.150
SAL-GRE	CCoWS	2000-2001	22	2.200	20.000	1.400
SAL-LOC	CCoWS	2000-2002	15	1.800	10.000	1.400
SAL-SOL	CCoWS	2000-2001	4	1.800	1.000	1.400
SAL-SPR	USGS-LOWESS	1969-1979+	3652	23.379	0.876	0.978
SLC-BIT	CCoWS	2000-2001	7	80.000	1.000	1.400
WIL-V6R	CCoWS	2001-2001	3	400000.000	0.000	0.900

Table 6.1. Sediment–rating curve parameters.

('+' denotes earlier USGS data that are now supplemented by CCoWS measurements.)

6.4 The RLDCL method: development of load duration curves

By convolving sediment rating curves for each monitored site with the corresponding flow duration curve, or one estimated by the regionalization procedure in Section 4.7, a set of load duration curves may be obtained. This provides a statistically based estimate of the long-term sediment being transported past each site. An overlay of many such curves from a single region is perhaps the most effective means of achieving a statistical understanding of the relative magnitude of sediment loads from various sites in the region. Such an overlay is presented in Figure 6.8, which contains data from all sites in the study area for which sufficient suspended sediment data have been collected. Each load duration curve comprises either direct flow duration data or regionalized flow duration data (see Section 4.7), and either historical USGS suspended sediment concentration data or more recent CCoWS suspended sediment data (see Table 3.1). The curves are colored to highlight the 'measured' portions of the curves. Red coloring denotes the sections of each load duration curve corresponding to the range of loads that have been measured in the field. The term 'measured' here means that suspended sediment concentration was determined through vacuum filtration of water samples, and flow was determined by measuring stream stage and referring to a stage–discharge curve determined for each site using discharge measurements made using current meters. White coloring indicates extrapolation beyond the measured range of the sediment–rating curve for each site.
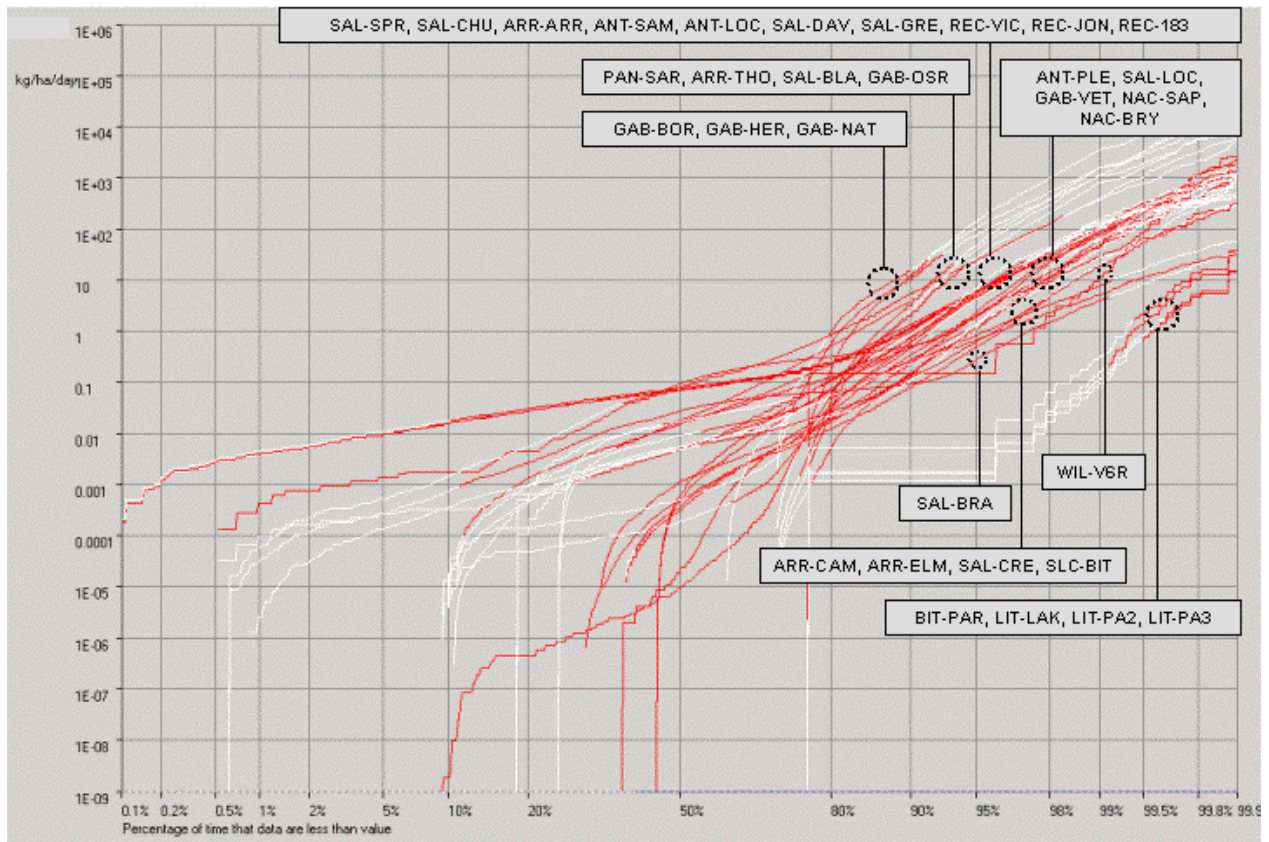
Figure 6.8. Load duration curves for suspended sediment, estimated for selected sites in the Salinas Watershed. Each curve has white and red portions: the red indicating the values within the range of field measurements, and the white indicating extrapolated values

6.5 The RLDCL method: inter-site comparison of sediment loads

In order for inter-site comparisons of long-term average flow or load data to be meaningful, they must be made at a common percentile, so that an unbiased representation of total monitoring time is given to each site. To illustrate the point that this is *not* the same as using a common recurrence interval, Figure 6.9 plots the ratio between the 99.5 percentile flow (Q99.5%) and the 2.33-year event from the annual maximum flood series (the mean annual flood, MAF). Not only does the ratio vary significantly, but the temporal bias that would result from using a fixed annual-flood recurrence interval varies with watershed area.

The best comparisons between sites are made at percentiles where all sites are within their measured range, such as the 90th percentile. Cumulative sediment loads up to this value may be safely calculated for almost all sites, because few sites require extrapolation of potentially significant load estimates below this percentile. Note that all sites require *some* extrapolation below minimum measured flows, but the resulting estimates of suspended sediment concentration are generally so small as to have a negligible effect on cumulative totals.
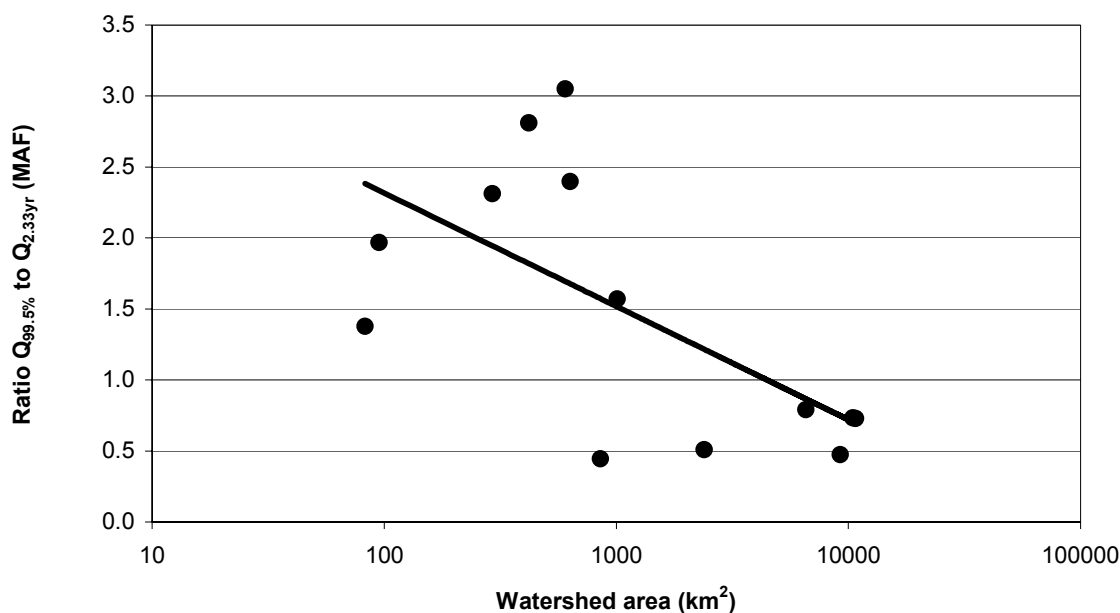

Figure 6.9. Ratio of 99.5 percentile flow to 2.33-year flood (from the annual flood series) for selected sites in the region of the Salinas Watershed.

The 90th percentile flow is not particularly large in the region of the Salinas watershed. It corresponds to the 37th largest daily flow in an 'average' year. For regulated streams, like the Salinas River, it is less than the 2-year annual peak flow. For unregulated streams, like Arroyo Seco, it is less than the 1.01-year annual peak flow, and for dry streams like Cholame Creek, it is zero. Given the highly episodic nature of sediment transport in the region, a much better inter-site comparison would be made using a higher percentile cumulative sediment load.

The 99.5 percentile flow was chosen as the compromise between the need to compare sites at a high enough percentile to include a significant proportion of their total transported sediment load, and the availability of data from a good range of sites throughout the watershed. This choice resulted in the elimination from the regional analysis of all data from the Gabilan Creek sites, where a number of storms were sampled, but most were lower than the 99.5, and even the 95 percentile flow. Using the 99.5 percentile does however allow inclusion of all the data from the small grazing watersheds on Little Cholame Creek and Bitterwater Canyon, which were deliberately monitored by CCoWS as sites representing grazing land. The only time these sites have flowed during the study period was during somewhere in the vicinity of a 35-year event (J. Varian, pers. comm.), so they are perhaps the only example where our measurements are biased too much toward rare flooding events, as opposed to storms that occur in most years.

Another attractive property of the 99.5 percentile is that it is in the same order of magnitude as the channel-full flow, or that flow that is just below out-of-channel flood flow. For example, the channel-full flow on the Arroyo Seco River occurs at a stage of about 7.5 feet – based on cross-section and other geomorphic measurements (Fig. 6.10). The USGS rating curve lists the flow corresponding to this stage as 6530 cfs. The 99.5th percentile flow at this site (based on a 100-year record) is about 55% as large – 3580 cfs. The sum of flows less than the 99.5th percentile is thus referred to in the present study as the **non-flood flow**. Correspondingly, the sum of sediment loads passed by flows less than or equal to the 99.5th percentile flow is referred to as the **non-flood load** or **non-flood yield**. This terminology is introduced here as a way of attaching an approximate level of physical significance to terms used to describe analytical results that are standardized about the 99.5th percentile flow.

An estimate of the fraction of the total load that is carried during all but the highest 0.5% of flows can be made by assuming, for a moment, that the 18.8 years of data at ARR–CAM represent 100% of time in the long-term. At this site, 60.9% of the USGS–estimated suspended sediment load was carried at flows less than the 99.5 percentile flow. This leaves a rough estimate of 39% of the long-term suspended load unaccounted for in our comparative analysis, an amount that was transported during the highest 35 days of flow in the 18.8–year record. The significance of this amount depends on the likelihood that spatial patterns of sediment transport differ during the largest 0.5% of flows – graphically corresponding to the degree to which the load duration curves for all sites are *not* parallel (Fig. 6.8). The curve for the SAL–SPR is steeper than for ARR–CAM, implying a greater bias toward loads carried at high flow. Indeed, during the 10–year record of daily sediment concentration measurements (and thus, load estimates) at SAL–SPR, only 26.3% of the load was passed during the lower 99.5% of flows (compared with 60.9% at ARR–CAM – although note the much shorter record at SAL–SPR). These shortcomings are the limits of the data. The only ways to address them are to collect load data during very large storms, or to use indirect methods such as natural tracer analysis (see review in Section 6.1).
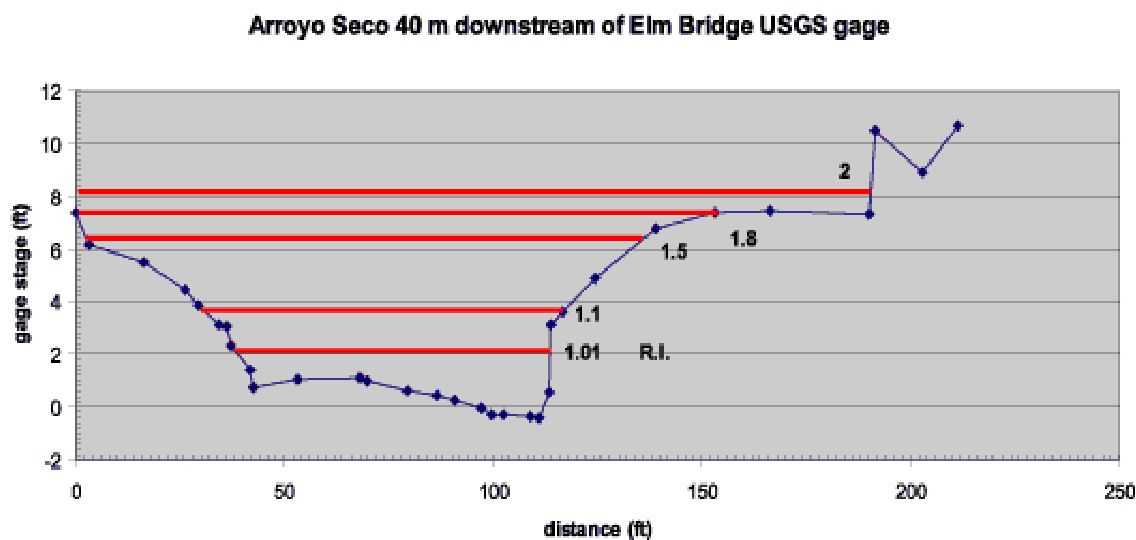

Figure 6.10. Channel cross–section on the Arroyo Seco River at Elm Rd (ARR–ELM) (50 m downstream from green bridge) (showing stages at recurrence intervals from 1.0001 to 2 years).

6.6 Results: regional suspended sediment load analysis using the RLDCL method

Estimated non-flood flows and suspended sediment loads for all eligible sites are tabulated in Table 6.2 and mapped in Figure 6.12 – with the 'non-flood' period defined for the present analysis by the 99.5 percentile. Flows were estimated using flow duration curves, or regionalized flow duration curves. Loads were estimated using the RLDCL method introduced in the present work. Of the 26 sites selected for this analysis, 13 required use of a regionalized FDC. Ten of these FDCs differed in watershed area from the target site by less than 40%, and the remaining three ranged between 3.8 and 6.2 times larger than the target site.

The RLDCL estimate of mean non-flood suspended sediment yield for Spreckels (SAL-SPR) is 64 tonnes/km²/yr (abbreviated hereafter to t/km²/yr). As noted above, we expect only about 26% of the total long-term load to occur in non-flood periods, so the RLDCL estimate translates to a total long-term load of 246 t/km²/yr. This is higher than the non-statistical estimate of 156 t/km²/yr made using the raw daily discharge and SSC concentration data from Spreckels (Section 5.1). The difference is an indication of both the inaccuracy of the RLDCL method due to the assumption of a uniform sediment-rating curve, and the inaccuracy of the non-statistical estimate based on just 10 years of data from a highly variable site.

The applicability of the above estimates as indications of the mean non-flood sediment yield per unit area is affected by the presence of thee large dams in the Salinas Watershed. The watershed area below these dams is 8765 km², or 81.7% of the Watershed above Spreckels. An upper limit for the areal sediment yield can be gained by assuming 100% sediment trapping efficiency for the dams. This increases the whole-Watershed estimate of mean non-flood yield per unit area from 64 to 78 t/km²/yr.

The estimates are also affected by changes in land use and river management, particularly the construction of the two largest dams in 1957 and 1964. The analysis presented here uses Spreckels flow data dating back to 1929, and assumes a constant sediment-rating curve throughout, based only on sampling

data from 1969 to 1979. Quantification of these effects on the analysis is beyond the present scope.

Site code	Watershed area (km2)	Regional flow duration curve used	USGS-LOWESS or CCoWS-manual sediment rating curve used	Dates of suspended sediment measurements	Number of suspended sediment measurements	Estimated 99.5 percentile flow (Q99.5%) (ML/day)	Estimated mean annual non-flood flow (Qave99.5%) (mm/yr)	Estimated 99.5 percentile suspended sediment load (L99.5%) (t/km2/day)	Estimated mean annual non-flood suspended sediment load (Lave99.5%) (t/km2/yr)	Annual estimate for fraction of watershed area below large dams (t/km2/yr)
ANT-LOC	562.0	ANT-LOC	USGS-LOWESS	1965-1974	3011	7006.1	143.9	27.6	76.30	
ANT-PLE	717.4	ANT-PLE	USGS-LOWESS	1961-1965	213	4924.0	76.5	12.6	31.60	
ANT-SAM	528.4	ANT-LOC	USGS-LOWESS	1961-1965	731	6586.4	143.9	34.1	81.21	
ARR-ARR	780.6	ARR-ELM	CCoWS	2000-2002	18	11034.5	201.3	25.6	76.60	
ARR-CAM	285.8	ARR-CAM	USGS-LOWESS	1962-1984+	6877	8849.9	472.1	12.5	27.42	
ARR-ELM	622.7	ARR-ELM	CCoWS	2000-2001	19	8802.7	201.3	1.6	7.29	
BIT-PAR	5.4	CHT-RWY	CCoWS	2001-2001	3	1.4	1.4	0.1	0.10	
LIT-LAK	18.1	CHT-RWY	CCoWS	2001-2001	5	4.9	1.4	0.2	0.27	
LIT-PA2	44.8	CHT-RWY	CCoWS	2001-2001	4	12.1	1.4	0.1	0.14	
LIT-PA3	27.8	CHT-RWY	CCoWS	2001-2001	4	7.5	1.4	0.1	0.08	
NAC-BRY	380.7	NAC-BRY	USGS-LOWESS	1960-1971	3100	11156.4	287.0	14.5	30.55	
NAC-SAP	419.6	NAC-SAP	USGS-LOWESS	1971-1974	1096	14576.2	305.9	25.3	39.74	
PAN-SAR	159.1	SLC-BIT	CCoWS	2000-2001	7	295.6	15.4	78.2	280.16	
REC-183	315.9	REC-JON	CCoWS	2001-2002	26	1016.8	52.0	25.6	88.93	
REC-JON	275.9	REC-JON	CCoWS	2000-2002	75	888.0	52.0	22.2	77.93	
RIT-TEM	47.1	RIT-TEM	USGS-LOWESS	1967-1972	1827	1024.6	183.7	23.8	51.04	
RTT-H46	7.6	RIT-TEM	USGS-LOWESS	1967-1972	1827	166.1	183.7	5.2	11.19	
SAL-BRA	6365.7	SAL-WUN	CCoWS	2000-2001	11	21752.0	55.7	0.8	3.76	4.60
SAL-CHU	10451.0	SAL-CHU	USGS-LOWESS	1966-1969+	1029	32461.2	35.6	11.9	48.79	59.73
SAL-CRE	1007.8	SAL-CRE	CCoWS	2001-2001	13	8464.9	65.0	1.4	5.85	8.21
SAL-GRE	8699.4	SAL-CHU	CCoWS	2000-2001	22	27020.6	35.6	23.2	78.77	96.43
SAL-LOC	7291.5	SAL-WUN	CCoWS	2000-2002	15	24915.6	55.7	17.9	50.16	61.41
SAL-SOL	9200.3	SAL-SOL	CCoWS	2000-2001	4	22715.2	31.4	10.9	29.50	36.11
SAL-SPR	10729.7	SAL-SPR	USGS-LOWESS	1969-1979+	3652	31387.1	25.4	21.8	63.94	78.27
SLC-BIT	606.7	SLC-BIT	CCoWS	2000-2001	7	1127.3	15.4	6.0	13.65	
WIL-V6R	16.4	CHT-RWY	CCoWS	2001-2001	3	4.4	1.4	7.4	9.59	

Table 6.2. Estimated 99.5 percentile flow, mean annual non–flood flow, 99.5 percentile TSS load, and mean annual non–flood TSS load for selected sites in the Salinas Watershed. These data are mapped in Figure 6.12.

1 '+' denotes earlier USGS data that are now supplemented by CCoWS measurements.

6.6.1 Tributaries

In looking at the spatial patterns of results from other sites, we use the non-flood range of 64 to 78 t/km²/yr at Spreckels as an indication of the basin average. Adjacent to Spreckels, predominantly urban loads in the Reclamation Ditch (REC-JON) yield 78 t/km²/yr, at the high end of the basin average. Just downstream at REC-183, after additional inputs from both urban and agricultural land, the mean load is 89 t/km²/yr.

The lowest estimated mean loads are from the eastern, grazing-dominated watersheds. A collection of small watersheds (5 – 45 km²)in the Little Cholame Creek area is estimated to produce non-flood loads between 0.08 and 9.6 t/km²/yr (BIT-PAR, LIT-LAK, LIT-PA2, LIT-PA3, WIL-V6R). The large grazing watershed (607 km²) drained by San Lorenzo Creek (SLC-BIT) has a similarly low estimated yield of 14 t/km²/yr. However, some very high loads are also estimated for this part of the region, as suggested by the data from Pancho Rico Creek, at 280 t/km²/yr. Pancho Rico Creek is unique in the Salinas Watershed, owing to the presence of a large, canyon, through which its middle reaches flow beneath 300 ft high eroding banks (Fig. 6.11). A large (550 m long x 600 m wide) landslide forms the right bank of the canyon at one point. The whole site is in the San Andreas Fault zone, 20 km from the site of a Magnitude 6.0 earthquake near Parkfield in 1966. We hypothesize that the high loads measured on Pancho Rico Creek are associated with the canyon. We recommend that this hypothesis be examined by repeated sediment sampling, and field survey of the canyon geomorphology.

The western, more-wooded watersheds are best exemplified by the Arroyo Seco River, which predominantly drains National Forest land. At the Campsite and Elm Rd sites (ARR-CAM & ARR-ELM), the mean non-flood loads are a low 27 and 7 t/km²/yr respectively. These are higher than long-term denudation rates inferred from Apatite Helium ages in the rocks of the Santa Lucia range in the past 2 million years (~0.9 mm/yr $\equiv$ 1-2 t/km²/yr, Ducea et al., 2003), perhaps due to the unusual severity of the Marble Cone Fire, which is prominent in the sampling record. Once the River reaches the Valley floor at ARR-ARR, below row-crops, vineyards, and grazing land, the estimated yield increases to 77 t/km²/yr, which is at the high end of the basin average. The Nacimiento River originates in the National Forest, and flows through wooded portions of Fort Hunter Liggett before passing the early USGS sites at Bryson and Sapaque Creek
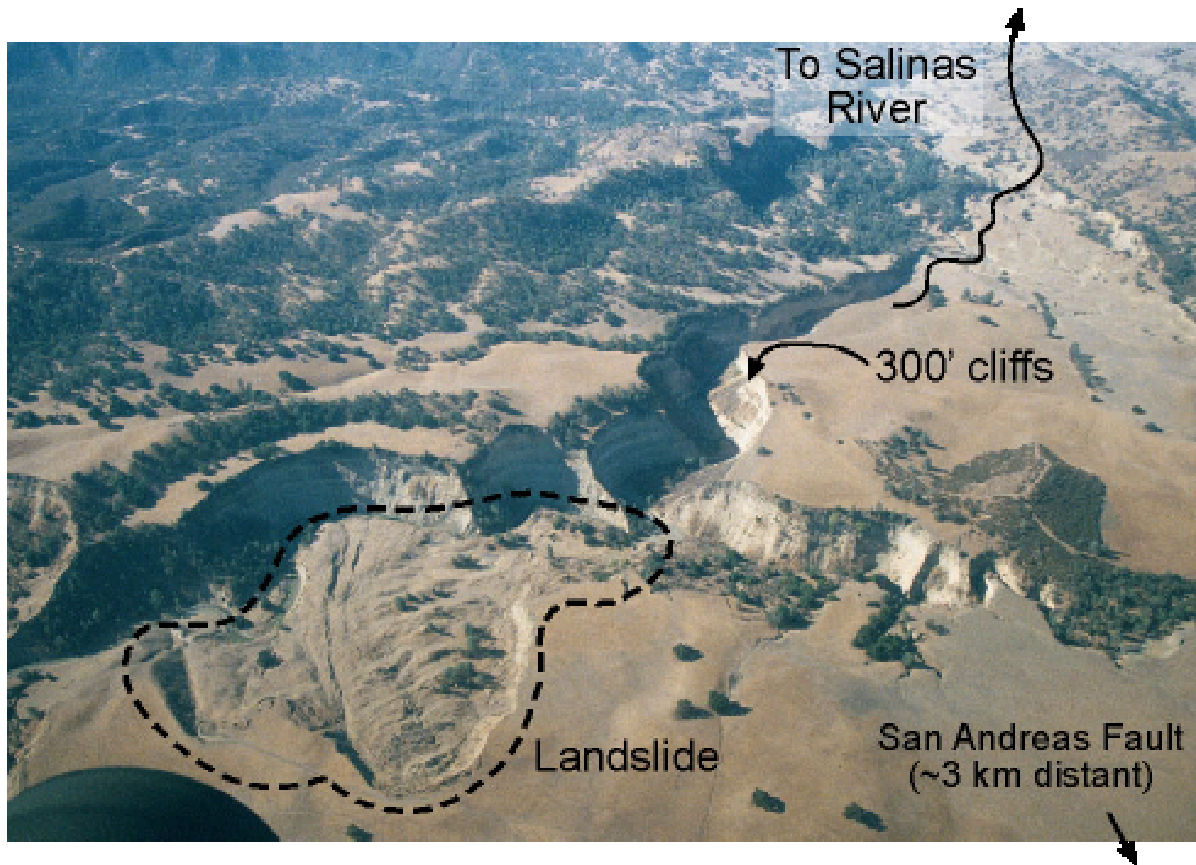
Figure 6.11. Deeply incised canyon on Pancho Rico Creek, looking southwest from above Peachtree Road. Note the large landslide in left foreground, probably associated with stream migration and 300' cliffs on opposite bank. Photo: Fred Watson, 3 Oct 2002.

(NAC–BRY & NAC–SAP). Here in the 1960s and 1970s, the watershed yielded a low-to-medium 31 and 40 t/km²/yr respectively. One might suppose that the slightly higher values relative to Arroyo Seco may be due to geology, fire, or military land use on the Fort, or they may simply be due to temporal sampling bias (further investigation may clarify this). The military hypothesis, however, is strengthened by the observation of even higher yields (32 – 81 t/km²/yr) from three sites on the drier San Antonio River watershed, which has a higher proportion of military land use, and a significant amount of data from a separate period to the Nacimiento data.
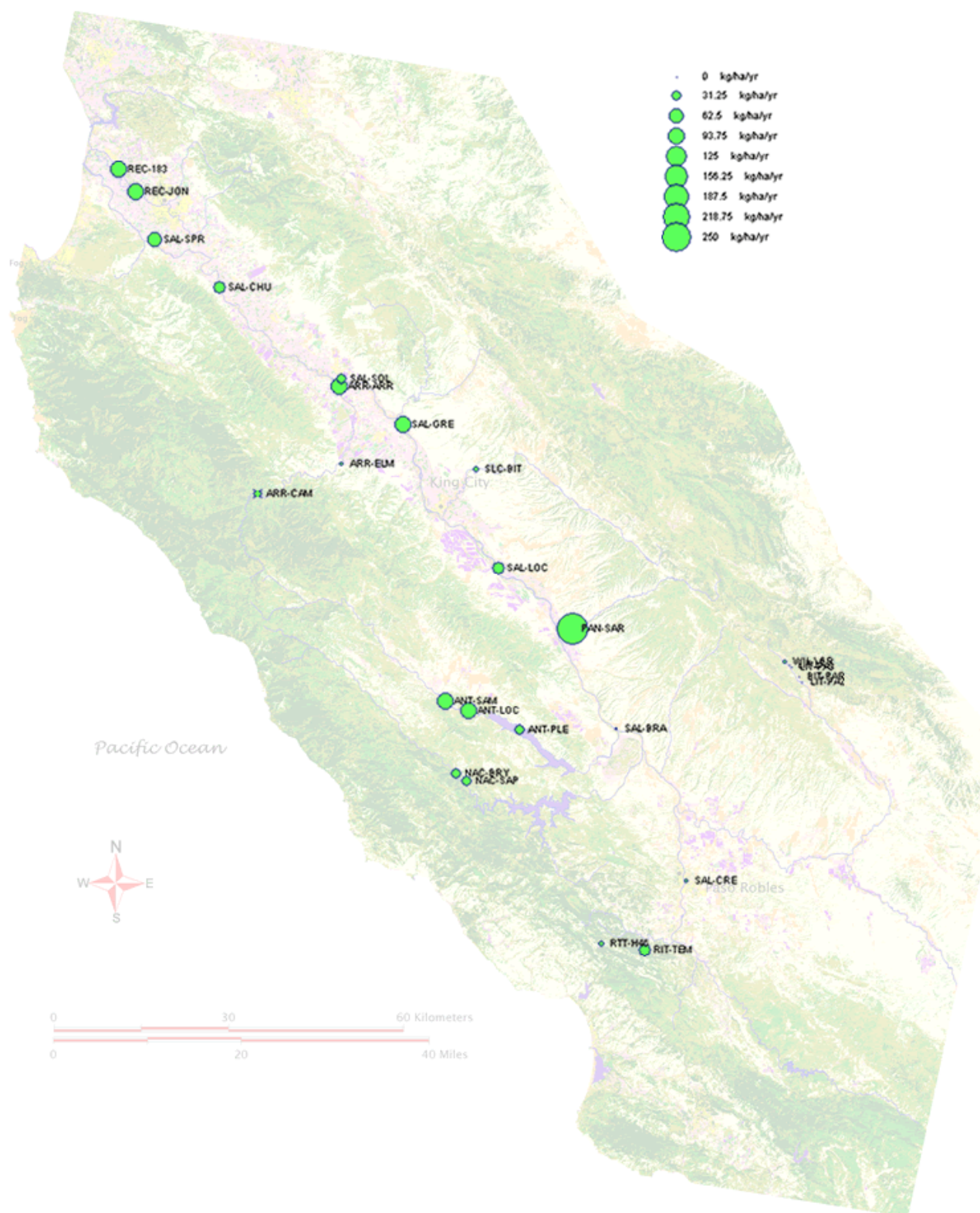
Figure 6.12. Estimated average annual non–flood suspended sediment load passing selected sites in the Salinas Watershed.

Low to medium yields (relative to the basin average) are also indicated for the southern-most portions of the Salinas Watershed in the Santa Rita Creek area, RIT-TEM and RTT-H46, with estimated non-flood loads of 51 and 11 t/km²/yr respectively. Sediment was sampled at both sites between 1967 and 1972. Some of the sediment from the watershed of the Santa Rita Creek site (RIT-TEM) is most likely trapped behind a 30-acre jurisdictional reservoir built in 1965 below the uppermost 22% of the watershed area. Correcting the yield estimate for this *pro rata* with the watershed area results in a new estimate of 65 t/km²/yr. This value is slightly above the basin average, as might be expected for a small watershed on the lower, southern crest of the Santa Lucia Range. The tributary site (RTT-H46) is below a much smaller watershed (7.6 km²) than RIT-TEM (47.1 km²), but relies upon the area-scaled RIT-TEM flow data for its flow duration curve. This discrepancy may account for the abnormally low sediment yield, 11 t/km²/yr, estimated for the site.

6.6.2 The main stem of the Salinas River

Turning now to the main stem of the Salinas River, estimates are given for a long sequence of sites starting at Paso Robles in the south (SAL-CRE), where the watershed area is 1008 km², extending past sites at Bradley (6366 km²), San Lucas (6,918 km²), Greenfield (8,325 km²), Soledad (8,826 km²), Chualar (10,451 (km²), and Spreckels (10,730 km²). The estimates indicate very low non-flood sediment yield at Paso Robles (5.9 t/km²/yr), past the inflow from the large watershed of the Estrella River, and again at Bradley (3.8 t/km²/yr).

These low values mainly reflect the low values of the contributing tributaries, their dry climates, and predominantly pastoral land uses. However, Lakes Nacimiento and San Antonio also have a very significant load-reducing effect, which can be calculated by estimating the load that may have reached the Salinas in the absence of the Dams. The following assumptions are made: at present, the entire suspended load above the reservoirs is deposited on the Lake beds; the historically measured areal loads above the Dams are indicative of their entire watersheds; and the present areal loads to the reaches between the Dams and the Salinas River can be estimated as the areal load passing Paso Robles. Given this, the load on the main stem at SAL-BRA would be 17 t/km²/yr rather than the actual 3.8 t/km²/yr. This estimated pre-dam value is still a low sediment yield relative to the watershed average, but one that is closer in

magnitude to both the load estimates for the tributaries upstream from it, and the load downstream at San Lucas (50–61 t/km²/yr).

The San Lucas (Lockwood Rd, SAL–LOC) site is downstream from the very high sediment loads that were measured in 2001 entering the Salinas from Pancho Rico Creek and experiences an estimated 50–61 t/km²/yr of non–flood suspended sediment load. Assuming 100% delivery from PAN–SAR to San Lucas, PAN–SAR contributes 12% (6 t/km²/yr) of SAL–LOC's load from only 2.2% of its area. Again, assuming no net deposition or scour during non–flood periods between SAL–BRA and SAL–LOC, the additional watershed area below SAL–BRA is estimated to contribute 93% of the load from 13% of the area upstream of SAL–LOC. Even given high loads from Pancho Rico Creek, and perhaps one or two similar neighboring tributaries, a discrepancy of this magnitude is suspicious. The most likely explanation must include errors in the estimation of non–flood load at any site, scour or bank–cutting in non–flood periods balanced by deposition in (here un–accounted) flood periods, and net long–term channel degradation. Only after these have been considered could potential contributions from rapidly expanding vineyards upstream of San Lucas be estimated using the present techniques.

Below San Lucas (SAL–LOC) are the first of the row–crops that gradually fill the entire Valley Floor on the 100 km journey to the Salinas River mouth. As many row–crop lands are devoid of vegetation during winter rains, their potential contribution to the Watershed sediment load is of interest. Although row crop agriculture comprises a 6% of the Salinas Watershed land use (Newman et al., 2002), no tributaries are dominated by it, and so no tributary loads may be measured in order to quantify it. Instead, a regional analysis such as the present one must attempt to discern the row–crop sediment load by inference after considering all other sources of sediment, and spatial sediment transport dynamics (more direct analyses are also presented in Sections 7.3.6 and 7.4.6).

The Salinas River at Greenfield (SAL–GRE) is downstream of a significant acreage of row–crops along the Valley floor and vineyards in the adjacent bench and rolling slopes. A major tributary, San Lorenzo Creek, also joins the River above Greenfield. This tributary has a low estimated non–flood load of 14 t/km²/yr at the point where it reaches the edge of the flat Salinas Valley floor some 10 km distant from the River itself. The estimated load at Greenfield is 79–96 t/km²/yr, an increase from the 50–61 t/km²/yr estimated at San Lucas. This may be due

to sampling bias, new agricultural inputs, or net scour from the streambed that originates as net deposition during flood periods that are un-accounted for in the present analysis. Channel degradation may account for about 10-20 t/km²/yr for each of these two reaches (assuming 36 km & 34 km reach lengths, 50 m active channel width, 0.03 m/yr degradation, 2 t/m³ bulk density, and 6000 km² watershed area). This does not account for all of the increases in load between Bradley and Greenfield. Either sampling bias or additional land use sources are likely.

The next site in sequence is at Soledad. The estimated non-flood load at Soledad is 30-36 t/km²/yr, which is lower than its upstream counterpart, and also lower than the basin average. Again, this is downstream of more agriculture, and an inflow from another major eastern tributary, Chalone Creek. This creek, like San Lorenzo, is a dry sandy wash surrounded by grazing land in its lower reaches (Fig. 6.13). It does however contain most of the naturally vegetated Pinnacles National Monument in its watershed, and thus would be
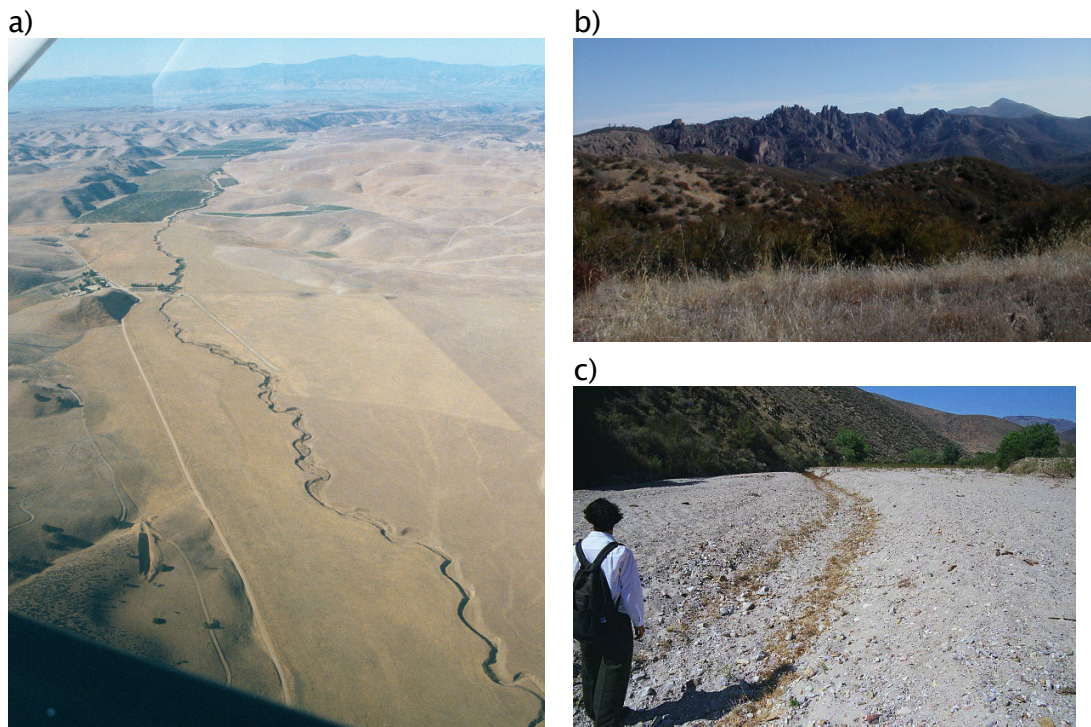

Figure 6.13. The Chalone Watershed (a tributary to the Salinas): a) Topo Creek (a tributary to the Chalone) drains typical grazing and feed crop lands (Oct., '02); b) the Pinnacles National Monument; c) Chalone Creek (note low-flow channel). Photos: a) Fred Watson, 3 Oct 2002; b) Thor Anderson, Fall 2000; c) Fred Watson, Fall 2000.

expected to exhibit relatively low sediment yield.

The Salinas at Chualar (SAL–CHU) is the first main stem site below the large inflow from the Arroyo Seco River, and yields an estimated 49–60 t/km²/yr during non–flood periods, an increase of 19–24 t/km²/yr over SAL–SOL. Some of this difference may be attributable to differences in the periods of record between the two sites (the relatively short SAL–CHU record includes the 1969 flood). The channel both aggrades and degrades at this near–sea–level site depending on winter storm severity, but a slight net long–term decline of about half a foot per decade appears to be evident in the record. This amounts to 9 t/km²/yr at Chualar, and could explain the increase in load between Soledad and Chualar (assuming 30 km reach length, 100 m width, 0.015 m/yr degradation, 2 t/m³ bulk density, 10,000 km² watershed area). New watershed sources are also possible. Based on limited sampling, the lower Arroyo Seco River (ARR–ARR) is estimated to yield 77 t/km²/yr in non–flood periods (apparently derived from the lower watershed, since the upper River (ARR–ELM) only yields 7.3 t/km²/yr). This is consistent with large areas of sloping agricultural and new vineyard land draining directly into the lower River (Fig.

Figure 6.14. New vineyards line the lower reaches of the Arroyo Seco River. Photo: Fred Watson, 3 Oct 2002.

6.14).

If a portion (e.g. 10 t/km²/yr) of the increase in Salinas River load between Soledad and Chualar was to be accounted for by watershed inputs (as opposed to sampling errors or channel degradation), the watershed area between the two sites (1251 km²) would have a mean non-flood suspended sediment yield of 84 t/km²/yr. After subtracting the high load that is estimated to be delivered by the Arroyo Seco River (77 t/km²/yr), the remaining watershed area between SAL-SOL and SAL-CHU (470 km²) would have a relatively high mean non-flood suspended sediment yield of 95 t/km²/yr. This watershed area includes a number of small, unnamed creeks draining the steep, wooded slopes of the Sierra De Salinas, Johnson Creek, which drains a small portion of wooded and grazing land in the Gabilan Range, and a large area of row-crop farming on the Valley floor. If one assumes that the wooded and grazing lands exhibit the low sediment yield measured at numerous similar sites throughout the study area then a large sediment yield of about 200 t/km²/yr is implicated for the row-crop lands (assuming they occupy about half of the 470 km² between Soledad and Chualar, excluding Arroyo Seco).

The last long-term gauged site on the Salinas is at Spreckels, and yields an estimated 64-78 t/km²/yr in non-flood times. This is higher than most of the

Figure 6.15. Recent floodplain deposition of sediment below the headwaters of Chualar Canyon, and subsequent channel maintenance using earth-moving equipment. Photo: Fred Watson, 2000.

large sub-watersheds. Long-term channel degradation would be minimal here, due to the proximity of the ocean. A figure of only 2 $t/km^2/yr$ is estimated for the 18 km reach, assuming degradation of 7 cm per decade. Sampling bias is unlikely, given the relatively long record at Spreckels, and the fact that the Chualar sampling was conducted during a fairly typical flow year. Additional land use inputs are thus the most likely source of the increased loads. If a portion (e.g. 13 $t/km^2/yr$) of the additional load between Chualar and Spreckels were to be accounted from watershed inputs, the areal load from the watershed between these two sites (279 km^2) would be a very high 500 $t/km^2/yr$. There are few tributaries along this reach. The largest is Chualar Creek, which may have a high load of sediment given the decomposed granite sands that are actively altering the floodplain drainage in Chualar Canyon (Figure 6.15), or a low load, due to dams that retain the Creek's waters just as it emerges from Chualar Canyon onto the main Salinas Valley floor. The latter is more likely because the Creek diminishes to a small ditch by the time it reaches the Salinas River. Its dimensions and substrate west of the town of Chualar are not indicative of high sand load. By exclusion, this leaves the likelihood that agricultural lands account for much of the increased load between Chualar and Spreckels. The capability for this level of sediment delivery from agricultural lands is supported by more detailed studies in Sections 7.3.6 and 7.4.6.

6.6.3   Load versus watershed area

Traditionally, differences in sediment yield between watersheds of different size are thought of within a context of an over-arching relationship between sediment yield and watershed area. The following analysis explores the Salinas data within this context.

From San Lucas downstream, all five main-stem monitoring sites experience higher non-flood sediment loads than any of the larger monitored tributaries draining to the Valley floor (including SAL-CRE, SAL-BRA, SLC-BIT, ARR-ELM, but excluding PAN-SAR). Graphically, in the Salinas Watershed, sediment yield per unit area increases with increasing sub-watershed area to about 200-500 km^2, and then levels off between 1000 and 10,000 km^2 (Fig. 6.16), a trend that shows no sign of changing for the un-accounted flows above the 99.5 percentile. This is either because contemporary re-mobilization of previously stored sediment is higher in these reaches, or because inputs from adjacent land uses are higher. The latter possibility, if borne out, implicates either

irrigated row-crop agriculture and vineyards, for these are the only significant land uses unique to the lower-Valley sites, or the small tributary watersheds in this area such as Chualar Creek. The former possibility contradicts general understanding that long-term sediment yield per unit area decreases with increasing watershed area (Gottschalk, 1964; Schumm, 1977; Shen & Julien, 1993), which is generally understood to be due to increasing storage of sediment in depressions and floodplains as one moves down a watershed (unlike shorter-term differences, which can be attributed to non-uniform rainfall). However, it is wise to examine the data that underlie this understanding (Renau & Dietrich, 1991).

In the original 'Handbook of Applied Hydrology' Gottschalk (1964) introduces the general idea of a negative specific-yield-area relationship based on 1096 measurements. This is re-stated in the sequel publication 'Handbook of Hydrology' by Shen & Julien, who give a power-function with exponent -0.3 - a straight down-sloping line on log-log axes (compare with the non-monotonic line in Figure 6.16). Dunne and Leopold's classic 1978 text discusses the same trend, but also notes that the dominant conclusion to be drawn from a scatter-plot of the same original yield-area data is *variability*, not trend. A series of down-sloping straight-line fits are also summarized in a book chapter by Walling (1994).

For reference, a contemporary database of 873 sites from all continents obtained from the UN Food and Agriculture Organization (FAO, 2001) is also shown in Figure 6.16. The data were screened to contain only the 80 sites with broadly similar climate to the Salinas Watershed. As expected from Dunne & Leopold's observations, there is considerable scatter. A straight-line regression fit to the log-log data produces a negative slope, in agreement with earlier authors. However, an objective LOWESS smoothing of the data (see Figure) suggests a more complex and uncertain relationship for watersheds between 100 and 10,000 km^2, and one with which the Salinas data generally agree.

The estimation that the lower Salinas main stem sites exhibit higher yields than the major tributaries just upstream contradicts the simplistic general statements cited above that 'yield decreases with increasing area'. But upon closer examination using the FAO data, the contradiction no longer applies. In the FAO data, yield increases with increasing area up to a point, and only declines clearly for watersheds considerably larger than the Salinas. In the context of the FAO

data, the downstream increases in sediment yield observed in the lower Salinas Valley may thus be explained by either:

- the same channel geomorphic processes (e.g. channel degradation, bank erosion, floodplain deposition) operating in both the Salinas and FAO data sets
- the same additional land use inputs (e.g. agriculture and vineyards) being manifested appearing in watersheds between 1,000 and 10,000 km^2 in both data sets
- or a statistically significant difference between the Salinas and the global average (FAO) that cannot be discerned given the present amount of available data
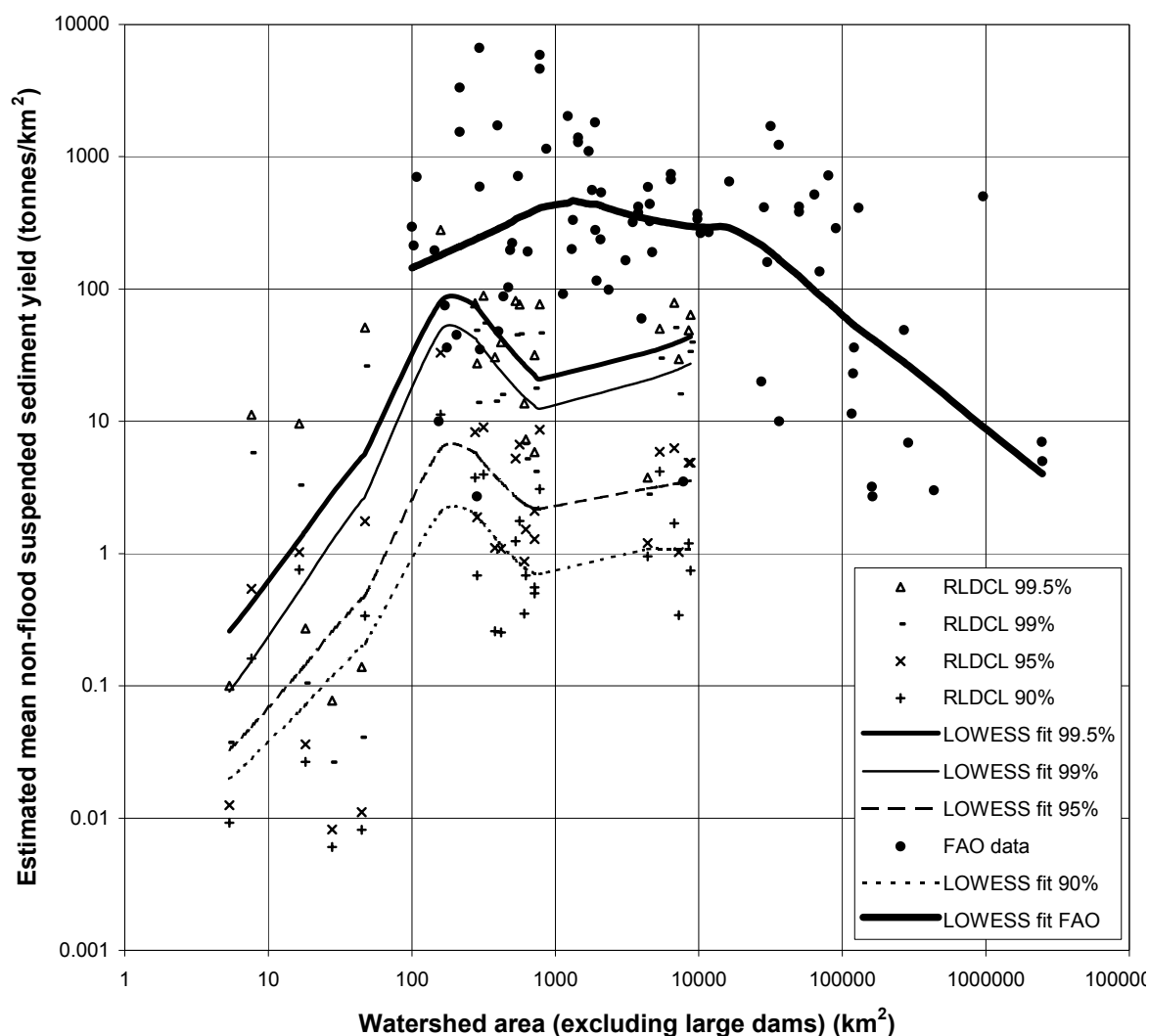
Figure 6.16. The balance of sediment yield amongst large and small streams, from the 90th percentile increasing to the 99.5th percentile. FAO Global Sediment Yield Database: watersheds with 300–700 mm annual rainfall (i.e. those climatically most similar to the Salinas Watershed). LOWESS smooth applied to data with Tension 0.5. Note that the FAO data represent total sediment load, whereas the RLDCL data represent non-flood suspended load – hence the overall difference in magnitude.

6.6.4 Caveat

At this point, it would be wise to recall the limitations of the present analysis. The major limitation is the paucity of data. The historic USGS sites were well monitored, but the recent CCOWS sites were only established for the present study. Although data from a number of sites were excluded from the present analysis due to sampling bias that could not be corrected, some of the *included* sites have only *three* suspended sediment measurements associated with them. Any conclusions drawn from such data must be considered very preliminary. On the positive side, the techniques presented herein are designed to yield increasingly accurate estimates as additional large storms are monitored in the future.

Other limitations include: the exclusion of flood data, and the exclusion of bedload data. The latter is expected to be only a minor limitation since bedload is generally expected to be less than 10% of suspended load (see for example Renau & Dietrich, 1991), except perhaps in granitic portions of the watershed where it may reach 50% (see Kondolf, 1982). Similarly, the inclusion of diverse sediment budget estimation techniques, such as the use of natural tracers, would benefit the work. Some additional techniques are explored in Chapter 0.

6.7 Comparison with reservoir sedimentation data

One of the most reliable techniques for estimating long term sediment yield from watersheds involves measurement of rates of reservoir sedimentation. Large reservoirs with capacity:inflow ratios of above 2, such as Lake San Antonio and Lake Nacimiento, trap as much as 95 – 100% of the sediment that enters them (Brune, 1953). The long-term rate may be estimated by periodically measuring the corresponding reductions in the capacity of the reservoir using bathymetric techniques. These estimates of volume must then be converted to an estimate of sediment mass, using an estimate of the mean bulk density of the sediment at the bottom of the reservoir (the dry weight of sediment divided by the volume it occupied on the reservoir-bottom – also known as specific weight) (USACE, 1989).

Previous investigators have documented volumetric reductions in reservoir capacity in three reservoirs in the study area and immediately adjacent areas:

Santa Margarita Reservoir, Los Padres Reservoir, and Lopez Reservoir (Knott, 1976; Glysson, 1977; Bloyd, 1981; Hecht, 1981; BAER Teams 1985, 1999). Lake Nacimiento has also been surveyed at least once, in the 1990s, but the results indicated an increase in capacity since dam construction in 1957 (SWRCB, 2001). This is due to an error in the original USGS-map-based capacity computations performed in 1954 prior to dam construction.

The bulk density of reservoir sediment depends on the texture of the sediment, the inundation regime, and the number of years since deposition (Edwards & Glysson, 1999). A range of measurements from 0.32 – 1.92 kg/m^3 was summarized by Lara & Pemberton (1965). These authors present a simple equation that estimates bulk density given a range of particle sizes of from recent, pure clay sediments (0.42 kg/m^3) to pure sand (1.59 kg/m^3). The particle size of reservoir sediments in the study area is uncertain. Beneath the granitic geology of the northern Santa Lucias, the sediments of San Clemente Reservoir contains approximately 95-100% sand and coarser material (Moffatt & Nichol Engineers, 1996, cited by Hecht, 2001; MEI, 2002). The majority of the study area is not granitic, so a larger proportion of silt and clay is expected in other reservoirs. Table 6.3 presents the previous volumetric estimates, converted to mass-based estimates under a range of estimated bulk densities and estimated trapping efficiencies.

The two smaller southern reservoirs exhibit relatively high yields of about 300 – 600 t/km^2/yr. The yield from Los Padres Reservoir reveals dramatic variation centered on the Marble-Cone fire of 1977. From 1947, the estimated yield is 33 t/km^2/yr, rising to 393 t/km^2/yr after 1961, and peaking at 8,365 t/km^2/yr in the year following the fire. The yield then rapidly subsides to pre-fire levels of 311 t/km^2/yr before 1980, and 374 t/km^2/yr thereafter.

Reservoir	Watershed area (km2)	Period	Sedimentation rate (m3/yr)	Primary source	Referral	Percent sand		Bulk density (kg/m3)		Sedimentation rate (t/km2/yr)		Assumed trap efficiency	Source	Watershed sediment yield (t/km2/yr)	
						Low	High	Low	High	Low	High			Low	High
Santa Margarita Reservoir	290.1		100787 (1977)	Glysson (1977)	BAER Team (1985)	40%	95%	1.08	1.51	376	526	85%	Brune (1953)	443	619
Lopez Reservoir	175.3		43168	Knott (1976)	BAER Team (1985)	40%	95%	1.08	1.51	267	373	85%	Brune (1953)	314	439
Los Padres Reservoir	161	Pre-Marble-Cone: 1947-1977	24916	Bloyd (1981)	Hecht (1981)	85%	95%	1.44	1.51	222	234	81%	BAER Team (1999) & Brune (1953)	274	289
"	161	Pre-Marble-Cone: 1947-1977	19415	Cal. Water & Telephone Co.	BAER Team (1999) & Hecht (1981)	85%	95%	1.44	1.51	173	183	81%	BAER Team (1999) & Brune (1953)	214	225
"	161	Pre-Marble-Cone: 1947-1961	2911	Cal. Water & Telephone Co.	BAER Team (1999)	85%	95%	1.44	1.51	26	27	82%	BAER Team (1999) & Brune (1953)	32	33
"	161	Pre-Marble-Cone: 1961-1977	33871	Hecht (1981)	BAER Team (1999)	85%	95%	1.44	1.51	302	319	81%	BAER Team (1999) & Brune (1953)	373	393
"	161	Post-Marble-Cone: 1978	684706	Hecht (1981)	BAER Team (1999)	85%	95%	1.44	1.51	6107	6441	77%	BAER Team (1999) & Brune (1953)	7932	8365
"	161	Post-Marble-Cone: 1979-1980	25471	Hecht (1981)	BAER Team (1999)	85%	95%	1.44	1.51	227	240	77%	BAER Team (1999) & Brune (1953)	295	311
"	161	Pre-Kirk: 1980-1998	29258	Cal.-Am. Water Co.	BAER Team (1999)	85%	95%	1.44	1.51	261	275	74%	BAER Team (1999) & Brune (1953)	355	374

Table 6.3. Summary of previous estimates of volumetric reservoir sedimentation (m3/yr) in the study area, and new estimates of mass-based watershed sediment yield (tonnes/km²/yr).

Some additional context is provided by estimates for the broader Californian Coast Range presented by Swanson Hydrology & Geomorphology (2001). These estimates are based on previous reservoir sedimentation studies from 15 watersheds. They are presented graphically, along with the estimates in Table 6.3 in Figure 6.17.
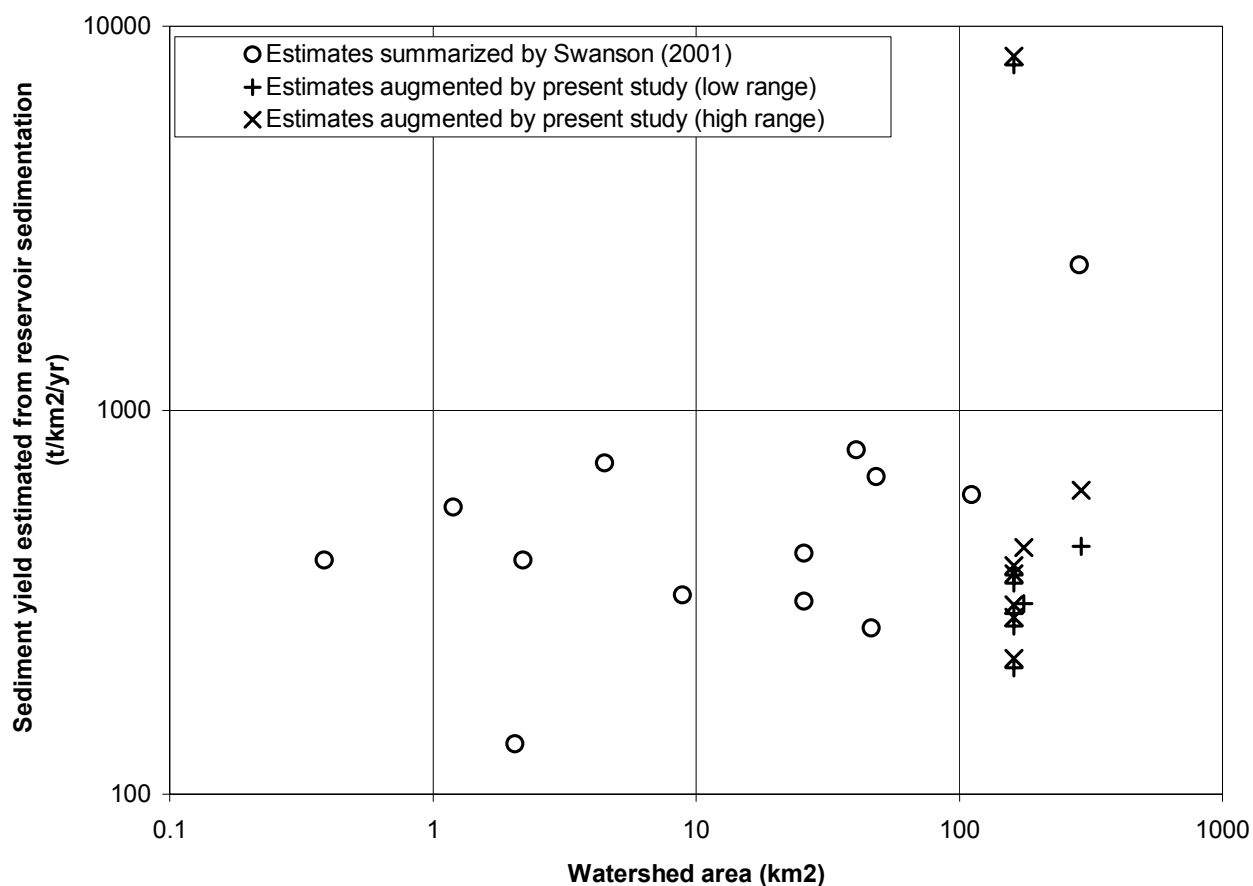

Figure 6.17. Sediment yield estimates based on reservoir sedimentation studies: comparison between broader Californian Coast Range watersheds (Swanson, 2001) and watersheds in and adjacent to the study area.

The study area estimates do not differ significantly to those from the wider geographic area, provided that some allowance is made for a possible relationship between yield and watershed area. Similarly, both sets of estimates do not differ significantly from the global data presented in Figure 6.16.

The reservoir–based data do however appear to differ from the RLDCL estimates in many cases. The comparison is difficult because the RLDCL estimates do not include 'flood' flows or bedload. The scaling factor for converting non–flood suspended load to total suspended load may be as high as 4 (Sec. 6.5). The factor for including bedload is thought to be less than 1.1 in the global literature, but could be as high as 1.5 in local granitic sub–watersheds (Kondolf, 1982; cited by Hecht, 1981). Thus the Southern Santa Lucia Range RLDCL suspended non–flood yields ranging from 11–51 $t/km^2/yr$ may scale (6x) to 66 – 306 $t/km^2/yr$. This just overlaps the range based on reservoir sedimentation (314 – 619 $t/km^2/yr$, Tab. 6.3). The remaining differences are unexplained, and but may include error inherent in the RLDCL method, further under–estimation of bedload fraction, or local differences in watershed characteristics. None of the other RLDCL sites fall within the watersheds of the reservoirs, and so further comparison is precluded.

The importance of bedload in accounting for the sediment load of mountainous streams should be investigated further. Similarly, further work should better quantify the amount of sediment unaccounted for by standardization at the 99.5th percentile flow, here termed the 'non–flood' flow (Sec. 6.5). Finally, further work should also examine the possibility that RLDCL estimates are biased to low values because of the log–log transformation of sediment–rating data prior to fitting sediment–rating curves. Note that this bias, if present, is less likely to effect comparison *among* RLDCL estimates than comparison *between* RLDCL estimates and estimates made using other methods (such as reservoir sedimentation analysis).

7   A closer look at sediment sources on the Valley Floor

7.1   Introduction

The regional sediment analysis of the previous chapter provided a large-scale, long-term context for sediment sources in the Salinas Watershed. It quantified long-term loads from the major different parts of the watershed, such as the wetter west, the drier east, and the Valley floor. However, the regional analysis concluded with uncertainty about the balance between in-channel and possibly agricultural sources of higher sediment loads in the main stem of the Salinas River as it flows through the Valley floor.

The present chapter presents four, additional studies involving more-detailed examination of valley floor sediment processes. The first is a brief analysis of the timing of suspended sediment concentration peaks in the main stem. The second is a summary and extension of a detailed study originally reported by Casagrande (2001), involving the construction of a one-year sediment budget for the small Gabilan Creek watershed (315 km²), a tributary to the Old Salinas River. The third study builds on work originally presented by Kozlowski (2001), and reports sediment loads measured directly from row-crop fields on a number of farms whose managers kindly collaborated with the project. The fourth study is a brief application of the RUSLE model, to facilitate comparison with standard erosion estimation techniques applied by agronomists with the USDA-NRCS.

7.2   Timing of runoff and sediment load on the main stem

One of the tenets of the long-term regional load analysis presented in the previous chapter was that there is a well-defined relationship between suspended sediment concentration and discharge at each monitoring site. Data were presented that showed this to be the case for many sites, including the main stem sites when examined over a very large range of discharges. However, for individual storms less than the mean annual flood, the sediment-discharge-rating relationship is confounded by concentrated sediment sources that are much closer to the monitoring site than the principal source of discharge flowing past the site. This behavior is examined in Figure 7.1, which shows the layout of a selection of key sites on the Valley Floor, and Figure 7.2, which overlays USGS flow data from these sites with sediment concentration data collected by CCoWS during an early storm in 2001.
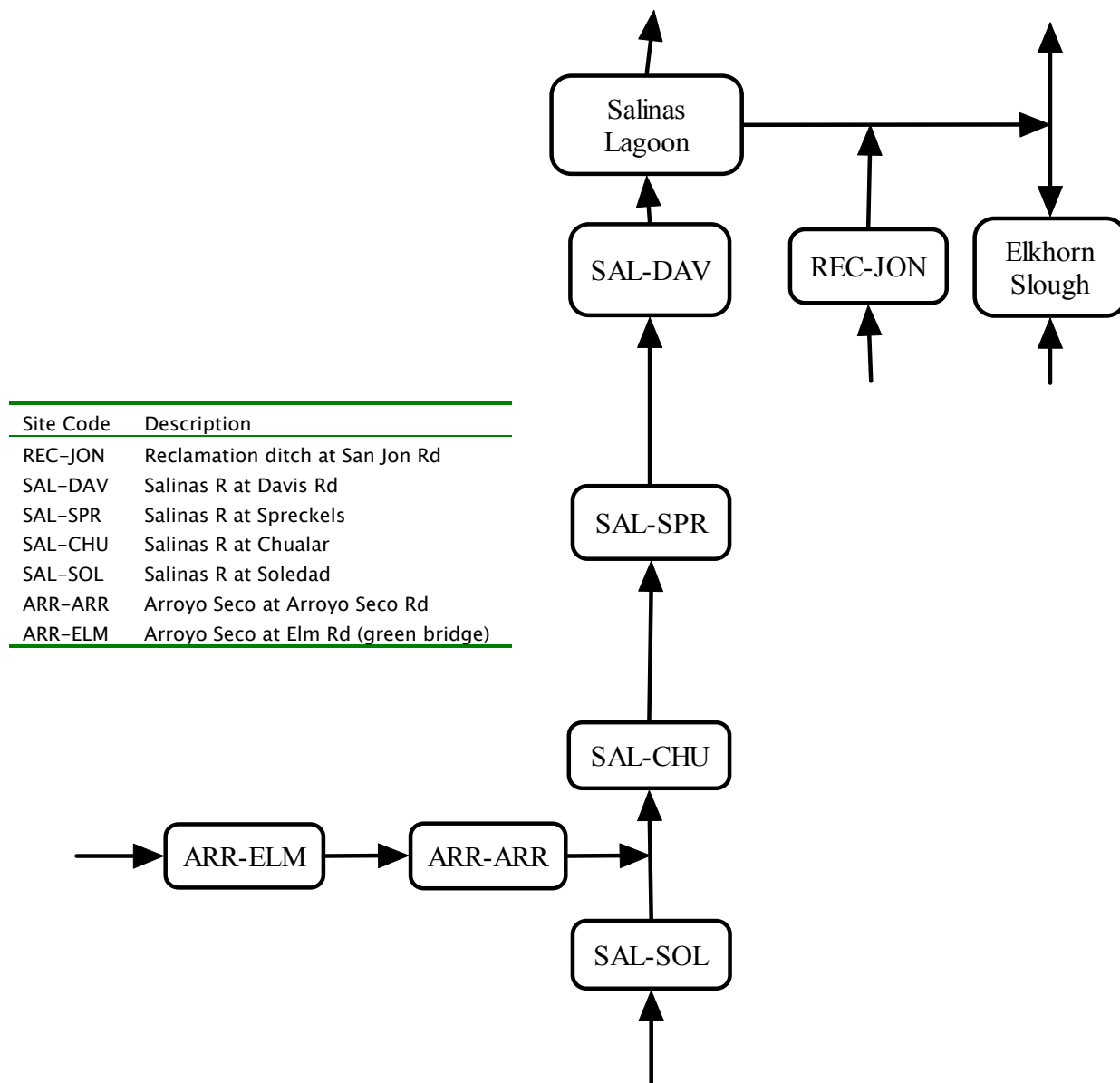
Figure 7.1. Schematic diagram of monitoring sites used for timing analysis in Figure 7.2. The Arroyo Seco River confluences with the Salinas River between Soledad and Chualar. The Reclamation Ditch confluences with the Old Salinas River on its way from the Salinas Lagoon, which is closed to the ocean except after storms, to Elkhorn Slough, which is always open to the ocean.
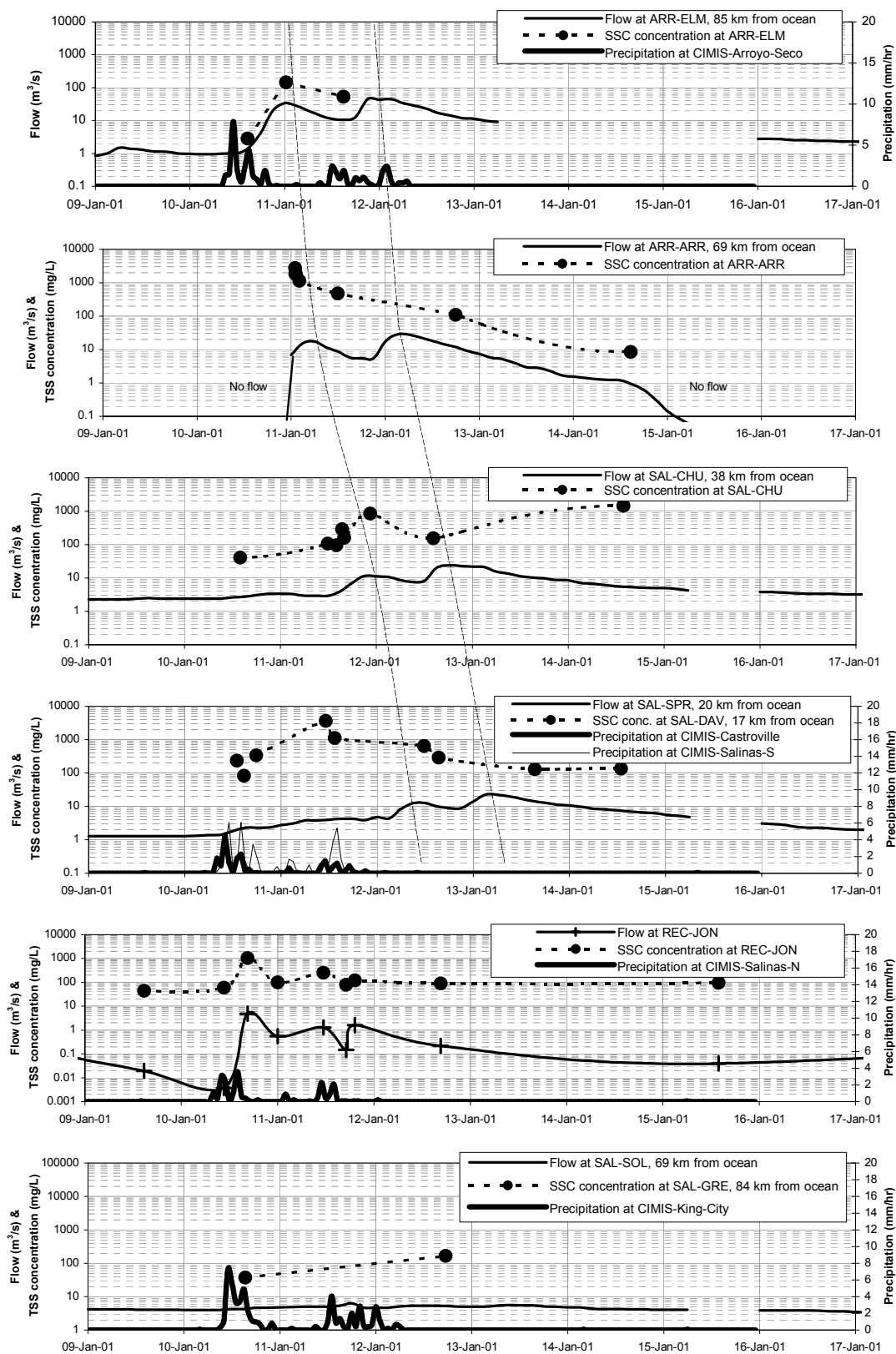
Figure 7.2. Timing of storm hydrograph progression down the Arroyo Seco / Salinas system, January, 2001.

The graphs in Figure 7.2 are intended to show that the highest sediment concentration and load at the lower main stem sites occurred well before the flow reaches a maximum value (Fig. 7.3). The first graph shows data for the Arroyo Seco River at Elm Rd (ARR-ELM). Significant rains fell midway through the 10th of January, and again late on the 11th. Each rain event resulted in a peak in discharge that flowed past ARR-ELM about half a day later. Prior to the events, clear water flowed at 1 m3/s. During the peaks, sediment concentrations remained relatively low (<200 mg/L) and flow reached 45 m³/s (1600 cfs), between the 1.01-year and the 2-year event for this site.
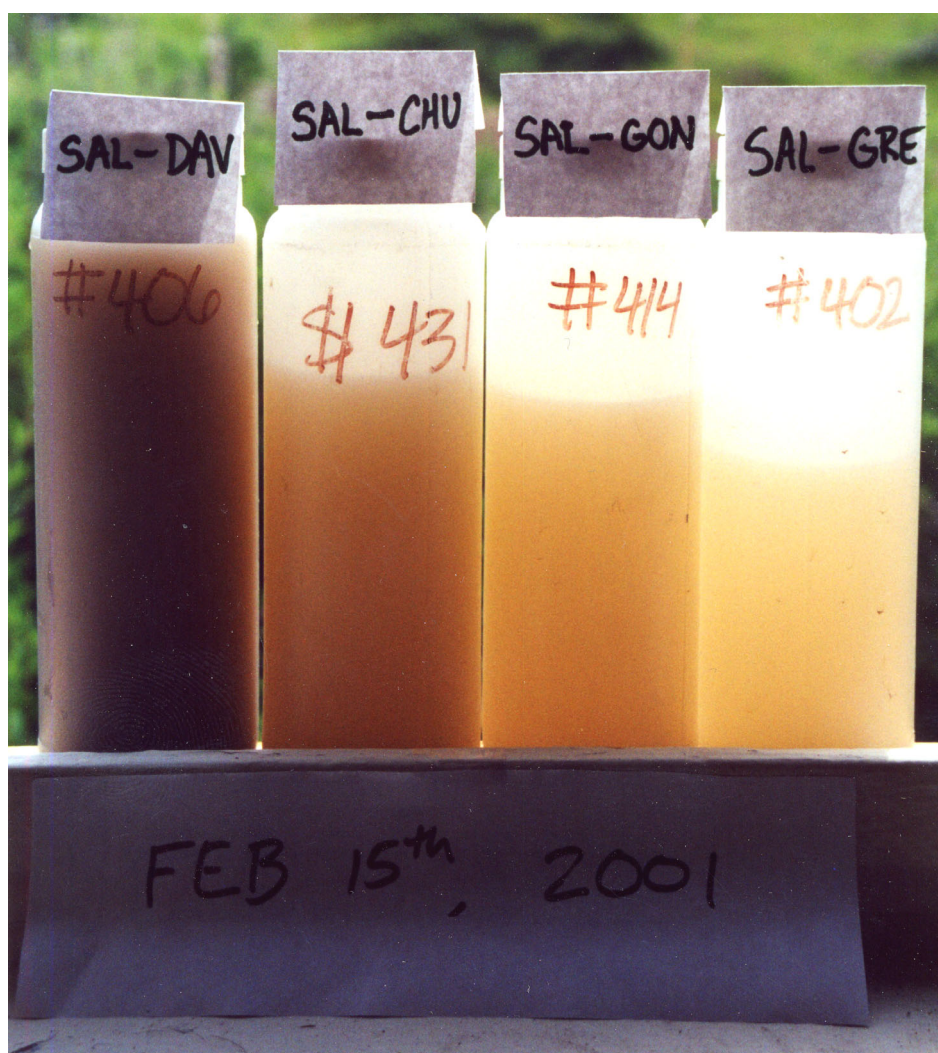
Figure 7.3. Suspended sediment samples taken during a 3-hour interval on the Salinas River during a storm: ranging from Davis Road near Salinas, upstream to Chualar, Gonzales, and finally Greenfield. Photo: Thor Anderson, Feb 2001.

Sixteen kilometers downstream, at Arroyo Seco Road (ARR–ARR), the streambed was completely dry prior to the event (2nd graph in Fig. 7.2). The first flow arrived at the site just after 1:00 AM on the morning of the 11th, bringing with it a concentrated foamy slurry of silt and leaves that had been accumulating in the dry bed for many months prior (Fig. 7.4). Within 2 hours, the flow reached 14 m^3/s (500 cfs). The sediment concentration was highest in the first few seconds (2738 mg/L), thereafter declining below 1000 mg/L in the first few hours. The second peak arrived in the early hours of the 12th, peaking at 27.9 m^3/s (985 cfs). Three days later, the river was dry again except for a few residual pools.
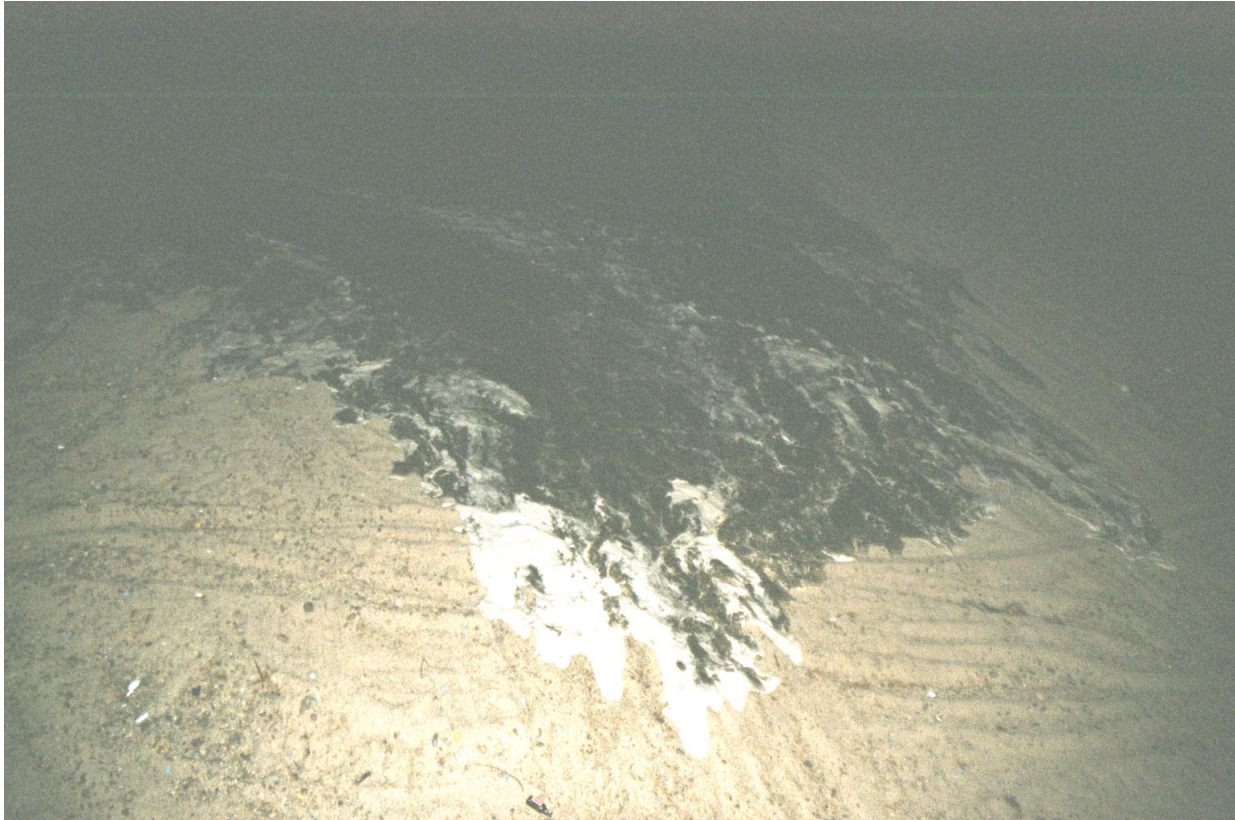
Figure 7.4. The first flow of the winter fills the wide sandy bed of the Arroyo Seco River at Arroyo Seco Road faster than one can outrun it (1:02 AM January 11th 2001). Photo: Fred Watson, 11 Jan 2001.

A few kilometers downstream from ARR–ARR, the Arroyo Seco River reaches the Salinas River. Just upstream of this confluence on the Salinas River side, at Soledad (SAL–SOL), conditions remained placid during this entire event, with flow gradually increasing from 4 m³/s to only 7 m³/s (Fig. 7.2, last graph). Downstream of the confluence, at Chualar (SAL–CHU), the flow dynamics in the Salinas River were therefore dominated by the influx from the Arroyo Seco River. With 31 km separating SAL–CHU from ARR–ARR, the flow peaks were delayed by a further 18 hours, and diffused down to peaks of 11.5 m³/s (405 cfs) and 24.2 m³/s (855 cfs) respectively. The highest concentration measured was 857 mg/L during the first peak, which broadly suggests a relationship between discharge and concentration at this site, although sampling was too infrequent to allow confirmation of this suggestion.

The flow peaks reached Spreckels (SAL–SPR) nearly 2 days after the rain events, reaching 12.6 m3/s (445 cfs) and 22.6 m³/s (798 cfs) on the 12th and 13th of January. Sediment concentration was measured at Davis Road, 3 kilometers downstream, owing to the busy traffic and high bridge at Spreckels. Sediment concentrations during the first event were fairly low, ranging between 83 and 337 mg/L. During the second event, however, a large sediment 'spike' at 3661 mg/L (a very high value capable of seriously affecting aquatic fauna) passed Davis Road carried by a flow of about 3.1 m³/s. The spike dissipated within a few hours to 1117 mg/L, still a high value for a large river discharging only 3.4 m³/s. By the time the second flood peak arrived at the site, borne of discharges from the Arroyo Seco River, the suspended sediment concentration was only about 300 mg/L. The highest instantaneous watershed sediment loads of the event occurred during the second rain, nearly two days before the highest discharges arrived from the Arroyo Seco River.

This pattern of an early sediment spike during rain, followed by declining concentrations as cleaner water arrives from upstream sources over the following days is indicative of a concentrated local runoff source, driven by rain. The source must be relatively large, because the instantaneous loads corresponding to the spike are larger than the 'regional' load measured during peak flow on the river a day or so later (Fig. 7.5). Data from the nearby Reclamation Ditch site at San Jon Rd (REC–JON, 5th graph in Fig. 7.2) confirm that the rains in this area were sufficient to produce peaks in runoff and sediment concentration from local streams other than the Salinas River main stem.

The source of the sediment spikes at Davis Road is likely to be either row-crop agriculture or urban stormwater, or a combination of both. A large stormwater drain discharges water into the Salinas River 450 m upstream of Davis Road from the City of Salinas. The watershed of the drain is approximately 20% of the City of Salinas, mainly comprising older areas of the City. Although storm runoff from these areas would be expected to be high, sediment loads would not – owing to the general lack of new development in this part of the City. The drain was sampled by CCAMP in 1999, but not during intense storms. Storm-sampling of the drain should be conducted in future in order to resolve the above uncertainties. Agricultural sources are equally likely, for opposite reasons. Although agricultural runoff ratios are much lower than urban runoff ratios, the associated sediment concentrations are much higher than for typical urban runoff. Making an inference based on field-level monitoring data (see Section 7.4 below), early-response agricultural loading of sediment to the Salinas River is probable under intense rainfall and antecedent soil saturation.
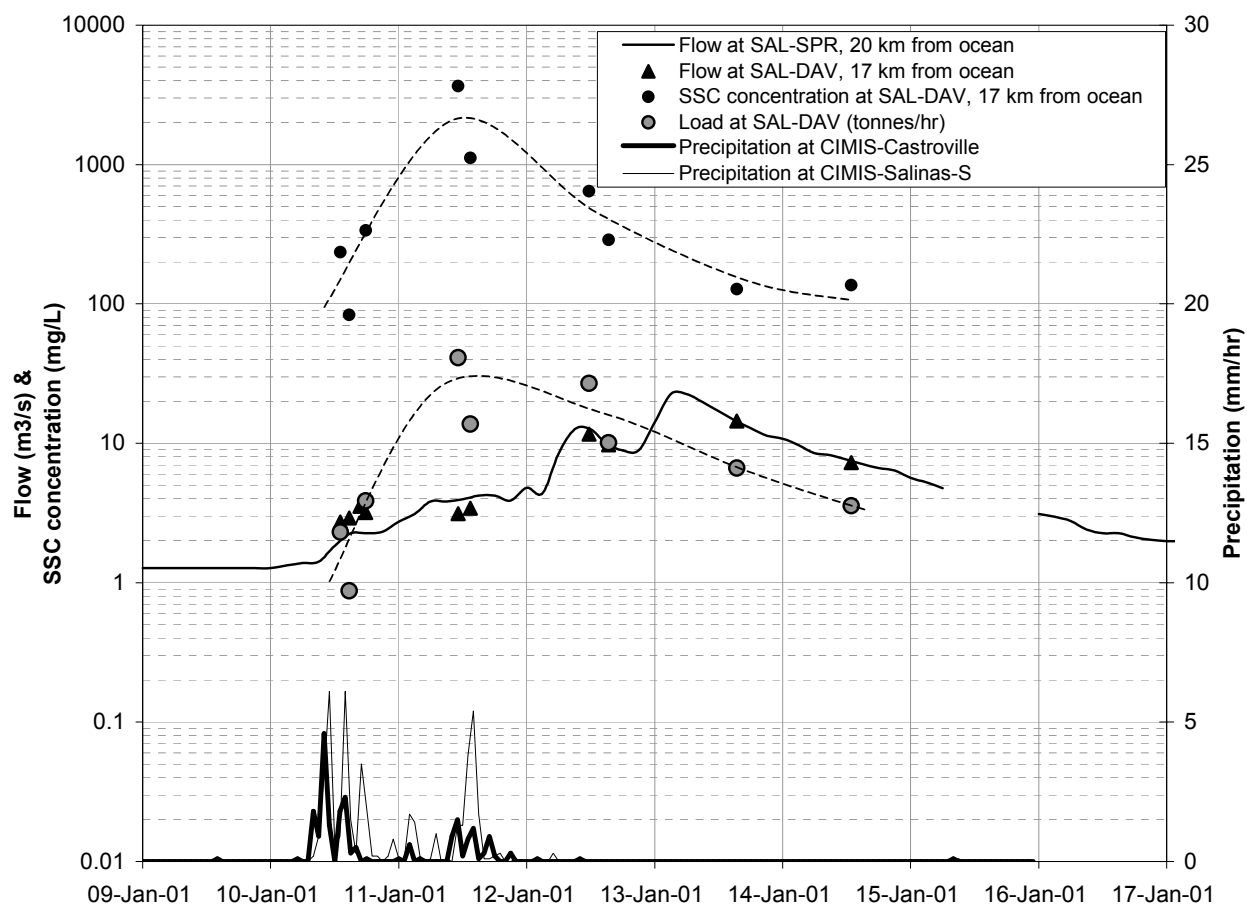
Figure 7.5. Timing of local sediment 'spikes' on the main stem of the Salinas River at Davis Rd (SAL–DAV) preceding the less–concentrated, regionally derived main stem flow peaks 2 days later. NB: Curves for TSS and load data were fitted manually.

7.3 Short-term sediment sources in the Gabilan Watershed

7.3.1 Watershed and channel description

The Salinas River has two mouths. Most of the flow reaching the ocean does so at the Salinas Lagoon, but some still travels down the Old Salinas River channel to the River's historical mouth at Moss Landing Harbor. Gabilan Creek is the major tributary of the Old Salinas River. It is discussed here both because of its inclusion in the historic Salinas River Watershed, and because it flows through all the major land types of the Salinas Watershed in a relatively short distance with many bridges for public access. This makes an excellent system to study as a model of the processes exhibited through the Central Coast region. The Gabilan Creek Watershed above Highway 183 comprises 315 km^2 and is approximately 36 km long (Fig. 7.7). Centered on the City of Salinas, its tributaries are Alisal Creek, Natividad Creek, and Santa Rita Creek.   Below Highway 183 the Creek flows into Tembladero Slough, which flows into the Old Salinas River channel.

The upper reaches are perennial until just downstream of the Old Stage Road crossing (Figs 7.6 & 7.8). Throughout this area the creek flows through steep canyons of oak and maple riparian communities.   The surrounding slopes include oak woodland, chaparral, and annual grassland used for grazing. Boulders and cobbles of granitic parent material are the dominant bed materials (Hager, 2001). After Old Stage Road the creek (still perennial) is slightly incised and begins flowing through a narrow cultivated valley for approximately 4.8 km out into the heavily cultivated Salinas Valley. Along this 4.8 km reach, the stream is lined with heavy to moderate stands of willow-oak communities and bed materials are now coarse sands and small cobbles (Fig.7.8).

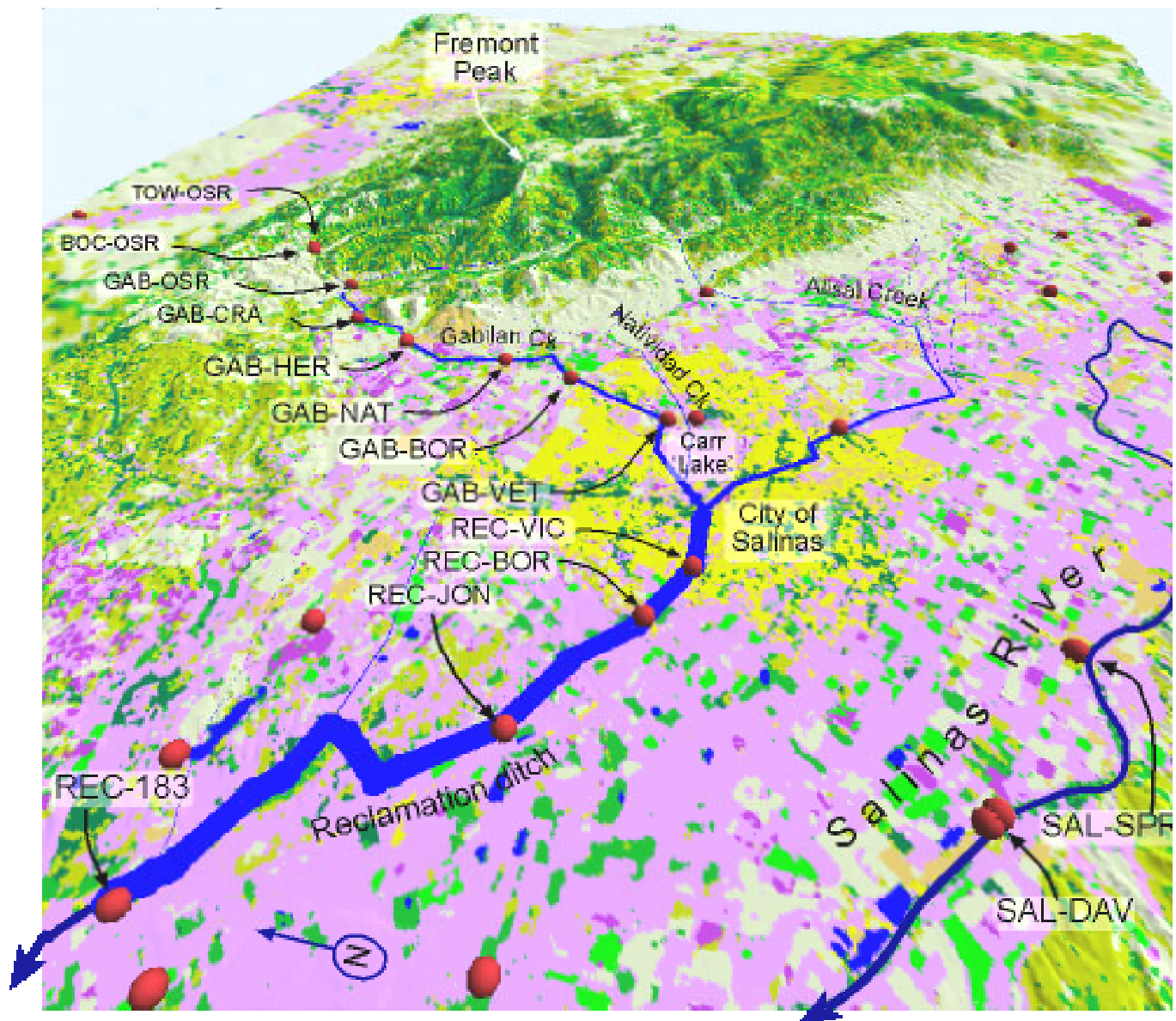Figure 7.6. Upper Gabilan Creek. Photo: Julie Hager, Fall 2002.

Figure 7.7. The Gabilan Creek Watershed, showing the location of CCoWS sampling sites.

Figure 7.8 Perennial flow: Gabilan Creek at Crazy Horse Canyon Road (downstream of Old Stage Road). Photo: Joel Casagrande.

Figure 7.9. Bulldozing of the creek channel between GAB–HER and GAB–CRA, Aug 2000. Photo: Joel Casagrande.

Once reaching the Salinas Valley at Herbert Road, the stream is consistently flat and bordered with cultivated fields for approximately 4.8 km. The channel is incised to depths ranging from one to six meters below the surrounding plains. Agriculture, predominantly lettuce and strawberries, has replaced much of the floodplain and riparian vegetation. Bulldozers are used to shape the channel in order to protect adjacent lands from flooding and erosion (Fig. 7.9).

Very little vegetation, except for various weeds and willow yearlings, are found along the banks at this point (Fig. 7.10). In this reach the stream only flows after intense rainfall. The bed substrate is made up of coarse sands and fine sediments that allow water to easily percolate into groundwater storage. Once reaching the eastern boundary of Salinas, the creek flows through man-made park areas that are lined with willow, cottonwood, and sycamore trees until reaching Veterans Park just upstream from Carr Lake. Gabilan Creek joins with Natividad and Alisal Creeks in Carr Lake located in the center of Salinas. Drainage out of Carr Lake leads into The Reclamation Ditch. Here, adjacent land areas are mostly urban with small amounts of crops.

In 1917, the lower portion of the Creek from Salinas down to Moss Landing Harbor was channelized into what is now known as The Reclamation Ditch and Tembladero Slough (Schaaf and Wheeler, 1999). With this change came the loss of almost all the riparian vegetation and alteration of the natural flow regime for the lower Gabilan Creek. Coastal marsh habitat was replaced with intense agriculture west of Salinas. The Reclamation Ditch runs through the center of urbanized Salinas, which is home to over 150,000 people, and continues through the coastal artichoke/lettuce fields to the west until reaching Tembladero Slough. Bed material in The Reclamation Ditch is primarily fine sediments (silt and clays) with small portions of sand in the lower reaches (Hager, 2001).

Figure 7.10. Gabilan Creek downstream from the Herbert Road Bridge. Note steep banks, bank failure, and lack of riparian vegetation. Photo: Joel Casagrande, 17 Aug 2000.

7.3.2 Aim

The aim of the work described here was to evaluate a single-year (2001 water year) sediment budget for the watershed by measuring the total sediment load passing each of 9 public bridges and two culverts (Fig. 7.7) along Gabilan Creek from its headwaters down to Highway 183 below Salinas. The watershed was chosen because of the approximately linear sequence of land uses along its banks: grazing, woodland, strawberries, vegetables, dense urban, and vegetables again. The sub-watersheds unique to each gauging and monitoring point in the study are shown in Figure 7.11.
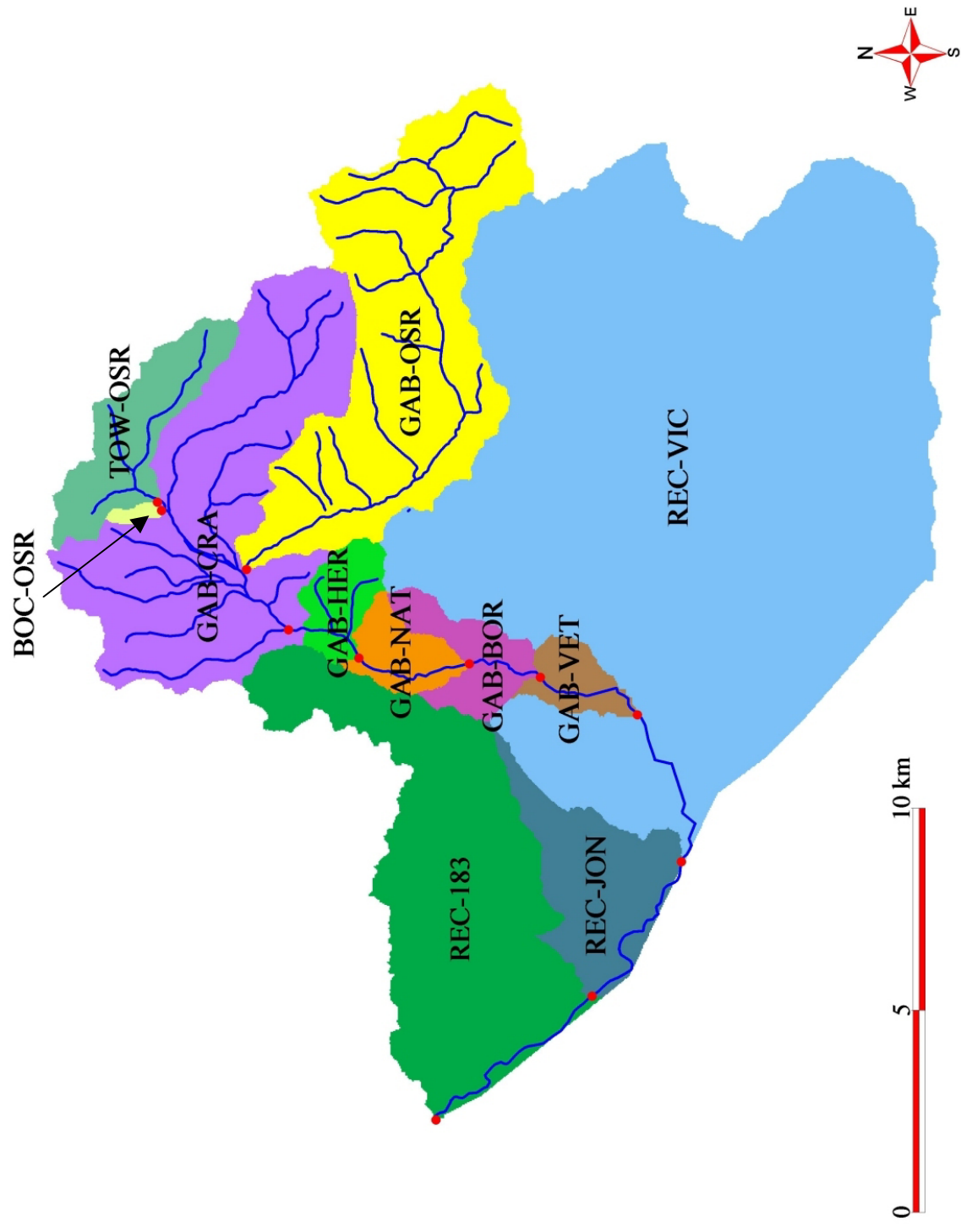
Figure 7.11. Gauged sub-watersheds of the Gabilan Creek Watershed.

7.3.3 Land use

The full watershed was partitioned into the sub-watersheds unique to the stream reaches upstream from each site, and the total area for each sub-watershed was calculated using the Tarsier Modeling Framework (Watson et al., 2002) (Figure 7.11, Table 7.1).

A digital land-use data set archived by the Association of Monterey Bay Governments shows 10 different land uses/ cover types in the Gabilan Watershed. These include grass, oak woodland/woody vegetation, shrub, artichoke, row crops, orchard/nursery, strawberries, greenhouses, golf courses, and urban land. These types were grouped as follows: 'grazing/natural' includes grass and woody vegetation classes; 'crops' includes artichoke, greenhouse, orchard/nursery, row crops, strawberries, and fallow covers; and 'urban' comprises of urban land and golf courses. The area of each of these classes is tabulated in Tables 7.2 and 7.3[11]. Of the 316 km^2 total watershed area above Highway 183, 188 km^2 (59.5%) are grazing and natural lands, 98.6 km^2 (31.2%) support crops, and 29.2 km^2 (9.3%) are urban.

7.3.4 Measurement of discharge and sediment transport

During the winter of 2000–2001, monitoring crews were maintained on standby, ready to measure discharge and sediment concentration in rotating 4 to 8-hour shifts around the clock during every major storm. The five largest storms were sampled adequately in this way, with storm hydrographs typically lasting about 5 days.

For each storm event, the total water and suspended sediment load passing each bridge was calculated using field and laboratory protocols described by Watson et al. (2002). In summary, staff plates were installed at each site and stage-discharge rating curves were constructed over a period of time for each

---

[11] The AMBAG data is from 1990–93. However, the Salinas Sediment Study has created a new land use data set (Newman & Watson, 2002) that estimates the GAB-OSR sub-watershed to be 14.1% (5.38 km^2) crop cover. Field observations indicate that there are large strawberry fields immediately upstream from the sampling site in this sub-watershed, but there is skepticism about the accuracy for the total area of these strawberries. Thus, it was decided that the area is approximately 2 km^2.

site using measurements of discharge (m³/s) based on lateral transects with a current meter (m/s). About 3 to 10 suspended sediment samples were taken during each storm, and their concentrations (mg/L) were multiplied by discharge from the stage–discharge curve (m³/s) to give instantaneous loads (g/s). These were integrated over the full duration of the storm hydrograph to estimate total suspended sediment load associated with each storm (tonnes). Bedload measurements (g/s) were also taken where possible, yielding similarly calculated total event bedload, albeit from fewer samples.

Inter–event loads were also estimated, based on interpolation between measurements taken at the end of the preceding storm, and just before the following storm. Such estimates are crude, but of sufficient accuracy to demonstrate that total inter–event loads are small relative to event loads.

Table 7.1. Sub–catchment and total drainage area for each monitoring site.

Sampling Site	Sub-watershed Area (km²)	Drainage Area (km²)
TOW-OSR	9.7	9.7
BOC-OSR	0.5	0.50
GAB-OSR	41.5	41.5
GAB-CRA	38.7	90.4
GAB-HER	4.3	94.7
GAB-NAT	4.1	98.7
GAB-BOR	5.4	104.3
GAB-VET	3.4	107.7
REC-VIC	155.7	263.3
REC-JON	12.5	275.9
REC-183	40.0	315.9

Table 7.2. Land use proportions within each sub-watersheds outlined in Figure 7.11.

Sub-watershed	Land Use							
	Grazing/ Natural		Crops		Urban		Total	
	Km²	%	Km²	%	Km²	%	Km²	%
TOW-OSR	9.7	100	0	0	0	0	9.7	100
BOC-OSR	0.5	100	0	0	0	0	0.5	100
GAB-OSR	41.5	100	0	0	0	0	41.5	100
GAB-CRA	38.2	98.6	0.55	1.4	0	0	38.7	100
GAB-HER	3.3	77.7	0.92	22.3	0	0	4.3	100
GAB-NAT	1.2	31	2.7	66.5	0.12	3	4.1	100
GAB-BOR	1.4	24.5	4.0	75.5	0	0	5.4	100
GAB-VET	1.2	35	1.0	29	1.2	35.6	3.4	100
REC-VIC	85.7	55	49.8	32	20.2	13	155.7	100
REC-JON	0.2	2	7.5	61	4.7	38	12.5	100
REC-183	5.1	13	31.9	80	2.9	7	40.0	100

Table 7.3. Cumulative land use proportions above each sampling point.

Sub-watershed	Land Use							
	Grazing/ Natural		Crops		Urban		Total	
	Km²	%	Km²	%	Km²	%	Km²	%
TOW-OSR	9.7	100	0	0	0	0	9.7	100
BOC-OSR	0.5	100	0	0	0	0	0.50	100
GAB-OSR	41.4	100	0	0	0	0	41.5	100
GAB-CRA	89.9	99.4	0.55	0.6	0	0	90.4	100
GAB-HER	93.3	98.5	1.5	1.5	0	0	94.7	100
GAB-NAT	94.5	95.6	4.2	4.2	0.12	0.1	98.7	100
GAB-BOR	95.9	92.0	8.2	7.9	0.12	0.1	104.3	100
GAB-VET	97.1	90.2	9.2	8.6	1.4	1.3	107.7	100
REC-VIC	182.7	69.4	59	22.4	21.5	8.2	263.3	100
REC-JON	182.9	66.3	66.6	24.1	26.3	9.5	275.9	100
REC-183	188.1	59.5	98.6	31.2	29.2	9.3	315.9	100

7.3.5 Results

Results from five storms are presented:

- October 25–31, 2000
- January 7–15, 2001
- January 23–26, 2001
- February 9–12, 2001
- February 18–19, 2001

Some storms were sampled in greater detail than others due to personnel availability. Typically 10 people were involved over a five-day period. A total of 293 suspended sediment samples were taken in the field along with 405 stage readings.

Event totals are summarized in Table 7.4, and inter-event totals are summarized in Table 7.5 and as percentages of total season load in Table 7.6. Season totals are shown Table 7.7. The details of each event are discussed at length by Casagrande (2001), who also gives plots of the key variables of each event.

Sample coverage for two of the events was limited relative to the other three, and so it was decided to base the watershed analysis on totals from just the three better-sampled events (Table 7.8). This enabled a more meaningful comparison to be made between sites. Figure 7.12 shows the longitudinal downstream progression of total (3-event) discharge, suspended load, and event mean concentration (EMC) moving down the watershed from the headwaters to Highway 183.

Table 7.4. Event totals for discharge, total suspended sediment, and bedload.

Sampling Site	Event 1 (October 25–31)			Event 2 (January 7–15)			Event 3 (January 23–26)			Event 4 (February 9–12)			Event 5 (February 18–19)		
	Discharge (m3)	SS (tonnes)	Bedload (tonnes)	Discharge (m3)	SS (tonnes)	Bedload (tonnes)	Discharge (m3)	SS (tonnes)	Bedload (tonnes)	Discharge (m3)	SS (tonnes)	Bedload (tonnes)	Discharge (m3)	SS (tonnes)	Bedload (tonnes)
TOW–OSR	*	*	*	6082.6	0.20	*	2900.2	0.9	*	1785.5	0.1	*	836	0.1	*
BOC–OSR	*	*	*	685.1	0.17	*	4709.8	8.1	*	1040.4	0.2	*	357	0.1	*
GAB–OSR	10957	15.2	0.3	16904.5	7.2	1.9	26509.9	29.3	1.8	14604.2	3.5	0.9	11068	7.8	14.6
GAB–CRA	61559	65.1	46.3	43363	7.7	7.2	69543	144.7	43.4	64173.6	37.8	18.7	25355	41.1	70
GAB–HER	21450	183.5	0.7	2367	2.8	0.0	9680.2	34.5	0.0	42183.2	124.5	0.0	8937	35.0	0.0
GAB–NAT	–	–	–	–	–	–	7928.4	53.2	0.6	26956.0	88.8	12.2	5842	39.3	11.9
GAB–BOR	–	–	–	–	–	–	–	–	–	10154.5	30.16	0.012	4006.1	23.9	0.0
GAB–VET	*	*	*	10241	0.1	0.0	31572	3.1	0.0	50833	4.96	0.3	20910	6.5	0.3
REC–VIC	*	*	*	656598	193.9	0.3	251610	103.8	*	*	*	*	105623	23	*
REC–JON	728334	543.5	0.0	616784	251.4	0.015	364252	245.2	*	*	*	*	225250	58	*
REC–183	*	*	*	963093	525.4	0.9	449047	399.2	*	*	*	*	112085	141	*

* Site not visited or not sampled for this parameter.

– No samples were taken due to no flow

Table 7.5. Estimated inter–event totals for discharge, suspended sediment, and bedload.

Sampling Site	Oct 31–Jan 7			Jan 16–Jan 22			Jan 27–Feb8			Feb13–17		
	Discharge (m3)	SS (tonnes)	Bedload (tonnes)	Discharge (m3)	SS (tonnes)	Bedload (tonnes)	Discharge (m3)	SS (tonnes)	Bedload (tonnes)	Discharge (m3)	SS (tonnes)	Bedload (tonnes)
TOW–OSR	41548.4	0.17	0.0	4888.0	0.02	0.0	7943.1	0.03	0.0	5499.1	0.02	0.0
BOC–OSR	927.7	0.01	0.0	109.1	0.002	0.0	177.3	0.003	0.0	122.8	0.00	0.0
GAB–OSR	22913.3	0.34	5.3	9362.5	0.34	0.6	15214.0	0.34	1.01	10532.8	0.34	0.7
GAB–CRA	71251.7	1.13	6.1	25235.6	1.13	0.7	41007.9	1.13	1.2	28390.1	1.13	0.8
GAB–HER	0.0	0.0	0.0	0.0	0.00	0.0	0.0	0.00	0.0	0.0	0.00	0.0
GAB–NAT	0.0	0.0	0.0	0.0	0.00	0.0	0.0	0.00	0.0	0.0	0.00	0.0
GAB–BOR	0.0	0.0	0.0	0.0	0.00	0.0	0.0	0.00	0.0	0.0	0.00	0.0
GAB–VET	318266	0.18	0.0	37443.1	0.02	0.0	60845.0	0.04	0.0	42123.4	0.02	0.0
REC–VIC	672799	26.59	0.0	79152.8	3.13	0.0	128623	5.08	0.0	89046.9	3.52	0.0
REC–JON	128535	4.76	0.0	15121.8	0.56	0.0	24572.9	0.91	0.0	17012.0	0.63	0.0
REC–183	137907	6.13	0.0	16224.3	0.72	0.0	26364.5	1.17	0.0	18252.4	0.81	0.0

Table 7.6. Inter–event load percentages of season total load for each monitoring site.

Sampling Site	Oct 31–Jan 7			Jan 16 – Jan 22			Jan 27 – Feb 8			Feb 13 – Feb 17			Totals		
	Discharge (%)	SS Load (%)	Bedload (%)	Discharge (%)	SS Load (%)	Bedload (%)	Discharge (%)	SS Load (%)	Bedload (%)	Discharge (%)	SS Load (%)	Bedload (%)	Discharge (%)	SS Load (%)	Bedload (%)
TOW–OSR	58.1	11.2	0	6.8	18.5	0	11.1	2.1	0	7.7	1.5	0	83.7	33.3	0
BOC–OSR	11.9	0.2	0	1.4	0.02	0	2.3	0.03	0	1.6	0.02	0	17.2	0.27	0
GAB–OSR	18	0.5	7.5	7.4	0.5	0.6	12.0	0.5	1.4	8.3	0.5	1.0	45.7	2	10.5
GAB–CRA	16.6	0.4	2.0	5.9	0.4	0.7	9.5	0.4	0.4	6.6	0.4	0.3	38.6	1.6	3.4
GAB–HER	0	0	0	0	0	0	0	0	0	0	0	0	0	0	0
GAB–NAT	0	0	0	0	0	0	0	0	0	0	0	0	0	0	0
GAB–BOR	0	0	0	0	0	0	0	0	0	0	0	0	0	0	0
GAB–VET	55.6	0.1	0	6.5	0.1	0	10.6	0.02	0	7.4	0.2	0	80.1	0.42	0
REC–VIC	33.9	0.9	0	4.0	0.9	0	6.5	1.4	0	4.5	1.0	0	48.9	4.2	0
REC–JON	6.1	0.1	0	0.7	0.1	0	1.2	0.1	0	0.8	0.1	0	8.8	0.4	0
REC–183	8.0	0.1	0	0.9	0.1	0	1.5	0.1	0	1.1	0.1	0	11.9	0.4	0

Table 7.7. Season totals for all sampling sites for discharge, total suspended sediment, and bedload.

Sampling Site	# of events monitored	Discharge (m3)	SS (tonnes)	Bedload (tonnes)	SS Mean Conc. (tonnes/m3)
TOW–OSR	4	71500	1.3	0.0	1.8×10^{-5}
BOC–OSR	4	8100	9	0.0	1.0×10^{-3}
GAB–OSR	5	127000	70	27.1	5.5×10^{-4}
			380	0.7	6.0×10^{-3}
GAB–NAT	5	41000	181	24.6	4.4×10^{-3}
GAB–BOR	5	14000	54	0.012	3.8×10^{-3}
GAB–VET	4	572200	15	0.6	2.5×10^{-5}
	3	1984000	320	0.3	1.6×10^{-4}
REC–JON	4	2120000	1098	0.0145	5.1×10^{-4}
REC–183	3	1723000	1066	0.9	6.1×10^{-4}

Table 7.8. Three-event totals for each monitoring site.

Sampling Site	3-event Totals (Jan 7-15, Jan 23-26, & Feb 18-19, of 2001)				
	Discharge (m³)	SS Load (tonnes)	SS EMC (mg/L)	Bedload (tonnes)	Bedload EMC (mg/L)
TOW-OSR	10000	1.2	121.4	0	0
BOC-OSR	6000	8.4	1460.3	0	0
GAB-OSR	54000	44.3	813.7	18.3	336.4
GAB-CRA	139000	193.4	1398.6	120.7	873.0
GAB-HER	21000	72.3	3444	0	0
GAB-NAT	14000	92.6	6722.2	12.4	903.4
GAB-BOR	4000	23.9	5960	0	0
GAB-VET	63000	9.8	155.8	0.3	4.8
REC-VIC	1014000	320.2	315.8	0	0
REC-JON	1206000	554.8	459.9	0	0
REC-183	1524000	1065.6	699.1	0	0

The data reveal a pattern dominated by percolation. All flow generated in the upper and upper-middle watershed above Boronda Road (GAB-BOR) percolated into the bed during the three summary events. No surface flow traveled past Boronda Road. Flow re-started again at Veteran's Park (GAB-VET), and continued to the ocean. The Gabilan Watershed was thus divided into two completely separate surface flow systems.

The total discharge (m^3) per unit area (m^2), was typically just above 1 mm for headwater sites with sand-bottomed channels draining mainly natural and grazing lands, with some agriculture (TOW-OSR, GAB-OSR, GAB-CRA). The smallest sub-watershed, a grazing area above the BOC-OSR site, delivered a higher volume per unit area (12 mm) but this was measured above any obvious access to a shallow sub-stream aquifers. Below Crazy Horse Road, a distinct decline in discharge is evident in the reaches passing through intense agricultural lands above the City of Salinas – indicating that percolation dominates the hydrology of small storm events at these sites (GAB-HER, GAB-NAT, GAB-BOR). Once in the City of Salinas, new urban flow occurred with an areal total of 3-5 mm that persisted past the City to the agricultural areas downstream. Figure 7.12 also shows 'Adjusted discharge' for these sites, based on just the area of the watershed below Boronda Road. In these terms, areal flow from the City and below was higher, at 6-7 mm. Below GAB-CRA, an 'Incremental discharge' was calculated by taking the increase or decrease in flow between each two successive sites, and dividing by the local sub-watershed area. This calculation shows that the reach upstream of Herbert Road percolated most of the water.

The suspended sediment load data plotted in Figure 7.12 echo the discharge data in many respects. Whenever flow is percolated, the sediment transport capacity of the remaining flow is reduced and sediment is deposited. The 0.5 km^2 grazing site at BOC-OSR generated 135 times more suspended load per unit area than the 9.7 km^2, well-vegetated grazing/natural site at TOW_OSR. The difference in area confounds the comparison, but the suggestion from the data is that a significant reduction in load may be associated with the vegetated banks of the TOW-OSR site.
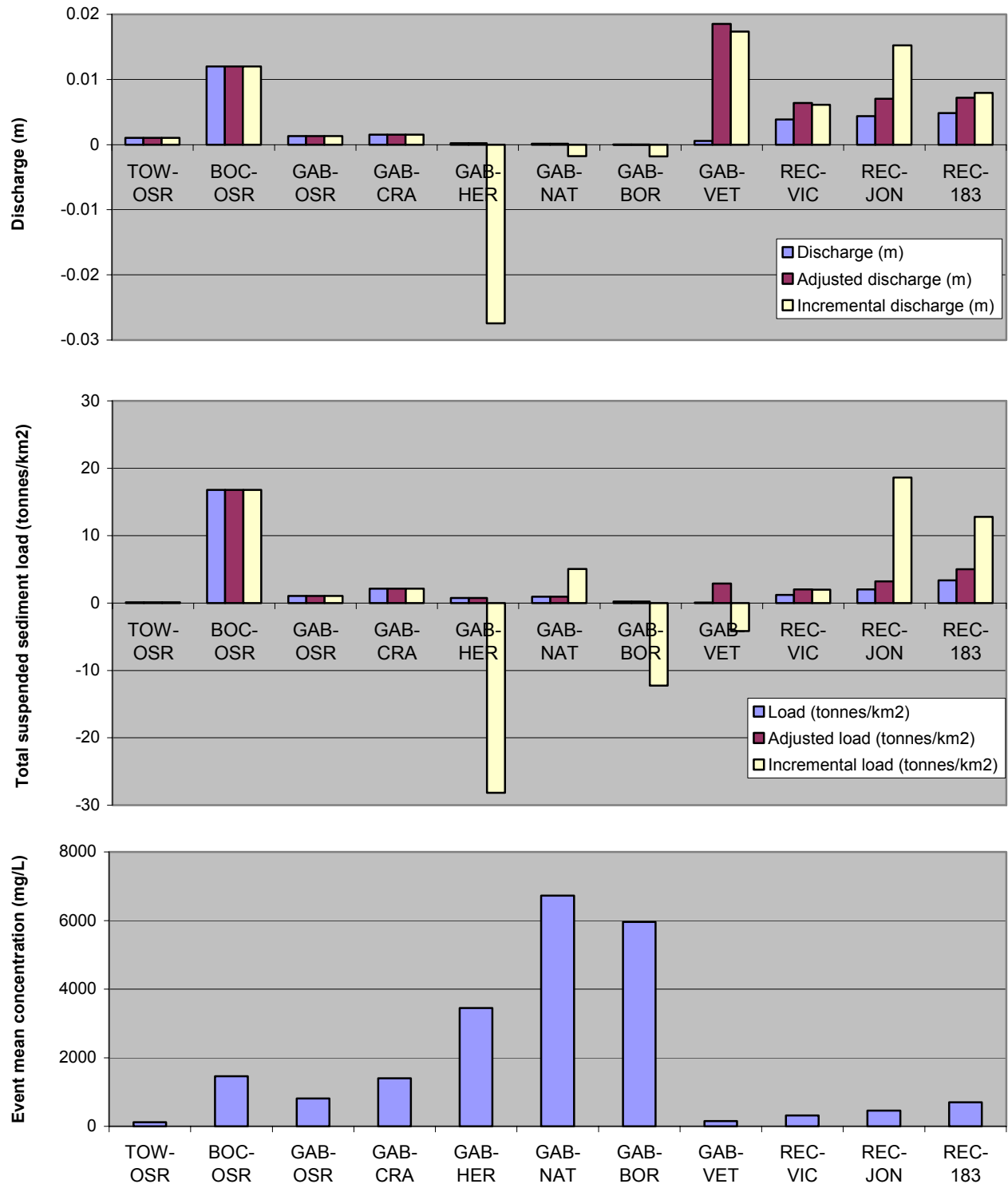
Figure 7.12. Total discharge, suspended sediment load, and event mean concentration for the three selected events. Note: 'adjusted load' is load that is specific to the watershed below the flow discontinuity at Boronda Road; 'incremental load' is specific to just the reach between the indicated site, and the next upstream site (if present).

Downstream, at the sites that integrate loads from a much larger area, 3-event total areal loads of 1.1 to 2.1 tonnes/km² were measured above Crazy Horse Road. Below this site, significant deposition takes place in association with the percolation described earlier. The incremental data show significant deposition above Herbert Road, but also some indication of higher loading rates from the agricultural lands between Herbert Road and Natividad Road. By Boronda Road, downstream, all surface water and sediment movement ceased.

Continuing downstream from Veteran's Park through the City and below to Highway 183, relatively high adjusted 3-event total areal loads of between 2.0 and 5.0 tonnes/km² were estimated. In incremental terms, there is evidence for a strong increase in load (after taking account of difference in watershed area) from the agricultural and urban lands below the City (between Victor Road and Highway 183).

The (non-adjusted) 3-event loads at REC-VIC, REC-JON, and REC-183 were 1.22, 2.01, and 3.37 t/km² respectively. If the increases in the downstream direction were to be explained by re-mobilization of channel sediment or bank erosion, they would imply an eroded streambed or bank thickness of approximately 4 to 5 mm (assuming reach lengths of 3000 m and 5000 m respectively, and bulk density of 2 kg/m³).

If, on the other hand, additional watershed sources were to account for the increased load, the following calculations apply. The incremental or reach-specific 3-event loads for the two reaches ('REC-VIC to REC-JON' and 'REC-JON to REC-183') are 18.6 and 12.8 t/km². These estimates can be compared to the regional RLDCL estimates (Sec.6.6) by estimating a factor for scaling from a 3-event suspended load to a mean annual non-flood suspended load. A simple assumption is that the spatial distribution of sediment yield is the same between 3-event and mean annual non-flood temporal scales, and thus that the ratios of RLDCL-estimated loads to 3-event loads for REC-JON and REC-183, are representative of the ratio between reach-specific (incremental) equivalents for the same sites. These ratios for REC-JON and REC-183 are 38.8:1 and 26.4:1 respectively, which leads to estimates of the mean annual non-flood suspended sediment yield for the lands specific to just the REC-JON and REC-183 reaches of 722 and 337 t/km²/yr respectively. These estimates indicate high sediment loads either from the agricultural lands that comprise 61% and 80% of the lands draining to the two reaches respectively, or from the remaining, largely urban

fraction. Urban sources are less likely, for they would also most likely be manifested in the GAB–VET and REC–VIC data. The estimated mean annual non-flood yields are approximately 5 to 10 times higher than the regional average, and are not unlike the high values suggested for agricultural lands between Soledad and Spreckels on the main stem (200–500 t/km²/yr, Sec. 6.6.2). It is possible that a combination of increased watershed loading and re–mobilization of streambed sediments is at work.

Event mean concentration was the highest at the agricultural sites between Herbert Road and Boronda Road (inclusive). A first hypothesis might be that this is due to higher agricultural inputs than from other land types. However, the observation may also be explained by the possibility that sediment concentration is increased as an artifact of removal of water by percolation. In turn, this latter explanation may be countered by noting that sediment transport capacity is best described as a power function with power greater than one, which would lead to lower concentration as percolation progressed because for every fraction of the flow that percolated, a greater fraction of sediment would be deposited. We are then left with the original hypothesis of relatively high sediment loadings from agricultural land during small storm events.

The urban–dominated flows at GAB–VET and REC–VIC are relatively free of sediment. Although concentration increases below the City at REC–JON and REC–183, the same levels as for GAB–HER through GAB–BOR are not observed below the City because of the dilution by the relatively sediment–free urban runoff.

Corresponding bedload data for the three selected events are shown in Figure 7.9. The blue bars in this Figure illustrate the total bedload that flowed past each site, divided by the total watershed of that site. The purple bars represent incremental data – the change in total bedload transport between a given site and the site immediately above it, expressed as a fraction of the watershed area specific to the given site. Negative incremental bedload thus indicates deposition. The only reaches to exhibit significant area–weighted bedload transport are those in the strawberry–agricultural region above the City of Salinas, including the GAB–OSR site which, while mainly draining natural and grazing lands, has a strawberry farm immediately upstream of it. As with the suspended sediment data, the reach above Herbert Road is 100% depositional of bedload. Bedload re–appeared downstream at Natividad road, indicating a

source specific to the reach between Herbert Road and Natividad Road. Again, this load was completely deposited in the reach between Natividad Road and Boronda Road. It is unlikely that all the bedload in transport is re-mobilization of existing bed material, because of the overall depositional nature of the hydrologic regime in this watershed during small storm events. Only much higher flows would be expected to exhibit net bed scour that could account for material measured passing a given site. Therefore, a concurrent land use loading is implicated, with the most likely bedload material source being agriculture, which in the areas in question, is dominated by strawberry farms. This is not unexpected, given the localized, high-velocity flows generated when rain falls on the plastic lining used in strawberry growing operations.

7.3.6 Conclusions of Gabilan study in relation to Salinas sediment sources

The conclusions that may be drawn from the Gabilan monitoring and analysis in relation to the determination of Salinas Valley sediment sources are as follows:

- Determination of watershed sediment budgets in non-perennial systems is confounded by the dominant influence of episodicity, percolation, and in-channel sediment storage, even when detailed storm-based monitoring is conducted at multiple sites simultaneously for a whole storm season. Conclusions based on monitoring data are thus limited. Decisions based on these data should be cognizant of the inherent uncertainty in the results.
- There is good evidence that row-crop agricultural lands contributed the highest suspended sediment loads per unit area under the conditions experienced in 2000-1.
- There is good evidence that urban lands contributed the greatest volume of runoff per unit area.
- There is some evidence for significant input of coarse material (transported as bedload) from strawberry lands.
- There is some evidence that sediment load from grazing lands can be high if not mitigated by stream-bank vegetation.

- More conclusive results based on in-stream monitoring could be gained through long term (5-10 years) storm-based monitoring programs capable of sampling from large flood flows. The high cost of such programs could be partly offset by carefully thought out improvements in site selection.
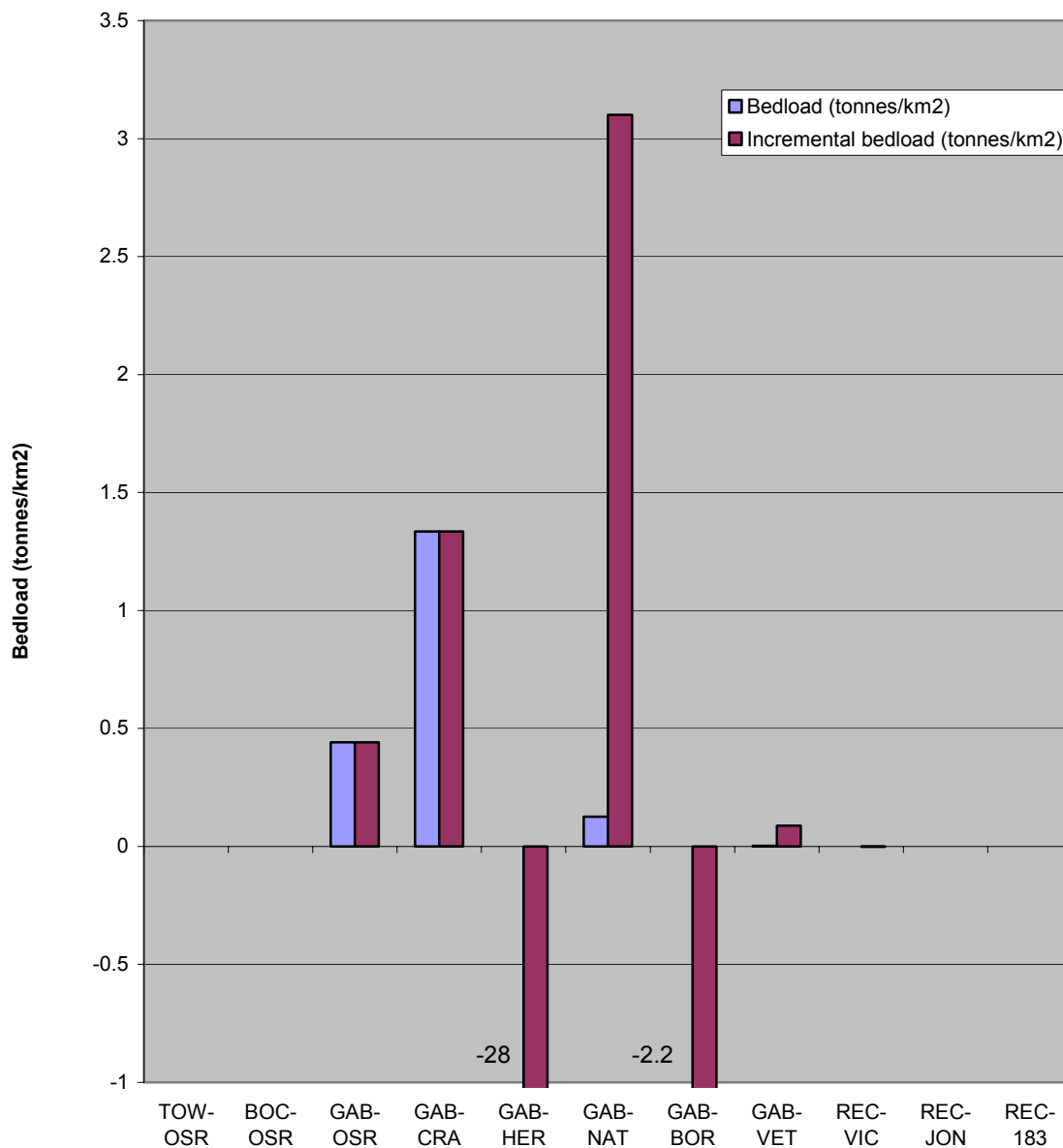

Table 7.9. Bedload totals for three selected events.

7.4 Direct measurement of sediment loads from agricultural fields

7.4.1 Introduction

Row-crop agricultural land has been suggested as a possible source of anthropogenically enhanced sediment loads both in the regional analysis of long-term sediment loads (Section 6.6.2), the brief analysis of the timing of sediment concentration and load in the main stem (Section 7.2), and the sub-watershed scale study on Gabilan Creek (Section 7.3). However, because there are no major tributaries of the Salinas River whose land use is dominated by row-crop agriculture, it is very difficult to make direct estimates of the net sediment load delivered to the main stem by row-crop agriculture over a large area.

An alternative means of obtaining direct information about the role of row-crop agricultural land in regional sediment budgets is to measure the sediment load from individual fields. The present section describes such work, which was conducted in collaboration with a number of generous private land-owners. More-detailed description of certain aspects of the work was given by Kozlowski (2001).

7.4.2 Sources of runoff and sediment from irrigated cropland

Runoff from irrigated land can arise not only after rainfall, but also after irrigation itself. There are three major classes of irrigation: furrow, sprinkler, and drip. Furrow irrigation is not common in the Salinas Valley, and in fact has become less common in California in general (Snyder, 1996). Sprinkler irrigation is common in the Salinas Valley. Water is delivered under pressure through pipes to be sprayed upward through nozzles mounted on pipes lying on or in the soil (Fig. 7.14). Normally in the Salinas Valley, the pipes or laid out for each irrigation event, and removed to allow access for tillage and other operations. On some Salinas farms, permanent pipes are laid into the ground with nozzles protruding up from the soil. "Linear" systems are not uncommon in the Salinas Valley. These deliver water sprayed downward from an overhead lateral on wheels that move along the field (Fig 7.14). Drip irrigation on vegetable crops is becoming more widely used. It is also used on certain fruits, particularly strawberries.

Figure 7.14. Sprinkler irrigation. Photo: Fred Watson, Oct 1999.

Figure 7.14. Linear irrigation. Photo: Thor Anderson, Summer 2000.

A typical irrigation event conducted using sprinkler or linear systems might deliver between half and one and a half inches of irrigation, depending on crop stage, soil moisture, and recent tillage. Under sprinkler irrigation, the water is delivered gradually over a period of almost a day. Under linear, the distribution is highly localized under the line of sprinkler heads, and must occur at a much higher instantaneous rate in order that all land gets enough water as the system moves from one end of the field to the other.

Whether or not runoff is produced depends upon many factors. Steep slopes are more likely to produce runoff than flat ones. Slopes with buried 'tile' drains (Fig. 7.16) reduce surface runoff by reducing soil saturation and allowing more water to infiltrate. Many soil surfaces become 'sealed' after rain or irrigation, such that subsequent rain or irrigation does not infiltrate and runs off easily. Tillage removes this problem, but cannot be accomplished during certain crop stages, and when the soil is very wet during winter. Water applied at a higher rate (such as under linear irrigation) infiltrates less readily and is more prone to runoff.

The concentration of sediment borne in runoff from row–crop fields also varies significantly. Runoff from mature crops or cover crops is expected to yield less sediment because of factors such as reduced drop impact, increased resistance to flow, and increased root strength. Certain soil types are also more erosive than others. Runoff from steeper fields has a higher sediment transport capacity, which may lead to higher runoff concentrations.

All farm runoff may be subject to a variety of practices aimed at reducing the delivery of runoff to downstream areas such as streams. Perhaps the most effective measures are sediment retention and detention basins (Fig. 7.16), which, if properly maintained, trap all sediment except the finest material under all but the most extreme rainfall situations.

Figure 7.16. Perforated 'tile drainage' pipes removed from beneath a field after clogging up. Photo: Fred Watson, Nov 2001.

Figure 7.16. Monitoring runoff entering an on-farm sediment detention basin. Photo: Fred Watson, 30 June 2000.

7.4.3 Sampling dates and sites

Monitoring of on-farm runoff was conducted opportunistically from April 2000 until the present, according to access to land, and other monitoring commitments. To date there have been 15 monitoring events covering separate 16 plots of land (i.e. fields or vineyards) on 7 properties. This has resulted in a total of 25 unique measurements of the total sediment yield from a specific plot of land during a specific irrigation or rainfall event. Sites were selected initially based on word-of-mouth access to land managed by collaborating growers. Later sites were selected based on particular features absent in the earlier sites, such as certain runoff management measures, and different terrain types. To preserve grower confidentiality, all sites are coded and their exact locations withheld from publication. All sites were in the Salinas Valley ranging from the Elkhorn Slough area south as far as the Greenfield area.

7.4.4 Methods

A detailed description of the relevant field and laboratory protocols is given in the CCoWS Protocols Document (Watson et al., 2002; Revision C; Sections 3.4, 3.5, & 4.1).

Both rainfall and irrigation events were monitored. In each case the primary aim was to quantify the total amount of water applied to the field, and the total amount of water and sediment running off. This was achieved by measuring rainfall and taking runoff water samples every 10 to 20 minutes during the full period of the event and subsequent runoff (usually about one day). The samples were analyzed for total sediment concentration, and integrated with discharge measurements to estimate total discharge and sediment load.

7.4.5 Results: field-scale sediment load

A total of 344 sediment samples and 452 runoff measurements were taken from 16 plots during 15 events, resulting in 25 measurements of total per-event plot runoff. Most of the events are described in detail by Kozlowski (2001).

Sampling setup and results for a typical sprinkler irrigation event are shown in Figures 7.18. Across all sprinkler events, water application rates ranged from 6 – 10 mm/hr. Total water applied ranged from 8 – 50 mm. Runoff timing lags behind irrigation timing, with peak runoff often occurring just as the sprinklers are turned off. Peak total sediment concentration often coincides with peak runoff.

Linear irrigation setup and results are shown in Figures 7.20. Water application rates were considerably higher than for sprinkler irrigation, ranging from 31.4 – 46.6 mm/hr. Runoff did not tend to lag behind irrigation timing as much as for sprinkler irrigation, and was more uniform in time. This is consistent with the linear systems constantly bringing new areas of soil to infiltration excess, resulting in a steady stream of runoff, albeit from a moving area. Small peaks occur from time to time as small soil dams are broken in the furrows and gutters draining the field.

Typical rainfall events are shown in Figure 7.22, with results from the left-hand (night time) event shown in Figure 7.22b. Average rainfall rate ranged from 1.6 – 3.8 mm/hr. Rainfall intensity varied between 1.9 and 13.2 mm/hr, based upon 10-minute sampling intervals. Peak runoff rates lagged behind peak rainfall rates, but runoff duration was not particularly different to rainfall duration.

Figure 7.18a. Measuring sediment runoff during sprinkler irrigation. Photo: Fred Watson, 30 June 2000.
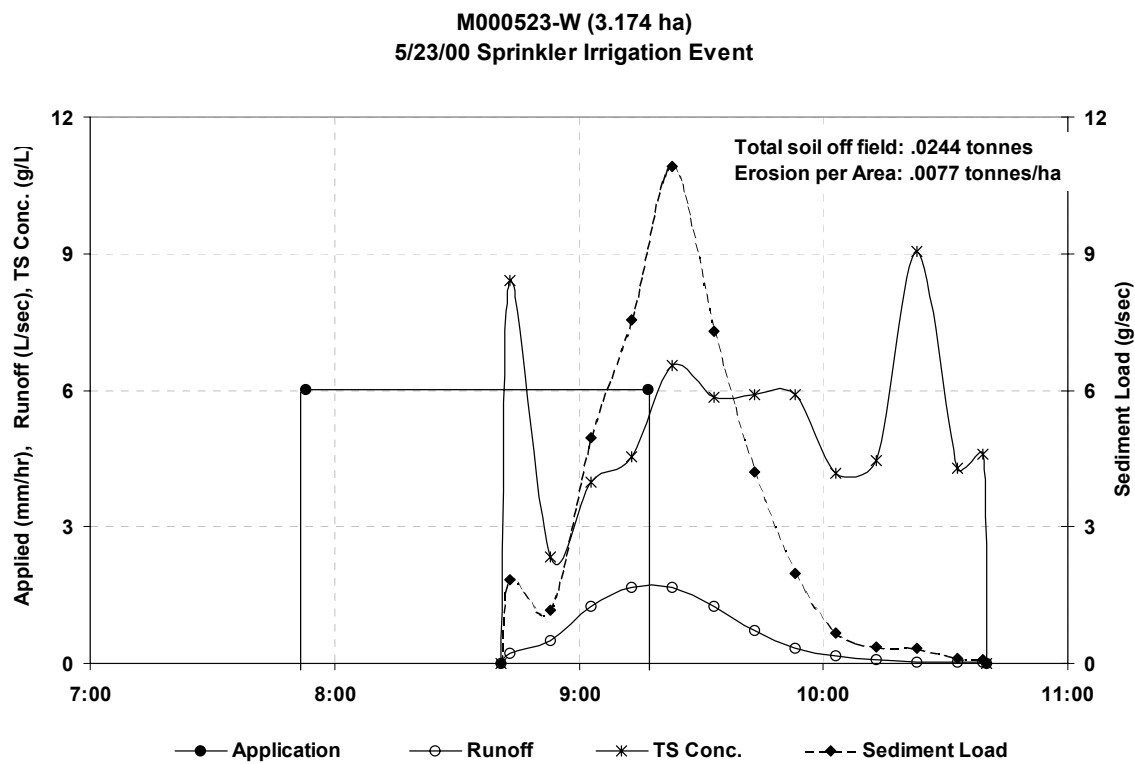

Figure 7.18b. Runoff results from a typical sprinkler irrigation event.

Figure 7.20a. Pipe used as sampling point draining field under linear irrigation. Photo: CCoWS, Summer 2000.
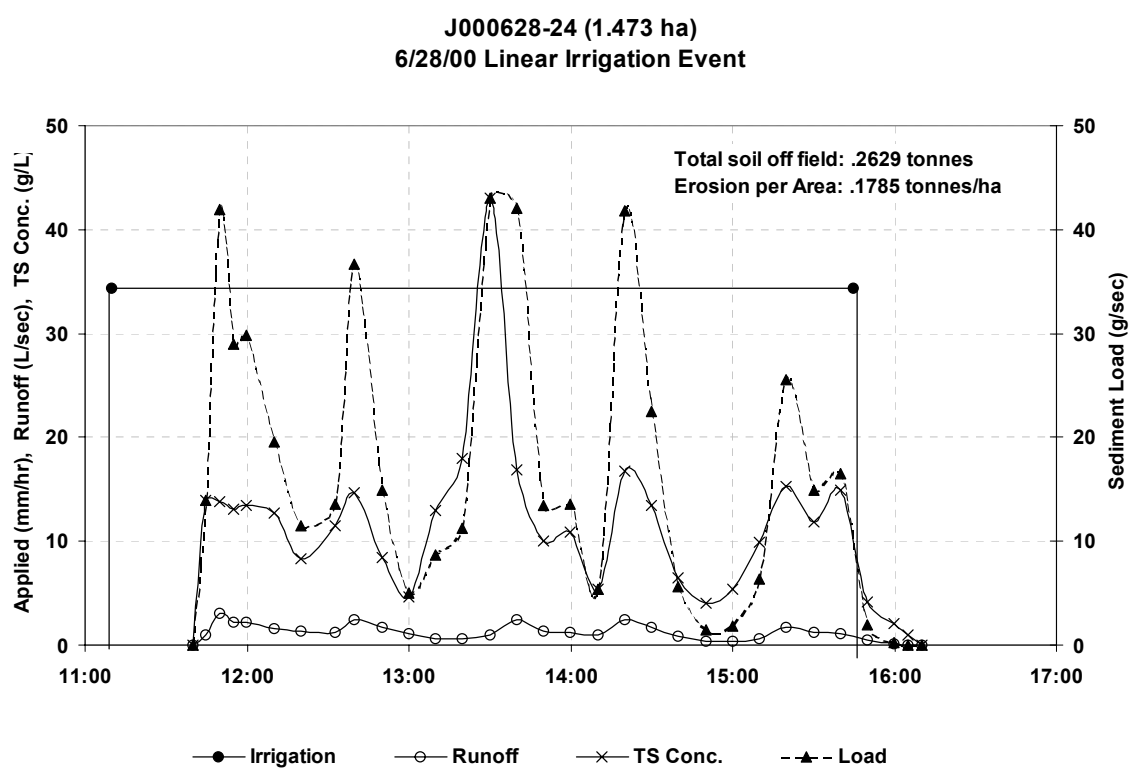

Figure 7.20b. Runoff results from a typical rain event.

Figure 7.22a. Sampling runoff from agricultural fields during rainfall events. Photos: Don Kozlowski, 19 Feb 2001; Fred Watson, 24 Nov 2001.
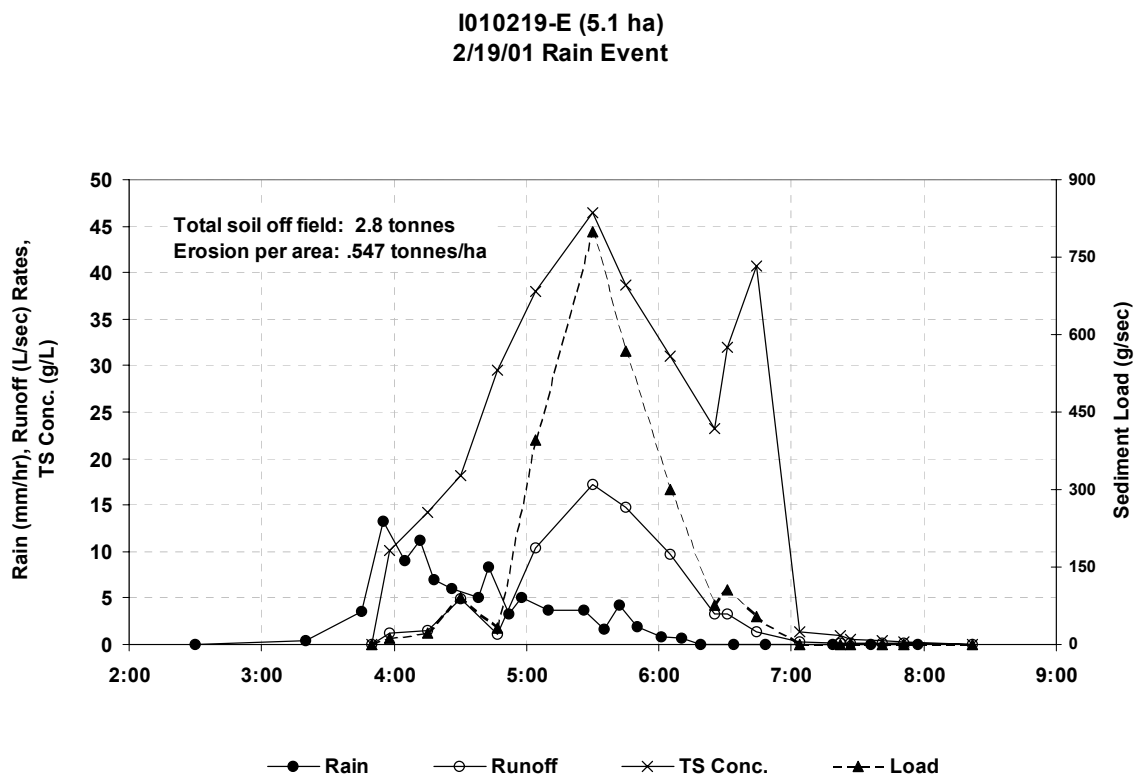
I010219-E (5.1 ha)
2/19/01 Rain Event

Figure 7.22b. Runoff results from a typical sprinkler irrigation event.

Results from all fields are summarized in Table 7.10 (with soil texture codes listed in Table 7.11), which is sorted from the highest sediment loads per area to the lowest loads. At the left of the figure are the basic attributes of each field. In the middle are summary attributes of the specific irrigation and rainfall events applied to the fields, and at the right are various expressions of the sediment load from the field. The most basic expression of sediment yield is the total load in tonnes per km^2 per event. Another useful measure is the event mean concentration (EMC) of sediment in the runoff, expressed in mg/L. Finally, a measure of the sediment 'cost' per unit of net irrigation is calculated, and expressed in tonnes per km^2 per millimeter of net irrigation (where 'net irrigation' equals irrigation applied minus irrigation tailwater).

All results presented in this Section are for sediment loads measured at the point of drainage from fields. They do not account for the beneficial effects of sediment and runoff detention systems that may be in place downstream of the sampling point. This is discussed further in Section 7.4.6.

Measured event load ranged from zero to 55 tonnes/km^2 (note that these figures are not comparable to long-term mean annual loads until appropriately scaled, as in Section 7.4.6). A consistent explanation of the variation between these values is not straightforward with respect to the field, irrigation, and rainfall attributes listed in Table 7.10. The largest measured load (55 tonnes/km^2) was from a relatively long 220-minute 13 mm rainfall event on a gentle (0–2%) sloped fallow field, although the same event yielded only 5.4 tonnes/km^2 from a steeper (0–5%) adjacent field. The high instantaneous irrigation application rates of linear irrigation systems (31–47 mm/hr) yielded the second and third highest loads (14–18 tonnes/km^2) when applied to sealed soils, but significantly lower loads (0–5.9 tonnes/km^2) when applied to cultivated soils. The lower application rates of sprinkler systems (6–10 mm/hr) can also lead to significant loads, even on cultivated soils, when the total amount of water is relatively high (48–50 mm or 2 inches).

Field	Date	Soil texture	Slope	Slope x surface erodibility	Crop	Crop stage	Soil state	Detention before sampling point?	Irrigation or rainfall	Area water applied to (m2)	App. rate (mm/hr)	Peak app. rate (mm/hr)	App. Duration (min)	Applied (mm)	Runoff (mm)	Runoff Coeff.	Sed. loss (tonnes /km2 /event)	EMC (mg/L)	Loss per net app. (tonnes /km2/mm)
D1	19-Feb-01	L, SL	0% - 2%	0.28%	None	Fallow	Cultivated	None	Rainfall	51230	3.8	13.3	220.00	14.0	1.49	10.7%	54.15	36,310	4.33
B3	28-Jun-00	L	~0-2%	0.28%	Red & green	Mature (last water)	Sealed	None	Linear	14731	34.35 / 5.67	34.35 / 5.67	45.37 / 275	26.0	1.36	5.2%	17.85	13,122	0.73
B2B	28-Jun-00	L	~0-2%	0.28%	Lettuce	Early (2nd water)	Sealed?	None	Linear	21535	46.6 / 4.03	46.6 / 4.03	24.19 / 280	18.8	1.62	9.4%	13.98	8,647	0.81
A2	30-Jun-00	FSL	~0-2%	0.20%	Red & green	Mature - last	Partly sealed	None	Sprinkler	13315	8.7	8.7	188.00	27.2	2.56	9.4%	7.77	3,033	0.32
C1	22-Jul-00	SiCL	0.01%-0.03%	0.01%	Cauliflower	Mid (17 days since)	Cultivated		Sprinkler	28387	10.1	10.1	301.00	50.4	0.79	1.6%	7.03	8,868	0.14
B2A	22-Jun-00	L	~0-2%	0.28%	Broccoli	Early (2nd water)	Cultivated	None	Linear	15834	31.42 / 3.75	31.42 / 3.75	24.93 / 209	13.1	0.94	7.2%	5.86	6,235	0.48
D1	12-Feb-01	L, SL	0% - 2%	0.28%	None	Fallow	Cultivated	None	Rainfall - tail	51230	5.0	7.5	24.00	2.0	0.46	23.0%	5.53	12,010	3.59
D2	19-Feb-01	L, SL	0% - 5%	0.70%	None	Fallow	Cultivated	None	Rainfall	38490	3.8	13.3	220.00	14.0	0.83	5.9%	5.42	6,561	0.41
C1	02-Aug-00	SiCL	0.01%-0.03%	0.01%	Cauliflower	Mid (28 days since)	Cultivated		Sprinkler	28387	8.4	8.4	345.00	48.4	1.51	3.1%	4.72	3,127	0.10
D1	11-Feb-01	L, SL	0% - 2%	0.28%	None	Fallow	Cultivated	None	Rainfall - tail	51230	1.6	3.0	137.00	3.8	0.35	9.2%	2.02	5,840	0.59
D2	12-Feb-01	L, SL	0% - 5%	0.70%	None	Fallow	Cultivated	None	Rainfall - tail	38490	5.0	7.5	24.00	2.0	0.20	10.2%	1.16	5,721	0.65
E3	24-Nov-01	LS	1% - 3.5%	0.23%	Brus. Spr.	Mature	Not cultivated	None	Rainfall	18723	4.7	7.2	240.00	16.0	0.10	0.6%	0.97	9,731	0.06
A1	30-Jun-00	FSL	~0-2%	0.20%	Red & green	Mature - last	Partly sealed	None	Sprinkler	14698	8.7	8.7	188.00	27.2	2.30	8.5%	0.88	384	0.04
A2	23-May-00	FSL	~0-2%	0.20%	Leaf lettuce	2 weeks	Mostly sealed	None	Sprinkler (artificial)	31736.5	6.0	6.0	84.00	8.4	0.30	3.6%	0.77	2,541	0.09
A1	23-May-00	FSL	~0-2%	0.20%	Leaf lettuce	2 weeks	Mostly sealed	Some water and	Sprinkler (artificial)	31736.5	6.0	6.0	84.00	8.4	0.11	1.3%	0.39	3,575	0.05
F1	28-29-Nov-01	C	6.8%	0.82%	None	Fallow	Composted, Sealed	None	Rainfall	42673	1.2	2.5	251.00	5.1	0.07	1.4%	0.35	4,986	0.07
E2	24-Nov-01	LS	1% - 6%	0.35%	Brus. Spr.	Mature	Not cultivated	Wetland	Rainfall	50392	2.0	7.2	240.00	16.0	0.14	0.9%	0.30	2,091	0.02
D2	11-Feb-01	L, SL	0% - 5%	0.70%	None	Fallow	Cultivated	None	Rainfall - tail	38490	1.6	3.0	137.00	3.8	0.14	3.6%	0.28	2,084	0.08
E1	24-Nov-01	LS	1% - 6%	0.35%	Brus. Spr.	Mature	Not cultivated	None	Rainfall	50392	3.7	7.2	240.00	16.0	0.36	2.3%	0.20	544	0.01
E4	24-Nov-01	LS	1% - 6%	0.35%	Brus. Spr.	Mature	Not cultivated	None	Rainfall	75127	7.7	7.2	240.00	16.0	0.03	0.2%	0.01	390	0.00
B1	Pre-5-Jul-00	L	~0-2%	0.28%	None	Fallow	Cultivated	None	Linear		35.66 / 3.57	35.66 / 3.57		31.2	0.00	0.0%	0.00	0	0.00
C1	28-29-Nov-01	SiCL	0.01%-0.03%	0.01%	Cauliflower	Pre-transplant			Sprinkler	28387	9.0	9.0	540.00	81.0	0.00	0.0%	0.00	0	0.00
F2	28-29-Nov-01	C	8.8%	1.06%	None	Fallow	Composted, Not-sealed		Rainfall	4736	1.2	2.5	251.00	5.1	0.00	0.0%	0.00	0	0.00
G1	28-Dec-01	L, GSL	~2-5%	0.98%	Vines	Dormant	Light grass cover		Rainfall		0.2	0.8	1920.00	5.7	0.00	0.0%	0.00	0	0.00
G1	02-Jan-02	L, GSL	~2-5%	0.98%	Vines	Dormant	Light grass cover		Rainfall		1.3	1.5	540.00	11.3	0.00	0.0%	0.00	0	0.00

Table 7.10. Summary of runoff and sediment data for a variety of agricultural fields under discrete irrigation or rainfall events. Note that linear irrigation systems only apply water to a fraction of the irrigated area at any given instant. The paired values for application rate and duration reflect both instantaneous irrigated areas and total irrigated areas.

Abbreviation	Texture	Fine / coarse
C	Clay	Finer
SiCL	Silty clay loam	...
L	Loam	...
FSL	Fine sandy loam	...
SL	Sandy loam	...
LS	Loamy sand	...
GSL	Gravelly sandy loam	Coarser

Table 7.11. Explanation of soil texture abbreviations used in Table 7.10, organized along an approximate gradient from fine to coarse textures.

Zero event loads were measured under a variety of circumstances. A linear irrigation event with zero load (apart from road runoff) was observed for well-cultivated decomposed-granite (DG) sloping soil. On a very flat ($< 0.03\%$) field, three inches of sprinkler irrigation also produced no runoff in a well-cultivated pre-plant situation. On one farm, zero runoff was achieved from steeply sloping land (8.8%) during a small rainfall event (5 mm at 1.2 mm/hr), apparently due in part to a combination of tile drainage and heavy composting leading to high soil water infiltration capacity. Preliminary work on a northern Salinas Valley vineyard also measured zero runoff, but the rainfall rates were so low (0.2–1.3 mm/hr) that comparison with the row-crop data is not possible.

Event mean concentration ranged from 0 to over 35,000 mg/L for the measured events. Most of the non-zero EMC values were well above 4000 mg/L, which would be considered a very high value if it were measured in a river or other stream. The variation in EMC approximately followed the variation in total load.

Sediment loss per unit of net irrigation was highest for linear irrigation systems (0.48–0.81 tonnes/km^2/mm). During sprinkler irrigation events where total sediment loss was relatively high (> 4 tonnes/km^2), these losses were relatively low (0.10–0.32 tonnes/km^2/mm) when compared with the net irrigation applied.

Soil texture and erodibility information for each field was obtained from maps made by the USDA-SCS soil survey (1978). The soils were predominantly loamy (SiCL, L, FSL, SL) or sandy (LS) in texture (see Table 7.11), and ranged from fine textures such as Clay (C) through to coarse textures such as Gravelly Sandy Loam (GSL). The USLE K-factor for soil erodibility is mapped for each soil type.

Table 7.10 lists the erodibility value for the surface layer, multiplied by the approximate mean slope of the field, yielding a measure of the erosion potential of the soil and slope (excluding other influences such as cover, rainfall, and management). There is no apparent correlation between slope erodibility and any of the measurements of erosion (areal loss, EMC, or loss per net application). This is most likely due to variation in other factors, such as rainfall intensity, and on-field management practices such as tile drainage and composting. Further monitoring is recommended.

Ideally, a predictive model could be formed that estimated soil loss from other parameters. However, the associated correlations are weak in the data set – as reflected in significant scatter in simple plots such as total soil loss versus total water applied (Fig. 7.23). Kozlowski (2001) demonstrated the *potential* for the row-crop data set to be summarized by a multivariate model. This potential would only be fully realizable with a much larger data set that repeatedly measured runoff from a wider range of combinations of field parameters and rainfall and irrigation conditions. Such data sets are compiled by the Natural Resources Conservation Service (NRCS) for calibration of the Revised Universal Soil Loss Equation (RUSLE) series of models. The present data could potentially be used to provide local Salinas Valley data to support a model based on the well-developed generic structure of RUSLE (a simple RUSLE application is presented for comparison in Section 7.5). Their immediate purpose, however, is to illustrate the range of sediment loads to be expected from Salinas fields, to suggest some of the factors that may contribute to variability within this range, and to provide the basis for an estimation, in the following section, of how sediment loads from agricultural fields may contribute to the regional average load.
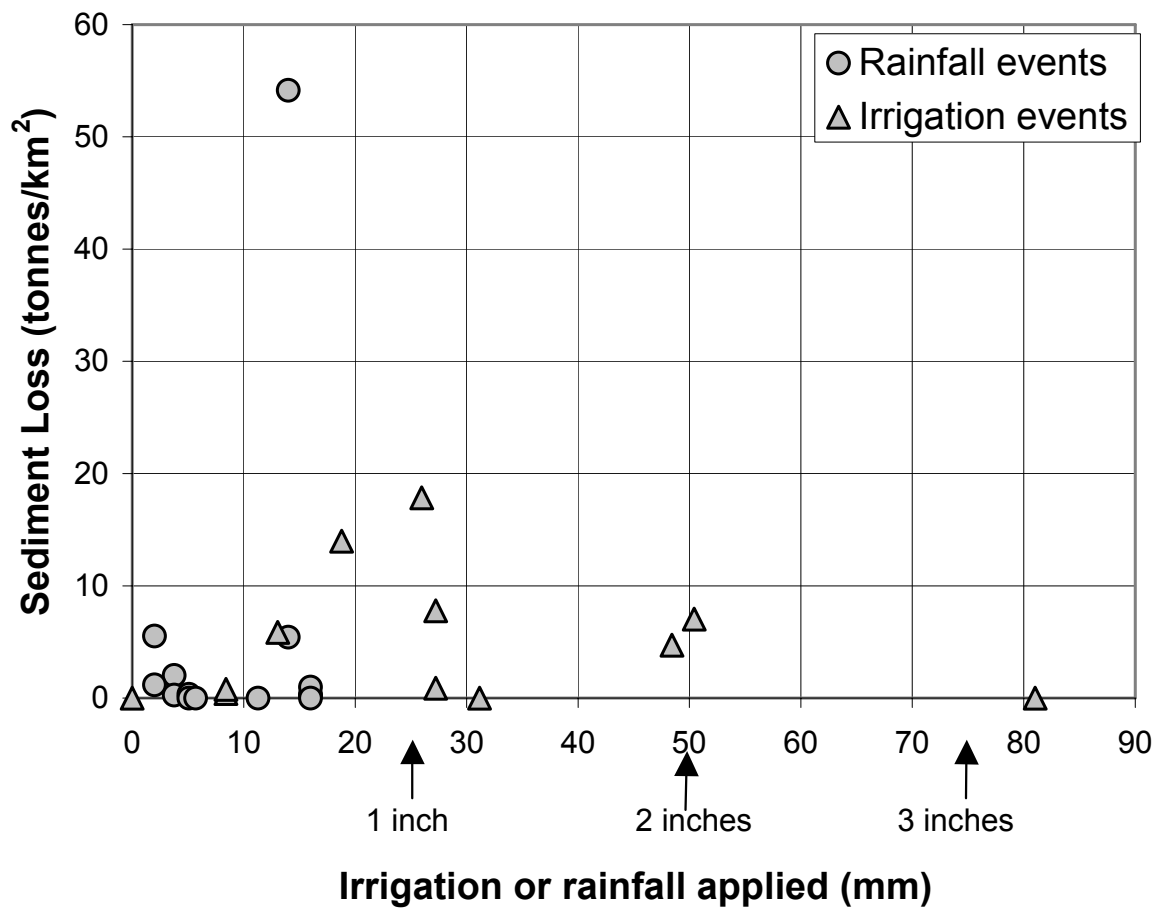
Figure 7.23. Sediment loss versus irrigation or rainfall totals for row-crop fields in the Salinas Valley.

7.4.6 Scaling of field-scale results to long-term regional averages

During the course of a year, a given field may export a range of sediment loads for each irrigation event that is applied to it, and each rainfall event to which it is subjected. A typical irrigation event delivers about an inch of water to the field. There may be 10 such events per crop, and two crops per year. As shown in the previous section, some events may produce no runoff or sediment load, and others from the same field may produce typical loads of about 5 tonnes/km^2, or as much as 55 tonnes/km^2.

Similarly, rainfall is highly variable. In a given year at the City of Salinas, there may be between 1 and 22 daily rainfall totals greater than or equal to half an inch, and between 0 and 6 daily rainfall totals greater than or equal to one inch (Fig. 7.24). An average rainfall year typically contains 8 to 12 half-inch events and 1 to 3 one-inch events.

In order to scale single-event load measurements to mean annual values, single-event values could be scaled by a conservative range of factors between about 5 and 20 for irrigation events, and between about 5 and 15 for rainfall events. Summing these ranges leads to scaling factors ranging between about 10 and 35. Taking 5 tonnes/km^2 as a typical single-event load, this leads to very approximate estimates of mean annual field loads of between 50 and 175 t/km^2/yr. In order to compare these numbers to the watershed averages estimated in Section 6.6, the delivery ratio must be examined as follows.
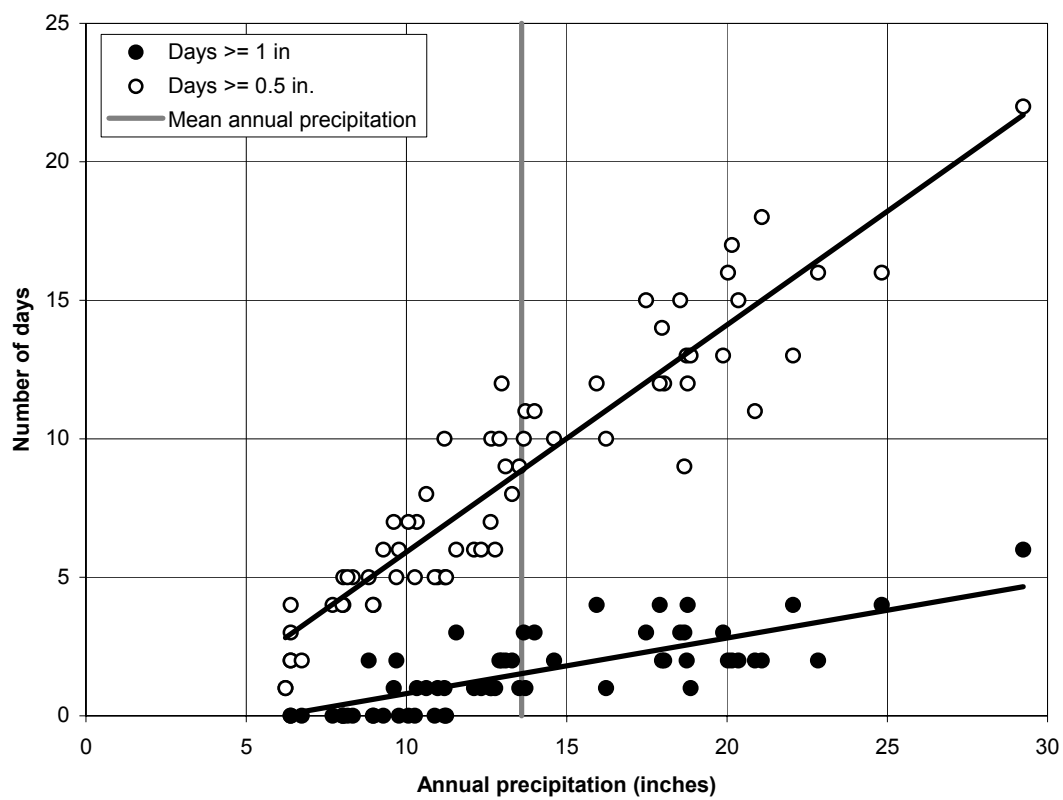
Figure 7.24. Frequency of significant rainfall events versus annual rainfall total – Salinas Airport.

Not all the sediment eroded from an agricultural field, is fully delivered to streams in the long-term. There are numerous retainment mechanisms in place in the Salinas Valley (SCS, 1984a, b). Perhaps the most prevalent are sediment detention and sediment retention basins. Detention basins are typically less than 20 meters long, and are designed to retain and deposit as much sediment as possible during a season, while allowing the remaining tailwater to overflow into downstream drainage pathways if necessary. Retention basins are larger, and are intended to retain a larger proportion of sediment and water. Some of these basins are installed under NRCS guidelines while others are situated and sized to take advantage of local topography or legacy features such as small quarries used for road construction. Certain farms also use a large array of small 'catch basins' only a few meters long, with each being manually maintained to clear sediment build-up after each irrigation event (Fig. 7.25). Material excavated from any basin may be applied back on to fields, or elsewhere at the grower's discretion. Basins may be placed at the runoff point of each field, or pair of fields, or farther downstream at the runoff point for an entire farm. In some cases, a series of basins are placed in series. Collectively, measures such as these may account for (i.e. trap) anywhere between zero and 100% of the load observed at the field runoff point.

Figure 7.25. A selection of on-farm measures for runoff control: (a) a typical detention basin with standpipe and outlet pipe, (b) a catch basin that can easily be manually excavated at regular intervals, (c) a broad vegetated area that intercepts and diffuses runoff from a small agricultural watershed. Photos: a) Don Kozlowski, Feb 2001; b) Fred Watson, 3 Oct 2001; c) Fred Watson, 24 Nov 2001.

Once beyond any on-farm measures such as detention basins, agricultural runoff may be conveyed to streams in agricultural ditches. At this time, the competence of the flow may be reduced due to factors such as reduction of drainage slope, and percolation into the bed of the ditch or stream. This results in sediment deposition, and a reduction in the proportion of sediment delivered to downstream areas. Once deposited in ditch or stream, the sediment may be later transported downstream by higher flows, or it may be excavated during channel 'maintenance' (Figure 7.26). Such maintenance is conducted both by private interests and by agencies such as the Monterey County Water Resources Agency. In either case, the long-term sediment delivery ratio (SDR) is reduced.

In the United States, sediment delivery ratios vary between close to 100% and as low as 1%, depending mainly on watershed area (NRCS, 1983). Agricultural systems on the Salinas Valley floor have low watershed area, and straightened, excavated channels with low resistance to flow. The associated SDR is expected to be at the high end of the national range. Values below 50% are unlikely. In some cases, farm runoff discharges directly into streams, and so the upper end of the delivery ratio range is 100%.

By combining a typical measured event load of 5 tonnes/km^2, with event-to-annual scaling factors of between 10 and 35, a possibility of up to 100% retention by on-farm basins, and a range of delivery ratios between 50% and 100%, the mean annual sediment load contributed by an agricultural field in the Salinas Valley to the Salinas River may vary from 0 to about 175 t/km^2/yr.

There are clearly considerable uncertainties in such an estimate, which thus only serves to indicate that it is possible that sediment loads from agricultural areas in the Salinas Valley are much higher (e.g. 175 t/km^2/yr) than the regional average load of 64 tonnes/km^2 (Section 6.6.2), and that it is also possible that agricultural loads are lower than the regional average. Future efforts should work to collect further monitoring data to reduce these uncertainties, in conjunction with similar measurements of runoff from other land types (e.g. grazing, vineyards, forests).

Figure 7.26. Sediment delivery ratio of agricultural ditches and streams: (a), (b) less than 100% delivery in excavated ditches, (c) greater than 100% delivery in an eroding ditch, (d) uncertain delivery ratio in a stream with riparian bank vegetation removed, (e) bank stabilisation along a grassed ditch, and (f) limited sediment retention in a cobbled ditch. Photos: Fred Watson: a) Jan 2001; b) 11 Feb 2000; c) 11 Feb 2000; d) Oct 2000; e) Feb 2002; f) Feb 2002.

7.5 Comparison with RUSLE estimates of field erosion

The Revised Universal Soil Loss Equation is a widely used tool for estimating erosion from agricultural and range lands at the plot scale. It was *not* used as the primary estimation tool in the present study because:

- regional-scale estimation of sediment yield is not possible with RUSLE
- field-scale estimation can be highly uncertain unless verified by local measurements

Thus, the present study emphasized the measurement of local field-scale erosion, before any attempts to estimate erosion using generic models. With some such measurements in hand (Sec. 7.4), some simple comparisons with RUSLE estimates can be made. The analysis presented below is offered only as a simple application of RUSLE for comparative purposes. A detailed application would involve much more detailed consideration of all the respective factors.

The form of RUSLE is very similar to USLE (Sec. 0), and is based around the following equation (Renard et al., 1996):

$$A = R \; K \; LS \; C \; P$$

where *A* is mean annual soil loss from an area, *R* is an average annual erosivity factor, *K* is a soil erodibility factor, *LS* is a topographic factor (combining slope (S) and slope length (L)), *C* is a cover management factor, and P is a support practice factor.

To give an approximate indication of the spread of RUSLE soil loss estimates for row-crops in the study area, the equation was applied to each farm upon which sediment was measured in Section 7.4. For each farm, Table 7.12 lists the values used for each factor, and the resulting estimate of mean annual soil loss. A uniform R-factor value of 30 was used, based on Figure 2-3 in Renard et al. (1996). In most cases, the slope was estimated as the mid-point of slope measured at each farm, but in some cases was determined from soil survey maps. Slope length was taken as the typical length of furrows, not including gutters running perpendicular to furrows, or agricultural drains downstream of gutters. A uniform value of 300 ft was assumed based on the size of the area

drained by a typical runoff collection point. The LS factor was then evaluated based on slope and slope length using Table 4-2 in Renard et al. (1996). The K-factor was taken from soil survey maps. The C factor was taken as 1, representing clean-tilled fallow fields, as was the P factor. In cases where crops or cover crops were present, or sediment detention basins were in place, the C and P factors would be lower.

In Table 7.12, mean annual soil loss estimates range from 124 t/km²/yr for a very flat farm (C), to 1243 t/km²/yr for a moderately steep row-crop farm (F) and a vineyard (G). The corresponding estimate based on field measurements (Sec. 7.4.6) was between 50 and 175 t/km²/yr – i.e. at the low end of the range of RUSLE estimates. Uncertainties with either method may account for this discrepancy, including inaccuracies in RUSLE itself, errors in the estimation of RUSLE parameters, and the many assumptions used to scale between single-event loads and mean annual loads in Section 7.4.6.

The RUSLE estimates compare well with previous estimates made using USLE in the Strawberry Hills Target Area, which borders the study area to its north (SCS, 1984a, b). The Strawberry Hills area has more sloping and erodible land than the row-crop areas of the study area, and as a consequence, its estimated mean annual sheet and rill erosion (Tab. 7.13) overlaps the upper range of estimates shown in Table 7.12. A combination of Modified USLE (MUSLE) and USLE estimates with limited field data was used in the proposed Morro Bay TMDL, resulting in estimated cropland sheet and rill yields of between 76 and 744 t/km²/yr (CCRWQCB, 2002).

The mean annual non-flood loads suggested for agriculturally dominated lands were 200-500 t/km²/yr in the regional analysis (Sec. 6.6.2), 337 to 722 t/km²/yr in the Gabilan Watershed analysis (Sec. 7.3.5), and up to 175 t/km²/yr based on on-farm measurements (Sec. 7.4.6). These numbers are very high within the context of the regional analysis, but are not contradicted by the RUSLE analysis. Note, however, that this comparison is distorted by the fact that the regional analysis is limited to suspended sediment, and non-flood loads.

Further study is warranted in order to account for the differences between the regional analysis described in Chapter 6, and the four different methods used to obtain supporting clarification of sediment sources in the watershed (i.e. in Sections 7.2, 7.3.5, 7.4.6, 7.5). At present, the results of the regional analysis

are the primary means by which the overall spatial distribution of sediment load in the study area is characterized. Given this, the differences obtained through comparison with other methods serve mainly to highlight the fact that sediment yield estimation in general is an uncertain undertaking.

Farm	Typical slope	Assumed slope length (ft)	Regional R factor	Mapped K factor	Estimated LS factor	Reference C factor	Reference P factor	A (tons/ac/yr)	A (tonnes/km2/yr)
A	1.00%	300	30	0.2	0.17	1	1	1.02	229
B	1.00%	300	30	0.28	0.17	1	1	1.43	320
C	0.02%	300	30	0.37	0.05	1	1	0.56	124
D	1.75%	300	30	0.28	0.35	1	1	2.94	659
E	3.19%	300	30	0.1	0.55	1	1	1.65	370
F	3.90%	300	30	0.24	0.77	1	1	5.54	1243
G	3.50%	300	30	0.28	0.66	1	1	5.54	1243

Table 7.12. Parameters and results of a simple application of the RUSLE (sheet and rill) soil loss model to the row–crop farms and vineyards measured during the present study.

	Area (acres)	Area (km2)	Erosion (tons/yr)	Erosion (tonnes/km2/yr)
Bushberry	36	0.15	540	3362.5
Dairy	70	0.28	280	896.7
Nursery	650	2.63	1625	560.4
Orchard	797	3.23	3191	897.5
Grain/Pasture	1237	5.01	3713	672.9
Strawberry	3900	15.78	38900	2235.9
Other row-crop	9000	36.42	45000	1120.8
Native veg.	40175	162.59	40175	224.2
Water	871	3.52	0	0.0
Other (includes res., urb., ind.)	4356	17.63	871	44.8

Table 7.13. USLE–based sheet and rill erosion estimates for sloping land in the nearby Strawberry Hills Target Area, to the north of the study area (SCS, 1984a, b).

8   References

American Public Health Association (APHA), American Water Works Association, and Water Pollution Control Federation (1995). Total Suspended Solids Dried at 103°–105° C. Method 2540 D.

American Society for Testing and Materials (ASTM) (2000) Standard Test Method for Determining Sediment Concentration in Water Samples. Method D 3977–97.

Armstrong, P., Silberstein, M., & Campbell, E. (1997). Wetlands. In: Monterey Bay Aquarium, A Natural History of the Monterey Bay National Marine Sanctuary, in Cooperation with the National Oceanic and Atmospheric Administration Sanctuaries & Reserves Division, Chapter 4.

Bloyd, R.M (1981). Letter of March 18, 1981 to Robert F. Blecker, hydrologist for Los Padres National Forest, which summarizes USGS studies of post–fire sedimentation in Los Padres Reservoir. (cited by Hecht, 1981)

Brown, W.M.III. 1973. Erosion processes, fluvial sediment transport and reservoir sedimentation in a part of the Newell and Zayante Creek basins, Santa Cruz County, California. U.S. Geological Survey Open File Report. Menlo Park, California. 31 pp.

Brune G.M. 1953, 'Trap efficiency of reservoirs', Transactions, American Geophysical Union Vol. 34, pp. 407 – 418.

Burned Area Emergency Response (BAER) Team – Las Pilitas Fire (1985). Preliminary Report – Damage and Rehabilitation – Las Pilitas Fire. Unpublished.

Burned Area Emergency Response (BAER) Team – Kirk Complex Fire (1999). Untitled. Preliminary Report on Kirk Complex Fire in Los Padres National Forest. Unpublished.

Central Coast Regional Water Quality Control Board (CCRWQCB) (2002). DRAFT: Morro Bay Total Maximum Daily Load for Sediment (including Chorro Creek, Los Osos Creek and the Morro Bay Estuary). 82 pp.

Church, M. (accessed 2002) Sediment Yield and Landscape Models, http://www.geog.ubc.ca/research/church6.html.

Curry, R. & Kondolf, G.M. (1983). Sediment Transport and Channel Stability, Carmel River Sediment Study. Completion report to Monterey Peninsula Water Management District.

Ducea, M.N., House, M., Kidder, S., (2003), Late Cenozoic denudation and uplift rates in the Santa Lucia Mountains, California. Geology, February 2003, v. 31, No. 2, p. 139–142.

Edwards, T.K. & Glysson, G.D. (1999). Field methods for measurement of fluvial sediment. United States Geological Survey, Techniques of Water Resources Investigations, Book 3, Chapter C2, pp 60–89.

Emmett, W.W. (1984). Measurement of bedload in rivers. In: Hadley, R.F. & Walling, D.E. Erosion and Sediment Yield: Some Methods of Measurement and Modelling, Geo Books, Norwich, England. Pp 91–109.

EPA (1999). Protocol for Developing Sediment TMDLs – First Edition. United States Environmental Protection Agency, EPA 841–B–99–004, 143 pp.

FAO (2001). http://www.fao.org/ag/agl/aglw/sediment/default.asp. Accessed August, 2002.

Farnsworth, K.L. (2000). Monterey Canyon as a Conduit for Sediment to the Deep Ocean. Monterey Bay Aquarium Research Institute. 33 pp.
http://www.mbari.org/education/internship/00interns/00internpapers/katie.pdf (Accessed, Jan 2003).

Friebel, M.F., Freeman, L.A., Smithson, J.R., Webster, M.D., Anderson, S.W., & Pope, G.L. (2001). Water Resources Data – California, Water Year 2001. Volume 2 – Pacific Slope Basins from Arroyo Grande to Oregon State Line Except Central Valley. USGS.

Fugro West, Inc. (2002) Paso Robles Groundwater Basin Study, Final Report to County of San Luis Obispo, http://slocountywater.org/pasoroblesbasin.

Glysson, G.D. 1977. Sedimentation in Santa Margarita Lake, San Luis Obispo County, CA. USGS Water Res. Investigation 77–56, 15 pp.

Glysson, G.D. & Gray, J.R. (2002) Total suspended solids data for use in sediment studies. Proc. Turbidity and Other Sediment Surrogates Workshop, April 30 – May 2, 2002, Reno, NV, 3 pp.

Gordon, N.D., McMahon, T.A., & Finlayson, B.L. (1992): Stream Hydrology: An Introduction for Ecologists, John Wiley & Sons Ltd., UK, 526 pp.

Gray, J.R., Glysson, G.D., Turcios, L.M., & Schwarz, G.E. (2000) Comparability of Suspended-Sediment Concentration and Total Suspended Solids Data. USGS Water-Resources Investigations Report 00–4191, 20 pp.
http://water.usgs.gov/osw/pubs/WRIR00-4191.pdf

Griffin, J.R. (1978). The Marble-Cone fire ten months later. Fremontia, 5:8–14.

Hampson, L. (1997). Sediment Transport Analysis: Carmel River Near Carmel – Water Years 1992–1995. Monterey Peninsula Water Management District, Tech. Memo. No. 97–03. 17 pp.

Hansen, R.T., Everett, R.R., Newhouse, M..W., Crawford, S.M., Pimentel, M.I., and Smith, G.A., 2002, Geohydrology of a deep aquifer system monitoring site at marina, Monterey County, California: U.S. Geological Survey, Water-Resources Investigations Report 024003, 36pp.

Hecht, B. (1981). Sequential changes in bed habitat conditions in the upper Carmel River following the Marble-Cone fire of August 1977. In: Warner, R.E. & Hendrix, K.M. (eds), California Riparian

Systems: Ecology, conservation and productive management. Univ. of California Press, pp. 134–141.

Hecht, B. (1993). South of the spotted owl: Restoration strategies for episodic channels and riparian corridors in central California. Proc. Soc. Wetland Scientists, Western Wetlands Conference, March 25–27, 1993, Davis, California, 18 pp.

Hecht, B. (2000). Sediment yield variations in the northern Santa Lucia Mountains. 9 pp. In: Zatkin, R. (ed.) Salinia/Nacimiento Amalgamated Terrane – Big Sur Coast, Central California. Guidebook for the Spring Field Trip, May 19–21, 2000. Peninsula Geological Society. 9 pp.

Inman, D.L. & Jenkins, S.A. (1999). Climate change and the episodicity of sediment flux of small California rivers. Journal of Geology, 107:251–270.

Inman, D.L., Jenkins, S.A., & Wasyl, J. (1998). Database for Streamflow and Sediment Flux of California Rivers. Scripps Institution of Oceanography, Reference Series, No. 98-9. 13 pp. plus tables and figures.

Johnson, K. S., C. K. Paull, J. P. Barry and F. P. Chavez. 2001. A decadal record of underflows from a coastal river into the deep sea. Geology, 29: 1019–1022.

Julien, P.Y. & Simmons, D.B. Sediment transport capacity of overland flow. Trans. American Society of Agricultural Engineers, 28:755–762.

Kistler, R.W., and Champion, D.E., 2001, Rb-Sr whole-rock and mineral ages, K-Ar, Ar/Ar, and U-Pb mineral ages, and strontium, lead, neodymium, and oxygen isotopic compositions for granitic rocks from the Salinian terrane, California: U.S. Geological Survey, Open File Report, 01-453, 84pp.

Knott, J.M. 1976. Sediment discharge in the Upper Arroyo Grande and Santa Rita Creek Basins, San Luis Obispo County, CA. USGS Water Res. Investigation 76-64. 29 pp.

Kondolf, G.M. (1982). Recent channel instability and historic channel changes of the Carmel River, Monterey County, California. M. Sc. Thesis, University of California Santa Cruz, 120 pp.

Lara, J.M. & Pemberton, E.L. (1965). Initial unit weight of deposited sediments. Proc. Federal Inter-Agency Sedimentation Conference, 1963. Misc. Publ. No. 970, USDA, pp. 818–845.

MacPherson, K. R. and Harmon, J. G. 2000. Storage Capacity and Sedimentation of Loch Lomond Reservoir, Santa Cruz County, California, 1998. USGS Water Resources Investigations Report 00-4016

Mattinson, J.M., and James, E.W., 1985, Salinian block U-Pb age and isotopic variations: Implications for the origin and emplacement of the Salinian terrane; in Howell, D.G., ed., Tectonostratigraphic terranes of the Circum-Pacific region, Circum-Pacific Council for Energy and Mineral Resources, Earth Sciences Series, v. 1, p.215–226.

Moffatt & Nichol Engineers (1996). San Clemente Reservoir dredging feasibility study, Carmel Valley, California. Consulting report prepared for California-American Water Company, Monterey Division.

Montgomery Watson Americas Inc., in association with CH2MHILL and Schaff and Wheeler Associates (1998a) Salinas Valley: Historical Benefits Analysis (HBA), Final Report to Monterey County Water Resources Agency.

Montgomery Watson & Raines, Melton & Carella Inc. (1998b), Salinas Valley Water Project, Project Plan Report, Draft, October, 1998, Prepared for Monterey County Water Resources Agency.

Monterey County Water Resources Agency (1997) Water Resources Data Report, Water Year 1994-1995.

Monterey County Water Resources Agency (MCWRA) & US Army Corps of Engineers (USACE) (2001). Draft Environmental Impact Report / Environmental Impact Statement for the Salinas Valley Water Project.
http://www.co.monterey.ca.us/mcwra/deir_svwp_2001/cover.htm

Moore, M.T., S. Testa III, C.M. Cooper, S. Smith, Jr., S.S. Knight, and R.E. Lizotte, Jr. 2001. Clear as Mud: The Challenge of Sediment Criteria and TMDLs. Water Environment and Technology (August 2001) pp. 49-52.

Mussetter Engineering, Inc. (MEI) (2002). Carmel River Dam Removal Study, Monterey County, California. Submitted to: California Department of Water Resources. Fort Collins, Colorado.

National Research Council (NRC) (2001). Assessing the TMDL Approach the Water Quality Management. National Academy Press, Washington, D.C., 109 pp.

Natural Resources Conservation Service, National Engineering Handbook, Section 3, Sedimentation (USDA, Washington, DC, 1983).

Newcombe, C.P. & Jensen, J.O.T. (1996). Channel suspended sediment and fisheries: a synthesis for quantitative assessment of risk and impact. North American Journal of Fisheries Management, 16:693-727.

Newman & Watson, land use, 2002.

Olley, J.M., Murray, A.S., Mackenzie, D.H., & Edwards, K. (1993) Identifying sediment sources in a gullied catchment using natural and anthropogenic radioactivity. Wat. Resour. Res., 29:4:1037-43.

Pasternack, G.B., Brush, G.S., & Hilgartner, W.B. (2001) Impact of historic land-use change on sediment delivery to a Chesapeake Bay subestuarine delta. Earth Surf. Process. Landforms, 26:409-427.

Pickup, G. & Warner, R.F. (1976) Effects of hydrologic regime on magnitude and frequency of dominant discharge. J. Hydrol., 29:51-75.

Prosser, I, Rustomji, P., Young, W., Moran, C., & Hughes, A. (2001) Constructing River Basin Sediment Budgets for the National Land and Water Resources Audit, CSIRO Land and Water, Tech. Rep. 15/01, Canberra, Australia.

Renard, K.G., Foster, G.R., Weesies, G.A., McCool, D.K, and Yoder, D.C., coordinators. Predicting Soil Erosion by Water: A Guide to Conservation Planning with the Revised Soil Loss Equation (RUSLE). U.S. Dept. of Agriculture, Agric. Handbook No. 703, 404 pp. 1997.

Renau, S.L. & Dietrich, W.E. (1991) Erosion rates in the southern Oregon Coast Range: evidence for an equilibrium between hillslope erosion and sediment yield. Earth Surf. Proc. & Landforms, 16:307-322.

Roberts, B.R., Shanahan, E., & Hecht, B. (1984). Salinas River Study - River morphology and behavior. In: Anderson-Nichols & Co., Inc., Consulting report to Monterey County Flood Control and Water Conservation District.

Soil Conservation Service (SCS) (1984a) Strawberry Hills Target Area: Watershed Area Study Report – Monterey County, California. United States Department of Agriculture, 55 pp.

Soil Conservation Service (SCS) (1984b) Strawberry Hills Target Area: Watershed Area Study Technical Report – Monterey County, California. United States Department of Agriculture, 234 pp.

Snyder, J.O. 1913. The fishes of the streams tributary to Monterey Bay, California. Bull. U.S. Bur. Fish. 32:49-72.

Snyder, R., M. Plas, and J. Grieshop. 1996. Irrigation methods used in California: grower survey. Journal of Irrigation and Drainage Engineering July-August 1996 v122 n4 p259(4).

State Water Resources Control Board (SWRCB).(2001). DECISION 1642. http://www.waterrights.ca.gov/Decisions/wrdec1642.htm

Sutherland, D.G., Hansler Ball, M., Hilton, S.J., & Lisle, T.E. Evolution of a landslide-induced sediment wave in the Navarro River, California. Geol. Soc. Am. Bull., 114:8:1036-1048.

Sutton, C. Herron, J.C, & Zappalorti, R. 1996. The Scientific Characterization of the Delaware Estuary. Product of the Delaware Estuary Program, April 1996. http://www.phillywater.org/Delaware/Watershed/hydrology.htm.

Swanson Hydrology & Geomorphology (2001). Technical Addendum to Zayante Area Sediment Source Study. For: Santa Cruz County Department of Environmental Health. 67 pp. http://www.co.santa-cruz.ca.us/eh/env_water_quality/sediment_study_appendices-final.pdf

Tooth, S. (2000). Process, form and change in dryland rivers: a review of recent research. Earth – Science Reviews, 51:67–107.

Trimble, S.W. & Crosson, P. (2000) U.S. soil erosion rates – myth and reality. Science, Vol. 289, No. 5477, 248–250.

United States Army Corps of Engineers (USACE) (1989, revised 1995). Engineering and Design – Sedimentation Investigations of Rivers and Reservoirs.
http://www.usace.army.mil/inet/usace-docs/eng-manuals/em1110-2-4000

United States Department of Agriculture, Soil Conservation Service (USDA-SCS) (1978). Soil Survey of Monterey County, California, 228 pp. plus maps.

United States Geological Survey (USGS). SUSPENDED-SEDIMENT DATABASE. Daily Values of Suspended Sediment and Ancillary Data.
http://webserver.cr.usgs.gov/sediment/introduction.html

Wallbrink, P.J. & Fogarty, P.J. (1998) Sediment sourcing in the Lake Burley Griffin Catchment, CSIRO Land and Water, Tech. Rep. 30/98, 37 pp.

Watson, F.G.R. & Rahman, J.M., 2002. The Tarsier environmental modelling framework. Submitted to: Environmental Modelling and Software.

Watson, F. & Vertessy, R., 2002. Development of a pilot local-scale environmental management support system for use in water supply sub-catchments in Pine Rivers Shire. Draft Final Report to Pine Rivers Shire Council and South East Queensland Water Corporation. CRC for Catchment Hydrology, 61 pp

Watson, F.G.R, Grayson, R.B., Vertessy, R.A., Peel, M.C., & Pierce, L.L. (2001a). Evolution of a hillslope hydrologic model. Invited paper, Proceedings International Congress on Modelling and Simulation (MODSIM 2001), pp. 461-467.

Watson, F., Rahman, J., & Seaton, S.. (2001b) Deploying environmental software using the Tarsier modelling framework. In: Rutherfurd, I., Sheldon, F., Brierly, G. & Kenyon, C. (eds). Proc. 3rd Australian Stream Management Conference, Brisbane 27-29 August, 2001, pp. 631-637.

Watson, F.G.R., Newman, W., Anderson T., Kozlowski, D., Hager, J., & Casagrande, J. 2002. Protocols for Water Quality and Stream Ecology Research. Watershed Institute, California State University Monterey Bay, Rep. No. WI-2002-05d.
http://science.csumb.edu/~Eccows/pubs/reports/CCoWS_Protocols_021014_VersionD.pdf

Willis, C.J., Manson, M.W., Brown, K.D., Davenport, C.W., and Domrose, C.J., 2001, Landslides in the Highway 1 corridor: Geology and slope stability along the Big Sur coast between Point Lobos and San Carpoforo Creek, Monterey and San Luis Obispo Counties, California: California Department of Conservation Division of Mines and Geology, pp.40.